Annual progress report of the Department of Solid State Physics 1 January - 31 December 1996

Jørgensen, Mikkel; Bechgaard, Klaus; Clausen, Kurt Nørgaard; Feidenhans'l, Robert; Johannsen, Ib

Publication date:
1997

Document Version
Publisher's PDF, also known as Version of record

RISØ

Risø-R-933(EN)

Annual Progress Report of the Department of Solid State Physics 1 January - 31 December 1996

Edited by M. Jørgensen, K. Bechgaard, K.N. Clausen, R. Feidenhans'l and I. Johannsen

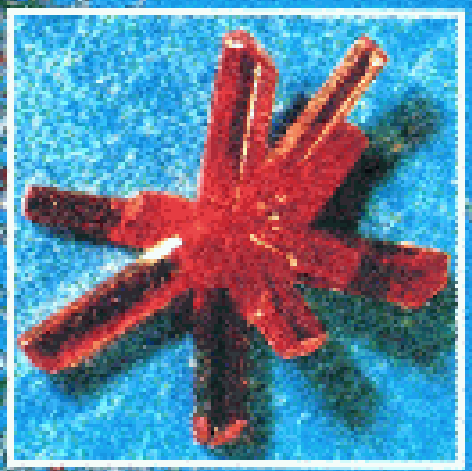

Risø National Laboratory, Roskilde, Denmark
January 1997

Annual Progress Report of the Department of Solid State Physics 1 January - 31 December 1996

Risø-R-933(EN)

Edited by M. Jørgensen, K. Bechgaard, K.N. Clausen, R. Feidenhans'l and I. Johannsen

Risø National Laboratory, Roskilde, Denmark
January 1997

Abstract
Research in the department is concerned with “Materials with Distinct Physical and Chemical Properties”. The principal activities of the department in the period from 1 January to 31 December, 1996, are presented in this Progress Report.

Neutron and X-ray diffraction techniques are used to study a wide variety of problems in condensed matter physics and include: two- and three-dimensional structures, magnetic ordering, heavy fermions, high T_c superconductivity, phase transitions in model systems, precipitation phenomena, and nano-scale structures in various materials. The research in chemistry includes chemical synthesis and physico-chemical investigation of small molecules and polymers, with emphasis on polymers with new optical properties, block copolymers, surface modified polymers, and supramolecular structures. Related to these problems there is work going on in theory, Monte Carlo simulations, computer simulation of molecules and polymers and methods of data analysis.

Frontpage illustration:

The $Mo_6Cl_{14}^{2-}$ cluster forms orange-yellow crystals with the planar trioxatricornane cation (insert). A perspective view of the structure is shown with Mo: Blue; Cl: Green; C: Grey; O: Red.

ISBN 87-550-2233-2
ISSN 0106-2840
ISSN 0907-0249

Grafisk Service - Risø - 1997

Contents

1 Introduction and Acknowledgements 9

2 Research Projects in the Department 14

2.1 Theory 15

2.1.1 Modelling Interface Properties on the Atomistic Level: Polymers Adsorbed to a Surface 15
2.1.2 Modelling Interface Properties on the Atomistic Level: Molecules Adsorbed to a Surface 16
2.1.3 Effects of Boundary Conditions on Magnetization Switching in Kinetic Ising Models of Nanoscale Ferromagnets 17
2.1.4 Towards a Systematic Classification of Protein Folds and Magic Number of Abundance 18
2.1.5 Spin-slip Structure and Central Peak Phenomena in Singlet-Doublet System, Praseodymium 19
2.1.6 Computer Simulation of Heteroepitaxial Film Structures 20
2.1.7 Monte Carlo Simulation Studies of Semidilute Solutions of Semiflexible Polymer Chains 21

2.2 Magnetic and Metallic Structures 22

2.2.1 Neutron Scattering Response in (U,Ce)Ru_2Si_2 22
2.2.2 Magnetic Properties of Holmium-Erbium Alloys 23
2.2.3 Observation of Coherent Magnetic Structures in Tb/Ho Superlattices 24
2.2.4 Resonant X-ray Magnetic Scattering at the K-edge from NiO 25
2.2.5 Magnetic Structure of Cs_2CuCl_4 in Applied Fields 26
2.2.6 The Structural and Magnetic Properties of Ho-Sc Alloys and Superlattices 27
2.2.7 Magnetic Fluctuations near a Quantum Phase Transition in the Heavy Fermion Alloy $CeCu_{6-x}Au_x$ at $x_c = 0.1$ 28
2.2.8 Development of the 'Small' Energy Gap of CeNiSn in High Magnetic Fields 29
2.2.9 Magnetic Resonant X-ray Scattering of Samarium Thin-Films 30
2.2.10 Structural Modifications in Cerium Thin-Films at Low-Temperatures 31
2.2.11 SANS Studies of the Incommensurate Magnetic Structures of Metal B20 Alloys 32
2.2.12 Polarized SANS Studies of Magnetic Structures in MnSi 33
2.2.13 Refinement of the Crystal Structure of a Single Crystal of $HoFe_4Al_8$ 34
2.2.14 Magnetic Neutron Scattering Studies of $DyFe_4Al_8$ at Very Low Temperature and Applied Magnetic Field 35
2.2.15 An X-ray Magnetic Scattering Study of $DyFe_4Al_8$ 36
2.2.16 Magnetic Fluctuations in Nanoparticles 37

2.3 Superconducting Materials and Phenomena 38

2.3.1 Microscopic Coexistence of Magnetism and Superconductivity in $ErNi_2B_2C$ 38
2.3.2 Observation of a Field-Driven Structural Phase Transition in the Flux Line

Lattice in $ErNi_2B_2C$ 39
2.3.3 Development of Decoration Chamber for Flux-Line Lattice Studies 40
2.3.4 Dynamics of Oxygen Ordering in $YBa_2Cu_3O_{6+x}$ Studied by Neutron and High- Energy Synchrotron X-ray Diffraction 41
2.3.5 Annealing of BiSCCO Wires Studied In-situ by High-Energy Synchrotron X-ray Diffraction 42
2.3.6 New Superstructures in $YBa_2Cu_3O_{6+x}$ Observed by High Energy X-Ray Diffraction 43
2.3.7 Monte Carlo Simulation Study of the Ortho-II, Ortho-III and Ortho-V Oxygen Ordering Superstructures in $YBa_2Cu_3O_{6+x}$ 44
2.3.8 Verification of Stripe Charge Correlations in $La_{1.775}Sr_{0.225}NiO_4$ by Hard X-Ray Diffraction 45
2.3.9 Softening of Lattice Vibrations and Superconductivity: Disappearance of the Mössbauer Spectrum of Non-Superconducting $PrBaCuFeO_{5+\delta}$ at Low Temperature 46
2.3.10 Evidence for Enhancement of T_c by Ortho-II Ordering in $YBa_2Cu_3O_{6.5}$ 47
2.3.11 Local Lattice Distortions in $YBa_2Cu_3O_{6.95}$: Evidence of a Small Polaron Formation 48
2.3.12 Magnetic Structures in $NdBa_2Cu_3O_{6+x}$ 49
2.3.13 Photoinduced Metastable State and Oxygen Ordering in $YBa_2Cu_3O_{6+x}$ 50

2.4 Structures and Defects 51

2.4.1 Soft Mode Behaviour and Lattice Melting in Na_2CO_3 51
2.4.2 Powder Neutron Diffraction Studies of the $K_2S_2O_7$-$KHSO_4$ System 52
2.4.3 Structure of the Cone Conformer of a Tetrakis(methylthio)-tetrapropoxy-calix[4]arene 53
2.4.4 The 154 K Phase Transition of Tetramethylammonium Tetrafluoroborate, NSLS 1996 54
2.4.5 Structural Studies of the Tetrathiafulvenyl Salt of Trichloroacetic Acid by Neutron Diffraction 55
2.4.6 Nuclear Density in MADMA and Borax for Charge Density Studies 56
2.4.8 Coarsening of Bimodal Coherent γ‘ Particle Size Distributions in Ni-Al-Mo Alloys 57
2.4.9 Coarsening of β‘ Coherent Particles in Fe-Ni-Al-Mo Alloys 58

2.5 Surfaces and Interfaces 59

2.5.1 Self Assembled Monolayers of Tetrakis(methylthio)-Tetrapropoxy-Calix[4]arene on Crystalline Gold(111) Surfaces 59
2.5.2 Structure and Orientation of Sn Precipitates in Epitaxial Layers of $Si_{1-x}Sn_x$ 60
2.5.3 Bismuth-induced restructuring of the GaSb(110) surface 61
2.5.4 Surface X-Ray Diffraction at the n-GaAs(001)/Electrolyte Interface 62
2.5.5 Surface X-ray Diffraction Study of the $\sqrt{3}x\sqrt{3}$ R 30^0 Structure of Sb on Cu(111) 63
2.5.6 Surface X-Ray Diffraction Studies of the Rb induced Ge(111)3x1 Structure 64
2.5.7 Surface X-Ray Diffraction Study of Ge(103) (1x1)-In 65
2.5.8 Surface X-Ray Diffraction Study of Ge(103)-(1x4) 66

2.5.9 Nanoclusters of the CWD Compound $Rb_{0.3}MoO_3$, Blue Bronze, Grown on $SrTiO_3$, Studied by Synchrotron x-ray Diffraction 67

2.5.10 Cu Films on Ni(100), Internal Faceting and Embedded Clusters Studied by Synchrotron x-ray Diffraction 68
2.5.11 Surface X-Ray Diffraction Study of Si(001)-(3x4)-In 69
2.5.12 X-ray Surface Structure Studies on Organic Crystals of Benzamide 70

2.6 Langmuir Films 71

2.6.1 X-ray Diffraction from Curved Thin Films 71
2.6.2 Studies of Phase Transitions in Langmuir Monolayers of a Triple Chain PE 72
2.6.3 Influence of Head Group Methylation on the Phase Behaviour of Lipid Monolayers 73
2.6.4 Binary Phase Diagram of Monolayers of Simple 1,2-Diol Derivatives 74
2.6.5 Influence of Polyelectrolyte Coupling on the Structure of Charged Monolayers 75
2.6.6 Superlattices of Crystalline Copper Complexes of α-Amino Acid Amphiphiles at the Air-Aqueous Solution Interface 76
2.6.7 Supramolecular Architecture Prepared *in-situ* at the Air-Aqueous Solution Interface; Thin Films of a 3x3 Grid Silver Complex 77
2.6.8 Oriented Crystalline Multilayers of Metal Dicarboxylic Acid Salts Self-Assembled at the Air-Aqueous Solution Interface 78
2.6.9 Chiral Separation of Diastereomeric Monolayers at the Air/water Interface 79
2.6.10 Interdigitated Chiral Architectures at the Air/liquid Interface: Role of Diastereomeric Interactions 80
2.6.11 X-Ray Synchrotron Studies of Polymer-Modified Lipid Monolayers on Water 81
2.6.12 Cyclic Peptides Forming Nanotubes at the Air-Water Interface 82
2.6.13 Crystallography of Monomolecular Protein Surface Layers Using X-ray GIXD 83
2.6.14 Temperature and Time Dependent Investigations of Cd-and Uranyl- Stearate Multilayers by means of Neutron Reflectivity Measurements 84

2.7 Microemulsions, Surfactants and Biological Systems 85

2.7.1 Isotropic Lifshitz Behavior in Block Copolymer-Homopolymer Blends 85
2.7.2 Pressure Dependence of the Phase Behavior of PEP-PDMS Diblock Copolymer 86
2.7.3 Diblock Copolymer Blends with Small Amounts of Homopolymer 87
2.7.4 Micro-phase Separation in Polymer Electrolyte Models PPO-$LiClO_4$ and PPO-$Mg(ClO_4)_2$ 88
2.7.5 Structure of PS-PEO Diblock Copolymers in Solution and the Bulk State Probed using Mechanical, Dynamic Light Scattering and Small-angle Neutron Scattering 89
2.7.6 Cubic Phase in a Connected Micellar Network of Poly(Propylene Oxide) 90
2.7.7 Scattering Studies of Aerogels During Gel-formation and Ageing 91
2.7.8 The Effect of Short Chain Alcohols on SDS Micelles 92
2.7.9 Reverse (Water-in-oil) Micelles of Amphiphilic Block Copolymers: A Small-angle X-ray and Neutron Scattering Investigation 93
2.7.10 Surface Induced Ordering of Triblock Copolymer Micelles at the Solid-Liquid Interface 94
2.7.11 Neutron Reflection from Biosensors 95
2.7.12 Order, Disorder and Composition Fluctuation Effects in Low Molar Mass Hydrocarbon-Poly(dimethylsiloxane) Diblock Copolymers 96

2.7.13 Composition Fluctuations at the Order-to-Disorder Transition in a Sheared Asymmetric Diblock Copolymer Melt 97
2.7.14 Phase Behaviour in Poly(ethyleneoxide)-*block*-poly(ethylethylene) Diblock Copolymers 98
2.7.15 Heat-induced Aggregation of β-Lactoglobulin Studied by Small-Angle Neutron Scattering 99
2.7.16 A Small-angle Scattering Study of the Polydispersity of Microemulsion Droplets 100
2.7.17 Structural Model of the 70S E. Coli Ribosome and Its RNA from Solution Scattering 101
2.7.18 Static Structure Factor of Worm-like Micelles 102
2.7.19 Aggregation Processes in AOT Water-in-Oil Microemulsions 103
2.7.20 Microemulsions as Model Systems for Hard and Soft Spheres 104
2.7.21 Phase Behaviour of Hydrocarbon-poly(dimethylsiloxane) Diblock Copolymer Melts Related to Temperature and Their Volume Fraction of Hydrocarbon 105
2.7.22 A Small-Angle Neutron Scattering (SANS) Study of Aggregates Formed From an Aqueous Mixture of Sodium Dodecyl Sulphate (SDS) and Dodecyl Trimethyl-ammonium Bromide (DTAB). 106
2.7.23 The Influence of Shape Fluctuations on the Size Distributions of Spherical Bilayer Vesicles and Droplet Microemulsions 107
2.7.24 An X-ray Photon Correlation Spectroscopy Experiment on a Diblock Copolymer System 108
2.7.25 The Effect of Cholesterol, Short Chain Lipids and Bola Lipids in Small Amounts on Lipid-bilayer Softness in the Region of the Main Phase Transition 109

2.8 Polymers 110

2.8.1 Holographic Data Storage Using Peptide Oligomers (DNO) 110
2.8.2 New Azobenzene Side-Chain Polyesters for Optical Information Storage 111
2.8.3 Side-Chain Liquid Crystalline Polyesters for Optical Information Storage 112
2.8.4 New Polyester Materials with Exceptionally Short Optical Storage Recording Times 113
2.8.5 Laser Induced Segmental Orientation in Cyanoazobenzene Side-Chain Polyesters 114
2.8.6 Studies on a Dilithium Initiator 115
2.8.7 Dilute Solution Properties of Segmentwise Deuterated Star-Shaped Polystyrenes 116
2.8.8 Synthesis of Hydrocarbon-Poly(dimethylsiloxane) Diblock Copolymers 117
2.8.9 Microstructure of Electropolymerized Polypyrrole Films 118

2.9 Organic Chemistry 119

2.9.1 Synthesis, Structure and Properties of 4,8,12-Trioxa-12c-phospha-4,8,12,12c-tetrahydrodibenzo[cd,mn]pyrene a Molecular Pyroelectric 119
2.9.2 Synthesis of Labile Molecules for Scanning Probe Microscopy-Induced Chemical Reactions 120
2.9.3 Synthesis of Some Novel 12c-Derivatives of 1,5,9-Trioxa-3,7,11-tris(tert-butyl)- tricornane 121
2.9.4 Synthesis of Two Container Molecules With Potential Liquid Crystalline Properties 122

2.9.5 Selective Halogen-Lithium Exchange Reaction of Bromine Substituted 25,26,27,28-Tetrapropoxycalix[4]arenes 123
2.9.6 Biaryl Cross-Coupling Reactions on 25,26,27,28-Tetrapropoxycalix[4]arenes 124
2.9.7 Van der Waals Interactions between Pyrene Substituted Calix[4]arene and Naphthalene 125
2.9.8 NMR Investigation of Solvent Dependant Conformational Change in Calix[4]arene Based Systems 126
2.10 Instrumentation 127
2.10.1 Flux Measurements on RITA 127
2.10.2 The Facility for Deformation of Germanium Wafers to be used as Monochromators 128
2.10.3 Polarised Neutrons at the Neutron Reflectometer, TAS8 129
2.11 Training and Mobility of Researchers - Access to Large Installations 130

3 Publications, Educational and Organisational Activities, Colloqia 132

3.1 Publications in International Refereed Periodicals 132
3.2 Other Publications 142
3.3 Conferences 144
3.4 Lectures 154
3.5 Meetings and Courses Organised by the Department 157
3.5.1 Symposium on Magnetism in Metals 157
3.5.2 Danish Polymer Centre Lecture Series 158
3.5.3 Polymer Research 159
3.5.4 Danish Polymer Centre Meeting 160
3.5.5 Polymer Surfaces and Interfaces 161
3.5.6 Third European Summer School on "Scattering Methods Applied to Soft Condensed Matter" 162
3.6 Membership of Committees and Boards 163
3.7 Colloquia held at the Department 165

4. Staff and Guest Scientists 167

4.1 Scientific Staff 168
4.2 Short Time Visitors 1996 170
4.3 Short Time Visitors under the CEC-TMR programme 1996 171

1 Introduction and Acknowledgements

In 1996 research of the Department of Solid State Physics was an integral part of Risø's long term programme "Materials with special physical and chemical properties". Starting January 1, 1997 the department has been asked to change its name to "Condensed Matter Physics and Chemistry Department", and the research will be performed in the programme area "New functional materials".

The research aims at creating an understanding of the relation between the atomic and molecular structure of materials and their electrical, optical, chemical or biological properties. the activities in 1996 were organised in three programmes: Macromolecular Materials Chemistry, Magnetism and Superconductivity, Surface and Interfaces. In addition the Department of Solid State Physics was in charge of a special programme under the Commission of the European Community (CEC) Training and Mobility of Researchers programme (TMR).

In 1996 Head of Research Programme Kurt Nørgaard Clausen was appointed Adjunct Professor of Physics at the University of Copenhagen.

Macromolecular Materials Chemistry

The purpose of this programme is the improvement of polymers and other macromolecular materials through integration of structural knowledge, synthesis and molecular design.

The Danish Polymer Centre
The Centre has now existed for more than two years as a collaboration between Risø, The Technical University of Denmark and 8 industrial partners. It is showing significant progress in a number of areas. Part of the work described in the projects below have been performed within the framework of the Centre. Industrial collaboration projects in a variety of areas ranging from medical adhesives to high performance injection moulded components are progressing and thus adding to the industrial impact of the Centre.

Some scientific highlights are

- **Materials for Optical Storage**

Materials based on azobenzene containing photorefractive macromolecules are expected to have potential as future materials for optical information storage. Recently, Risø has contributed to this development with a new class of peptide based materials, which holds particular promise for erasable holographical storage devices. The new, so-called DNO materials are designed to form a stacking pattern of the photoactive chromophores resembling the helical geometry as seen in DNA. The results show that it is possible to write diffraction patterns in thin DNO films with a higher efficiency than in any other photorefractive material. The holograms also exhibit exceptionally good thermal stability up to 180 ^{o}C.
Within a more traditional class of photoanisotropic materials based on side-chain liquid crystalline polyesters significant progress has been achieved. New insight into the basic mechanism of the storage process has been obtained using polarised infrared light to study the reorientation of both the chromophores and the polymer chain. Studies of new materials with

systematic variations in the molecular architecture led to new materials with significantly shorter writing time (50 ms).

- **Unusual Pressure Dependence of the Phase Behaviour of Block Copolymers**

Block copolymers play an increasing role in technical applications - thermoplastic elastomers being one example. At room temperature, these materials tend to have ordered structures, which are responsible for their elastic properties. At high temperature the materials become disordered and processable by i.e. injection moulding. Theoretical predictions have indicated that transition from order to disorder is influenced by pressure. This was experimentally proven by application of pressure to a block copolymer melt while studying the structure by small angle neutron scattering.

- **Complex Phase Behaviour in Solvent Free Macromolecular Surfactants**

Unsolvated block copolymers share important similarities with low-molecular weight amphiphilic molecules with respect to ordered microstructures. Amphiphilic molecules such as surfactants, phospholipids, and ionic soaps self-assemble in aqueous solutions into highly organised structures because of the hydrophobic effect. As the concentration of the amphiphile increases, thermodynamically stable supramolecular aggregates form with a variety of ordered state symmetries. Block copolymer melts are a separate class of soft materials that spontaneously form ordered phases below a critical temperature. In the attempt to make the link between such block copolymer melts and solvated surfactants, Risø has, in collaboration with the University of Minnesota, synthesised and studied a new class of medium size block copolymers of poly(ethylene oxide) and poly(ethyl ethylene), PEO-PEE. The PEO-PEE polymer systems exhibit a variety of ordered phases. Transition from one ordered state to another is found to occur only when the lattice spacing is closely matched, highlighting the importance of the epitaxy and molecular conformation of soft materials.

- **Molecular Sensors Based on Calixarenes**

Molecular sensors are gaining growing importance for medical, industrial, and environmental analysis and monitoring. Calixarenes are bowl shaped molecules which can be used as a template for creating complex sensor materials exhibiting molecular recognition. New methods have been developed for selective insertion of functional groups that will bind to specific target molecules. Similarly, new synthetic methods allow the attachment of molecular fragments that will change in fluorescent properties when the binding site is occupied.
Furthermore, fundamental studies on structural rearrangements of this group of materials, due to changes in the chemical environment of the molecule, have been performed.

- **Magic Numbers of Proteins**

A goal in the chemistry and physics of macromolecules is to attempt to make large molecules (hetero-polymers) using the tricks nature has developed during evolution.
The self-organisation of the chemical processes that nature masters, is based on an interplay between the enthalpy (basic forces) and the entropy (the complexity of matter). One of the most intriguing problems in this context is protein folding: How can a large molecule consisting of thousands of atoms spontaneously and consistently fold up to a dense unit which has precise functional abilities - and this in a matter of seconds? A simple physical theory and model based on symmetry principles explaining this has been proposed. Surprisingly a sequence of magic numbers for the abundance of certain protein sizes, as well as their predominant size, were found - and confirmed with statistics on available data bases.

- **The Structure of Wormlike Micelles: Neutron Scattering and Computer Simulations**

Microemulsions are homogeneous mixtures of oil and water with amphiphilic (soap-like) molecules situated at the interface between them. Understanding the phase behaviour and microscopic structure of microemulsions is very important due to their biological and medical relevance and the numerous technological applications of microemulsions in particular in the food and pharmaceutical industry. From a fundamental point of view microemulsions in which the soap molecules form long and flexible aggregates are fascinating model systems for so-called equilibrium polymers. Their main difference in comparison with long polymer molecules is the finite life time, i.e. the fact that these aggregates are constantly breaking up and recombining whereas 'classical' polymers are firmly bonded. The structure of such microemulsions has been studied by small-angle neutron scattering and computer simulations. The combination of the two approaches has provided us with detailed information with regard to the local structure, the flexibility and the average length of the aggregates. The work is a collaboration with the Polymer Institute, ETH-Zürich, Switzerland.

Surfaces and Interfaces

The purpose of this programme is to investigate the relationship between atomic/molecular structure and properties of surfaces, boundary layers and thin films**.**

Some scientific highlights are

- **Restructuring of III-V Semiconductor Surfaces**

Metal-semiconductor interfaces are of considerable interest for both fundamental and technological reasons. Most vapour-deposited metals react with III-V semiconductors to form complex, nonstoichiometric interfaces, however, it is generally believed that the semimetals Sb and Bi form non reactive, ordered interfaces. Column-V metals on III-V semiconductors are frequently regarded as examples of ideal adsorbate-semiconductor hetero junctions. However, we have shown that this simple picture is generally not true and that column V elements can induce significant restructuring of the substrate by studying the case of a monolayer of Bi deposited on the GaSb(110) surface.

- **Contacts Problems Between Crystals**

Computer simulation of interfaces between mismatched crystals is an important tool for understanding the complex phenomena observed. It is of relevance for example in the new field of tribologi, in corrosion protection, in lubrication and many other technological applications. We have investigated a model system of one alkali halide on another for which the interface is nontrivial, while the interatomic forces are well known. Our simulations provide a new interpretation of the interfacial structures which can be verified by X-ray scattering. The method has the advantage that quite large systems can be simulated and consequently the statistical properties be assessed.

- **Magnetic Superlattices**

Using advanced deposition techniques such as Molecular Beam Epitaxy (MBE) it is now possible to design magnetic materials at the atomic level. These materials are of importance for future generations of magnetic storage media. In collaboration with Oxford University the magnetic properties of superlattices fabricated from the rare earth metals have been studied using a mixture of neutron and X-ray scattering. In their bulk state the rare earths display a rich variety of magnetic structures, which have been shown to be modified in the superlattice in

unexpected ways. In superlattices formed from magnetic holmium and non-magnetic scandium the helical magnetic order of the holmium is essentially confined to lie within the holmium layers. This contrasts with the case of superlattices formed from holmium and other non-magnetic elements.

- **Internal Faceting in Cu Thin Films**

The smallest existing crystals contain only from ten to hundreds of atoms and due to their smallness the finite size and the external shape become important for all their properties. Such nanoclusters are studied both for the interest in their optical and electrical properties and because they play an important role in epitaxial growth of thin films. Risø has measured the detailed atomic construction of such nanoclusters and the strain field using synchrotron x-ray diffraction, which determines their size and shape. A particular example is a new type of nano-clusters in Cu-films grown on Ni substrates. Here the clusters are imbedded inside the Cu film, and they are believed to constitute a new, quite general and important phenomena in epitaxial film growth.

Magnetic and Superconducting Materials

The purpose of this programme is to investigate the relationship between atomic/molecular structure and properties of magnetic and superconducting materials.

Some scientific highlights are

- **Interaction Between Magnetism, Superconductivity and Magnetic Field**

In general magnetic and superconducting states of a material are mutually exclusive. However, in a class of materials with the formula $R\mathrm{Ni_2B_2C}$, where R is a rare earth element, antiferromagnetism and type-II superconductivity coexist. By exposing these materials to a magnetic field, and thereby generating a lattice of quantized magnetic flux lines, it is possible to study the interplay between magnetic ordering and superconductivity. In corporation with Bell Laboratories, Risø has investigated the flux-line lattice in $\mathrm{ErNi_2B_2N}$ using small-angle neutron scattering. The principal result of the initial study show evidence of microscopic interaction between magnetism and superconductivity. Moreover, the flux-line lattice has square symmetry as opposed to the hexagonal lattice usually observed.

- **New Superstructures in $\mathbf{YBa_2Cu_3O_{6+x}}$**

The charge transfer leading to high-T_c superconductivity in $\mathrm{YBa_2Cu_3O_{6+x}}$ is strongly dependent on the oxygen stoichiometry and structural ordering. New superstructures related to the formation of copper-oxygen chains in specific layers of the structure have been observed in carefully prepared single crystals, by neutron and high energy X-ray diffraction. The superstructures are characterised by alternating copper-oxygen chains that are oxygen rich and oxygen poor. Experimental studies of the superconducting properties have shown strong influence of these factors on the superconducting transition temperature. From neutron diffraction studies evidence for local lattice distortions related to the charge transfer have been established.

Neutron Programme

The special programme under the CEC training and mobility of researchers (TMR) obtained in late 1995 a new contract covering the period 1996 until the end of 1998.

- **RITA: The Next Generation of Neutron Triple-Axis Spectrometer**

RITA (Reinvented Triple Axis Spectrometer) incorporates many innovative features that greatly improves the efficiency with which dynamical processes can be studied in the solid state. The first experiments on this new instrument have been performed and demonstrate that the overall gain in efficiency can exceed an order of magnitude. Investigations that will particularly benefit from the design features of RITA are the study of novel metals (so-called heavy fermion materials), low-dimensional magnetic systems and the quest to understand the origin of high-temperature superconductivity.

Acknowledgements

The Department of Solid State Physics receives its basal budget through Risø National Laboratory from The Ministry of Research. Additional financial support, which is gratefully acknowledged, has been received from The Ministry of Energy, The Natural Science Council, The Technical Science Council, The Danish Materials Technology Development Programme (MUP II), The European Community (DG XII and DG XIII), NATO, The Academy of Technical Sciences (ATV) and The Research Academy, Novo Nordisk A/S, Danfoss A/S, Haldor Topsøe A/S and the Carlsberg Foundation.

2 Research Projects in the Department

The work is divided into the following subject categories:

2.1 Theory

2.2 Magnetic and Metallic Structures

2.3 Superconducting Materials Phenomena

2.4 Structures and Defects

2.5 Surfaces and Interfaces

2.6 Langmuir Films

2.7 Microemulsions, Surfactants and Biological Systems

2.8 Polymers

2.9 Organic Chemistry

2.10 Instrumentation

2.11 Training and Mobility of Researchers - Access to Large Installations

2.1 Theory

2.1.1 Modelling Interface Properties on the Atomistic Level: Polymers Adsorbed to a Surface

P. Sommer-Larsen, *Department of Solid State Physics, Risø National Laboratory, Denmark*

The properties of interfaces between different materials are often determined by layers so thin that the atomistic structure of the materials plays a crucial role. Adhesion of a polymer to a surface is one property, where the interaction energy between the surface and an organic material are important. Such surface energies can be calculated using molecular mechanics and dynamics methods combined with quantum chemical methods. If surface energies for interfaces with inorganic materials like quartz is studied, it is extremely important to be able to calculate accurate surface charges on the inorganic material.

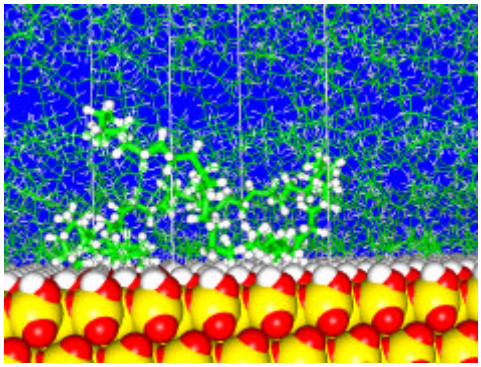

Fig 1. Snapshot from a molecular dynamics simulation of polyethylene on a quartz (110) surface. One molecule among many is highlighted. Parts of the chain is adsorbed flat on the surface. Other parts form loops or dangling ends into the polymer bulk.

The interaction between polymers and surfaces can be studied with molecular dynamics methods (see Fig. 1). It is however often useful to apply coarse grained models for the same kind of problems. An example is given below.

Mixing inorganic powder into a polymer results in a material with desirable properties for a number of applications. In order to improve the mechanical properties - especially the toughness - of the mixture, the inorganic filler particles should be strongly attached to the polymer chains. We have studied a model for grafting a long polymer chain to a surface. The polymer is a copolymer with a very low degree of a surface active segment. This is modelled by a sequence $A_nBA_nB\ldots A_nBA_n$ where n>>1. We have used Theodorou's implementation of Scheutjens and Fleers lattice model[1] for a block-copolymer. As input the model an interaction parameter describing the strength of the attractive interaction between the B-segment and the surface: $c = -U_{BS}/kT > 0$. U_{BS} is the interaction energy between surface and B-segment.

Fig. 2 shows the volume fraction of B-segments adsorbed to the surface. It can been seen that even at bonding strengths corresponding to a true covalent bond, the surace is far from covered with the surface active B-segments.

Fig. 2.
The volume fraction of B-segments in the first layer, corresponding to the number of attached chains. Points indicates results calculated with the model. Full lines corresponds to a simplified model, where $\varphi_B(1)$ scales approximately as $\sqrt{c}$.
The strength of the interaction parameter is indicated on the x-axis.

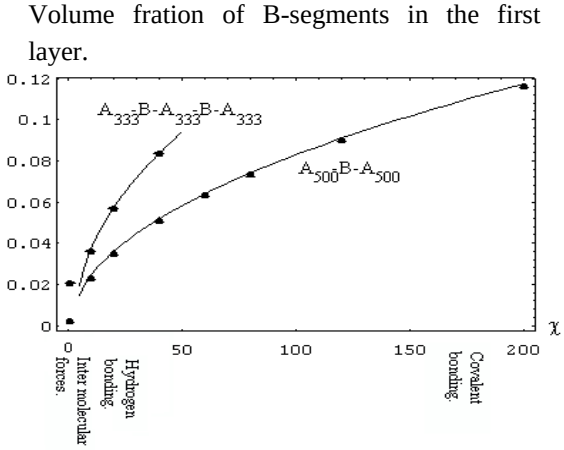

[1] D. N. Theodorou, Macromolecules, **21**, 1411 (1988)

2.1.2 Modelling Interface Properties on the Atomistic Level: Molecules Adsorbed to a Surface

P. Sommer-Larsen and I. Johannsen, *Department of Solid State Physics, Risø National Laboratory, Denmark*

Single molecules may today be visualised on a surface by scanning probe microscopy. This allow for manipulation of surface layers on a molecular scale. Modelling is a complementary tool to experimental investigations. It is helpful both in visualising molecules on surfaces and in predicting their geometry. Modelling results often form the basis for the interpretation of experimental findings.

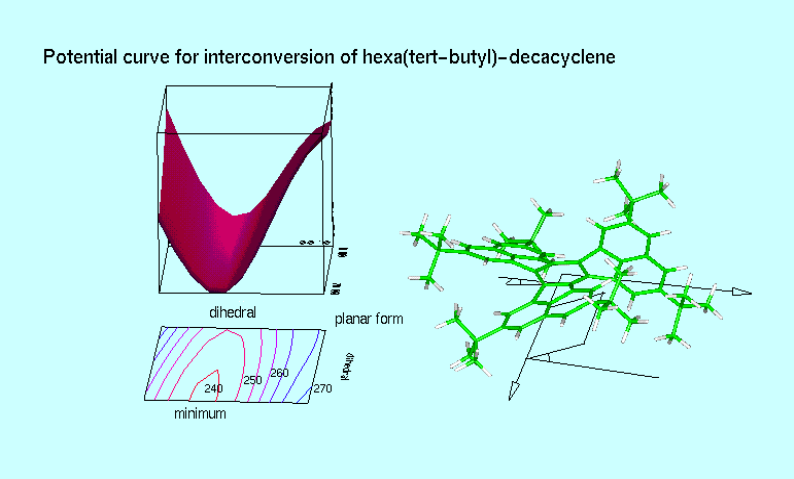

Fig. 1. Potential curve for inter conversion between the two enantiomeric forms of the molecule. The potential energy is calculated using molecular mechanics as a function of two dihedral angles depicted in the right figure. The transition state corresponds to a planar geometry some 25 kcal·mol^{-1} higher in energy than the ground states. The planar form corresponds to the upper right corner of the countour map.

In the following example a large molecule with threefold symmetry is studied. Molecular mechanics calculations predict that the molecule hexa(tert-butyl)-decacyclene is optically active and show a propeller like geometry in agreement with X-ray crystallographic data for the parent decacyclene compound. No rapid interconversion between the two enantiomeric forms is however expected for the isolated molecule. The potential barrier for interconversion is calculated to be more than 100 kJ·mol^{-1} - quite a high value (see Fig. 1).

Interaction with a surface may non the less drastically change the geometry of the molecule. Fig. 2 predict the geometry to be planar, when the centre of the molecule adsorbs over a hole in the Cu (111) surface and to be propeller like when it adsorbs directly on top of a Cu atom.

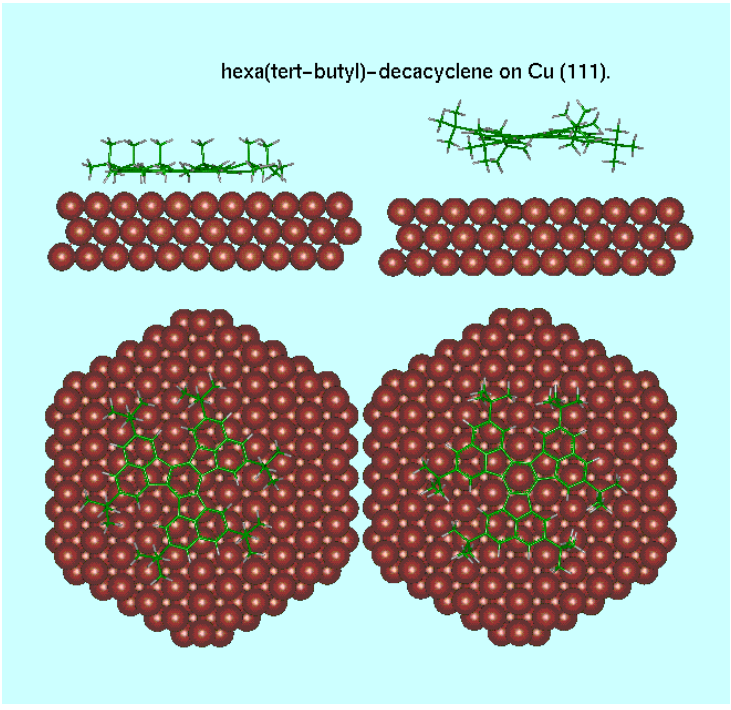

Fig. 2. Molecular mechanics simulation of the molecule on a Cu (111) surface. The centre of the molecule may either adsorb over a hole in the Cu (111) surface or directly on top of a Cu atom. For each situation, the figure shows a side wards and a vertical view of the structure. In the first situation, the attraction to the surface force the molecule to become planar, whereas it retains its propeller like geometry in the other situation.

2.1.3 Effects of Boundary Conditions on Magnetization Switching in Kinetic Ising Models of Nanoscale Ferromagnets

H.L. Richards[a,b], M. Kolesik[a], P.-A. Lindgård[a], P.A. Rikvold[b], M.A. Novotny[b]. [a]*Department of Solid State Physics, Risø National Laboratory, Denmark.* [b]*Center for Materials Research and Technology, Department of Physics and Supercomputer Computations Research Institute, Florida State University, USA*

The next generation of high-density magnetic recording media should have much higher storage densities without sacrificing large coercivity. The experimentally observed nonmonotonic dependence of the coercivity on particle diameter implies that the optimum size of ferromagnetic grains for use in recording media is small enough to be single-domain but large enough to be nonsuperparamagnetic. We have extended earlier studies which used Ising systems to model the nonequilibrium statistical mechanics of magnetization reversal. Specifically, we investigate the dependence of the switching field, which is usually measured in static or slowly increasing fields, on the boundary conditions. We show that the boundary conditions strongly influence switching phenomena for weak applied fields and small systems, and that this influence is observable in the switching field. Some preliminary results of the present study have been published in ref.1.[1]

Kinetic nearest-neighbor Ising models form a class of high anisotropic model systems that have become popular subjects for Monte Carlo simulations of metastable decay. The reasons for this are easy to understand. A great variety of exact results have been obained for the equilibrium two-dimensional Ising model in zero field. As a nontrivial model for which a number of exact results are known, it has become a favorite of researchers in statistical mechanics, and it has been a standard in investigations of universality, finite-size scaling, and various approximation schemes, such as series expansions. *Kinetic* Ising models with a variety of stochastic spinflip dynamics have proven useful as simple but nontrivial models for the study and testing of ideas in nonequilibrium statistical mechanics, such as dynamic universality and critical exponents, and metastability. Below we show, as an example, the obtained switching field for octagonal systems.

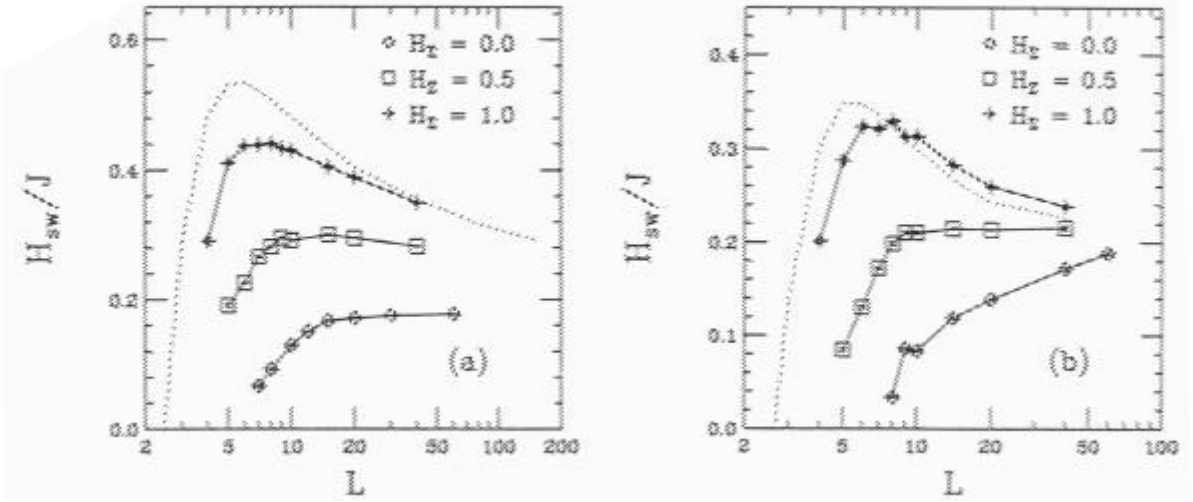

The switching field as a function of system size for octagonal system with various values of H_z. Data for periodic systems (dotted lines) were taken from Ref. 4. (a) $T = 1.3J \approx 0.57T_c$ and τ = 1000 MCSS. (b) $T = 0.8T_c \approx 1.81J$ and τ = MCSS.

[1] M. Kolesik, H.L. Richards, M.A. Novotny, P.A. Rikvold and P.-A. Lindgård, J. Appl. Phys., submitted

2.1.4 Towards a Systematic Classification of Protein Folds and Magic Number of Abundance

P.-A. Lindgård, *Department of Solid State Physics, Risø National Laboratory, Denmark.* H. Bohr, *Center for Biological Sequence Analysis, Department of Physical Chemistry, The Technical University of Denmark, Denmark*

In almost half a century large databases of protein sequences and of protein structures have been building up. And, like the case of for example atomic elements or isotope tables, it is natural to ask for some classification that can group the proteins into related families other than those that arise from homology analysis of the sequence of amino acids in the polypeptide chain. What we here have in mind is a kind of atomistic taxonomy, where the proteins are grouped according to the number of typical elements.

A lattice model Hamiltonian has been invented for protein structures that can explain the division into structural fold classes during the compactification stage of the folding process. Proteins are described by chains of secondary elements, with the hinges in between being the important degrees of freedom. The protein structures are given a unique name, which simultaneously represent a 1-dimensional string of physical coupling constants describing hinge spin interactions. We have defined a metric and a precise distance measure between the fold classes. An automated procedure is constructed in which any 3-dimensional protein structure in the usual *PDB* coordinate format can be transformed into the proposed chain representation. Taking into account hydrophobic forces we have found a mechanism for formation of domains containing predicted magic numbers of secondary structures and multiple of these domains. We have performed a statistical analysis of available protein structures and found agreement with the predicted preferred abundances of proteins with a predicted magic number of secondary structures. Thermodynamic arguments are given for the increased abundance and a phase diagram has been calculated yielding the folding scenario, which is shown on Fig.1. We estimate the upper limit of the total number of possible fold classes to be around 4000, and confirm this through an explicit calculation of the possible chain configurations that are tightly packed on a small 3D regular lattice. A brief accont has been published.[1]

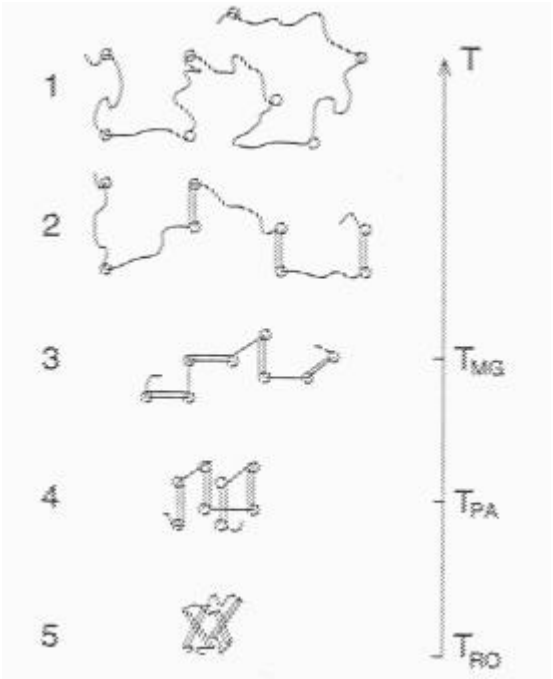

Fig.1. A schetch of the five stage folding scenario from
1) the unfolded state at high temperatures to
2) a partly secondary structure forming stage,
3) the *Molten Globule* (MG) stage,
4) the *Parent Stage* (PA), and finally
5) the *Native,* twisted stage at about room temperature T_{RO}.
The double lines indicate formerd secondary structures and single straight lines interconnections formed by loops.
The ° indicates the considered eight 'hinge' residue positions.

[1] P.-A. Lindgård and H. Bohr, Phys. Rev. Lett., **77**, 779 (1996)

2.1.5 Spin-slip Structure and Central Peak Phenomena in Singlet-Doublet System, Praseodymium

P.-A. Lindgård, *Department of Solid State Physics, Risø National Laboratory, Denmark*

The magnetic response from singlet ground state magnets has attracted considerable attention for many years. The more intriguing ones are the spin 1/2 quantum antiferromagnetic systems with frustration, among which we find e.g. the high T_c super conducting materials and nuclear magnetism in Ag. In a somewhat simpler class of singlet ground state systems, the singlet character is not of co-operative nature, but is caused by the effect of the crystal field. In such systems Cooper showed that the transition to magnetic order is accompanied by a softening of the excitations to the excited states. The question is whether this is a pure soft mode transition or if it is over taken by a 'central peak' representing the dynamics of locally induced cluster of magnetic ordering. This response is that found in the isotropic Heisenberg magnet, and is associated with the divergence of the longitudinal Curie-Weiss susceptibility $\_^{zz}(\mathbf{q})$, at the ordering vector **q**. For the singlet-singlet system $LiTb_xY_{1-x}F_4$ existence of a 'central peak' at the transition to magnetic order was demonstrated experimentally.[1] It was explained in terms of fluctuating regions of induced magnetic order in analogy to the anharmonic theories for structural phase transitions. A similar, although more complex phenomenon for the singlet-doublet case has been found only in Pr, and the origin is still under debate. A double peaked intensity is developing at $\mathbf{Q}_1 \approx 0.125\boldsymbol{\tau}_{100}$, the latter being close to the wave vector at which magnetic ordering occurs.The two puzzling features:1) that there is more than one quasi-elastic peak, and 2) that there is an intensity increase below T = 4.2 K where there is no further softening of the exitations, have been taken as a sign of, that we might not have a full description of the rare earths in terms of the localized 4 - *f* moments subject to the crystalline electric field of the lattice and weakly interacting via the conduction electrons. We have shown that the observed quasi-elastic behavior can be understood on the basis of the correlation theory[2] for the singlet-doublet system, and the localized model for the rare earths, when the well known complications of the Praseodymium system are taken into account. The proposed (short range ordered) structure is a distorted spiral with spin-slips.

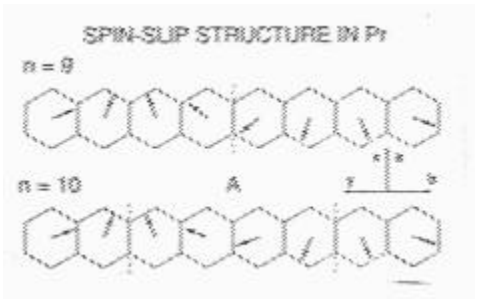

Fig.1. Spin-slip structure for *y*-order (longitudinal) with period $n = 8$, and phase-locked *x*-order (transverse) with period of $n = 9$ and $n = 10$. The dashed lines indicate possible slip positions. Notice that the spins in the distorted spiral tilt towards the easy direction (corner of hexagon). In Pr every second spin is furthermore flipped.

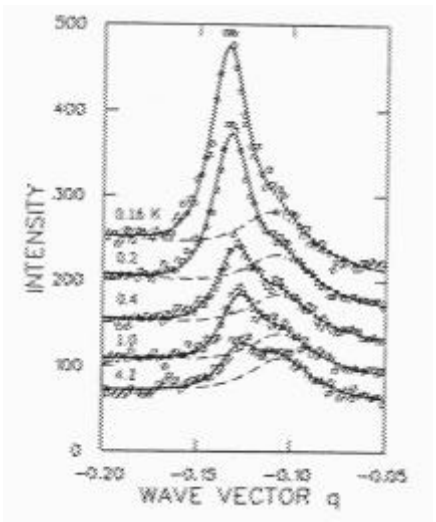

Fig.2. The ° shows data for the 'central peaks' in Pr for various temperatures.[3] The *x*- and *y*- polarized modes are equally visible in this scan with q=[q,0,3]. The full line represents a fit with two amplitude parameters (and a skew background).

1 R.W. Youngblood, G. Aeppli, and J.D. Axe, Phys. Rev. Lett. **49**, 1724 (1982)
2 P.-A. Lindgård, Phys. Rev. Lett. **50**, 690 (1983)
3 H.B. Bjerrum Møller, J.Z. Jensen, M. Wullf, A.R. Macintosh, O.D. McMasters and K.A. Gschneider, Jr. Phys. Rev. Lett. **49**, 482 (1982)

2.1.6 Computer Simulation of Heteroepitaxial Film Structures

J. Baker and P.-A. Lindgård, *Department of Solid State Physics, Risø National Laboratory, Denmark*

Computer simulation is an important tool for understanding the complex phenomena often observed at interfaces between mismatched crystals. We have investigated the case of NaCl on KBr,[1] where the lattice mismatch is very large (≈17%), and the shape of the interface is non-trivial. Helium Atom Scattering (HAS) data from the surface of films of 2 to 6 monolayers indicate the presence of superstructure,[2] but do not reveal the real-space morphology of the surfaces. The film structures were simulated by extending the continuous Monte Carlo method of Vives and Lindgård[3] to allow for several monolayers of adsorbed atoms, multiple atom types, and the behavior of atoms in the dimension perpendicular to the substrate. In addition, a novel dipole summation technique was developed to calculate the ionic energies. The simulations provided real-space visualisations of the films, an example of which is given in the left figure below. Shown is the equilibrium structure of the 3 monolayer case after all of the film layers and two of the substrate layers have been allowed to relax. The superstructure is a two-dimensional pattern of height modulations, the profile of which is clearly visible in the figure. In addition, the simulation reveals that the substrate relaxes much more than the film and that the substrate and film modulations are in phase. For each of the coverages simulated, the amplitude of the surface rumple found by fitting profiles such as the one on the left to cosine curves is in excellent agreement with amplitudes calculated from HAS peak intensities; this is pictured in the right hand frame below. This work is being extended to the similar system KCl/NaCl(001), which relieves misfit strain by rumpling at low coverages and by forming networks of dislocations at thicker coverages. These mechanisms are likely general features of heteroepitaxial growth, and this work will hopefully be extended to other more technologically relevant systems as well.

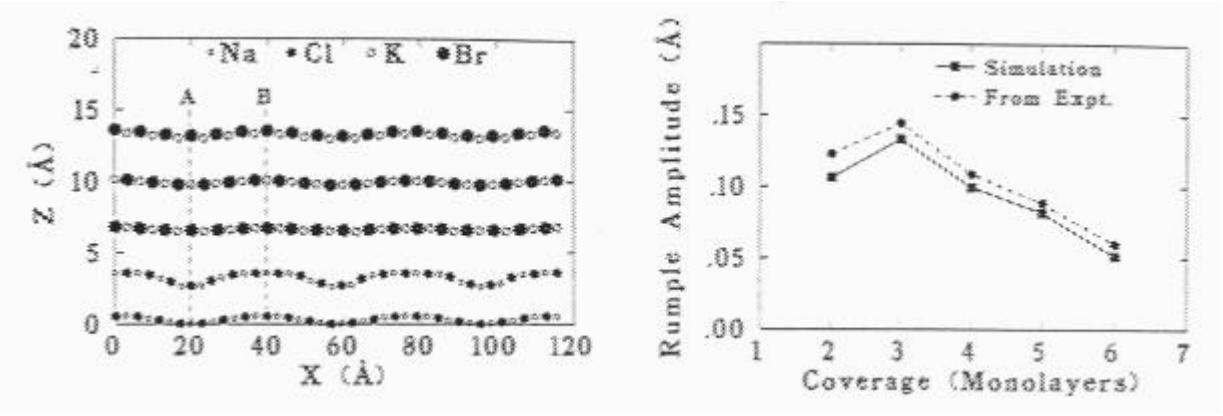

Fig. 1. On the left is a cross section of the simulated 3 ML film of KBr on a 2 ML NaCl substrate, showing the superstructure rumpling caused by the misfit. The lines A and B mark a maximum and minimum of the corrugation, respectively. It can be seen that the film and substrate modulations are in phase, and that the substrate is much more affected by the misfit than is the film.
On the right is a comparison of the simulated rumple amplitude with that calculated from HAS diffraction peak intensities. Both the maximum at 3 ML and the overall behavior *vs.* thickness are well reproduced by the simulation.

---

1 J. Baker and P.-A. Lindgård, Phys. Rev. Rapid Comm. **B54**, Oct. 15 1996
2 J. Duan *et al.*, Surf. Sci. **272**, 220 (1992)
3 E. Vives and P.-A. Lindgård, Phys. Rev. **B46**, 4788 (1992)

2.1.7 Monte Carlo Simulation Studies of Semidilute Solutions of Semiflexible Polymer Chains

J.S. Pedersen, *Department of Solid State Physics, Riso National Laboratory, Denmark*, M. Laso, P. Schurtenberger, *Institut für Polymere, ETH Zürich, Switzerland*

We have performed Monte Carlo simulation studies on the Kratky-Porod model for semiflexible chains used in our previous studies of single chain properties.[1,2] The model has a fixed valence angle and free rotation about the bonds. Hard spheres are placed along the chains to simulate the excluded volume of the polymer. The chains have 6-8 spheres per statistical segment length b and the systems typically contains 10000 spheres of radius $R/b=0.1$. The strength of the excluded volume interactions corresponds to that found for polystyrene in a good solvent as well as for wormlike micelles[1]. Simulations have been performed for contour length of L/b=3, 10.9, 30 and 90 using a box with periodic boundary conditions. For each of the contour lengths, the concentration was varied from very dilute concentration well below the overlap concentration c^* up to a volume fraction of 0.1-0.2. In the dilute region we used pivot moves[1] in which the longest part of the chains are pivoted. This is very efficient at low concentrations but becomes quite inefficient at higher concentrations. Therefore a reptation ('cut-and-paste') type of move was used at higher concentration. The total number of Monte Carlo steps in a simulation was 10^6-10^7. The scattering function $S(q)$ was calculated as described in[3] and sampled together with the radius of gyration, the end-to-end distance, the end-to-middle distance and the distance between two inner points. Figure 1 shows the scattering function for $L/b=10.9$. The expected reduction of the intensity and descrease of the correlation length is observed. The functions were fitted in the region of small scattering vectors by the Debye function for a single Gaussian chain and the forward scattering $S(0)$ and the correlation length ξ were obtained. We determined the product of A_2Mc, where A_2 is second virial coefficient, M is the molar mass and c the polymer concentration for the different chain length from the intial concentration dependence of $S(0)$. This then allowed us to calculate a reduced concentration $X = (16/9)A_2c$ for all volume fractions simulated. We found that both $S(0)$ and ξ display a universal behavior in their dependence upon X which closely follow the experimentally observed behavior for polymers in good solvvents or polymerlike micelles with characteristic deviations from the renormalization group predictions at high values of .

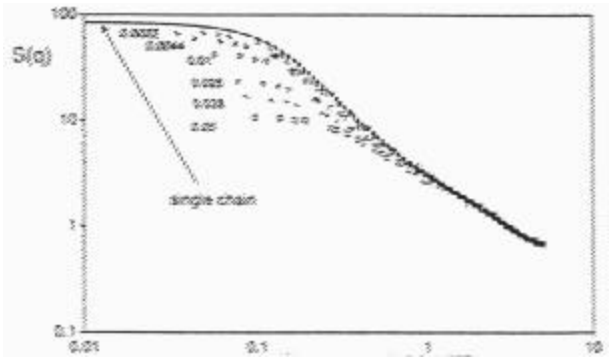

Fig.1. Scattered function $S(q)$, as a function of scattering vector q for $L/b=10.9$. The single chain scattering function is also shown.

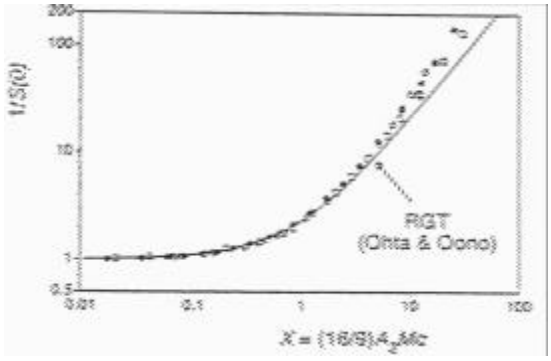

Fig.2. Volume fraction dependence of the inverse forward scattering $S(0)^{-1}$ for three chain lengths. The full curve is from renormalization group calculations.[4]

1 J.S. Pedersen, M. Laso, P. Schurtenberger, Phys. Rev. E **54**, 5917 (1996)
2 J.S. Pedersen, P. Schurtenberger, Macromolecules **29**, 7602 (1996)
3 D. Frenkel, R.J. Vos, C.G. de Kruif, A. Vrij, J. Chem. Phys. **84**, 4625 (1986)
4 T. Ohta, Y. Oono, Phys. Lett. **89A**, 460, (1982)

2.2 Magnetic and Metallic Structures

2.2.1 Neutron Scattering Response in (U,Ce)Ru_2Si_2

S. Mataš[†*], M. Mihalik[†], [†]*Institute of Experimental Physics SAS, Slovak Republic,* A. Schröder[*], J.-G. Lussier[*], [*]*Department of Solid State Physics, Risø National Laboratory, Denmark* and A. A. Menovsky, *Van der Waals-Zeeman Lab., University of Amsterdam, Netherlands*

The ternary heavy-fermion compounds URu_2Si_2 and $CeRu_2Si_2$ attract much attention because of their unusual low-temperature properties. In our previous papers we studied magnetic and transport properties of the pseudoternary system (Ce,U)Ru_2Si_2 for small concentration of Ce in URu_2Si_2.[1,2] Our measurements, taken on single crystals on the U rich side, showed that Ce substitution strongly affects anomalies in resistivity, susceptibility and heat capacity data which are related to the magnetic phase transition in URu_2Si_2.[2] The single crystal $U_{0.975}Ce_{0.025}Ru_2Si_2$ has been studied by neutron scattering using the triple axis spectrometer *TAS7* at the Risø National

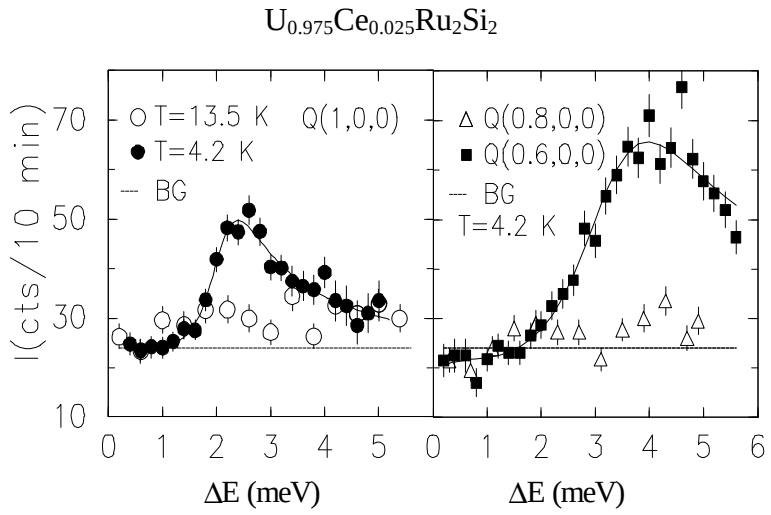

Fig. 1. Constant Q-scans at Q=(1,0,0), Q=(0.8,0,0) and Q=(0.6,0,0) at low temperatures. Lines are guides to the eye.

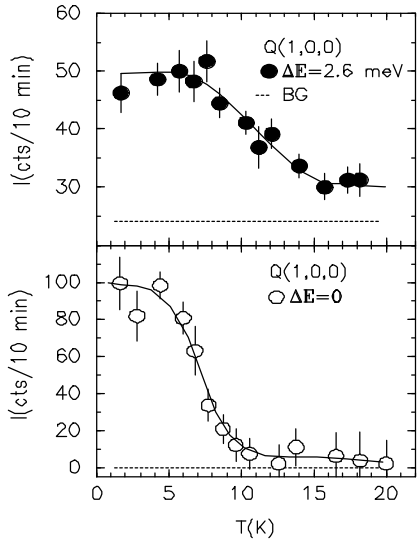

Fig.2. Temperature dependence at Q=(1,0,0). Lines are guides to the eye

Laboratory. Sharp dispersive excitations like in URu_2Si_2[3] were observed at low temperatures (see Fig.1). Similar to URu_2Si_2, two spin gap minima occur at wavevectors Q_1=(1,0,0) and Q_2=(0.6,0,0), however the difference of two gap values Δ_1=2.4 meV and Δ_2=4 meV has decreased. With increasing temperature the gap at Q=(1,0,0) in the magnetic excitation spectrum softens and vanishes at around 15 K (see Fig.2).

From elastic neutron diffraction, an antiferromagnetic ordering of the alloyed sample $U_{0.975}Ce_{0.025}Ru_2Si_2$ could be detected at temperatures below T_N =10 K (see Fig.2). A very small magnetic moment of (0.006±0.003) μ_B/U atom was estimated from comparison of the integrated magnetic intensity at (1,0,0) to the intensity of the nuclear peak (1,0,1). The magnetic moment is polarised along the c-axis. The main characteristic features - a characteristic spin gap and an antiferromagnetic order - still remain in this alloyed compound $U_{0.975}Ce_{0.025}Ru_2Si_2$, however the size of the magnetic moment and the transition temperature to an ordered state is reduced with Ce substitution for U in URu_2Si_2.

---

1 M. Mihalik *et al*., Physica B, **186-188** 507-510 (1993)
2 M. Mihalik *et al*., IEEE Trans. on Mag., **30** 1142-1145 (1994)
3 C. L. Broholm, Ph.D. Thesis Risø-**M-2731** (1989)

2.2.2 Magnetic Properties of Holmium-Erbium Alloys[1]

H.M. Rønnow, *Department of Solid State Physics, Risø National Laboratory, Denmark*

The magnetic properties of holmium[2] and to some extent erbium[3] have been studied thoroughly and are well described by a standard MF model[4]. This provides an ideal starting point for examining the effect of alloying. Single crystals of Ho-Er random alloys have been investigated by neutron diffraction measurements on the TAS1 spectrometer.

Apart from the slightly different strength of the exchange coupling, the crystal field has opposite sign for the two elements. As a result the alloys show both scaling behaviour of properties like the anti-ferromagnetic transition temperature T_N and the cone angle (as well as new behaviour like an increased cone phase stability and new spin-slip structures. Most of these properties have been described by a Virtual-Crystal MF model which has been developed on basis of the interaction parameters found for the elements. This essentially parameter free model fits the measured scattering along the [0,0,l] and the [1,0,l] directions satisfactory.

Below 25 K the $Ho_{90}Er_{10}$ alloy exhibits a structure with 7/36 periodicity but broadened higher harmonics. Upon closer examination the spin slip structure performs alternating 4/6 and 3/6 rotations between each spin slip. If these blocks are mixed at random rather than perfectly alternating, the resulting scattering cross section is in good agreement with the experiment.

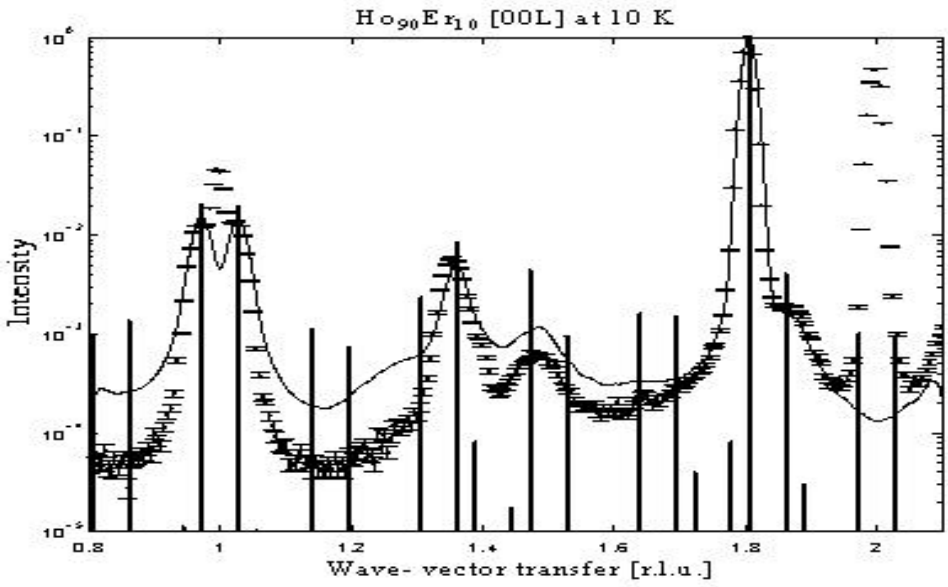

Fig. 1. Scattering along [0 0 L] in $Ho_{90}Er_{10}$ at 10 K. Vertical lines are scattering cross-section from a pure 7/36 structure, solid line from a mixed (4+3)/36 structure.

The origin of this short range disorder is a combination of different circumstances as the periodicity 7/36 corresponding to two alternating blocks. The influence of the opposite crystal fields is being investigated further through more calculations.

---

1 Ms.C. Thesis, University of Copenhagen (1996) ISBN 87-550-2221-9
2 J. Jensen, Phys. Rev. B, **54,** 16098 (1996)
3 R. Cowley and J. Jensen, J. Phys. C, **4**, 9673
4 J. Jensen and A. R. Mackintosh, *Rare Earth Magnetism,* Clarendon Press, Oxford (1991)

2.2.3 Observation of Coherent Magnetic Structures in Tb/Ho Superlattices

C. Bryn-Jacobsen, R.A. Cowley, J.P. Goff, R.C.C. Ward, M.R. Wells, *Oxford Physics, Clarendon Laboratory, UK*, D.F. McMorrow, *Department of Solid State Physics, Risø National Laboratory, Denmark*

Despite the large number of recent studies of superlattices grown by MBE, there have been relatively few reports of magnetic/magnetic rare-earth combinations. We have now completed an investigation of the Tb/Ho system. Three samples were studied, with nominal compositions Tb_{10}/Ho_{30}, Tb_{20}/Ho_{20}, and Tb_{30}/Ho_{10}, where the subscripts refer to the number of planes per bilayer. High resolution x-ray diffraction measurements undertaken at the Clarendon Laboratory revealed that the samples are of high crystalline quality. Neutron diffraction measurements were performed at Risø using TASI. Scans with the wave-vector transfer along the [00*L*] and [10*L*] directions of reciprocal space were made at temperatures in the region T=10-240 K. To elucidate the magnetic structures formed at each temperature examined, the nuclear neutron scattering was first subtracted from the total neutron scattering data using profiles constructed from the modelling of x-ray and neutron structural data. The resulting profiles were then fitted to detailed models for the magnetic scattering, yielding good fits to the data as shown in Fig. 1 for Tb_{20}/Ho_{20} at T=10 K.

For all samples between T≈10-130K, it is found that the Ho moments order in a spiral, and the Tb moments align ferromagnetically. For both the Ho and Tb, moments are confined to the basal plane, and the magnetic structures formed are coherent over several bilayers. The turn angle per plane in the Ho blocks changes with temperature such that the total turn angle between adjacent Tb blocks is $n\pi/3$. For T≈130-225K, only the Tb moments remain ordered, and continue to adopt a ferromagnetic structure that is coherent over intermediate Ho blocks. However, for Tb_{30}/Ho_{10} above T≈205K, a fraction of the Tb moments order in a basal-plane spiral so that the Tb exhibits a mixed helical/ferromagnetic phase.

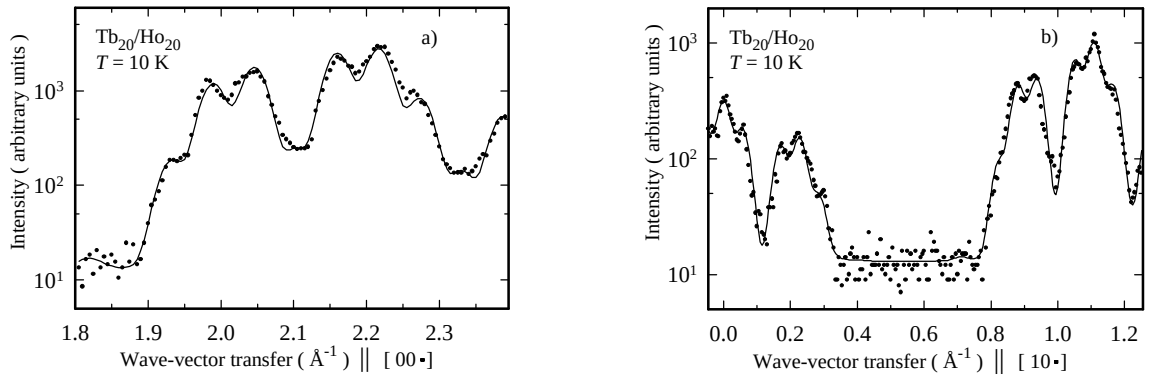

Fig. 1. The magnetic scattering from Tb_{20}/Ho_{20} at T=10 K with wave-vector transfer along the directions a) [00*L*], and b) [10*L*]. The solid line is a fit to the data using a model where the Ho moments are ordered in a spiral structure, and the Tb moments are aligned ferromagnetically, with both the Ho and Tb moments confined to the basal plane.

2.2.4 Resonant X-ray Magnetic Scattering at the K-edge from NiO

J.P. Hill, *Department of Physics, Brookhaven National Laboratory, USA*, C.-C. Kao, *National Synchrotron Light Source, Brookhaven National Laboratory, USA*, D.F. McMorrow, *Department of Solid State Physics, Risø National Laboratory, Denmark*

Resonant x-ray magnetic scattering exploits enhancements in the cross-section occurring when the incident photon energy is tuned through an atomic absorption edge. Large enhancements were first observed at the L edges in Ho and explained in terms of electric multipole transitions. In addition to the L edges much larger enhancements are expected, and observed, at the M edges of the actinides for which the dipole excitation is to the highly polarized 5f levels. Conversely, resonant scattering at a K-edge is expected to be considerably weaker because the strong (dipole) transitions involve *s* and *p* levels for which there is no spin-orbit correlation of either the core level or the intermediate state. Nevertheless, K-edge studies would be of some interest because of the window they would provide on transition metal compounds.

We report the observation of K-edge resonant magnetic scattering in the antiferromagnet NiO, for which an approximately two-fold increase in the scattering is observed at an energy corresponding to a *quadrupolar* feature in the absorption spectrum (Fig.1). Quadrupole excitations couple to *d*-like states at a K-edge and for transition metals these are the magnetic states. Thus, the high degree of polarization of the localized $3d^8$ states compensates for the small size of the quadrupolar matrix elements and an observable enhancement results. From the ratio of the non-resonant to resonant magnetic scattering, we estimate that the first order quadrupolar resonant scattering amplitude is $0.016r_0$, which is of the same order of magnitude as similar terms in the rare earths. These studies provide for the possibility of element specific magnetic diffraction in such notable transition metal oxides as the high T_c cuprates and colossal magnetoresistance manganites.

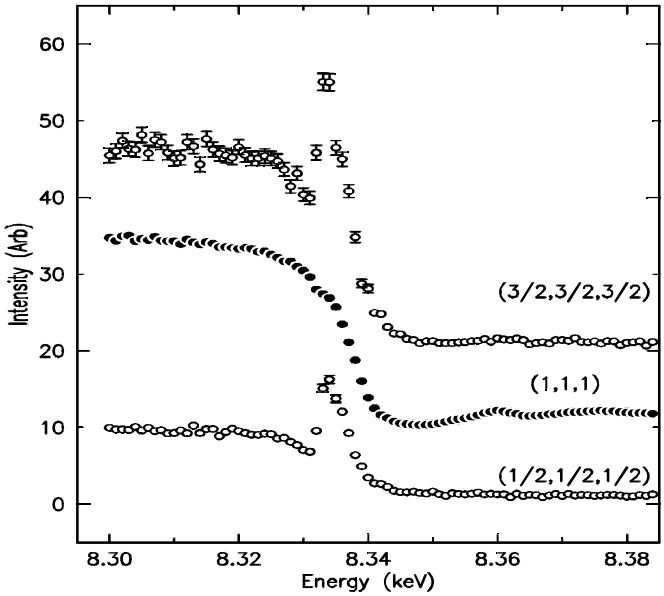

Fig. 1. The energy dependences of the (1,1,1) charge peak, and the (1/2, 1/2, 1/2) and (3/2 3/2 3/2) magnetic peaks from NiO at room temperature.

2.2.5 Magnetic Structure of Cs_2CuCl_4 in Applied Fields

R. Coldea, D.A. Tennant, R.A. Cowley, *Oxford Physics, Clarendon Laboratory, UK*, D.F. McMorrow, *Department of Solid State Physics, Risø National Laboratory, Denmark*

Magnetic susceptibility measurements[1] have shown that Cs_2CuCl_4 behaves like a nearly 1D S=1/2 Heisenberg antiferromagnet with an exchange interaction J=0.34 ±0.02 meV between spins in the one-dimensional chains, and a small exchange coupling between chains. The crystal structure is orthorhombic and magnetic chains are parallel to the *b*-axis. Neutron scattering experiments[2] performed on a single crystal sample using TAS7 have shown that 3D magnetic ordering occurs below T_N = 0.62 K, and is incommensurate along the chain direction with a wave vector **q**=(0,0.472,0)[rlu]. In the *(a,b)* scattering plane magnetic peaks were observed at (h,k±q,0) for either h even and k odd, or h odd and k any integer. Analysis shows that the low-temperature spin ordering is cycloidal with spins rotating in a plane that contains the propagation direction *b* and makes a small angle with the *(b,c)* plane. The occurrence of the incommensurate structure is the consequence of frustration on the spins induced by the interchain exchange coupling and a mean field calculation of the ground state energy gives the value for the interchain coupling J'/J=0.17.

The effect of an applied field on the magnetic structure was studied for the field parallel to the *c*-axis, i.e. almost in the plane of rotation of the spins. The intensity of magnetic reflections decreases monotonically on increasing field and magnetic peaks could not be detected above a critical field B_C=1.66 T at T=0.32 K. The position and width of elastic peaks are constant for $B \leq B_C$. The transition to the high-field phase shows a significant hysteresis effect, as shown in Fig. 1. Magnetic reflections corresponding to ordering of spin components along *y* and *z*-axis disappear at the same value of the field, and no magnetic peaks could be detected along any symmetry directions for higher fields, suggesting that the transition is to a phase with no long-range magnetic order. The critical field is independent of temperature for $0.3<T<0.45$ K and decreases rapidly and monotonically with temperature for $0.45\ \text{K}<T<T_N$. The latter part of the transition line is probably from the incommensurate 3D ordered phase to the paramagnetic phase. Further inelastic neutron scattering experiments at ILL in the low-temperature high-field phase have shown that 1D quantum effects are important.

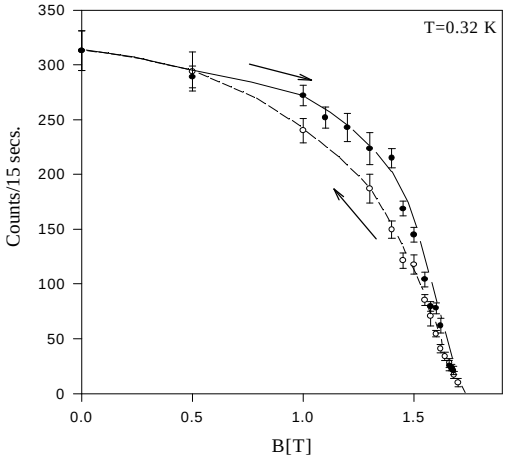

Fig. 1 Peak amplitude of the (0,1.47,0) magnetic reflection as a function of applied field. The lines are guides to the eye.

[1] R.L. Carlin, *et al* (1985). J. Appl. Phys. **57** 3351

[2] R. Coldea, D.A. Tennant, R.A. Cowley, D.F. McMorrow, B. Dorner and Z. Tylczynski, (1996). J. Phys.: Condens. Matter **8**, 7473

2.2.6 The Structural and Magnetic Properties of Ho-Sc Alloys and Superlattices

C. Bryn-Jacobsen, R.A. Cowley, J.P. Goff, R.C.C. Ward, M.R. Wells, *Oxford Physics, Clarendon Laboratory, UK,* D.F. McMorrow, *Department of Solid State Physics, Risø National Laboratory, Denmark*

We have extended our previous studies of Ho-based alloys and superlattices grown by MBE to the Ho-Sc system. The samples were grown at the Clarendon Laboratory and consist of six alloys Ho_x:Sc_{1-x} (with nominal Ho concentrations x=0.25, 0.40, 0.50, 0.75, 0.85, and 1.00); and three superlattices Ho_{30}/Sc_{10}, Ho_{20}/Sc_{20}, and Ho_{20}/Sc_{40} (where the subscripts refer to the nominal number of planes per bilayer). Both x-ray and neutron diffraction techniques were employed to study the structural properties of the samples. It was revealed that the alloys have different *a* lattice parameters for the Sc seed layer and the Ho:Sc alloy grown on top of the seed layer; whilst the superlattices have different *a* lattice parameters for the Sc seed, and for *both* the Ho and Sc in the superlattice. Neutron diffraction techniques were used to determine the characteristics of the magnetic structures formed in the temperature region T=2-140K. For the alloys, it is found that the Ho 4*f* moments form a basal-plane helix at all temperatures, and Fig. 1 illustrates the change with temperature of the helical wave vector, $\boldsymbol{q}$. As for Ho:Y and Ho:Lu alloys, a good description of the dependence of Néel temperature upon concentration is given by a virtual crystal model where the peak in the conduction electron susceptibility varies linearly between that of the pure constituents. In the superlattices, the Ho moments also form a basal-plane helix upon first ordering, with the temperature variation of the helical wave vector per plane in the Ho layers, $\boldsymbol{q}_{Ho}$ (or equivalently the turn angle per Ho plane, θ_{Ho}), shown in Fig. 2. However in contrast to Ho/Y or Ho/Lu superlattices, there is no long-range coherence of helically arranged Ho moments over the non-magnetic interlayers. Instead it is found that in the helical phase, Ho_{10}/Sc_{30} and Ho_{20}/Sc_{20} exhibit a short-range coherence of an overall antiferromagnetic coupling between adjacent Ho blocks; whilst for Ho_{20}/Sc_{40} ordering is confined to individual Ho blocks. For Ho_{20}/Sc_{20}, there is low temperature transition from the helical to a ferromagnetic phase, in which moments are ferromagnetically aligned within Ho blocks and coupled antiferromagnetically between adjacent Ho blocks.

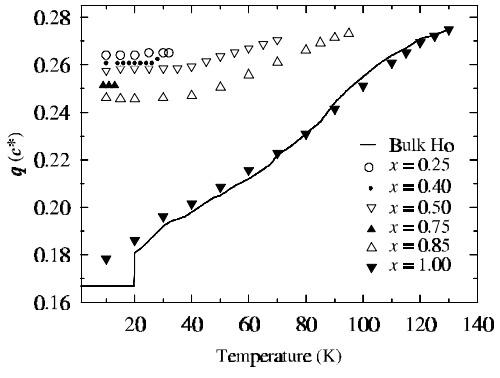

Fig. 1. The temperature dependence of the helical wave vector, $\boldsymbol{q}$, for the Ho:Sc alloys compared to bulk Ho.

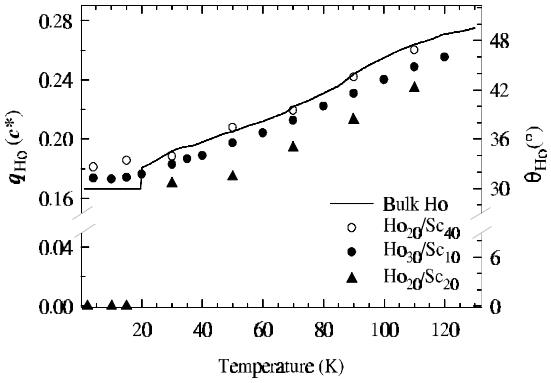

Fig. 2. The temperature dependence of the helical wave vector per plane in the Ho layers, $\boldsymbol{q}_{Ho}$ (or θ_{Ho}), for the Ho/Sc superlattices compared to bulk Ho. $\boldsymbol{q}_{Ho}$ reduces to zero for Ho_{20}/Sc_{20} when the moments adopt a purely ferromagnetic arrangement.

2.2.7 Magnetic Fluctuations near a Quantum Phase Transition in the Heavy Fermion Alloy $CeCu_{6-x}Au_x$ at $x_c = 0.1$

A. Schröder, *Department of Solid State Physics, Risø National Laboratory, Denmark,*
G. Aeppli, *NEC, Princeton, USA,* E. Bucher, *Universität Konstanz, Germany, and Bell Lab. Innovations, Murray Hill, USA*

To study the non-Fermi-liquid behavior near a quantum phase transition ($T_N \rightarrow 0$), the heavy fermion system $CeCu_{6-x}Au_x$ was investigated by cold neutron scattering at the extrapolated critical concentration of the onset of magnetic order $n_c = 0.1$, where strong deviations from the Fermi-liquid behavior were observed in the low temperature bulk properties,[1] e.g. $C/T \sim \ln T$ instead of $C/T \approx$ const. for $x = 0$. The measurements of a single crystal of $CeCu_{5.9}Au_{0.1}$ were performed in the Bell Lab. dilution refrigerator at TAS7 with $E_f = 3.7$ meV using a BeO-filter. The magnetic correlations found here are reminiscent of these observed in $CeCu_6$.[2] Like in $x = 0$, the dynamic correlations (with short anisotropic correlation lengths) are centered around $Q_1 = (1,0,0)$ (see Fig. 2) and at $Q_2 = (0,0.85,0)$, although for $x = 0.1$, the intensity at Q_1 exceeds already the intensity at Q_2 (see Fig. 3) as a preparation for the static magnetic order with only one wave vector near Q_1 at higher x. For $x = 0.2$ $Q = (0.79,0,0)$ below $T_N \approx 0.25$ K.[3] What has changed is the energy scale. The energy width Γ (Lorentzian HWHM) of the quasielastic fluctuations near Q_1 at $Q = (0.8,0,0)$ (see Fig. 1) is much smaller for x_c ($\Gamma \approx k_B T$ for $T > 1$ K) and does not saturate below 1.5 K as is does for $x = 0$.[2] At the lowest temperature, $T = 0.07$ K, the energy width even goes below the resolution of HWHM = 0.07 meV and therefore seems to be the critical quantity driving to a phase transition at lower temperatures or higher x. What is very different from the Fermi-liquid regime and typical for this scaleless critical behavior, is the lack of the saturation of Γ, no Kondo scale can be defined (for $T > 0.07$ K). Our first data do not give a precise temperature scaling for the magnetic susceptibility χ, but show, that $\chi''(\omega=0,Q)$ which has to be considered at a special wave vector like $Q = (0.8,0,0)$ rises faster towards low temperatures than χ_{bulk}.[1] The competition of the interactions leading to the complicated scenario of more than one correlation vector is certainly responsible for the very low ordering temperature T_N in $CeCu_{5.9}Au_{0.1}$ and has to be considered beside the onsite Kondo compensation to understand the 'nonmagnetic-magnetic' transition in this compound.

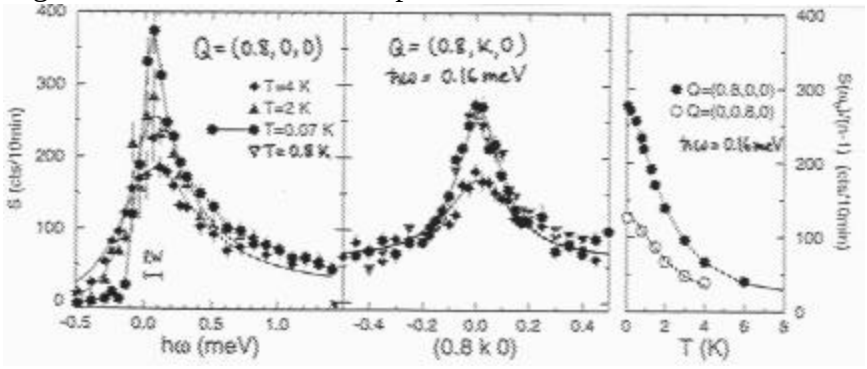

Fig. 1: Neutron intensity of $CeCu_{5.9}Au_{0.1}$ of constant-Q scans at $Q = (0.8,0,0)$ at different temperatures T.

Fig. 2 presents the constant-E scans at $\hbar\omega = 0.16$ meV along (0.8,k,0).

Fig. 3: Temperature dependence of the (unconvoluted) neutron intensity divided by $n(\omega)+1$ as an estimate for χ'' at $\hbar\omega = 0.16$ meV at wave vectors close to Q_1 and Q_2 like $Q = (0.8,0,0)$ and $Q = (0,0.8,0)$.

---

1 H. v. Löhneysen et al, Phys. Rev. Lett. **72**, 3262 (1994)

2 G. Aeppli et al, Phys. Rev. Lett.57, 122 (1986); J. Rossat-Mignod et al, J. Magn.Magn Mater. **76-77**, 376 (1988)

3 O. Stockert et al, SCES'96, to be published in Physica B, or see RISØ-R-863(EN), p. 31 (1996)

2.2.8 Development of the 'Small' Energy Gap of CeNiSn in High Magnetic Fields

A. Schröder, *Department of Solid State Physics, Risø National Laboratory, Denmark,* G. Aeppli, *NEC, Princeton, USA,* T.E. Mason, *University of Toronto, Canada,* E. Bucher, *Universität Konstanz, Germany, and Bell Lab. Innovations, USA*

Cold neutron scattering measurements were performed on single crystals of CeNiSn in the 9T-magnet at TAS7 with E_f = 3.5 meV, to investigate, how the smaller magnetic energy gap with $\hbar\omega_2^{max}$ = 2.5 meV[1] at wave vectors like Q_2 = (0,1,0) behave in a high magnetic field H, driving this 'Kondo insulator' towards a metallic phase.[2] Here also the width of this sharp excitation is getting broader with field as well as with temperature like the higher excitation with $\hbar\omega_1^{max}$ = 4.1 meV at wave vectors like Q_1=(0,0.5,1)[3] (see Fig. a),b)). In contrast to Q_1, where $\omega_1^{max}(H)$ = const., ω_2^{max} is shifted towards higher energies, which cannot be explained by a simple Zeeman splitting. This leads to a reduction of the low energy excitations below ω_2^{max} in high magnetic field. The strong oscillation at ω_2^{max} present in 0 T are suppressed in 8.9 T (see Fig. c),d)). The field behavior of the lower energy gap at Q_2 cannot account for the restoring of the very low energy excitations observed in the specific heat.[2] The magnetic correlations at Q_1 and $\hbar\omega_1^{max}$ = 4.1 meV dominate the spectrum in high field without leading to a magnetic instability, leaving the $1/\omega$ weighted integrated intensity, the static susceptibility $\chi(\omega=0,Q_1)$, unchanged.[3] When doping induces magnetic order in $CeNi_{1-x}Cu_xSn$, the wave vector Q_1 of the high gap, not Q_2 of the small gap, describes the static magnetic order.[3]

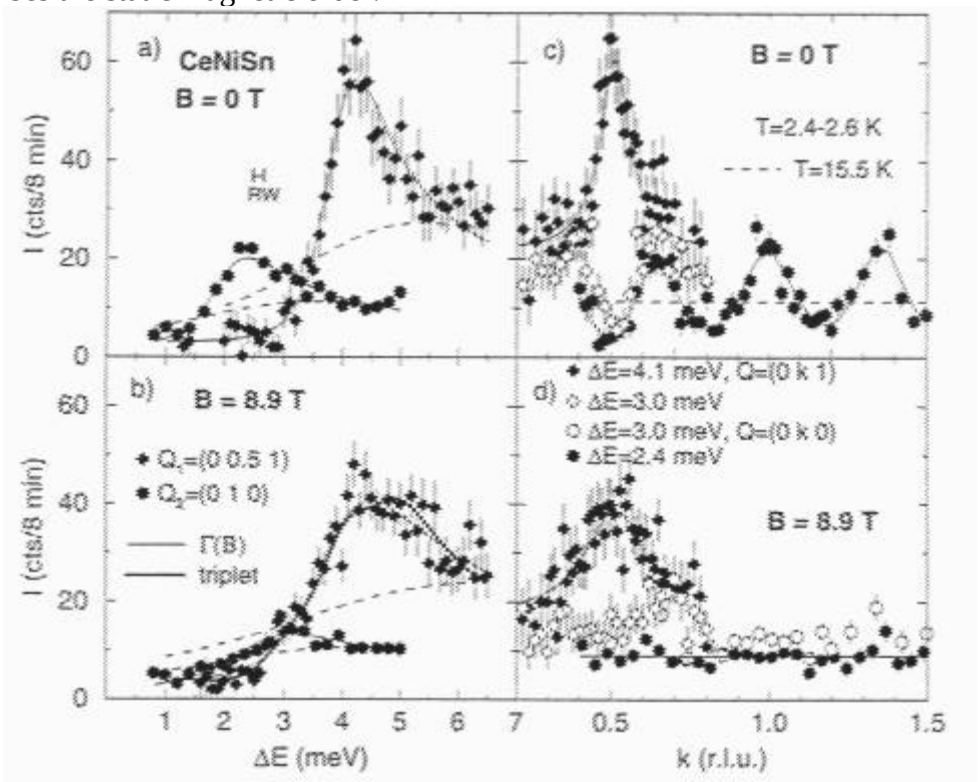

Fig.: Neutron intensity of CeNiSn in magnetic fields of H=0 T (top) and H=8.9 T (bottom) at low temperatures T. a) and b) show constant-Q scans at Q_1 = (0,0.5,1) and Q_2 = (0,1,0), b) and c) show constant-E scans mainly at $\hbar\omega_1^{max}$ = 4.1 meV and $\hbar\omega_2^{max} \approx$ 2.4 meV along (0,k,1) and (0,k,0).

[1] T.E. Mason et al, Phys. Rev. Lett. 69, 490 (1992)
[2] T. Takabatake et al, Phys. Rev. B 45, 5740 (1992)
[3] A. Schröder et al, ECNS'96, to be published in Physica B, see also RISØ-R-863(EN), p.30 and p. 29 (1996)

2.2.9 Magnetic Resonant X-ray Scattering of Samarium Thin-Films

J.-G. Lussier, A. Madsen, R. Feidenhans'l, D.F. McMorrow, *Department of Solid State Physics, Risø National Laboratory, Denmark,* J.P. Hill and D. Gibbs, *Department of Physics, Brookhaven National Laboratory, USA*

The magnetism of Sm cannot be well studied by neutron scattering. In its natural form, Sm has several isotopes which contribute to the large absorption cross-section and give a large incoherent background. Historically, the magnetic structure of Sm was discovered on single isotope samples.[1] Another, more modern approach, which is not sensitive to isotopic differences, is to use an atomic absorption edge to enhance the magnetic X-ray cross-section (magnetic resonant X-ray scattering). We performed a series of measurements at the X-22c beamline, Brookhaven National Laboratory on two thin-films grown at the MBE facility, Risø National Laboratory. The films were grown with the sequence: Nb(1000Å) / Y (200Å) / Sm(5000Å) / Y(375Å) / Nb (1000Å) / Sapphire and Nb(1000Å) / Y (500Å) / Sm(10000Å) / Y(250Å) / Nb (1000Å) / Sapphire. Bulk-Sm has a rhombohedral crystal structure and one of the complication in the growth of Sm thin-films is the possible formation of HCP-Sm. Our study has shown that, although the rhombohedral structural phase of Sm is observed, Fig. 1 a) and b), the films failed to reveal any magnetic Bragg peaks using the L_{II}- and L_{III}-edge radiation of Sm. The mosaic spread (≈0.4°) and strains in the film (Fig. 2) may have prevented the magnetic order to develop or to be observable. A soft annealing procedure has been applied on the 10000Å-film and will be studied again in a near future.

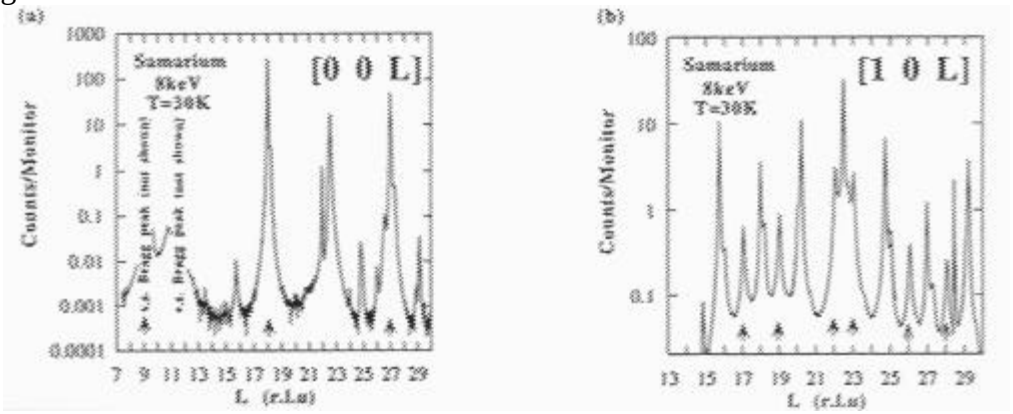

Fig. 1. X-ray scattering scans: a) along the (00L) and b) along the (10L) direction at 8keV. Both labeling refer to the hexagonal representation of the rhombohedral structure. The expected peaks for RH-Sm are shown by the arrows. The other peaks are due to the substrate and other components of the films.

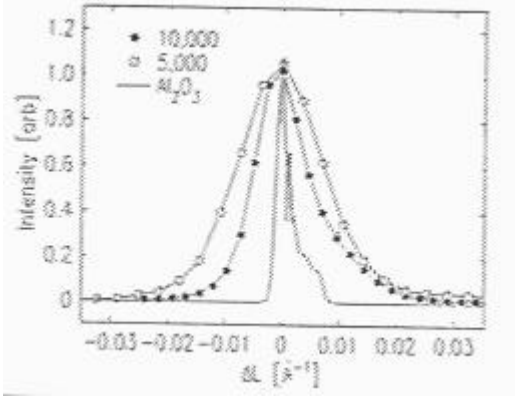

Fig. 2. The lineshape broadening, which reveals the level of strains in the films, is an order of magnitude larger in the Sm-films than what was found in Ho films previously studied at the X-22c beamline.

[1] W.C. Koehler and R.M. Moon, Phys. Rev. Lett. (1972) **29**, 1468

2.2.10 Structural Modifications in Cerium Thin-Films at Low-Temperatures

J.-G. Lussier, A. Madsen, R. Feidenhans'l, *Department of Solid State Physics, Risø National Laboratory, Denmark*

Elemental cerium exists under many allotropic forms. Upon cooling and under normal conditions of pressures, γ-Ce (fcc) transforms into β-Ce (dhcp) and eventually into α-Ce (fcc; 7% collapse of the γ-Ce unit cell) below ≈100K. Experimentally, however, bulk samples usually contain a mixture of several allotropic forms depending on the thermal history of the sample. The preparation of single phase samples of Ce is a long standing problem and is particularly important because of the very different magnetic and transport properties associated with each allotropic forms. In that regard, thin-films may provide a way to stabilize the growth of only one allotropic form. Several Ce thin films were grown at the molecular beam epitaxy (MBE) facility, Risø National Laboratory. In the present report, a low-temperature structural investigation of two of those films are presented. In Fig.1, a Ce film grown on a Vanadium substrate was studied by neutron scattering at the *TAS7* spectrometer. As shown in the figure, in addition to the peak at Q=2.11Å^{-1} associated with the growth of γ-Ce or β-Ce, two temperature dependent peaks at 2.05Å^{-1} (60K<T<30K) and at 1.93Å^{-1} (T<30K) have been observed. Although it is not clear whether these new peaks are magnetic or structural in origin, the new wavevectors do not correspond to any known bulk crystal structures for Ce. In the second film studied, shown in Fig. 2, the X-ray scattering performed on a Ce film grown on a Y substrate shows a reordering similar to what is observed in bulk Ce samples. At high temperature the Q=2.11Å^{-1} is present, while on cool down, the onset of a peak at Q=2.24Å^{-1} clearly indicates the formation of a mixed phase containing α-Ce below 60K. This transition temperature appears lower in the film than in the bulk. On warm-up (not shown), the α-peak remained visible until 220K showing the large hysteresis associated with the transition. Also visible is a small shoulder at ≈2.07Å^{-1} which is reminescent of the peak at 2.05Å^{-1} of Fig.1. The small peak at 1.93Å^{-1} was temperature independent in the Ce/Y film. Other studies are needed to establish the effect of the thicknesses and the substrate layer chosen on the overall phase diagram associated with the films.

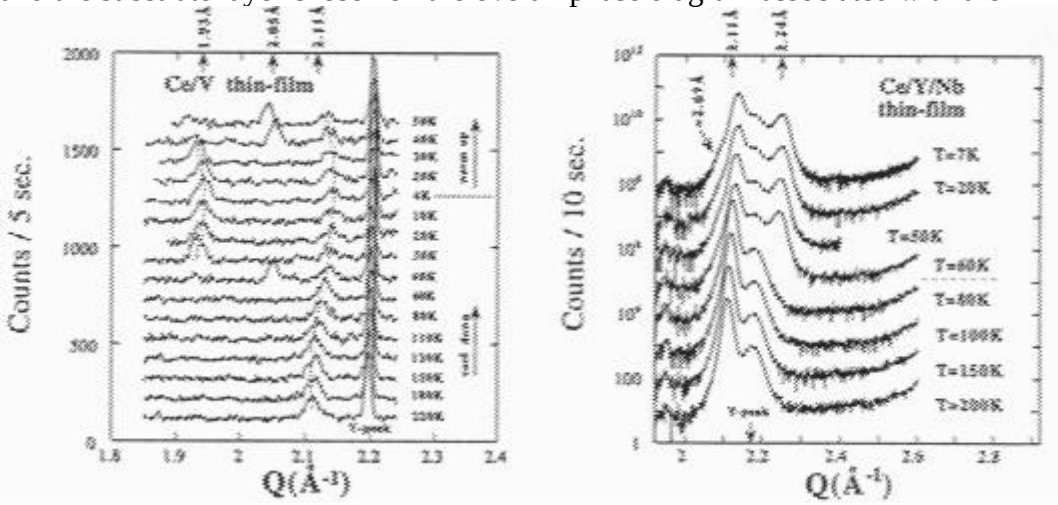

Fig. 1. Neutron scattering study of a Cerium thin-film grown with the sequence: Nb (1000Å) / Y (250Å) / Ce (2000Å) / V (1000Å) / Sapphire (Al_2O_3). The longitudinal scans have been shifted by a constant factor for clarity. The dashed lines are guide to the eyes.

Fig. 2. X-ray scattering study of a Cerium thin-film grown with the sequence: Nb (1000Å) / Y (150Å) / Ce (2200Å) / Y (250Å) / Nb (1000Å) / Sapphire (Al_2O_3). Each curve have been scaled by a factor for clarity. Note the log scale.

2.2.11 SANS Studies of the Incommensurate Magnetic Structures of Metal B20 Alloys

J.G. Booth, E.W. Achu, H.J. Al-Kanani, *Physics Department, Joule Laboratory, University of Salford, UK,* M.M.R. Costa, *Department of Physics, Faculty of Science and Technology, University of Coimbra, Portugal* and B. Lebech, *Department of Solid State Physics, Risø National Laboratory, Denmark*

Metal alloys with the B20 ($P2_13$) crystal structure which lack inversion symmetry are capable of supporting an antiferromagnetic static spin density wave at low temperatures. The helical magnetic structure is extremely long range and propagate along high symmetry directions. The variation of the Néel temperature, the high field magnetisation and the magnetic propagation vector $\boldsymbol{q}$ all suggest a dependence on the electron concentration[2] which have not however been finally confirmed. In order to confirm the suggested behaviour we have fabricated a wide range of polycrystalline intermetallic silicides and germanides with the B20 crystal structure which span the electron concentration range of interest and have characterised these magnetically and crystallographically using neutron diffraction.

The first experiment was aimed at determining the length of the magnetic propagation vector of some representative alloys as a function of temperature using small angle neutron scattering and powdered alloy samples. Eight alloys from the series CrSi/FeSi, CrSi/MnSi, CrSi/CoSi, MnSi/CoSi and CrGe/FeGe have been successfully examined below the Néel temperature and in zero magnetic field over a q-range up to 0.1 Å^{-1}. The data were corrected by the subtraction of a high temperature spectrum and the satellite occurring at low-q was found to be prominent. The radial average of the magnetic intensities were fitted to a Lorentzian line shape. For comparison a powdered MnSi sample as briefly examined and the corresponding q-value agreed with the previously published value.[3]

The results obtained for $Mn_{0.9075}Cr_{0.0925}Si$ are shown in Fig. 1 and indicate that q is practically independent of temperature and of the same order of magnitude as that observed in pure MnSi with $q \sim 0.035$ Å^{-1} (180 Å). For the FeGe/CrGe alloy samples we found high Néel temperatures and modulation vectors of about 0.01 Å^{-1} (630 Å), i.e. in full accord with the results reported for FeGe[4]. The FeSi/MnSi series paralleled that reported previously for FeSi/CoSi[5] over the same range of electron concentration and in general, the results showed that the relationship between the magnetic properties and the electronic structure is strongly supported.

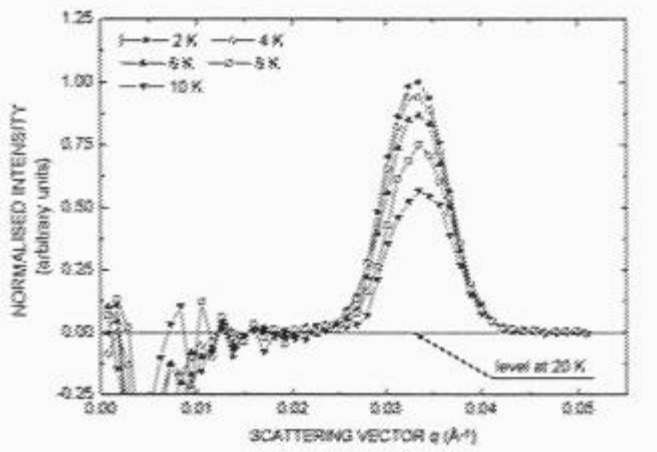

Fig. 1 Radial distribution of the magnetic scattering for $Mn_{0.9075}Cr_{0.0925}Si$ derived from SANS spectra at low temperatures. The 20 K data (background) has been subtracted and the data normalised to the intensity at 2 K and q = 0.0334 Å^{-1}.

[2] B. Lebech in "Recent Advances in Magnetism of Transition Metal Compounds". Eds. A. Kotani and N. Suzuki. World Scientific, Singapore, New Jersey, London, Honkong , 167 (1993).

[3] Y. Ishikawa, K. Tajima, D. bloch and M. Roth, Solid State Commun. **19**, 525 (1976).

[4] B. Lebech, J. Bernhard and T. Freltoft, J. Phys.: Condens. Matter **1**, 6105 (1989).

2.2.12 Polarized SANS Studies of Magnetic Structures in MnSi

S.Aa. Sørensen, M.C. Gerstenberg and B. Lebech, *Department of Solid State Physics, Risø National Laboratory, Denmark,* P. Høghøj, *Institute Laue Langevin, France*

The cubic compound MnSi is an example of a so-called Dzyaloshinskii-Moriya (DM) system, where the helicity of a helical magnetic structure is locked to the chirality of the crystal structure. Due to the weakness of the anti-symmetric Dzyaloshinskii-Moriya interactions, the periods of the magnetic structures observed in these systems are generally very long, making Small Angle Neutron Scattering (SANS) the preferred microscopic technique for the study of these systems. In the case of MnSi, the period is 180 Å corresponding to a magnetic modulation vector of length 0.035 $Å^{-1}$. The use of an incident beam of polarized neutrons for SANS experiments on DM systems combines the resolution properties and the high rate of data acquisition of the SANS setup with the possibilities to determine the helicity of the magnetic structure and to get detailed information about the spatial arrangement of the spins.
In a collaboration between Risø and the instrumentation group of Institut Laue Langevin, a polarizing band-pass filter for neutrons has been implemented at the Risø SANS instrument and successfully tested with MnSi. The filter is based on a principle of double reflection of the neutrons in multilayers of Fe-Si sputtered on each side of a 0.5 mm thick Si wafer and magnetized in an external magnetic field. According to its spin state, a neutron will either be transmitted through the device by reflection in the two multilayers or be absorbed in a layer of Gd deposited on top of the multilayers. In the sputtering process, the d-spacing of the multilayer is modulated to allow neutrons with wavelength within a 20% bandwidth around 7 Å to be transmitted by the filter. The main advantages of this design are: The combining of polarizer and monochromator minimizes the total loses, the filter fits the geometrical constraints of the SANS setup and by rotating the device to a setting where the neutrons go straight through the wafer, one can rapidly switch from a polarized to a non-polarized neutron beam. The transmission of the neutrons with the desired spin state was approximately 50 % and the flipping ratio of the polarizer was 20. These figures of performance are expected to be slightly improved in the near future.

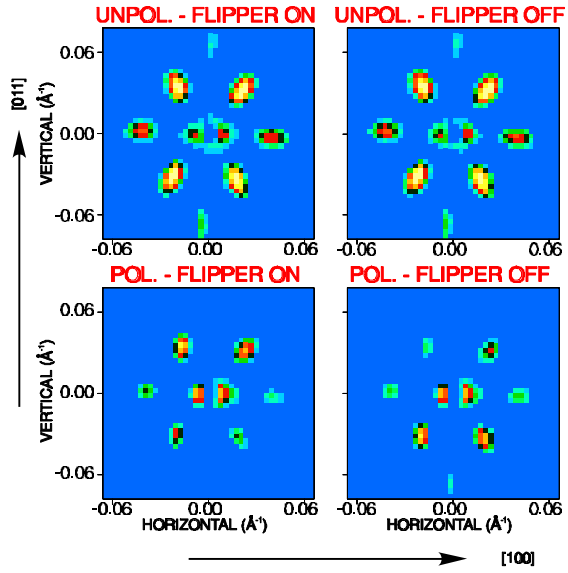

Fig. 1. The diffraction pattern in the [100]-[011] plane of MnSi recorded with the polarizing band-pass filter at the Risø SANS instrument. Note, that when the filter is oriented to reflect neutrons, intensity is moved from the one set of magnetic satellites to te other as the direction of the incident neutron spin is reversed by a Mezei flipper.

[5] J. Beille, J. Voiron, F. Towfiq, M. Roth and Z. Y. Zhang, J. Phys F.: Met. Phys. **11**, 2153 (1991) and J. Beille, J. Voiron and M. Roth, Solid State Commun. **47**, 399 (1983).

2.2.13 Refinement of the Crystal Structure of a Single Crystal of $HoFe_4Al_8$

J.A. de Carvalho Paixão, M.R. Silva, *Department of Physics, Faculty of Science and Technology, University of Coimbra, Portugal*, S.Aa. Sørensen and B. Lebech, *Department of Solid State Physics, Risø National Laboratory, Denmark*

The objective of this experiment was the structural characterisation of a single crystal of the intermetallic compound $HoFe_4Al_8$ by neutron diffraction, a task undertaken in view of future work to investigate the magnetic structure and properties. Similarly to other RFe_4Al_8 (R = rare earth), the crystal structure is the $ThMn_{12}$ structure (space group I4/mmm) with the Ho atoms in the (2*a*) sites, the Fe atoms in the (8*f*) sites and the Al_I and Al_{II} atoms in the (8*i*) and (8*j*) sites, respectively. The cell parameters were obtained from a least-squares refinement of the orientation matrix (UB-matrix) using the angular positions of 25 intense and well centered reflections. At ambient temperature $a = b = 8.669(5)$ Å and $c = 5.005(2)$ Å in good agreement with previous x-ray work. During the data collection 860 reflections were measured out to $\sin\theta/\lambda = 0.70$ Å^{-1} on the 4-circle diffractometer TAS2. After averaging symmetry equivalent reflections, a total of 162 independent reflections were obtained. The atomic positions (*x*, *y*, *z*), temperature parameters (U_{11}, U_{22}, U_{33}, U_{12}, U_{13}, U_{23}) and site occupancies (*OCC*) were refined by least-squares fitting the model structure factors to the measured intensities. We obtain a good agreement with the structural model with a final residual factor of $R = 3.2\%$ (see Table 1). The crystal proved to be rather perfect and some extinction was found to affect the measured intensities ($y_{min} = 0.49$, $y_{mean} = 0.92$). An extinction correction based on the Becker-Coppens model with a Lorentzian isotropic mosaic distribution was included in the refinements. The refined value of the average mosaic spread was $\eta = 0.19'$. It can be concluded from this experiment that our crystal is ordered, in particular that within the experimental uncertainty there is no disorder of the Fe atoms into the Al positions.

ATOM	*x*	*y*	*z*	U_{11}	U_{22}	U_{33}	U_{12}	U_{13}	U_{23}	*OCC*
Ho	0	0	0	66(8)	= U_{11}	53(14)	—	—	—	—
Fe	1/4	1/4	1/4	52(6)	= U_{11}	40(14)	2(3)	6(3)	= U_{13}	0.99(1)
Al_I	0.3424(3)	0	0	53(14)	58(15)	48(20)	—	—	—	0.96(2)
Al_{II}	0.2790(3)	1/2	0	69(14)	25(13)	19(10)	—	—	—	0.98(2)

Table 1. Results of the least-squares refinement of the crystal structure data for $HoFe_4Al_8$. The elements of the tensor U_{ij} are given in 10^4 Å units.

2.2.14 Magnetic Neutron Scattering Studies of $DyFe_4Al_8$ at Very Low Temperature and Applied Magnetic Field

S.Aa. Sørensen and B. Lebech, *Department of Solid State Physics, Risø National Laboratory, Denmark,* J.A.de Carvalho Paixão and M.R Silva, *Department of Physics, Faculty of Science and Technology University of Coimbra, Portugal*

As part of an ongoing combined neutron and X-ray scattering study of the magnetic $ThMn_{12}$-structure compounds MFe_4Al_8, where M is a rare earth or actinide element,[6] we have investigated the system $DyFe_4Al_8$ by neutron scattering at temperatures down to 350 mK and applied magnetic fields up to 5 Tesla. In previous neutron experiments performed at TAS2, Risø and D10, ILL the Fe-sublattice was found to order at 180 K in a so-called G-type antiferromagnetic structure propagating along equivalent <110>-directions. The G-type structure has superimposed on it a long-wavelength amplitude modulation with $\boldsymbol{q}$ = (q,q,0), q=0.14 r.l.u. Below approximately 100 K, the modulation vector locks into the value q=2/15 and remains independent of temperature on further cooling. At about 25 K, the Dy-sublattice starts ordering with the same modulation vector as observed for iron. Below 15 K, higher order harmonics of the modulation are observed. From an X-ray magnetic scattering experiment it is believed that, the Dy-moments form a basal plane cycloid.

In the neutron experiments a broad profile of diffuse scattering is observed in scans along $\boldsymbol{q}$ at temperatures below 10 K (see Fig. 1). The intensity of this scattering has been observed to increase steadily when cooling down to 2 K. To further investigate this phenomenon, we did a new diffraction study at TAS1, Risø, with the sample mounted in an Oxford Instruments "Heliox" $^4He/^3He$-cryostat allowing us to reach 350 mK as the base temperature. No changes in neither the peaks nor the diffuse scattering were observed in the temperature range from 2 K down to 350 mK. The data are not yet fully analyzed, but at the moment we are interpreting the diffuse component of the scattering in a model of a "floating" spin-slip.

Experiments on $DyFe_4Al_8$ in magnetic field applied along the $[1\bar{1}0]$-direction were performed at the TAS1 and TAS3 spectrometers at Risø. In Fig. 2, the intensity of the nuclear (110) and (220) peaks and their first order magnetic satellites are shown *vs.* field at the temperature 4.2 K. Note, that the satellites around the (220) nuclear reflection are gone already at a field of 0.75 Tesla. From the structure it follows, that these satellites are exclusively due to Dy-ordering. Hence, the antiferromagnetic coupling of the Dy-moments is broken by the external field of 0.75 Tesla.

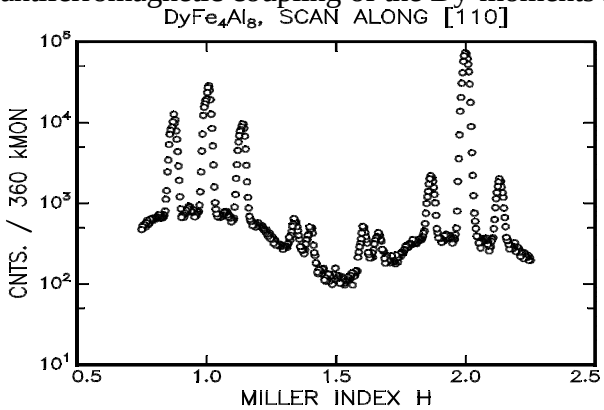

Fig. 1. Neutron diffraction profile along [110]. TAS1, Heliox, T = 4.2K.

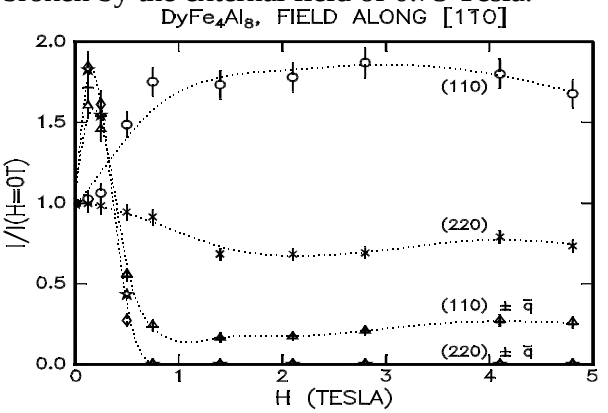

Fig. 2. Normalized intensity of the (110) and (220) nuclear peaks and their first order magnetic satellites. The dotted lines are guides to the eye.

[6] J A. Paixão, S. Langridge, S. Aa. Sørensen, B. Lebech, A. P.Goncalves, G. H. Lander, P. J. Brown, P. Burlet and E. Talik , to appear in proceedings of the ECNS, October 1996, Interlaken, Switzerland

2.2.15 An X-ray Magnetic Scattering Study of $DyFe_4Al_8$

S. Langridge, *ESRF, France and European Commission, JRC, Institute for Transuranium Elements, Germany,* J.A. Paixão, *Department of Physics, University of Coimbra, Portugal,* S.Aa. Sørensen, *Department of Solid State Physics, Risø National Laboratory, Denmark,* C. Vettier, *ESRF, France,* G.H. Lander, *European Commission, JRC, Institute for Transuranium Elements, Germany,* D. Gibbs, *Physics Department, Brookhaven National Laboratory, USA,* A. Stunault, D. Wermeille and N.B. Berhoeft, *ESRF, France,* E. Talik, *Institute of Physics, University of Silesia, Poland*

The magnetic structure of the $ThMn_{12}$-structure compound $DyFe_4Al_8$ is complicated and not yet fully understood. The general features of the magnetic ordering determined mainly from neutron scattering experiments are summarized in 2.2.14. A central problem has been to establish whether the Dy-moments when ordering below approximately 25 K are forming a transverse amplitude modulated structure in the basal plane of the *bct* crystal structure or the moments are rotating in some helical or cycloidal structure. An X-ray resonant magnetic scattering experiment was performed on the ID20 beamline of the European Synchrotron Radiation Facility. As shown in Fig. 1, the intensities of the first order magnetic satellites around (*hh*0) reciprocal lattice points were measured at the Dy L_{III}-edge at the temperature 12 K. In the figure, the intensity is shown as a function of the Bragg-angle, θ with the $DyFe_4Al_8$ single crystal sample in two different orientations. In orientation (A), the reciprocal lattice [110]-[$\bar{1}$10] plane is parallel to the diffractometer plane defined by the incident wavevector, $\boldsymbol{k}_i$ and the outgoing wavevector, $\mathbf{k}_f$. In the orientation (B), the sample has been rotated by 90 degrees around the [110] relative to the first orientation, thus bringing the basal plane of the crystal perpendicular to the diffractometer plane. From the angular dependence of the satellite intensities in the two orientations it is concluded, that the Dy moments must rotate in the basal plan. In the experiment, the intensity of the (330) + $\boldsymbol{q}$ and (440) + $\boldsymbol{q}$ satellites were measured at the Dy L_{III}-edge as a function of temperature. A steep drop in the intensity was observed in the temperature range between 11 K and 20 K corresponding to the disordering of the Dy 4f-moments. However, a weak signal was detected all the way up to the temperature of disordering of the Fe-moments. This is a sign of the importance of hybrydization of the Dy-5f and Fe-3f bands in mediating the interaction between the two magnetic sublattices.

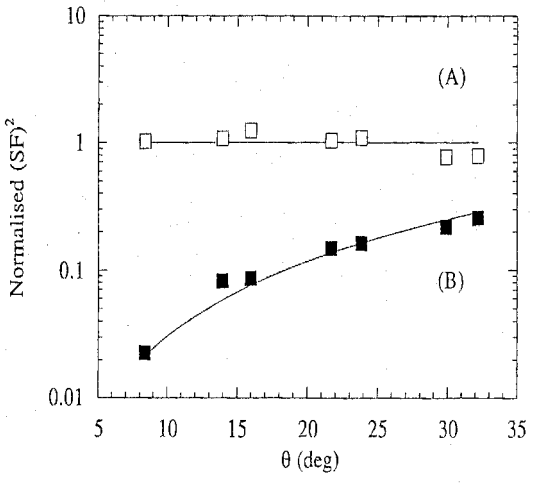

Fig. 1. Lorentz-corrected intensity of the 1st order magnetic satellites measured in the σ→π channel.The average intensity of all satellites measured in orientation (A) has been normalized to unity. For orientation (B), the solid curve has been drawn to predict the intensities with no adjustable parameters.

2.2.16 Magnetic Fluctuations in Nanoparticles

F. Bødker, M.F. Hansen, S. Mørup, *Institute of Physics, Technical University of Denmark*, and K. Lefmann, K.N. Clausen, P.-A. Lindgård, *Department of Solid State Physics, Risø National Laboratory, Denmark*

Magnetic particles below a certain size will consist of a single magnetic domain. At low temperatures the magnetization will be aligned along a so-called easy axis, but at higher temperatures the thermal fluctuations may cause the magnetization to fluctuate among different easy directions. This phenomenon is known as superparamagnetic relaxation.
At TAS6/RITA we have studied a sample of nanosized (about 10 nm) hematite particles. In bulk hematite the moments of the two sublattices are antiferromagnetic aligned below 260 K, but above this temperature they are canted by about 0.1 degree with respect to each other leading to weak ferromagnetism. Our small hematite particles, however, are weakly ferromagnetic down to the lowest temperatures with a particle moment which is small, but significantly larger than expected from the bulk properties. The amplitude and frequency of the fluctuations of the particle moment were studied by inelastic neutron scattering. Figure 1 shows the measurements of the energy transfer at the antiferromagnetic (111) reflection. At the lowest temperature, only the static magnetization is seen, but with increasing temperature a broader component appears, indicating the onset of thermally activated fluctuations.

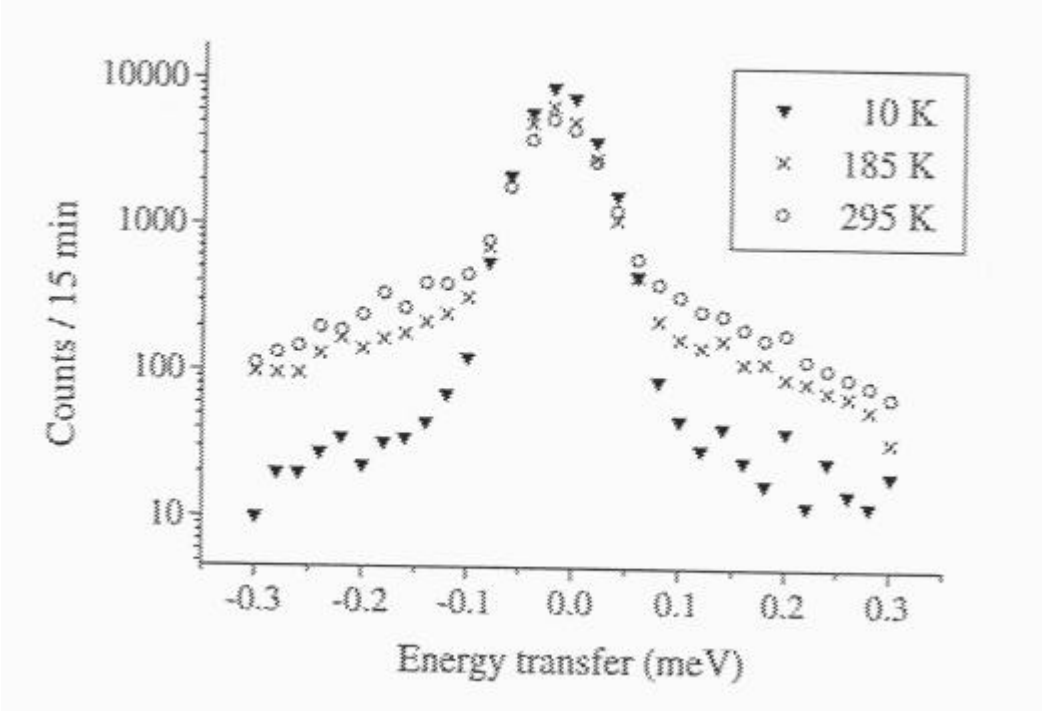

Fig. 1. Scattered neutron intensity in three constant-q scans at temperatures of 10 K, 185 K, and 295 K shown in one semi-logarithmic plot. The central peak around zero energy transfer is resolution limited and is seen at all temperatures. In contrast, an inelastic tail is present only at the two highest temperatures.

2.3 Superconducting Materials and Phenomena

2.3.1 Microscopic Coexistence of Magnetism and Superconductivity in $ErNi_2B_2C$

U. Yaron, P.L. Gammel, A.P. Ramirez, D.A. Huse, D.J. Bishop, *Bell Labs., Lucent Technologies, USA,* A.I. Goldman, C. Stassis, P. Canfield, *Iowa State University, USA,* K. Mortensen and M.R. Eskildsen, *Department of Solid State Physics, Risø National Laboratory, Denmark*

It general magnetic and superconducting states of a material is mutually exclusive. However, in a class of materials with the formula RNi_2B_2C, where R is a rare earth, antiferromagnetism (AF) and superconductivity coexist, which makes these a priori interesting subjects of investigation. We have performed small-angle neutron scattering (SANS) studies of the flux-line lattice (FLL) in $ErNi_2B_2C$[1], which has a zero field critical temperature, T_c = 10.5K, and a Neel-transition, T_n = 6K as shown in the phase diagram in fig. 1.

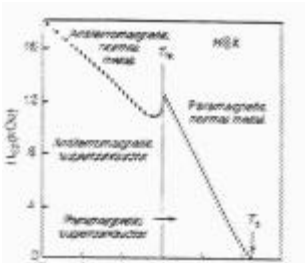

Fig. 1. The phase diagram for $ErNi_2B_2C$.[2]

The principal result of our investigation is shown in fig. 2. This is a typical SANS pattern after background subtraction. It shows a four-fold symmetry including second order peaks, which should be contrasted to the hexagonal FLL usually observed. By moving the detector to within one meter from the sample it was possible to reach the 11th order AF Bragg peaks which folds into the first Brillouin zone near the centre as shown in the insert. As the AF peaks are aligned with the [1,0,0]/[0,1,0] directions we can deduce that the FLL locks into the [1,1,0] direction.

In fig. 3. is shown the FLL scattering form factor vs. field which allows us to extract the penetration depth, $\lambda \approx 500$Å, and coherence length, $\xi \approx 135$Å. The square root of the FLL reflectivity versus temperature is also shown. Assuming mean-field temperature dependence of λ this should give a straight line, which is seen to agree reasonably well.

We believe that our results show that there will be a rich and interesting phenomenology to be studied in this system and others belonging to the same class.

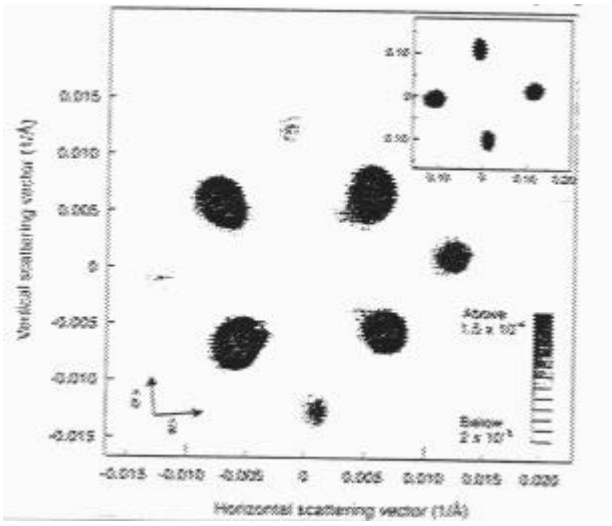

Fig. 2. Greyscale image of FLL Bragg scattering pattern. This was obtained after field-cooling the sample to 1.6K in a field of 4kOe. The inset shows the 11th order magnetic peaks at 1.6K with no applied field.

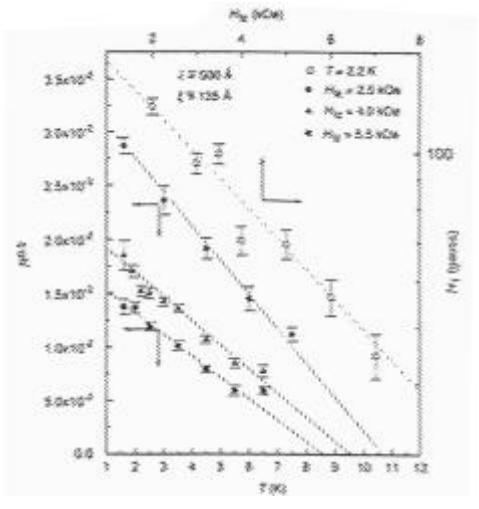

Fig. 3. The log of the form factor versus applied field at 2.2K (open symbols), and the square root of the reflectivity versus temperature for various fields (solid symbols).

[1] U. Yaron *et al.*, Nature **382**, 236 (1996)

[2] B. K. Cho *et al*. Phys. Rev. B **52**, 3684 (1995)

2.3.2 Observation of a Field-Driven Structural Phase Transition in the Flux Line Lattice in $ErNi_2B_2C$

M.R. Eskildsen, N.H. Andersen, K. Mortensen, *Department of Solid State Physics, Risø National Laboratory*, P.L. Gammel, B.P. Barber, U. Yaron, A.P. Ramirez, D.A. Huse, D.J. Bishop, *Bell Labs, Lucent Technologies, USA*, C. Bolle, C.M. Lieber, *Harvard University, USA*, S. Oxx, S. Sridhar, *Northeastern University, USA* and P. Canfield, *Iowa State University, USA*

The flux-line lattice (FLL) found in type-II superconductors usually show hexagonal symmetry. However a square FLL is found in $ErNi_2B_2C$.[1] This square symmetry has to be stabilized by an anisotropy in the system which could be either an in-plane anistropy in H_{C2} or due to a magneto-elastic coupling induced by the antiferromagnetic ordering of the Er spins. We have performed small-angle neutron scattering (SANS) studies of the FLL at low fields which show a structural transfor-mation of the FLL into a hexagonal symmetry as the field is lowered.

Fig. 1. shows how the symmetry transformation manifests itself. In the top panel the normalized peak position , q/q_0 with $q_0 = 2\pi\sqrt{(B/\varphi_0)}$, of the observed Bragg peaks is shown. For a square lattice we expect respectively 1 and $\sqrt{2}$ for first and second order refelctions, whereas a hexagonal lattice gives 1.07 for the first order reflection. It is clearly seen that over a range from 1100 to 500 Oe the first and second order peaks of the square lattice converge to the value exected for a hexagonal lattice. Shown in the lower panel is the azimuthal width of the first order peaks as the field is lowered. The azimuthal broadening that occurs as the field is lowered below 500 Oe also signals the square to hexagonal transition, as the limited resolution of the SANS experiment prevents us from resolving individual peaks.

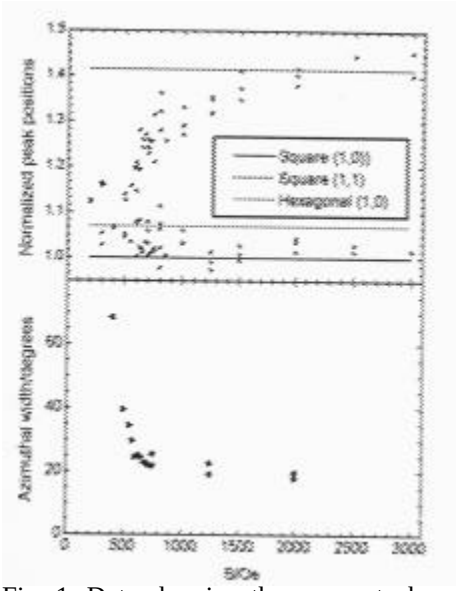

Fig. 1. Data showing the square to hexagonal FLL symmetry trans-formation. Top panel shows normalized peak position and bottom panel shows the azimuthal width of first order Bragg peaks.

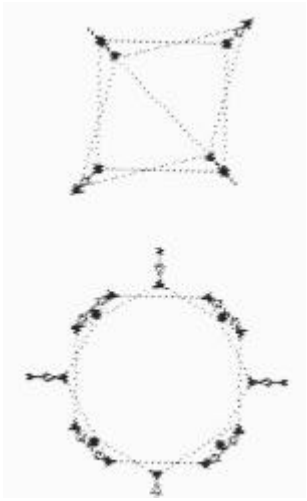

Fig. 2. Schematic picture of square to hexagonal transformation. Top is direct space and bottom is reciprocal space.

In Fig. 2. we show the structural transformation which proceed by an area preserving rhobohedral distortion along the (1,1) directions of the square FLL, giving rise to a double degeneracy and hence twelve peaks in the hexagonal symmetry. In top of Fig. 2 the transformation is shown in direct space. Square points indicate square lattice vortex positions and triangular peaks indicate hexagonal lattice vortex positions. In bottom the transformation is shown in reciprocal space, where the splitting of and movement of the square lattice peaks as the field is lowered is shown with arrows.

In conclusion this system provides an ideal model for studying the effects of anisotropy on the symmetry of the FLL.

[1] U. Yaron *et al.*, Nature **382**, 236 (1996)

2.3.3 Development of Decoration Chamber for Flux-Line Lattice Studies

M.R. Eskildsen, S. Nielsen and N.H. Andersen, *Department of Solid State Physics, Risø National Laboratory, Denmark*

In the process of strengthing the department reasearch into the properties of the magnetic flux-line lattice (FLL) in type-II superconductors, a decoration chamber has been constructed.
The Bitter decoration technique is a direct imaging method which can be used to independent studies of the FLL, or as a supplement to small-angle neutron scattering (SANS) experiments. Bitter decoration works by field cooling the sample to below the critical temperature, T_c, in a low pressure He atmosphere, and then evaporate magnetic particles of e.g. iron or nickel into the back-ground gas. The magnetic particles then therma-lize in the background gas and diffuse onto the sample surface and prefentially decorate where flux lines are exiting the sample. Once decorated the magnetic particles are fixed by the van der Waals force, allowing the sample to be heated up and imaged in a SEM. A scematic figure of the decoration chamber is shown in figure 1.

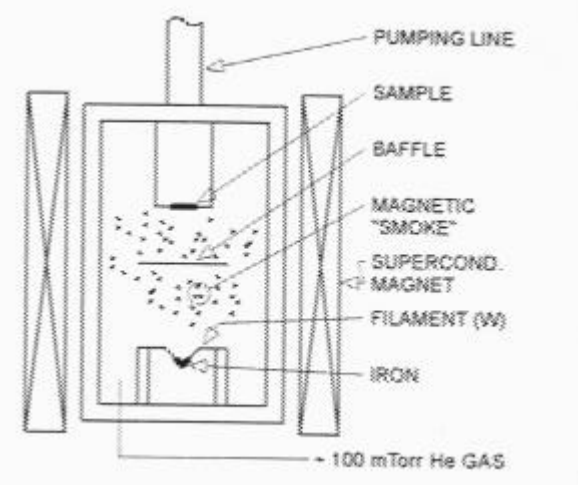

Fig. 1. Scematic drawing of the decoration chamber.

An example of a decoration image is shown in figure 2. The characteristics of the decoration chamber is as follows: The chamber is cooled by insertion into liquid He, and hence the operating temperature is 4.2K. The chamber is designed to fit into a liquid helium transport dewar and therefore no seperate cryostat is needed. Arrangements for reclaiming the boiled off He gas are included.
The magnetic field is generated by coils of superconducting NbTi wire in a copper matrix, and it can be applied over the entire temperature range from 4.2K to room temperature, with the advantage that no power is dissipated when cooled to base temperature. The field range is up to 200G with a precission of ±0.5G with the power supply used.
A tungsten filament and iron wire is used for the decorations.

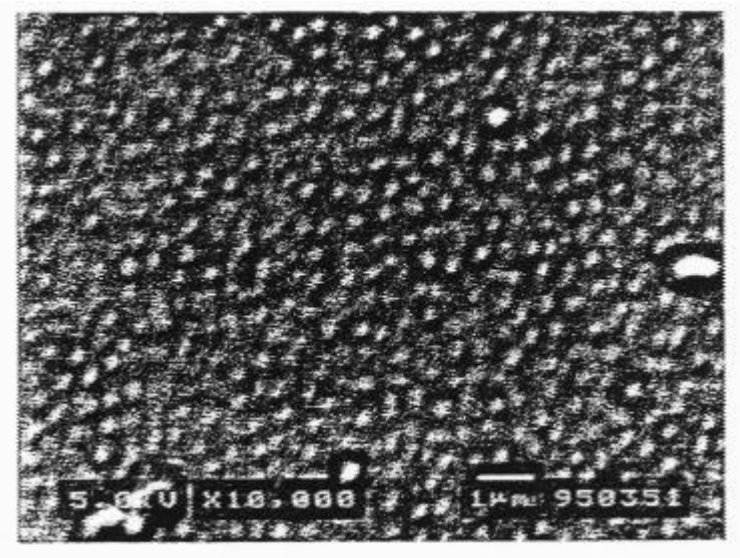

Fig. 2. SEM image of decoration pattern. The material is $YBa_2Cu_3O_7$ decorated in a field of 77.6G.

2.3.4 Dynamics of Oxygen Ordering in $YBa_2Cu_3O_{6+x}$ Studied by Neutron and High-Energy Synchrotron X-ray Diffraction

T. Frello, N.H. Andersen, J. Madsen, M. Käll, O. Schmidt, *Department of Solid State Physics, Risø National Laboratory, Denmark,* M. von Zimmermann, J.R. Schneider, *HASYLAB, Germany,* T. Wolf, *Forschungszentrum Karlsruhe, Germany,* H.F. Poulsen, *Materials Department, Risø National Laboratory, Denmark*

The close relation between oxygen ordering and superconductivity in $YBa_2Cu_3O_{6+x}$ with $0 \leq x \leq 1$ has stimulated many structural studies of this material. Of particular interest has been the orthorhombic double cell structure, called ortho-II, which is found for oxygen stoichiometries $0.35 \leq x \leq 0.67$ and leads to a plateau of $T_c \approx 60$ K. It results from oxygen ordering in CuO chains along the *b* axis in the basal plane of the unit cell with the oxygen being preferentially on every second chain. Among the unsettled structural properties are the reasons why the ortho-II structure does not develop long range order, and why the single cell ortho-I structure remains stable down to temperatures that are significantly lower than predicted by most theoretical models. We have studied the dynamics of the ortho-II ordering process in a high purity single crystal by neutron and high-energy synchrotron X-ray diffraction in time intervals from a few seconds to several weeks, and for temperatures from 20 to 200 °C. Our studies reveal a two-step ordering process. When the temperature is changed below 100 °C, an initial change in the ordering properties occurs instantaneously (within seconds) followed by a very slow ordering process, that does not seem to develop long range order even on a time scale of several years. Our data show that the optimal temperature for developing ortho-II ordering is around 80 °C. The observed properties may be interpreted on the basis of recent theoretical model predictions that suggest a strong variation of the oxygen chain length distribution function with temperature.[1] As the temperature is lowered a rapid increase of the average chain length is predicted.[1] Locally the chains may combine but thermodynamic equilibrium is only established via a more long range oxygen diffusion process that is frozen out before the chain length distribution saturates.

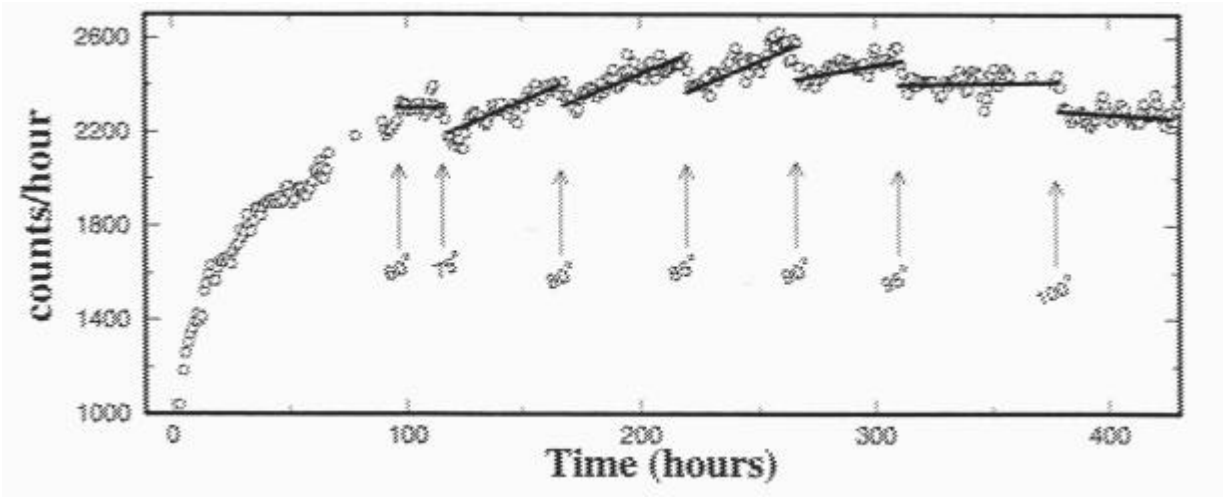

Fig.1. The time-development of the intensity of the (½ 0 0) reflection (the ortho-II phase) measured by neutron diffraction at the TAS1 Risø neutron spectrometer. The sample was quenched from 170 °C to 70 °C at t=0 hours. Additional temperature changes are indicated on the figure by arrows. Circles are experimental data, the lines are guides to the eye.

[1] G. Uimin, Phys. Rev. B, **50**, 9531 (1994)

2.3.5 Annealing of BiSCCO Wires Studied In-situ by High-Energy Synchrotron X-ray Diffraction

T. Frello, N.H. Andersen, A. Abrahamsen, *Department of Solid State Physics, Risø National Laboratory, Denmark*, H.F. Poulsen, S. Garbe, *Materials Department, Risø National Laboratory, Denmark*, M.D. Bentzon, *NKT Research Center, Denmark*, M. von Zimmermann, *HASYLAB, Germany*

Much effort is put into the development of superconducting wires for power transmission. The most widely used method is the Powder-In-Tube technique, where superconducting $Bi_2Sr_2Ca_{n-1}Cu_nO_{2n+4+x}$ (BiSCCO) powder is filled into a silver tube which is subsequently subjected to thermomechanical treatments. A key point in obtaining a high critical current density j_c is the optimisation of the heat-treatment of the wires. During annealing at ≈840 °C the BiSCCO-2212 phase (T_c=85 K) is transformed into the BiSCCO-2223 phase (T_c=110 K) inside the silver cladding. The influence of the silver on the phase transformation as well as the texture development is not yet well understood. We have used High-Energy Synchrotron X-ray Diffraction for an *in-situ* study of the solid state transformation and texture formation of the BiSCCO powder inside the silver cladding during annealing. The photon energy used was 100 keV, having sufficient penetration power to allow for X-ray diffraction in a transmission geometry. To our knowledge, this is the only technique suitable for such *in-situ* measurements. The diffraction patterns were recorded by a two-dimensional CCD detector, enabling us to obtain simultaneous information of both phase development as well as texture formation, see Fig. 1. Experiments were performed for mono- and multifilament wires with annealing temperatures of 820, 835 and 850 °C for up to 26 hours. The heating and cooling rates were varied, showing that very fast heating is detrimental to the phase development. The solid state transformation generally runs faster for the multifilament wires and the optimum annealing temperature also seems to be lower than for the singlefilament wires.

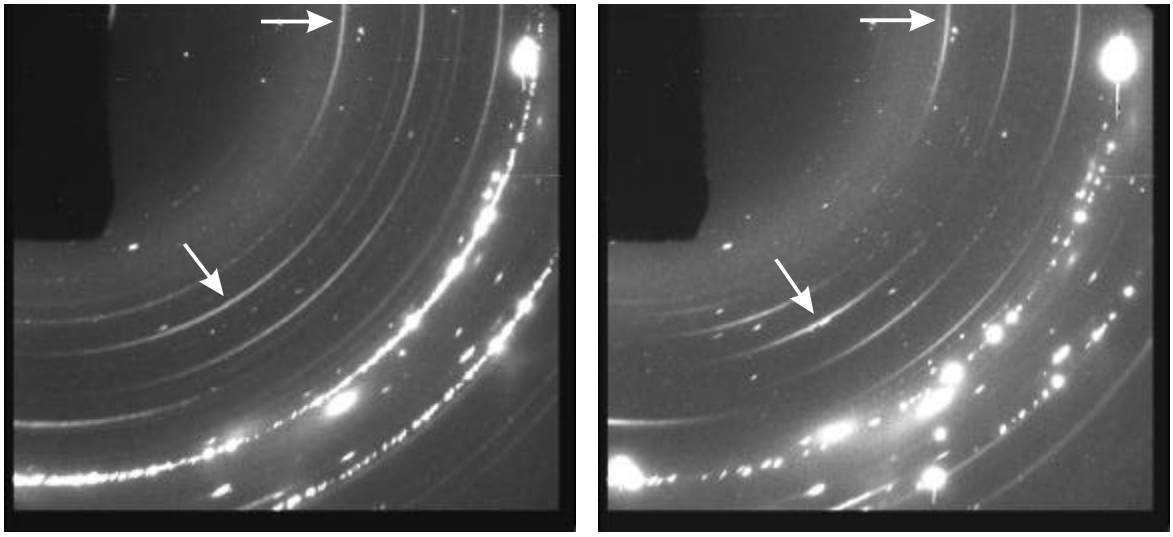

a) b)

Fig. 1. Diffraction images for a monofilament wire annealed at 835 °C for a) 0 hours and b) 26 hours. The ring segments indicated by arrows on the figure are diffracted signals from the BiSCCO. The full rings and bright spots originate from the silver cladding. The images show that the 2212 phase in a) is totally transformed into the 2223 phase in b). Furthermore, the texture of the 2223 phase is considerably more narrow than that of the 2212 phase. The annealing also leads to a recrystallisation of the silver.

2.3.6 New Superstructures in $YBa_2Cu_3O_{6+x}$ Observed by High Energy X-Ray Diffraction

T. Frello, J. Madsen, O. Schmidt, N.H. Andersen, *Department of Solid State Physics, Risø National Laboratory, Denmark*, M. von Zimmermann, J. Schneider, *HASYLAB, Germany*, R. Liang, P. Dosanjh and W.N. Hardy, *UBC, Canada*

The oxygen ordering in the CuO_x basal plane has significant influence on the charge transfer leading to superconductivity in $YBa_2Cu_3O_{6+x}$. The tendency of the system to form Cu-O chains along the *b* axis for $0< x < 1$ leads to weak orthorhombic distortions of the basic tetragonal structure with different sequences of superstructure ordering of *full* (CuO) and *empty* (Cu) chains along the *a* axis. Most notably we have observed the double cell ortho-II[1] and the triple cell ortho-III[2] superstructures with chain ordering sequences: *full-empty* and *full-full-empty* at ideal oxygen stoichiometries of $x = 0.5$ and $x > 0.67$, respectively. Weak superstructures of more complex ordering sequences have been observed by electron microscopy,[3] but so far never by structural techniques that probe the bulk of the material. We have prepared well equilibrated single crystals with stoichiometries, $x = 0.62$ and $x = 0.67$ and studied their oxygen ordering properties with high energy synchrotron X-ray diffraction. In the $x = 0.62$ crystal we find commensurate superstructure peaks with modulation vectors (2/5,0,0), and finite correlation lengths which at room temperature are 10.2 Å along the *a* axis and 73 Å along the *b* axis (see Fig. 1). We interpret the (2/5,0,0) peaks to be the second harmonic of an ortho-V superstructure with periodicity 5*a* and a chain ordering sequence of *full-full-empty-full-empty*, which has ideal oxygen stoichiometry, $x = 0.6$. Simple structure factor calculations show that the intensity of primary peaks at (1/5,0,0) is almost an order of magnitude smaller than that of the (2/5,0,0) peak and may therefore hardly be seen on the background and the tails of the Bragg peaks. The ortho-V peaks are centred around ortho-II peaks at (1/2,0,0) which have correlation lengths at room temperature of 17 Å along the *a* axis and 83 Å along the *b* axis. There is a clear *c* axis modulation of the ortho-II superstructure and a weaker one for ortho-V, but it is not possible to deduce values for the correlation lengths. The ortho-II intensity increases slightly when the ortho-V superstructure starts to decrease at 55 °C, before it disappears at around 110 °C. In the crystal with $x = 0.67$ we observe incommensurate superstructure peaks with ordering vector (0.38,0,0). The correlation lengths at room temperature are 11.5 Å along the *a* axis, 56 Å along the *b* axis, and rather weak correlations along the *c* axis similar to those found for the ortho-III superstructure.[2] Although the superstructure peaks may be fitted nicely with a single Lorentzian we cannot preclude that the apparently incommensurate superstructure peaks are combinations of ortho-III and ortho-V peaks. Neither can we preclude weak traces of ortho-II superstructure peaks. The (0.38,0,0) superstructure has a broad transition between 45 and 140 °C. Our eksperimental observations are in good agreement with recent Monte Carlo simulation model studies (see contribution 2.3.5).

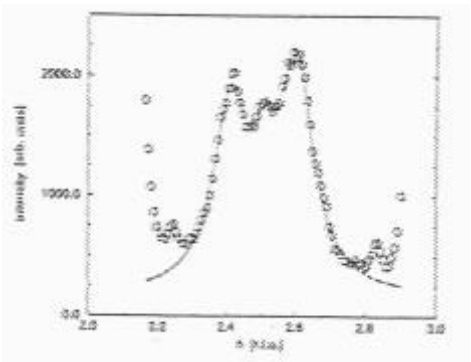

Fig. 1. Observation of combined ortho-V ($h = 2.4$ and 2.6) and ortho-II ($h = 2.5$) superstructure peaks at room temperature in $YBa_2Cu_3O_{6.62}$ Full line is a fit with three Lorentzians. The peaks at $h \approx 2.24$ and 2.83 have not been identified. The scattering densities at $h \rightarrow 2$ and 3 are the tails of the Bragg peaks.

[1] P. Schleger *et al*., Phys. Rev. Lett. **74**, 1446 (1995)
[2] P. Schleger *et al.* Physica C **241**, 103 (1995)
[3] R. Beyers *et. al.* Nature **340**, 619 (1989)

2.3.7 Monte Carlo Simulation Study of the Ortho-II, Ortho-III and Ortho-V Oxygen Ordering Superstructures in $YBa_2Cu_3O_{6+x}$

D.M. Jensen, T. Fiig, *UNI-C, Denmark*, N.H. Andersen and P.-A. Lindgård, *Department of Solid State Physics, Risø National Laboratory, Denmark*

Different superstructures from oxygen ordering in Cu-O chains along the *a* axis of orthorhombic $YBa_2Cu_3O_{6+x}$ ($0.35 < x < 1$) have been observed experimentally. The ordering properties of the most notable phases, the tetragonal disordered, and the orthorhombic ordered ortho-I with periodicity *a* and ortho-II with periodicity 2*a* have previously been studied by use of the 2*d* ASYNNNI lattice gas model with three interaction parameters, V_1, V_2 and V_3. V_1, the repulsive nearest neighbour interaction, and V_2, the attractive next nearest neighbour interaction for oxygen atoms bridged by a Cu atom, stabilise the Cu-O chain formation at low temperatures, and the repulsive next nearest neighbour interaction, V_3, for oxygen atoms that are not bridged by Cu atoms (transverse to the Cu-O chains), stabilises the ortho-II structure for $x \approx 0.5$. However, the ASYNNNI model cannot account for the ortho-III structure with periodicity 3*a*, and some higher order superstructures observed experimentally (*cf.* contribution 2.3.3). We have added a fourth repulsive interaction parameter, V_5, between oxygen atoms that are separated by the distance 2*a* without intervening Cu atoms to the ASYNNNI model and studied the oxygen ordering properties of this model by Monte Carlo simulation technique. As in previous studies we have chosen the parameters, $V_1 \equiv 1$, $V_2 = -0.36\ V_1$ and $V_3 = 0.12\ V_1$, and estimated $V_5 = 0.04\ V_1$ to be a reasonable choice for further studies. The simulations have been performed by use of the SGI PowerChallenge at UNI-C for which a parallel algorithm has been developed. Preliminary results from a 64×64 oxygen system with periodic boundary conditions at a temperature $T = 0.08\ V_1/k_B$ are shown in Fig. 1 for $x = 0.5$, $x = 0.6$ and $x = 0.7$. Upper figures are snapshots of the oxygen atoms (notice that the *a* and *b* axes are along the <1,1> directions) and the lower figures are the corresponding structure factors *S(Q)* calculated along the *a** direction *(h,0).* The results show that the addition of the V_5 parameter to the ASYNNNI model stabilises the ortho-III structure with peaks at $h = n/3$ (n = integer) for $x = 0.7$ (close to the ideal composition $x = 0.67$). For $x = 0.6$ a superstructure with periodicity 5*a* and superstructure peaks at $h = n/5$ are anticipated and actually found in the simulations. For $x = 0.5$ the ortho-II superstructure with peaks at $h = n/2$ is dominant as expected. Notice that none of the superstructures has developed long range order.

Fig. 1. Model studies of the oxygen ordering in the CuO_x basal plane of $YBa_2Cu_3O_{6+x}$ (see the text)

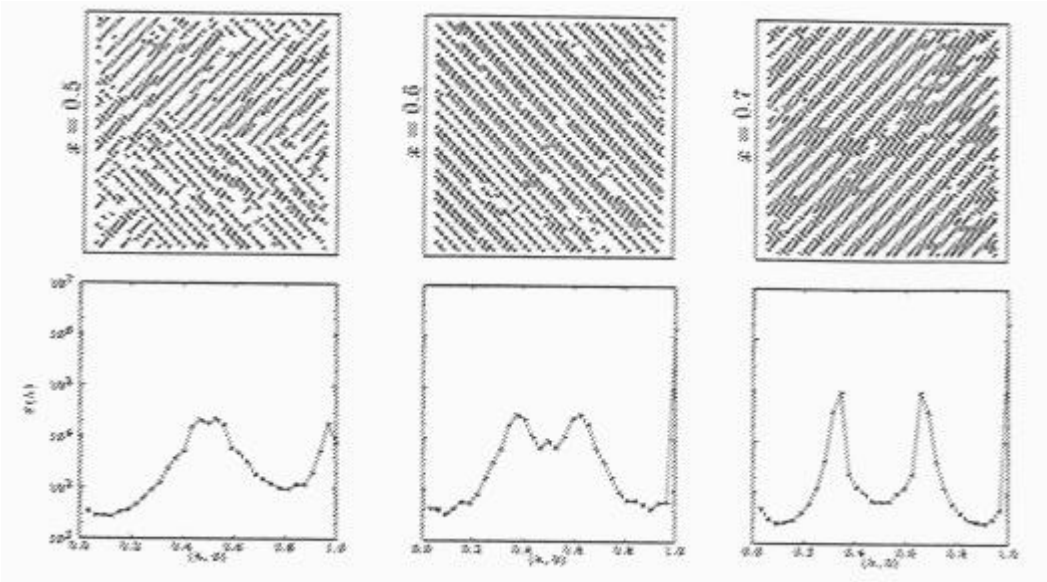

2.3.8 Verification of Stripe Charge Correlations in $La_{1.775}Sr_{0.225}NiO_4$ by Hard X-Ray Diffraction

M. von Zimmermann, J.R. Schneider, *HASYLAB, Germany,* T. Frello, J. Madsen, N.H. Andersen, *Department of Solid State Physics, Risø National Laboratory, Denmark,* A. Vigliante, J.M. Tranquada, D. Gibbs, *Department of Physics, Brookhaven National Laboratory, USA*, and D.J. Buttrey, *University of Delaware, USA*

Recent neutron scattering studies have shown very intriguing stripe correlations of spins and holes in nickelates and cuprates,[1] but no X-ray diffraction experiment has confirmed the neutron results. We have carried out an X-ray diffraction study of $La_{2-x}Sr_xNiO_4$ (x = 0.225) at the hard X-ray wiggler beamline BW5 at HASYLAB and verified the presence of stripe charge correlations in this material. We use 100 keV photons, which imply an absorption length of 0.08 cm and allow us to perform the experiment in Laue geometry and study the bulk of the same crystal as in the previous neutron experiment.[2] Ta-SiO_2 crystals with a mosaicity of 50 arc seconds used as monochromator and analyzer gave a resolution of 0.009 $Å^{-1}$ (longitudinal) and 0.001 $Å^{-1}$ (transverse). The sample was initially cooled to 10 K where eight independent incommensurate superstructure reflections at $Q = G - g_{2\varepsilon}$ were observed. G is a reciprocal lattice vector and $g_{2\varepsilon}$ = (2e,0,1) is the charge density modulation vector for which it is expected that e » x. In Fig. 1 are shown h scans (along a^*) through (4-2e,0,3) at 10 K in the stripe ordered phase and at 170 K, where the ordering has disappeared. After the initial cooling to 10 K the (4-2e,0,3) peak intensity was measured as function of increasing temperature, and subsequently for decreasing temperature. The results are shown in Fig. 2. Below 40 K the peak intensity decreases steadily, and hysteresis is observed when the sample is cooled again after the initial heating study. The temperature dependence of the incommensurate splitting parameter, e, and the correlation lengths were measured, and the results are comparable with those obtained by neutron diffraction.[2] The largest correlation lengths of 46 Å in the a direction, 74 Å along b and 14 Å along c were found at 50 K close to where the peak intensity is maximum.

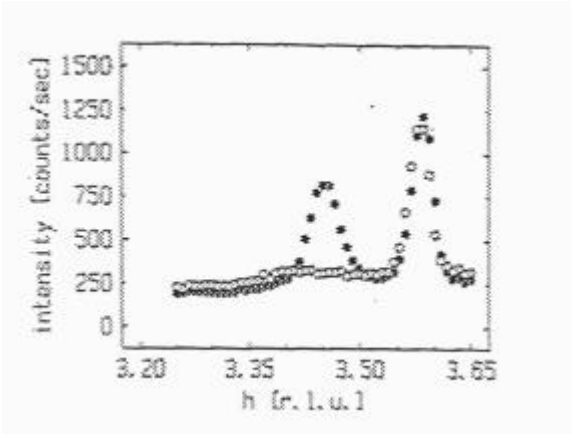

Fig. 1. h scan through the charge-order peak at (4-2e,0,3) at 10 K (filled circles) and 170 K (open circles). The temperature independent peak at h=3.58 is an Al powder line from the cryostate.

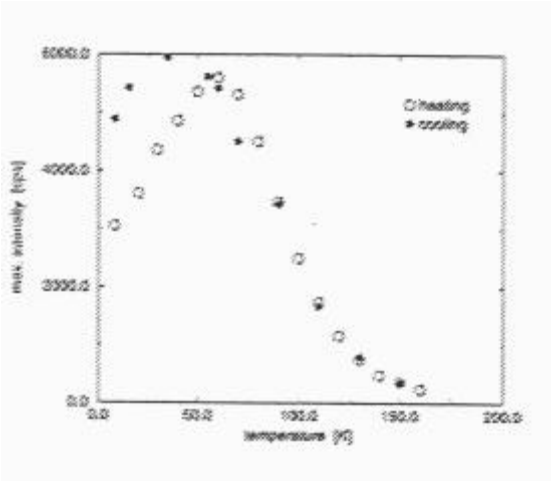

Fig. 2. Temperature dependence of the (4-2e,0,3) charge order peak measured during initial heating (open circles) and subsequent cooling (closed circles).

[1] J.M. Tranquada *et al*., Nature **375**, 561 (1995) ; J.M. Tranquada *et al.*, Phys. Rev. B **54**, 7489 (1996)
[2] J.M. Tranquada *et al.* Phys Rev. B **54**, 12318 (1996)

2.3.9 Softening of Lattice Vibrations and Superconductivity: Disappearance of the Mössbauer Spectrum of Non-Superconducting $PrBaCuFeO_{5+\delta}$ at Low Temperature

U. Amador, *Fac. Cc. Químicas, Universidad Complutense, Spain*, N.H. Andersen, *Department of Solid State Physics, Risø National Laboratory, Denmark*, J.L. Martínez, *Instituto de Ciencia de Materiales de Madrid, Spain*, N. Menéndez, J.Tornero, *Dpto. Química Física Aplicada, Universidad Autónoma, Spain*, E. Morán, and M. Ruiz-Aragón, *Dpto. Química Inorgánica. Fac. Ciencias Químicas, Universidad Complutense, Spain*

Since the discovery of high T_c superconductors much attention has been paid to understand their basic superconducting mechanisms. Some experimental results show that phonons could play an important role. Several authors have found that the absorption area of the Mössbauer spectra diminish below T_c, and these anomalies have been associated with a substantial softening of particular vibrational modes localized in the Cu-O bonds, which has been interpreted as a precursor of the onset of superconductivity in the framework of a modified BCS model.

The structure of the family of materials $REBaFeCuO_5$ (RE=Y, rare earth) (Fig.1), closely related to that of $YBa_2Cu_3O_{6+x}$, consists of double layers of squared pyramids [BO_5] (B=Fe/Cu) sharing the apical oxygen, where Ba^{2+} ions occupy the perovskite-like cuboctahedral A position and RE^{3+} is located in between the layers. The B positions are partially occupied by copper and iron, giving rise to [BO_2] layers with both metals randomly distributed. Thus, no pure copper-oxygen planes are present. Although the structure exists for all the rare earth metals, the anomalous dependence of the absorption area has only been observed, so far, in the praseodymium-containing compound. In this connection, the refinement of our neutron diffraction data revealed that some extra oxygen is located at (1/2, 1/2, 1/2) (Fig.1), with the amount of extra oxygen being as high as 0.24(1). As a first approach, the Cu and Fe atoms have a fivefold pyramidal coordination; however, due to the extra oxygen, about 25% of the B atoms are octahedrically coordinated. In this connection Mössbauer spectroscopy suggests that only the iron ions have a sixfold coordination in $PrBaCuFeO_{5.24}$. This material shows an abrupt drop of the resonant area of the Mössbauer spectra below ~180 K (Fig. 2) probably associated with the softening of a vibrational mode at the Cu/Fe-O_{apical} bond at a pseudo-octahedral $(Cu/Fe)O_6$ position. This effect is similar to that observed in some superconducting materials like Fe-doped $La_{1.85}Ba_{0.15}Ca_xFe_xCu_{1-2x}O_4$, $Bi_4Sr_3Ca_3(Cu,Fe)_4O_{16}$, $(Bi,Pb)_2Sr_2Ca_2Cu_3O_{10}$ and $YBa_2(Cu,Fe)_4O_8$ and in Sn-doped $EuBa_2Cu_{2.98}Sn_{0.02}O_7$. However, since the title material is not superconducting down to 1.7 K (Fig. 3) the phonon softening is not always a precursor of superconductivity.

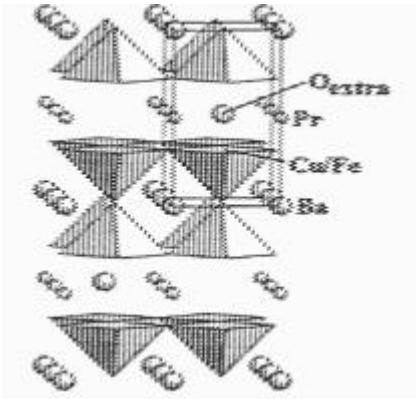

Fig. 1. Structure of $PrBaCuFeO_{5.24}$

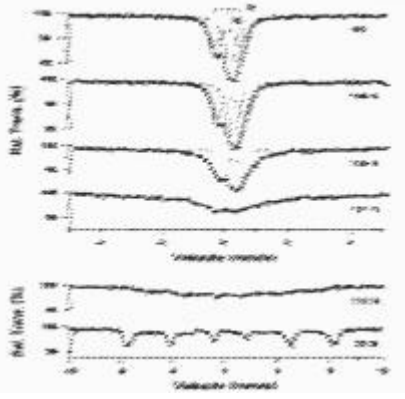

Fig. 2. Mössbauer spectra of $PrBaCuFeO_{5.24}$

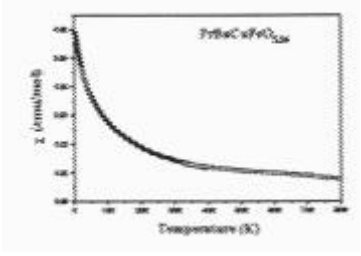

Fig. 3. Magnetic susceptibility of $PrBaCuFeO_{5.24}$

2.3.10 Evidence for Enhancement of T_c by Ortho-II Ordering in $YBa_2Cu_3O_{6.5}$

J. Madsen, N.H. Andersen, *Department of Solid State Physics, Risø National Laboratory, Denmark,* M. von Zimmermann, *HASYLAB, Germany*, T. Wolf, *ITP, Germany*

It is well known that the superconducting transition temperature T_c of $YBa_2Cu_3O_{6+x}$ ($0.35<x<1$) is time dependent if a crystal is quenched from the tetragonal disordered phase into the ordered orthorhombic phase in liquid nitrogen (LN_2). Theoretical model studies[1] have shown that this time dependence follows a redistribution of the oxygen atoms in the CuO_x basal plane into chains along the crystallographic *b* direction in the orthorhombic phase. This formation of oxygen chains in the basal plane is closely related to the charge transfer to the superconducting planes, and thereby to T_c.

Studies of the structural phase diagram have revealed that the orthorhombic phase consists of a high temperature ortho-I phase where chains form along the *b* direction with no ordering along *a*, and low temperature orthorhombic superstructure phases with additional ordering of the chains in the *a* direction. The T_c vs. *x* phase diagram shows a plateau like behaviour around x=0.5, which is believed to result from an enhanced charge transfer stabilised by the formation of an orthorhombic superstructure called the ortho-II phase.

Jorgensen *et al.*[2] have studied the effect on T_c of quenches from the tetragonal phase directly to the ortho-II phase on powder samples. We have investigated the effect of a possible additional oxygen ordering in the ortho-II superstructure phase by quenching a single crystal from the ortho-I phase to the ortho-II phase, to see if the initial ordering in the ortho-I phase is sufficient for an optimal charge transfer and T_c.

The crystal was prepared to x=0.5 under equilibrium conditions using a gas volumetric system. The diffuse ortho-II structure was detected in a diffraction experiment with room temperature correlation lengths of x_a=64Å, x_b=198Å and x_c=30Å along the *a*-, *b*- and *c*-directions respectively, and was seen to disappear as the temperature was increased above 180°C.

The sample was heated to 200°C in a furnace and then quenched to 77K with three different cooling rates. After each quench T_c was measured by the onset of the third harmonic in the ac-susceptibility signal. The faster the crystal is cooled to LN_2 temperature the less ortho-II ordering and thereby a lower amount of oxygen atoms in ortho-II domains. The first "quench" was performed by lowering the crystal from the furnace into an atmosphere of LN_2 gas. The next "fast quench" was done by lowering the bottom of the sampleholder into LN_2 while blowing LN_2 gas onto the crystal. The "very fast quench" was performed by pouring LN_2 directly on the crystal. The results of the experiment are seen in Fig. 1. The difference in T_c from the fully ordered ortho-II phase to the non ordered phase is 5K. After the "very fast quench" sequences of low temperature annealing and subsequent T_c measurements were performed. This showed a minimum temperature of 250K for the oxygen atoms to increase their order.

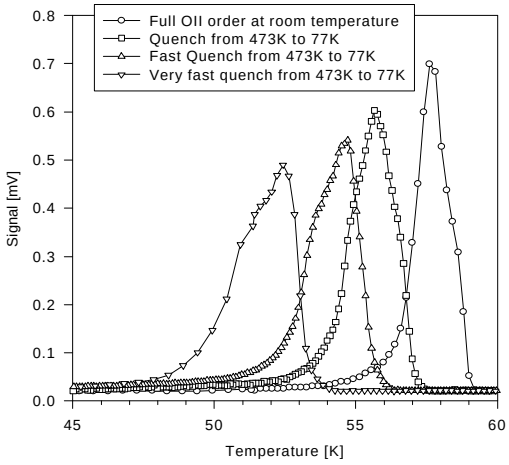

Fig. 1. Third harmonic ac-susceptometer signal measured on $YBa_2Cu_3O_{6.5}$ for 4 different quench treatments. The faster the temperature has been lowered from 473K to 77K, the lower the T_c. T_c is defined as the onset of the third harmonic signal.

[1] H. F. Poulsen *et al*. Phys. Rev. Lett. **66**, 465 (1991)

[2] J. D. Jorgensen *et al*., Physica C **167,** 571 (1990)

2.3.11 Local Lattice Distortions in $YBa_2Cu_3O_{6.95}$: Evidence of a Small Polaron Formation

L. Karlsson, R.L. McGreevy, *Studsvik Neutron Research Laboratory, Sweden,* N.H. Andersen, *Department of Solid State Physics, Risø National Laboratory, Denmark,* and L. Börjesson, *Department of Applied Physics, Chalmers University of Technology, Sweden*

The influence of the structural ordering on superconductivity in $YBa_2Cu_3O_{6+x}$ has been studied extensively by many techniques, but most of the structural information has been obtained from standard diffraction techniques that give the time and space average unit cell information. There are few studies, that have focused on the local structural distortions, in particular the existence of a double well potential and a split of the apical O(4) oxygen site bridging Cu(1) in the CuO_x basal plane and Cu(2) in the superconducting CuO_2 planes, but these studies have not established unambiguous results. We have obtained clear evidence for the existence of such local lattice distortions from analyses of the total scattering (*i.e.* both Bragg and energy integrated diffuse scattering) density of an $YBa_2Cu_3O_{6.95}$ powder sample. Measurement were performed on different diffractometers and samples, and the data have been carefully corrected and normalised to obtain a proper total scattering function *S(Q).* A radial distribution function *G(r)* consistent with *S(Q)* has been constructed by use of the inverse method, MCGR,[1] and *G(r)* has been used to establish a structural model via the RMC (Reverse Monte Carlo) method.[2] We have studied a model consisting of 12×12×4 unit cells, in which the positions of the 7459 atoms corresponding to $O_{6.95}$ are modified by a Monte Carlo method until *G(r)* calculated from it agrees with that constructed from *S(Q)*. The average crystallographic positions were determined by Rietveld refinement and used as the starting configuration in the initial RMC model. From the final equilibrated RMC model we have derived the partial radial distribution functions, $g_{ij}(r)$, and calculated the average crystallographic structure by mapping the atomic positions in the 576 unit cells onto one. Good agreement with the Rietveld results has been obtained. In particular, there is no split site for the average apical O(4) oxygen. Fig. 1 shows $g_{CuO}(r)$ for the crystallographically distinct pairs of Cu and O atoms. The positions and the widths of the first peaks for Cu(2)-O(2), Cu(2)-O(3), Cu(1)-O(4) and Cu(1)-O(1) at $r \approx 1.8$ Å are similar (O(2) is on the *a* axis and O(3) is on the *b* axis). However, the peak for Cu(2)-O(4) at ≈ 2.3 Å is about twice as wide and shows signs of splitting. This crucial result indicates that Cu(2) and O(4) are simultaneously both either closer or more distant from their centre of mass. Since the charge transfer from the CuO_x basal pane to the superconducting CuO_2 planes depends on the local Cu(2)-O(4) separation this is direct evidence of small polaron formation. Assuming that bipolarons with charge $2|e|$ are essential for superconductivity[3] their size may be estimated to be ≈ 13 Å, in close agreement with the superconducting correlation length.

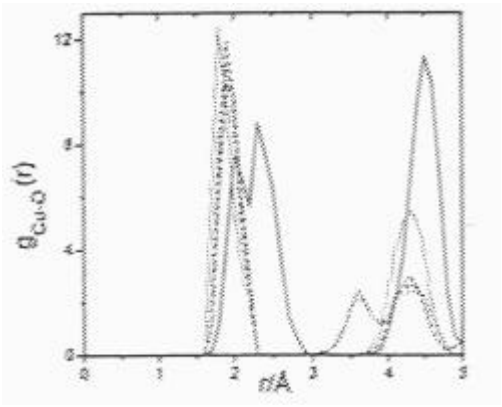

Fig. 1. Partial radial distribution functions: $g_{Cu(2)O(2)}(r)$ (dot), $g_{Cu(2)O(3)}(r)$ (short dot), $g_{Cu(1)O(1)}(r)$ (dash, divided by 2), $g_{Cu(1)O(4)}(r)$ (short dash) and $g_{Cu(2)O(4)}(r)$ (solid, multiplied by 4)

1 R.L. McGreevy, Materials Forum **166-169**, 45 (1994)
2 R.L. McGreevy, Nucl. Inst. Methods in Phys. Res. A **354**, 1 (1995)
3 A.S. Alexandrov and N.F. Mott, Prog. Phys. **57**, 1197 (1994)

2.3.12 Magnetic Structures in $NdBa_2Cu_3O_{6+x}$

A.T. Boothroyd, J.M. Reynolds, *Clarendon Laboratory, Oxford University, UK*, E. Brecht, *INFP, Forscungszentrum Karlsruhe, Germany*, T. Wolf, *ITP, Forscungszentrum Karlsruhe, Germany*, and N.H. Andersen, *Department of Solid State Physics, Risø National Laboratory, Denmark*

The ordering of the Pr ions in non-superconducting $PrBa_2Cu_3O_{6+x}$ was recently found to induce a significant change in the magnetic structure of the Cu sublattice.[1] It is of interest to know if the same type of rare-earth - Cu coupling exists in other compounds of the series. Accordingly, we have studied the Nd and Cu magnetic ordering in $NdBa_2Cu_3O_{6+x}$.

One reduced and one oxygenated crystal of $NdBa_2Cu_3O_{6+x}$ were investigated, together with several other reduced crystals of the same compound doped with various cations. The reduced crystals all exhibited Cu antiferromagnetism, with ordering temperatures above room temperature, and the AFI - AFII reorientation at lower temperatures (30 - 100 K). Nd antiferromagnetism was observed below T_{Nd} = 0.62 K in the oxygenated $NdBa_2Cu_3O_{6+x}$ crystal (Fig. 1) with a (1/2, 1/2, 1/2) arrangement of Nd moments. In the reduced crystal T_{Nd} = 1.6 K (Fig. 2), but the nature of the ordering was quite different. Instead of sharp magnetic Bragg peaks we observed a continuous ridge of scattering parallel to the crystal *c*-axis, indicative of strongly 2-dimensional ordering. Since powder neutron diffraction measurements did not reveal such 2*d* ordering[2] we are inclined to believe it is brought on by the AFI - AFII Cu spin reorientation which was only partly complete at 1 K in our crystal. Careful analysis of the Cu spin structure is underway to detect any changes associated with the Nd ordering.

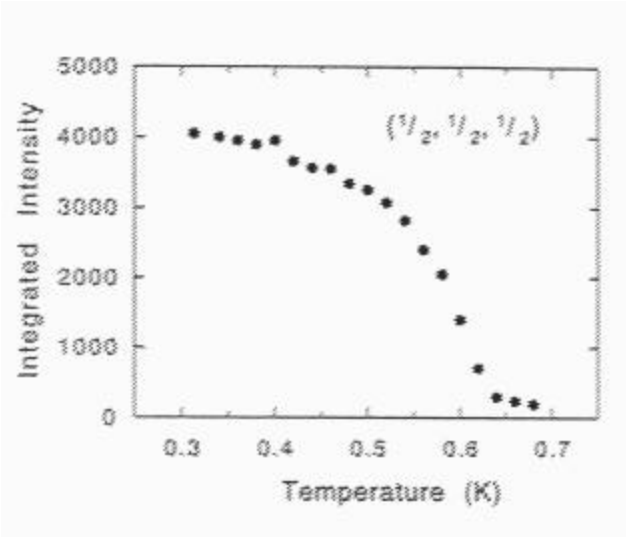

Fig. 1. Temperature dependence of the (1/2,1/2,1/2) magnetic reflection in an oxygenated crystal of $NdBa_2Cu_3O_{6+x}$

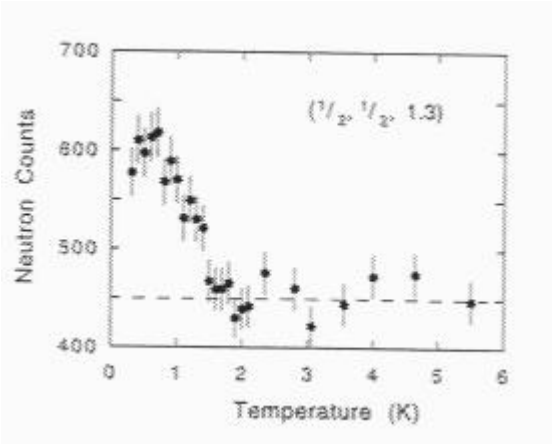

Fig. 2. Temperature dependence of the scattering at (1/2,1/2,1.3), a point on the ridge of diffuse scattering observed in the reduced crystal of $NdBa_2Cu_3O_{6+x}$

[1] A.T. Boothroyd, A. Longmore, N.H. Andersen, E. Brecht and Th. Wolf, to appear in Phys. Rev. Lett.

[2] T.W. Clinton, J.W. Lynn, J.Z. Liu, Y.X. Jia, T.J. Goodwin, R.N. Shelton, B.W. Lee, M. Buchgeister, M.B. Maple and J.L. Peng, Phys. Rev. B51 (1995) 15429.

2.3.13 Photoinduced Metastable State and Oxygen Ordering in $YBa_2Cu_3O_{6+x}$

M. Käll, N.H. Andersen, *Department of Solid State Physics, Risø National Laboratory, Denmark,* M. Osada, M. Kakihana, L. Börjesson, *Department of Applied Physics, Chalmers University of Technology, Sweden,* R. Liang, P. Dosanjh and W.N. Hardy, *Department of Physics, University of British Columbia, Canada*

Raman scattering spectra of oxygen deficient single-crystal $YBa_2Cu_3O_{6+x}$ superconductors with local ortho-III order exhibit intense multiple-phonon scattering from normally Raman forbidden vibrational modes.[1] The origin of this unusual scattering is found to be a broad electronic resonance centred at ~2.1 eV, see Fig 1. The resonance can only be excited if the light is polarised along the CuO-chains, and moreover, it can be "bleached" away if the sample is illuminated for sufficiently long time, as can be seen in Fig. 1. If the sample is kept in the dark at room temperature (RT) the resonance returns within ~24h. At higher temperatures the recovery time increases rapidly and above ~125 ^oC it is no longer possible to bleach the resonance. This activated behaviour is illustrated in Fig. 2, which shows the equilibrium strength of the resonance, *i.e.* after bleaching in a laser-field, as a function of temperature. The transition has a midpoint at ~75 ^oC and mirrors the temperature dependence of the ortho-III superstructure reflections detected by hard X-ray measurements of the same de-twinned $YBa_2Cu_3O_{6.77}$ single crystal.[2] The striking similarity between the two experiments can be explained if one assumes that the light induces an electronic transition that relax through a structural modification of the CuO-chains. Increasing the temperature above the threshold energy for oxygen diffusion will then both destabilise the bleached state and disorder the ortho-III structure. Although the exact nature of the electronic resonance and the photo-induced structural modification is not clear at present, the Raman measurements illustrate the strong coupling between electronic and structural degrees of freedom in the CuO-chains, and constitute the first inelastic scattering measurements of the superstructure phase transition in $YBa_2Cu_3O_{6+x}$ superconductors.

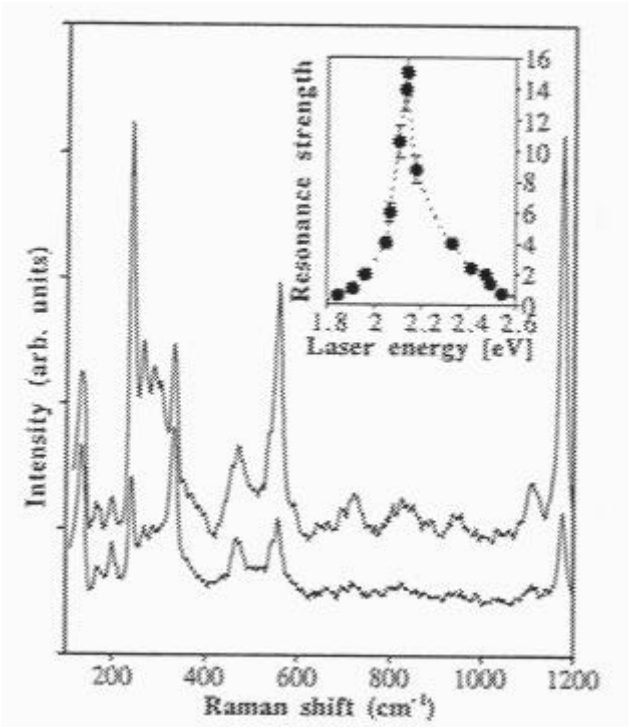

Fig. 1. Ramann spectra of $YBa_2Cu_3O_{6.77}$ at RT. Upper spectrum measured during the first 100 sec of illumination (unbleached state) and lower spectrum (bleached state) measured after 1 hour of illumination with 2.41 eV photons (100 W/cm^2). Inset shows resonance profile at 120 ^oC.

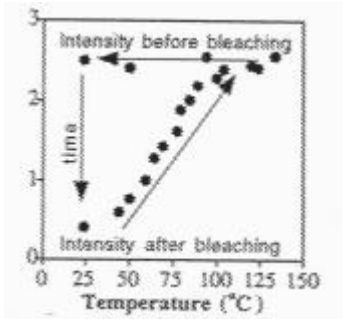

Fig. 2. Resonance strength in bleached and unbleached states for an incident laser energy of 2.41 eV as function of temperature in the vicinity of the ortho-III phase transition.

---

1 M. Käll *et al.*, Risø-R-863(EN), 50 (1996)

2 P. Schleger *et al.*, Physica C **241**, 103 (1995)

2.4 Structures and Defects

2.4.1 Soft Mode Behaviour and Lattice Melting in Na_2CO_3

M.J. Harris, *Rutherford Appleton Laboratory, ISIS Facility, Didcot, UK*, D.F. McMorrow, *Department of Solid State Physics, Risø National Laboratory*, K.W. Godfrey, *Oxford Physics, Clarendon Laboratory, Oxford, UK*

It is thought that when a crystal melts, the atomic displacements diverge, producing a complete breakdown of the crystalline order. Theoretical studies have shown that a similar divergence of the atomic displacements should also occur at a structural phase transition that is driven by a two-dimensional phonon softening; this is known as lattice melting. In contrast with conventional melting, crystalline order returns continuously on heating above the lattice melting transition, so that it is a fully reversible and continuous process.

The only compound known to exhibit this unusual behaviour is Na_2CO_3, where the process of lattice melting occurs at a hexagonal-to-monoclinic transition at 760 K.[1,2,3,4] This transition is driven by a complete softening of the transverse acoustic modes over all wave vectors in the **a*-b*** plane, and we set out to investigate it in detail using TAS7. We had two main objectives; the first was to characterise the lineshape of the soft transverse acoustic mode at T_c, and the second was to obtain the detailed temperature-dependence of the soft elastic constant, C_{44}, by measuring the dispersion of the phonon branch as it softens on approaching the transition. Both of these objectives were achieved, and in particular, the lineshape of the soft mode turned out to be very interesting. Constant-*Q* scans for [*h*,0,2] wave vectors showed that the soft mode is characterised by quasielastic scattering across the whole of the **a*-b*** plane at T_c. Rather than being Lorentzian (as is usual for dynamic critical scattering), the lineshape of the quasielastic scattering is closer to being exponential, as shown in the Fig. 1. This implies that the time correlations decay algebraically, which is an unusual result.

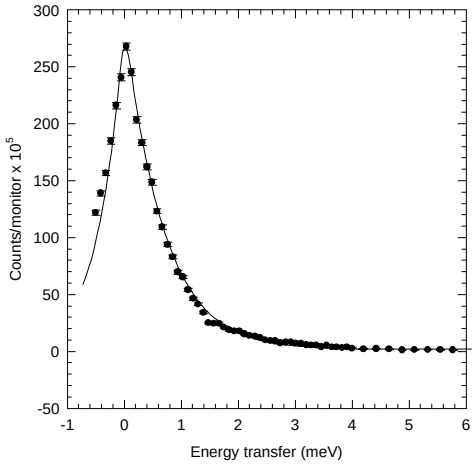

Fig. 1. A constant-Q energy scan at T_c (752.5 K) at Q=(0.2,0,2) from Na_xCO_3. The solid line represents the fit of an exponential lineshape to the data.

1 M.J. Harris *et al*., (1993). Phys. Rev. Lett. **71**, 2939
2 I.P. Swainson *et al*., (1995). J. Phys: Condensed Matter. **7**, 4395
3 M.J. Harris *et al*., (1985). Phys. Rev. B **51**, 6758
4 M.J. Harris *et al*., (1996). J. Phys: Condensed Matter. **8**, 7073

2.4.2 Powder Neutron Diffraction Studies of the $K_2S_2O_7$-$KHSO_4$ System

K. Nielsen, *Department of Chemistry, Technical University of Denmark*, B. Lebech, *Department of Solid State Physics, Risø National Laboratory, Denmark* and Hae Seop Shim, *Korea Atomic Energy Research Institute, Taejon, Korea*

Catalysts for the production of sulphuric acid and for flue gas cleaning are based on V_2O_5 dissolved in pyrosulfate/hydrogen sulphate melts. The detailed chemical and structural information about the binary $K_2S_2O_7$-$KHSO_4$ system is therefore important for the understanding of the structure and stability of the catalytically active vanadium complexes.

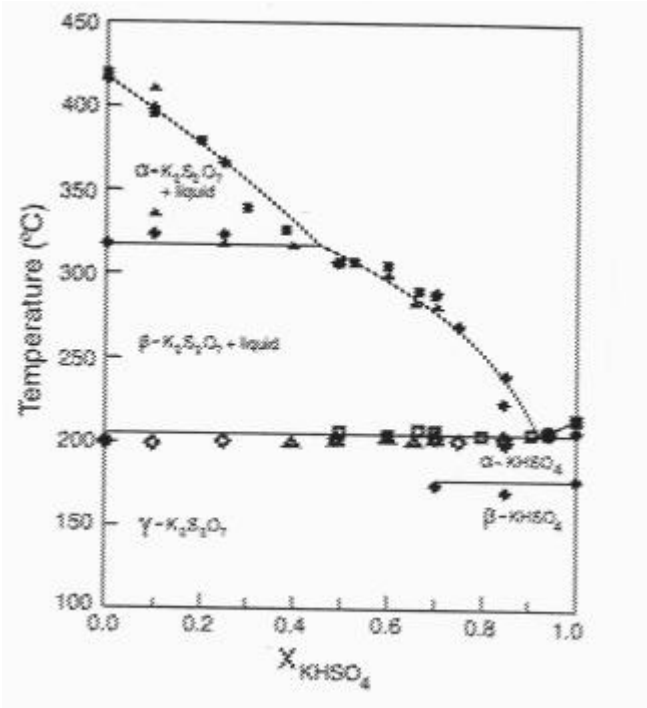

Based on the phase diagram for the binary system (see Fig. 1) by Eriksen et. al.[1] neutron powder diffraction at temperatures in the range 25 to 340°C have been performed on the pure compounds and a mixture with a 0.25 mole fraction of $KHSO_4$. Both $KHSO_4$ and $K_2S_2O_7$ undergo solid-solid phase transitions, $KHSO_4$ at 178°C, and $K_2S_2O_7$ at 318°C. The structures of these two high temperature compounds are unknown. The enthalpy change (ΔH) at the phase transition for $K_2S_2O_7$ is of the same order of magnitude as the enthalpy change (ΔH_{fus}) at the melting temperature (420°C), so major structural changes are expected.

Quite unexpectedly, the diffraction data at 187°C of the solid mixture does not show any of the pure $KHSO_4$ Bragg reflections despite the fact that the phase diagram does not indicate any formation of mixed compounds. A detailed examination of the powder diffraction data is in progress.

[1] K.M. Eriksen, R. Fehrmann, G. Hatem, M. Gaune-Escard, O.B. Lapina and V.M. Mastikhin, J. Phys. Chem. **100**, 10771 (1996)

2.4.3 Structure of the Cone Conformer of a Tetrakis(methylthio)-tetrapropoxy-calix[4]arene

T. Schultz, *Department of Solid State Physics, Risø National Laboratory, Denmark,* R.G. Hazell, *Department of Inorganic Chemistry, Aarhus University, Denmark* and M. Larsen, *Department of Solid State Physics, Risø National Laboratory, Denmark*

Calixarenes are a class of macrocyclic compounds comprising 4-16 or more phenolic moieties joined in a cyclic array at the meta positions by methylene groups. They are prepared from p-alkyl-phenols and formaldehyde in the presence of a catalytic amount of base. The size of the ring can be controlled by the nature and amount of the base. The 5,11,17,23-tetrakis(methylthio)-25,26,27,28-tetrapropoxy-calix[4]arene contains four methylthio groups, introduced, in order to make a calixarene suitable for self assembly on gold surfaces. Modified calixarenes having thiol groups anchored to the rim of the bowl shaped assembly of aromatic rings, have are known to produce monolayers on clean flat gold surfaces.[1]

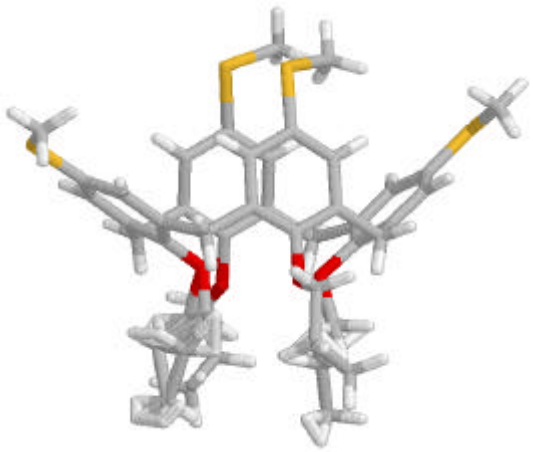

Fig. 1 Rasmol drawing of one calixarene molecule, displaying the disordered propoxy groups.

The calixarenes have an outstanding capacity as molecular receptors, due to their variable chemical modification potential and their conformational pliability which enables them to adapt to the shape of suitable guest molecules. The possibility of making well defined monolayers of calixarenes, opens up a whole new range of experimental characterization techniques, among those Grazing Angle X-ray Diffraction using synchrotron radiation. The present calixarene, 5,11,17,23-tetrakis(methylthio)-25,26,27,28-tetrapropoxy-calix[4]arene, is believed to form a monolayer on gold(111) surfaces, however we do not yet know to what extent a crystallographically ordered surface is obtained. In order to interpret grazing angle X-ray diffraction data, recorded at the BW2 beamline, Hasylab, Hamburg, we needed to determine the 3-D crystallographic structure which is reported here.

The data was collected within one week at the Department of Inorganic Chemistry Aarhus University, using a 4-circle Huber diffractometer, equipped with a conventional Mo X-ray tube. During data collection the crystal was cooled to 120 K in order to reduce thermal motion. Data were corrected for background, Lorentz and polarization effects. The structure was solved using SIR92 and the positions of H atoms were calculated. Non-H atoms were refined anisotropically using a modification of ORFLS. The propoxy groups attached to the two phenyl groups inclined to the axis of the molecule exhibit a two-fold disorder. The disorder influences only the two middle atoms of the propoxy groups, and the occupation factors were refined to 0.50:0.50 for one propoxy group and 0.43:0.57 for the other.

Space group	Monoclinic, P 21/n
a	12.479(3) Å
b	27.145(8) Å
c	12.591(4) Å
β	97.40°
Volume	4240(2) $Å^3$
Z	4
Temperature	120 K
Density	1.22 g/cm^2
R-factor	5.2 %
G.O.F.	1.458

[1] B. Huisman, E.U.T. Velzen,., C.J.M. Veggel, J.F.J. Engbersen, and D.N. Reinhoudt, Tetrahedron Letters (1995) **18**, 3273-3275

2.4.4 The 154 K Phase Transition of Tetramethylammonium Tetrafluoroborate, NSLS 1996

T. Schultz, *Department of Solid State Physics, Risø National Laboratory, Denmark,* F.K. Larsen, *Department of Inorganic Chemistry, Aarhus University, Denmark*

Tetramethylammonium Tetrafluoroborate (TMT) is an organic salt used as a supporting electrolyte in the field of electrochemistry. TMT has a number of temperature dependent, structural features, which have been only partly described in the litterature. G. Zabinska et al.[1] have calculated transition enthalpies for the two known phase transitions at 154K and 601K using DSC, and G. Guseppetti et al.[2] have solved the room temperature structure of TMT using single crystal X-ray diffraction techniques, though the description of the disordered BF_4^- unit is inadequate.

Single crystal measurements performed at 298K (see Fig. 1), 160K and 140K at Aarhus University, has established a description of the structural changes occurring in TMT at 154K. From these measurements it is clear that TMT has a tetragonal unit cell at 298K containing 16-fold disordered BF_4^- ions and ordered $(CH_3)_4N^+$ ions. Lowering the temperature to 160K diminishes the disordering of BF_4^- to 8-fold, freezing out a lowest energy configuration of these ions. At around 160K diffuse diffraction peaks appear at half order h- and k-values, the intensity of these grows rapidly upon further cooling. At around 155K the half order diffraction peaks, start to split into 2 or 4 components. This splitting is explained by a model containing 4 monoclinic (or possibly orthorhombic) twins, with unit cells twice as big as the tetragonal room temperature cell.

In the period August 21 to August 31, 1996, we performed single crystal measurements at the 4-circle instrument at beam-line X3A1, NSLS, Brookhaven National Laboratory, New York. Using Imaging Plates, we collected TMT data sets at 298K, 240K, 155K, 145K and 15K. In addition careful measurements of the diffuse half order Bragg peaks and of the unit cell volume as a function of temperature (see Fig. 2) was carried out which will enable us to calculate the order parameter of the 154K phase transition.

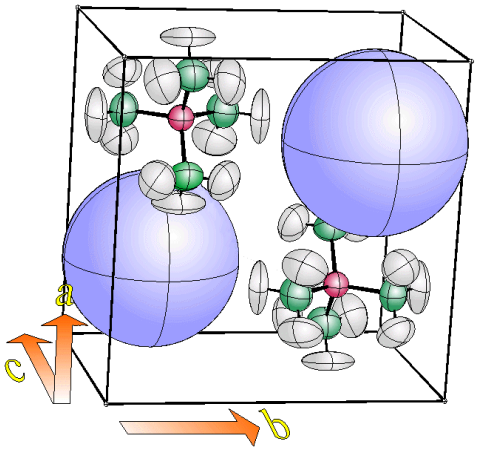

Fig. 1 The tetragonal unit cell of TMT at 298K, showing the ordered tetramethylammonium ions and the disordered tetrafluoroborate ions (indicated using blue balls).

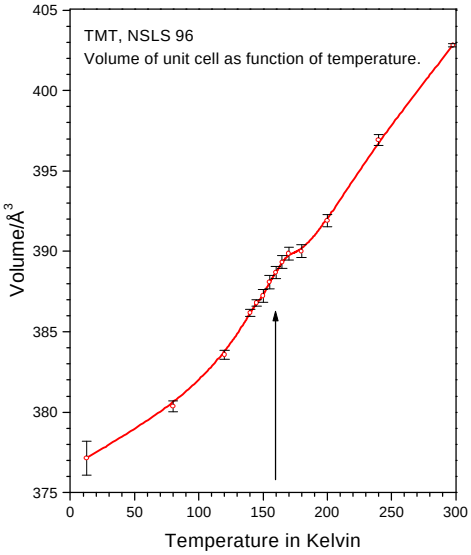

Fig. 2 The variation of the TMT unit cell volume as a function of temperature, clearly showing the continuous phase transition at around 154K. (NSLS, October 1996)

[1] G. Zabinska, P. Ferloni, and M. Sanesi, Thermochimica Acta **122**, 87-94(1987)

[2] G. Giuseppetti, F. Mazzi, C. Tadini, P. Ferloni, and S. Torre, Zeitschrift für Kristallographie **202**, 81-88(1992)

2.4.5 Structural Studies of the Tetrathiafulvenyl Salt of Trichloroacetic Acid by Neutron Diffraction

F.C. Krebs and B. Lebech, *Department of Solid State Physics, Risø National Laboratory, Denmark*

Recent studies[1] of the solvent dependency of the reaction between TTF and trichloroacetic acid have shown very different reaction pathways leading to different crystalline products. In one particular case the structure of the crystalline product was solved by X-ray diffraction[2] and found to contain hydrogen bonded trichloroacetate dimers. Very large crystals of the material could be grown and these showed to be suitable for neutron diffraction studies so as to establish the nature of the hydrogen bonds.

An initial data collection on a large crystal of the material (using TAS2, the 4-circle neutron diffractometer at RISØ) was undertaken to establish whether the crystal diffracted well enough for complete structural resolution by neutron diffraction. The initial data collection have shown the crystal to be of sufficient quality for a full data collection which will be launced in November 1996 with a two month duration. Structure refinement with the structure obtained by X-ray diffraction using the initial dataset obtained by neutron diffraction (approximately 600 reflections) with constraints gave R1 = 0.0358 and wR2 = 0.0553.

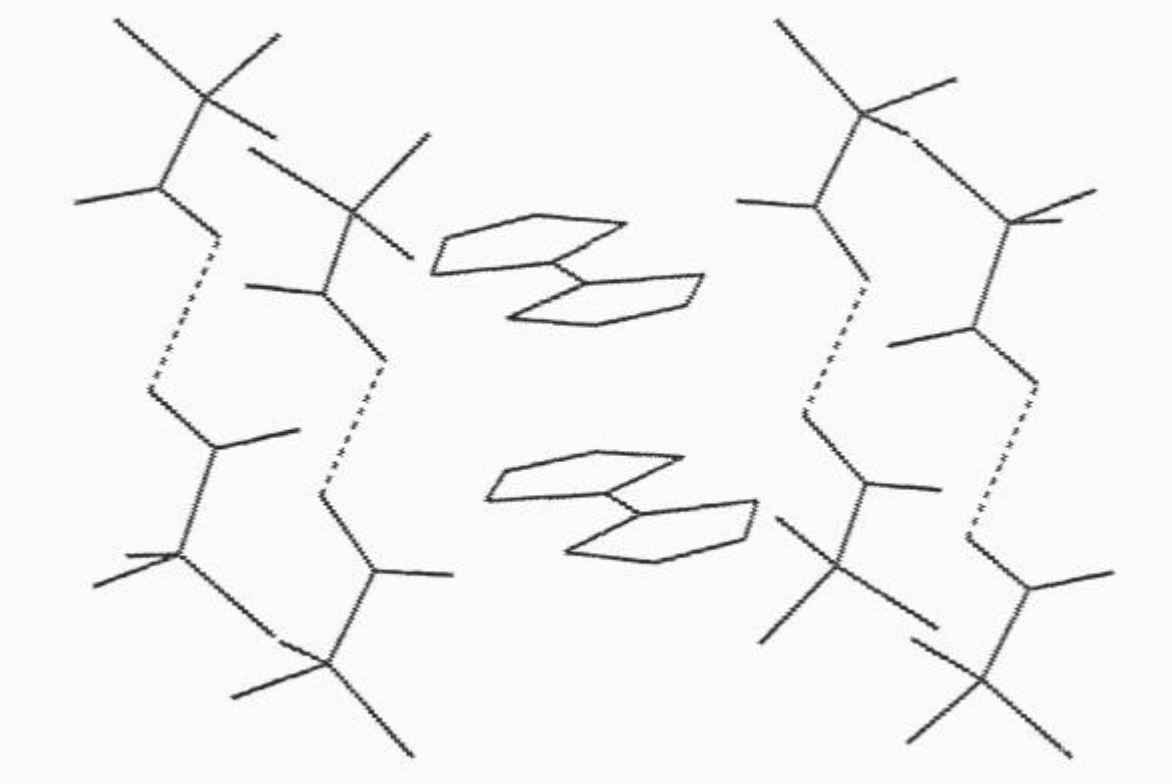

Fig. 1. Showing the TTF dimer surrounded by hydrogen bonded trichloroacetate dimers.

[1] F.C. Krebs, M. Fourmigué and P. Batail in the D.E.A. report by Frederik C. Krebs, Construction de Matériaux Sagaces à Partir de Molécules Organiques Fonctionnalisées: Vers un Contrôle des Structures et des Proprietés, Institut des Matériaux de Nantes, France (1995)

[2] T. Pittelkow, S.B. Schougaard and F.C. Krebs, private communication

2.4.6 Nuclear Density in MADMA[1] and Borax for Charge Density Studies

H. Birkedal, D. Madsen, P. Harris, S. Larsen, *Centre for Crystallographic Studies, Copenhagen, Denmark* and B. Lebech, *Department of Solid State Physics, Risø National Laboratory, Denmark*

Among intermolecular interactions, hydrogen bonds play an important role in the determination of significant topological features of chemically interesting systems. As an example can be given protein/DNA folding and molecular recognition. One of our main interests is therefore to obtain an understanding at a detailed level of intra- and intermolecular interactions in molecular crystals. Investigations of the electronic charge density in the regions of interaction give information on the character of these, thereby enabling us to understand which features are dominant in these interactions. In studies of the charge density of crystals using x-ray diffraction it is essential to have detailed information about nuclear positions and motion. This information can be obtained from the x-ray diffraction experiment for heavier atoms only. This is especially a problem when the compound of interest contains hydrogen or deuterium, because their electron distribution is removed from the nuclei by chemical bonding. Furthermore hydrogen/deuterium atoms are often engaged in some of the most important interactions − hydrogen bonds − thus a very important feature cannot be accurately studied by x-ray diffraction alone. This problem can be solved by supplementing the x-ray data with neutron diffraction data. In order to obtain an accurate description of especially the hydrogen/deuterium nuclear parameters we have therefore performed single crystal diffraction experiments at the four-circle neutron diffractometer TAS2.

Last year both x-ray and neutron data were collected on methylammonium deuterium maleate (MADMA). The space group of MADMA could not be determined unambiguously by the results from the x-ray experiment, however, the neutron data set was used to determine that MADMA crystallizes in the centric space group Pnam. The two very short hydrogen bonds are thereby imposed a crystallographic symmetry. The displacement parameters for the hydrogen/deuterium atoms were fixed in the multipole refinement of the x-ray data[2]. The analysis of the multipole model for MADMA showed transferability of the properties of the electron density in all bonds in the cation compared to the cation in a previous investigated compound, Methylammonium hydrogen succinate monohydrate[3]. With the purpose of studying hydrogen bonds in boron compounds we have collected neutron data on deuterated borax ($Na_2B_4O_7{\cdot}10D_2O$). We are currently processing the borax data.

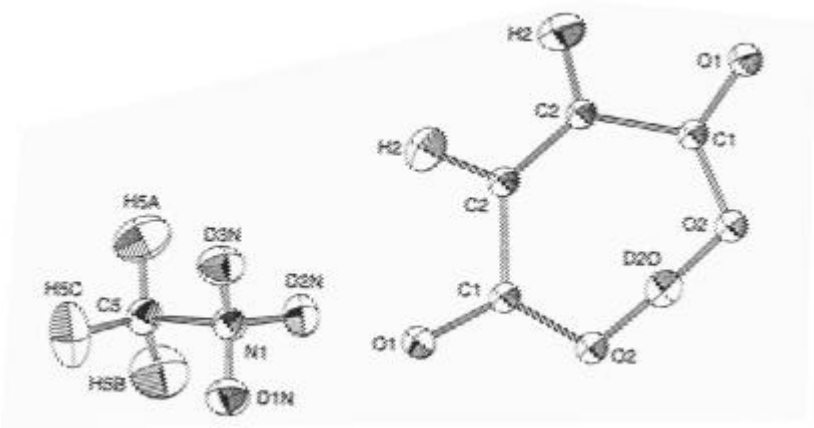

Fig. 1. Refined neutron structure of MADMA shown with 50% nuclear probability ellipsoids (ORTEP-II[4]).

[1] Methylammonium Deuterium Maleate
[2] D. Madsen, C. Flensburg and S. Larsen, to be submitted to J. Phys. Chem. (1996)
[3] C. Flensburg, S. Larsen and R. F. Stewart, J. Phys. Chem. **99**, 10130 (1995)
[4] C.K. Johnson, Report ORNL-5138, Oak Ridge National Laboratory, Tennessee, USA (1976)

2.4.8 Coarsening of Bimodal Coherent γ‘ Particle Size Distributions in Ni-Al-Mo Alloys

J.J. Cruz, H.A. Calderon, *Departamento de Ingeniería Metalúrgica. ESIQIE-IPN, Mexico,*
J.S. Pedersen, *Department of Solid State Physics, Risø National Laboratory, Denmark*

The coarsening kinetics of bimodal distributions of coherent γ‘ particles in Ni-base alloys is investigated. The bimodal distribution of particles is created by aging at two different temperatures. Small angle neutron scattering (SANS) experiments have been carried out in order to determine the particle size distributions (PSD) of the smaller particles. The alloys investigated have the following compositions: Ni-14 at.% Al, Ni-10 at.%Al-5 at.%Mo and Ni-6.5 at.%Al-10 at.%Mo. The statistical reliability provided by SANS is difficult to use owing to the complications in the determination of particle size distribution. Common quantities determined in SANS analysis are subject to large uncertainty (*e.g.* the Guinier radius) in cases where an anisotropic distribution of particles is present. Most metallic systems investigated in the field of coarsening present anisotropic scattering patterns and therefore it is important to develop a method to evaluate reliably the particle size distribution from SANS intensities.

The current results show some progress in the determination of PSDs from anisotropic scattering patterns. The method should be appropriate to deal with particles that show strong spatial and orientational correlations. The strong correlations result in characteristic peaks in the bidimensional SANS pattern. Instead of simulating these 2D patterns and adjusting model parameters to fit them (about 10 000 positions), projections of the scattered intensity on selected directions have been obtained. This produces one dimensional scattering curves which are used for the subsequent analysis. An earlier described method based on clusters containing only a small number of particles is used for determining size distributions.[1] Results are given in Fig. 1 for one of the investigated alloys. Fig. 2 shows a comparison to measurements made by transmission electron microscopy. It can be seen that a relatively good agreement has been reached between the two experimental methods. Comparison to TEM results is still incomplete and research is being done to satisfy this objective.

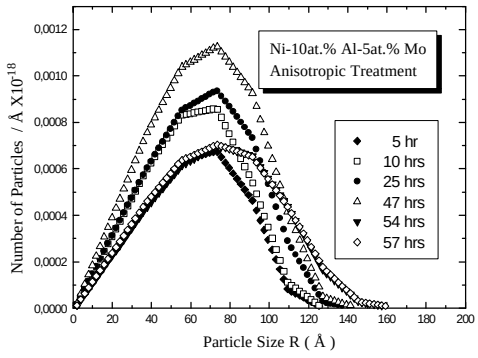

Fig. 1. Particle size distributions in the alloy Ni-10 at.%Al-5 at.%Mo.

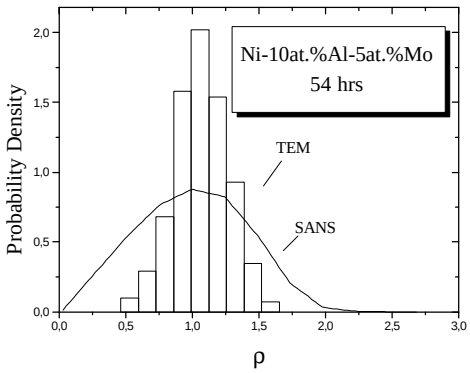

Fig. 2. Comparison of PSDs determined by SANS and TEM.

[1] P. Vyskocil, Dissertation ETH-Zürich Nr. 10396, 1994

2.4.9 Coarsening of β‘ Coherent Particles in Fe-Ni-Al-Mo Alloys

H.J. Dorantes, H.A. Calderon, *Departamento de Ingeniería Metalúrgica. E.S.I.Q.I.E.-I.P.N., Mexico,* J.S. Pedersen, *Department of Solid State Physics, Risø National Laboratory, Denmark*

The alloys Fe-10at.%Ni-15 at.%Al and Fe-10 at.%Ni-15 at.%Al-1 at.% Mo have been investigated. Bimodal distributions of precipitates have been created by double aging procedures. Small angle neutron scattering is being used to determine the particle size distribution of the smaller particles created by aging at 923 K. A larger population of particles is also present in the specimens but these particles are too large to be detected by a SANS measurement. Single crystals with a cylindrical form, having the direction [100] parallel to their long axis have been used for the measurements. The SANS patterns have anisotropic shapes, *i.e.*, they show interference peaks along [001] directions and they do not have circular symmetry. The distribution of particles is not homogeneus in space as shown by the interfence peaks in the patterns. Nevertheless investigation of the coarsening kinetics requires analysis of such patterns since common quantities (*e.g.* Guinier Radius) are subject to extremely large uncertainities. The analysis technique employed to determine the particle size distributions is based on linear averages done on the bidimensional patterns. Specific directions have been selected to average the measured intensity. An earlier described method based on clusters containing only a small number of particles is used for determining size distributions.[1] This is done instead of calculating the scattered intensity for a system with many particles. Fig. 1 shows results of the determination of particle size distributions in the two alloys under investigation for different aging times. Comparison to measurements made by transmission electron microscopy is in progress.

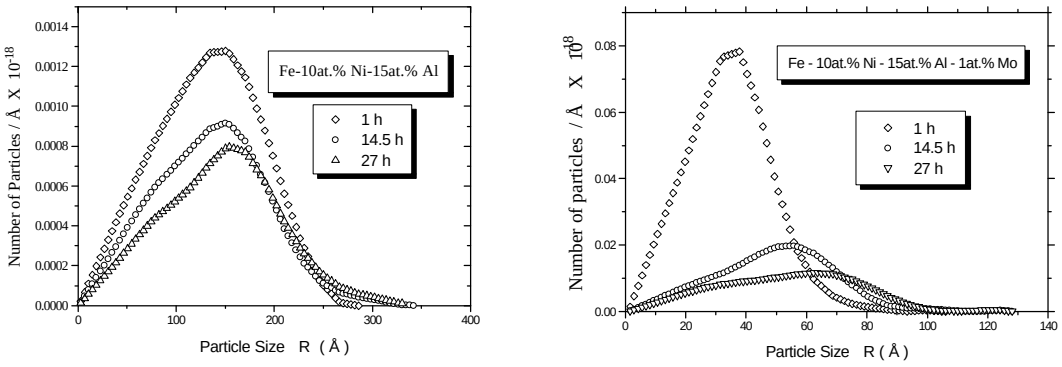

Fig. 1. Particle size distributions after different aging times in the two alloys under investigation.

[1] P. Vyskocil, Dissertation ETH-Zürich Nr. 10396, (1994)

2.5 Surfaces and Interfaces

2.5.1 Self Assembled Monolayers of Tetrakis(methylthio)-Tetrapropoxy-Calix[4]arene on Crystalline Gold(111) Surfaces

T. Schultz, R. Feidenhans'l, I. Johannsen, M. Jørgensen, M. Larsen, *Department of Solid State Physics, Risø National Laboratory*

The 3-dimensional structure of tetrakis(methyl-thio)-tetrapropoxy-calix[4]arene is described in contribution 2.4.3. The methyl-thio groups anchored to the rim of the bowl shaped assembly of aromatic rings, are responsible for the ability of this compound to produce monolayers on clean flat gold surfaces.

The possibility of making well defined monolayers of calixarenes, opens up a whole new range of experimental techniques for studying the mechanisms that gives them their outstanding capacity as molecular receptors. Of these we have until now performed in-house X-ray Photoelectron Spectroscopy and Grazing Angle X-ray Diffraction at the BW2 beam-line, Hasylab, Hamburg.

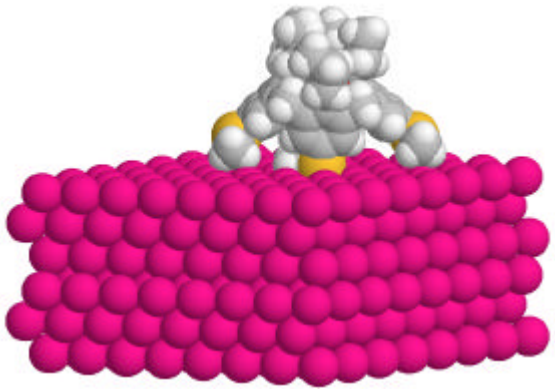

Fig. 1 Rasmol drawing of one calixarene molecule on top of a (111) oriented gold crystal, artists impression.

The process of self assembly of the calixarenes on gold, occurs within minutes, when a gold substrate is immersed into a dilute (mM) solution of calixarene in a mixture of ethanol and chloroform. For X-ray diffraction measurements, a gold(111) single crystal is chosen due to the inertness of gold and in order to increase the likelihood that the calixarene monolayer has crystalline properties. In-house XPS measurements, have shown that the chemical composition of a gold(111) surface after chemisorption of the calixarenes, corresponds closely to that expected from a single monolayer (Table 1). After a few days of exposure to ambient air, the amount of oxygen on the surface increases drastically, a process which is not yet understood but may be due to either oxidation of the methylthio groups or binding of carbon dioxide to the surface.

Table 1 Results from XPS measurements on a calixarene coated Au(111) single crystal.

XPS results	C	O	S	Au
Freshly prepared monolayer	48.8%	2.4%	2.1%	46.5%
After exposure to air (2 weeks)	29.6%	30.4%	1.5%	38.5%

In order to determine the microscopic structure of the calixarenes as they sit on top of the gold surface, we have performed grazing angle X-ray diffraction experiments at Hasylab. However these experiments have indicated that the crystalline quality of the monolayer is not sufficient for that kind of experiments. Atomic Force Microscope measurements are planned and hopefully will increase our knowledge on the calixarene monolayers in direct space enabling us to optimize the crystalline quality.

2.5.2 Structure and Orientation of Sn Precipitates in Epitaxial Layers of $Si_{1-x}Sn_x$

M.F. Fyhn, J. Chevallier, S.Y. Shiryaev, A.N. Larsen, *Institute of Physics and Astronomy, University of Aarhus, Denmark.* R. Feidenhans'l and J. Als-Nielsen, *Niels Bohr Institute, University of Copenhagen, Denmark*

Binary group IV alloys have gained considerable interest during the last decade. These alloys can be used to make devices, compatible with conventional Si technology, which are faster than structures based on Si alone. The research has primarily been devoted to $Si_{1-x}Ge_x$, and $Si_{1-x}C_x$ while $Si_{1-x}Sn_x$ only recently was grown of high structural quality.[1] $Si_{1-x}Sn_x$ has a smaller bandgab than Si and is expected to have electrical properties suitable for heterostructure devices.[2]

We have grown $Si_{1-x}Sn_x$, x~5.5% by molecular beam epitaxy on Si <001> and $Si_{1-x}Ge_x$ substrates.[3] Due to the large difference in lattice constant between Si and Sn (20%) and the low solubility of Sn in Si (~0.1%) the $Si_{1-x}Sn_x$ layers are metastable, and we are currently studying the relaxation of $Si_{1-x}Sn_x$ at different temperatures. The relaxation channels have been found to be precipitation and generation of misfit dislocations. The Sn precipitates in epitaxial $Si_{1-x}Sn_x$ layers have been studied by transmission electron microscopy, and the figure below shows a plan-view micrograph of the diffraction pattern from $Si_{1-x}Sn_x$, x=5.3% annealed at 950°C for 1 hour. The additional spots seen between the ones related to the diamond-structure of $Si_{1-x}Sn_x$ are due to precipitates, which have lattice constants different from the surrounding matrix. X-ray diffraction measurements at Risø National Laboratory and at DESY, Hamburg have been performed to measure the lattice constants in a more precise way and to determine the orientation of the precipitates. These measurements confirm the texture seen by TEM (as figure) and verifies that two different solid phases of Sn (α-Sn and β-Sn) are present.

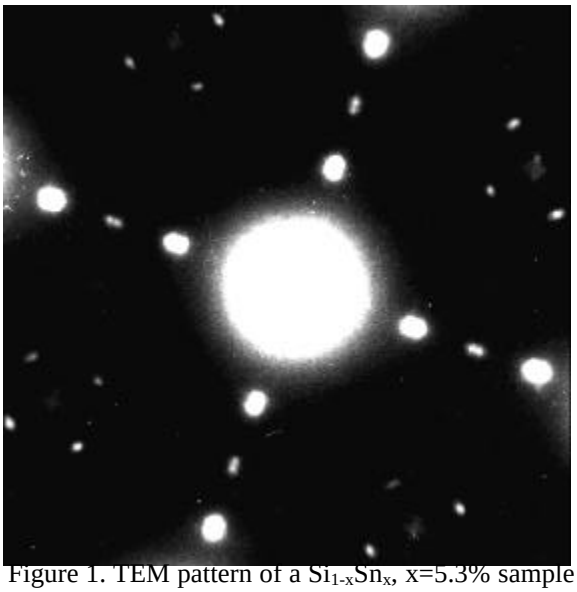

Figure 1. TEM pattern of a $Si_{1-x}Sn_x$, x=5.3% sample annealed at 950°C for 1 hour

[1] S. Yu. Shiryeav, J. Lundsgaard Hansen, P. Kringhøj and A. Nylandsted Larsen, Appl. Phys. Lett. 67, 2287 (1995)

[2] A. T. Khan, P. R. Berger, F. J.Guarin and S. S.Iyer, Appl. Phys. Lett. 68, 3105 (1996)

[3] M. F. Fyhn, S. Yu. Shiryaev, J. Lundsgaard Hansen and A. Nylandsted Larsen, Appl. Phys. Lett. 69, 394 (1996)

2.5.3 Bismuth-induced restructuring of the GaSb(110) surface

T. van Gemmeren, L. Lottermoser, G. Falkenberg, L. Seehofer, and R.L. Johnson, *II. Institut für Experimentalphysik, Universität Hamburg, Germany,* L. Gavioli, and C. Mariani, *Dipartimento di Fisica, Universita di Modena, Italy,* R. Feidenhans'l, E. Landemark, D.-M. Smilgies, and M. Nielsen, *Risø National Laboratory, Denmark*

Metal-semiconductor interfaces are of considerable interest for both fundamental and technological reasons. Most vapor-deposited metals react with III-V semiconductors to form complex, nonstoichiometric interfaces, however, it is generally believed that the semimetals Sb and Bi form nonreactive, ordered interfaces. Column-V metals on III-V semiconductors are frequently regarded as examples of ideal adsorbate-semiconductor heterojunctions. We present a new structural model which shows that this simple picture is generally not true and that column V elements can induce significant restructuring of the substrate.

The structure of the GaSb(110)(1×2)-Bi reconstruction was determined using surface x-ray diffraction, scanning tunneling microscopy and photoelectron spectroscopy. The x-ray diffraction experiments were performed at the wiggler BW2 beamline in HASYLAB. The ideal GaSb(110) surface is terminated with zigzag chains of anions and cations running in the $[1\,\bar{1}\,0]$ direction. In the Bi induced (1×2) reconstruction we find that every second zigzag chain in the uppermost substrate layer is missing. The surface is terminated by a full monolayer of Bi atoms which also form zigzag chains. The Bi atoms in the chains are alternately bonded to the first and second layer substrate atoms and the Bi chains are tilted 34.2° with respect to the (110) plane. We propose that the formation of the reconstruction is driven by the very favorable bonding geometry in the adsorbate chains.

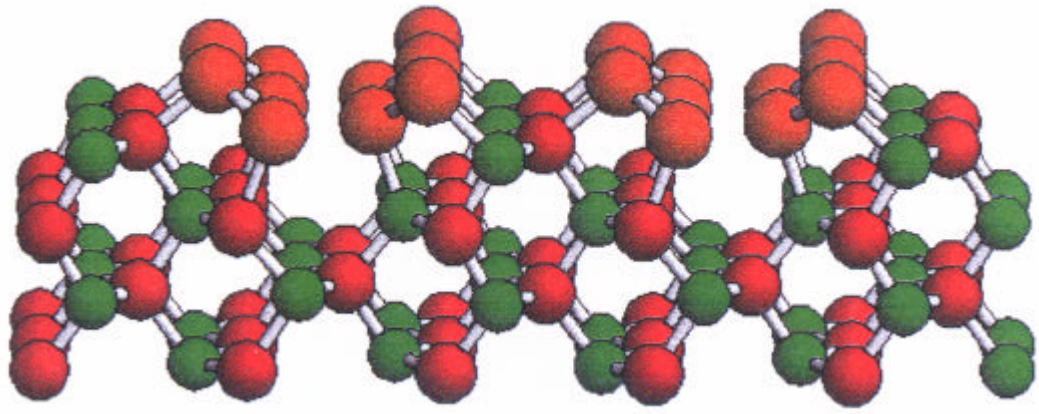

Fig. 1. The Bi induced 1x2 structure of the GaSb(110) surface. Bi atoms are shown orange, Ga atoms green and Sb atoms red.

2.5.4 Surface X-Ray Diffraction at the n-GaAs(001)/Electrolyte Interface

G. Scherb, A. Kazimirov, J. Zegenhagen, *MPI-FKF Stuttgart, Germany,* T. Schultz, R. Feidenhans'l, *Risø National Laboratory, Denmark,* D.M. Kolb, *University of Ulm, Germany*

In-situ surface x-ray diffraction (SXD) has shown to be a powerful method for getting atomic scale structural information from the metal/electrolyte interface. We have extended the application of this technique to the challenging field of semiconductor/ electrolyte interfaces, and the first system under study is n-GaAs(001) in acidic aquous electrolytes (H_2SO_4, HCl). The experiments were performed at beamline BW2 at HASYLAB, Hamburg, using a thin layer electrochemical cell equipped with a 6 μ mylar window and working in the classical three-electrode configuration.

Whereas in-plane scattering yields details about the atomic arrangement in the interfacial plane, information on surface roughness, facetting and also on the electron density at the electrolyte side of the interface can be derived from the intensity distribution along the crystal truncation rods (CTR). Measuring the potential dependence of the (11*l*) rod intensity, we monitored the roughness transitions at the GaAs(001)/H_2SO_4 interface associated with anodic oxidation (increase in roughness) and cathodic reduction (decrease in roughness).[1] Our measurements of the specular (00*l*) rod at the n-GaAs(001)/HCl interface have clearly shown that surface roughness is not the only factor contributing to the rod shape (Fig. 1). While around $l = 4$ the intensity profile can be fitted using only a roughness parameter, the rod at $l = 2$ shows a remarkable broadening that is not described in terms of roughness. This peak, being much weaker in intensity than the (004) reflection, is rather sensitive to electron density variations, and the ions in the electrochemical double layer present at the interface have to be considered. In terms of a simple model for additional electron density due to chloride ions, the fit of the specular rod was greatly improved. Best agreement was achieved for ~ 1ML chloride. However, these preliminary results are derived from a real simple model which has to be refined on the basis of further measurements.

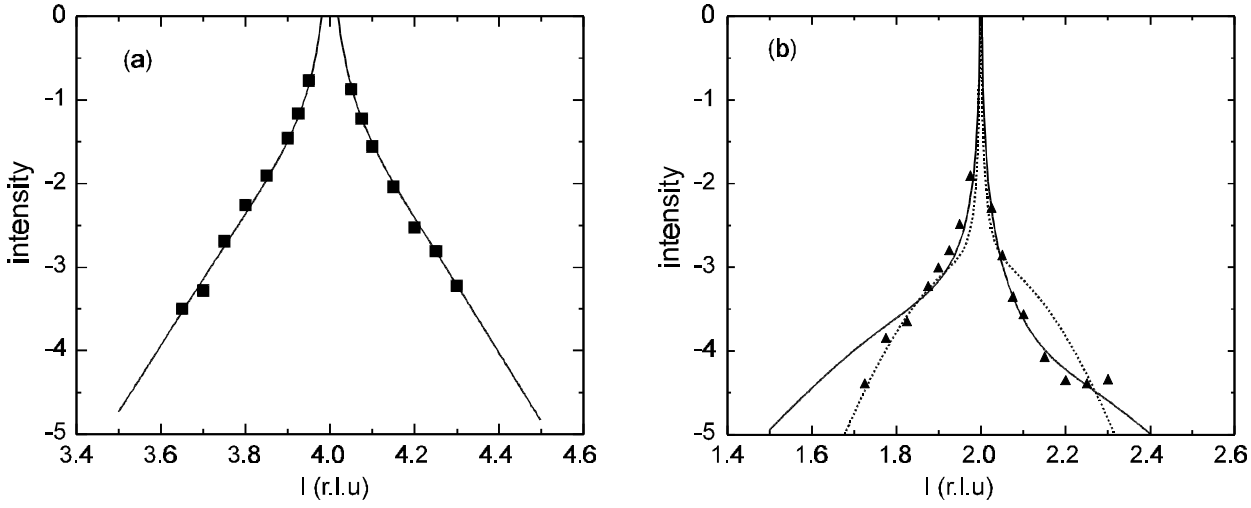

Fig .1: Specular (00*l*) rods at the n-GaAs(001)/HCl interface at -1.0V. (a) Rod at (004), fitted with rms = 4.3 Å. (b) Rod at (002), fitted for roughness only (broken line, rms = 6.4 Å) and for the roughness obtained from (004) and 1ML of chloride (solid line).

[1] J. Zegenhagen, A. Kazimirov, G. Scherb, D.M. Kolb, D.-M. Smilgies, and R. Feidenhans'l, Surf. Sci **352-354**, (1996) 346

2.5.5 Surface X-ray Diffraction Study of the √3x√3 R 30° Structure of Sb on Cu(111)

J.M. Gay, G. Le Lay, *CRMC2, France*, R. Feidenhans'l, F.B. Rasmussen, J. Baker, T. Schultz, M. Nielsen, *Department of Solid State Physics, Risø National Laboratory, Denmark*, O. Bunk, G. Falkenberg, L. Seehofer, R.L. Johnson, *II. Institute for Experimental Physics, University of Hamburg, Germany*

Antimony is known to have a surfactant effect in epitaxial growth on both semiconductor and metal films. This property is closely related to its strong tendency to superficial segregation. The growth of Sb on Cu(111) has been recently studied by Auger Electron Spectroscopy (AES), Low Energy Electron Diffraction (LEED) and Photo Electron Spectroscopy (PES).

The dissolution kinetics at 400°C of 1 ML of Sb deposited on Cu(111) stops at a steady state with a √3x√3 R 30° structure. On the other hand, the segregation kinetics of Sb on the surface of a Cu(Sb)(111) solid solution (0.45 at%) gives similarly rise to the √3x√3 R 30° superstructure, as shown by LEED studies. The microscopic mechanisms of dissolution and segregation of Sb are still unclear. PES experiments have shown different binding states in the Sb monolayer deposited at room temperature and in the annealed layer. More precisely, two chemical states are observed after annealing when the √3x√3 R 30° structure appears. The purpose of the surface x-ray diffraction study was to investigate in detail the atomic structure of the Sb √3x√3 R 30° structure after annealing of a monolayer deposited at room temperature.

Integer and fractional order in-plane reflections have been measured, as well as rods. The analysis of the experimental data is in progress.

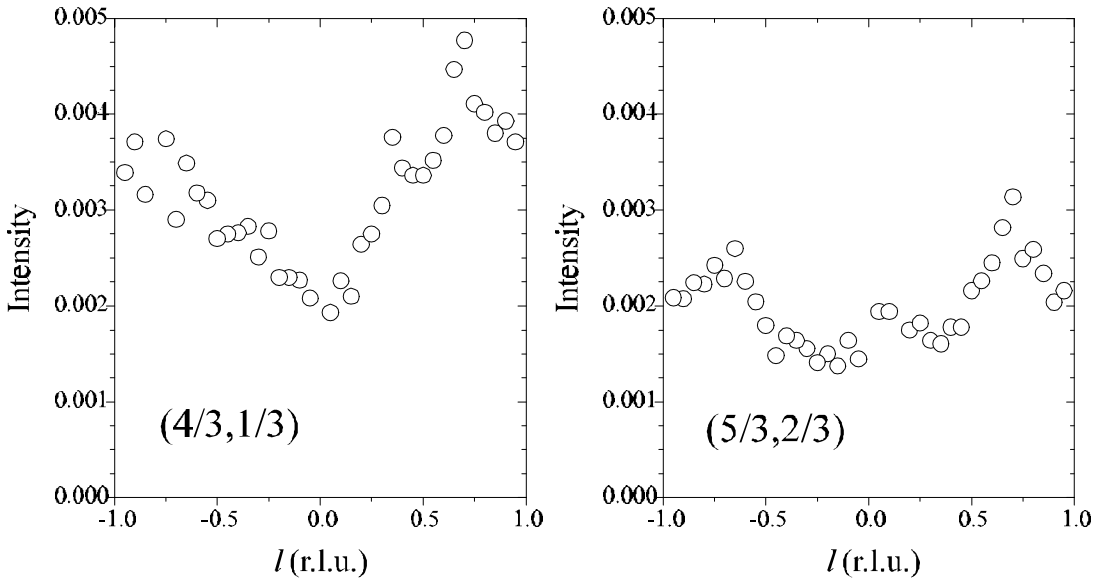

Fig. 1. Fractional order rods scan of the (4/3,1/3) and (5/3,2/3) reflections.

2.5.6 Surface X-Ray Diffraction Studies of the Rb induced Ge(111)3x1 Structure

E. Landemark, M. Nielsen, R. Feidenhans'l, *Department of Solid State Physics, Risø National Laboratory, Denmark,* L. Lottermoser, O. Bunk, L. Seehofer, G. Falkenberg, R.L. Johnson, *II. Institut für Experimentalphysik, Universität Hamburg, Germany*

There is currently a large interest for the metal induced 3x1 reconstructions of the Si(111) surface. Similar 3x1 reconstructions are induced by sub monolayer coverages of different adsorbates, such as Li, Na, K and Ag. Despite an extensive amount of studies presented during the last years, the atomic structure of these surfaces is still controversial. While the adsorbate coverage now generally is believed to be ~1/3 monolayer, the number of Si atoms per unit cell participating in the reconstruction is unknown and vary between 2 and 6 in recently proposed models.[1,2] Previously, we have studied the Si(111)3x1 Li, Na and Ag surfaces by XRD. In order to obtain more information of the 3x1 systems, we have now extended our studies to include the 3x1 reconstruction induced by Rb adsorption on the Ge(111) surface.

The contour maps of the 2D Patterson functions show similar interatomic vectors for the three Si surfaces (Fig. 1.). The variation in height of corresponding peaks can be explained by different Z values for the involved atoms and is an indication of ordered positions for the metal atoms. The Patterson function for the Ge(111) surface is more unlike. This might indicate a different surface structure but it might also be explained by the difference in Z and scattering factor between the two substrates.

The data analysis of the out of plane, rod scan, data sets is still in progress. We have not been able to reproduce the data by calculating the diffracted intensity from earlier proposed models. Instead we have found better agreement with a new model, consisting of four substrate atoms building up a ”double zig-zag chain” structure. We are presently testing out our new data analyzes program that also includes minimization of the Keating energy. The idea is to use the Si/Li data, where the metal scattering can be neglected, to find the positions of the substrate atoms. The next step is then to find the positions of the metal atoms and completely determine the atomic structure for the four surfaces.

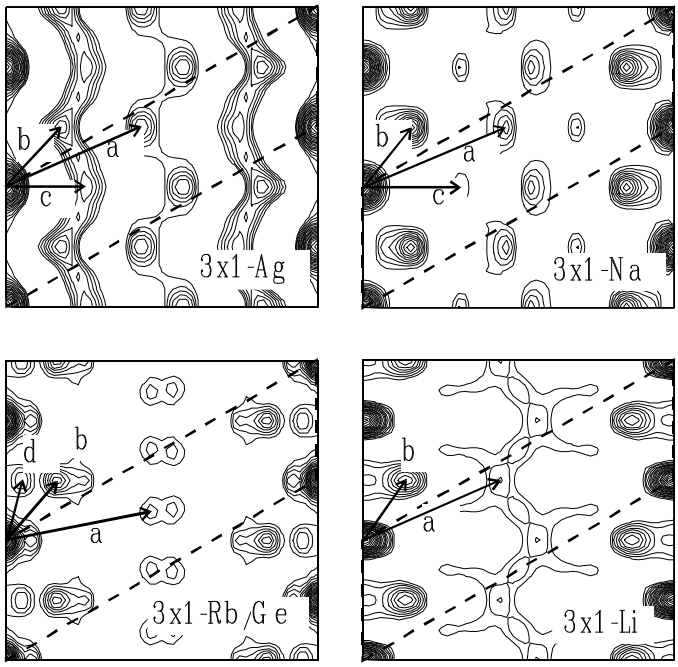

Fig. 1. Contour maps of the experimental Patterson functions for the Si(111)3x1-Ag, Si(111)3x1-Na, Ge(111)3x1-Rb and Si(111)3x1-Li surfaces.

[1] H.H. Weitering, N.J. DiNardo, R. Péres-Sandoz, J. Chen and E.J. Mele, Phys. Rev. B 49, 16837 (1994)
[2] Steven C. Erwin, Phys. Rev. Lett. 75, 1973 (1995)

2.5.7 Surface X-Ray Diffraction Study of Ge(103) (1x1)-In

O. Bunk, J. Zeysing, L. Seehofer, G. Falkenberg, R.L. Johnson II. *Institut für Experimentalphysik, Universität Hamburg, Germany,* M. Nielsen, R. Feidenhans'l, *Department of Solid State Physics, Risø National Laboratory, Denmark*

The self-organisation of atoms on surfaces is of fundamental importance and has great potential as a method for producing highly regular three-dimensional nanoscale structures. We have found that very uniform clusters, similar in shape to the well-known "hut-clusters" produced by Ge deposition on Si(001), are formed after annealing an indium-covered Ge(001) surface.[1] The clusters are bounded by In-terminated {103} facets. A knowledge of the exact positions of the In and Ge atoms in the clusters would allow the strain relief in the cluster to be determined, which would provide insight into the fundamental mechanism driving the formation of the nanostructures. When In is deposited on a Ge(103) surface a stable (1x1) reconstruction with large domains[2] is formed. This surface is therefore a good starting point for determining the surface crystallography of the (103) facets. The sample was prepared at the photoemission system FLIPPER II and then transferred in a small portable UHV-chamber with a hemispherical Be window to the surface diffractometer on the wiggler beamline BW2 at HASYLAB in Hamburg. The recorded data consists of 297 measurements along 13 rods and 102 symmetry inequivalent in-plane reflections. A model for the reconstruction is shown in Fig. 1. A key aspect of this model is that the threefold-coordinated In atoms saturate all the surface dangling bonds and thereby minimize the surface free energy.

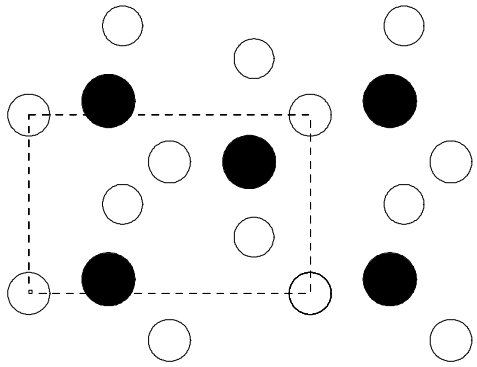

Fig. 1. A model of the Ge(103) (1x1)-In reconstruction. In atoms are represented by filled circles and the Ge atoms by open circles.

[1] M. Nielsen, D. Smilgies, R. Feidenhans'l, E. Landemark, G. Falkenberg, L. Lottermoser, L. Seehofer and R.L. Johnson, Surf. Sci. **430**, 352-354 (1996)

[2] L. Seehofer, G. Falkenberg and R.L. Johnson, Phys. Rev. B in press (1996)

2.5.8 Surface X-Ray Diffraction Study of Ge(103)-(1x4)

O. Bunk, L. Seehofer, G. Falkenberg, R.L. Johnson *II. Institut für Experimentalphysik, Universität Hamburg, Germany*, M. Nielsen, R. Feidenhans'l, *Department of Solid State Physics, Risø National Laboratories, Denmark*

A new way of deriving a structural model for a complex high-index surface reconstruction has been successfully tested. The basic model for the reconstruction has been developed using a combination of an in-plane dataset with a small rod-scan dataset.[1] All the fractional order rods were calculated from this preliminary model. Using these theoretical calculations we were able to select rods with high intensity and distinctive features for the measurements which avoided wasting time measuring featureless rods.

The sample was prepared at the photoemission system FLIPPER II and then transferred in a portable UHV-chamber to the diffractometer on the wiggler beamline BW2 at HASYLAB in Hamburg. The recorded dataset for the final analysis consists of 237 measurements along 10 rods and 235 symmetry inequivalent in-plane reflections. The Patterson function is shown in Fig. 1a. The most important distance corresponding to the main feature of the reconstruction, a double step, is marked by ”1”, in Fig. 1. Two rod-scans are shown in Fig. 1b. The main features of these rods can already be explained with the model. Further structural refinements, now in progress, will reveal the exact atomic positions.

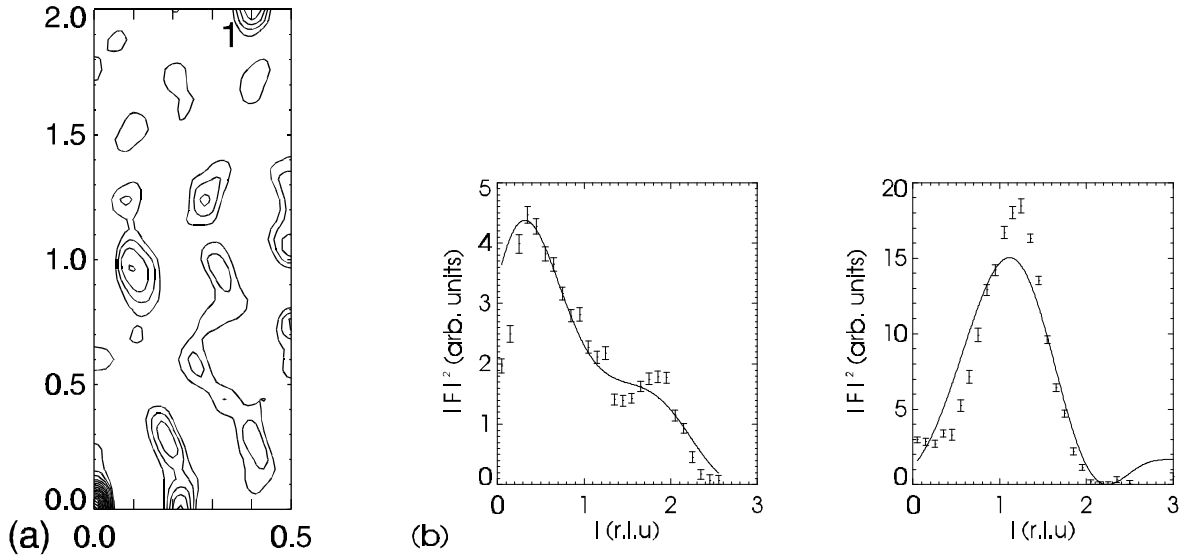

Fig. 1. a) Patterson function of the in-plane projected electron density calculated from the fractional order reflections (The asymmetric unit is shown. b) Rod-scans along (0,-4¼,*l*) and (4,- ½,*l*).

[1] L. Seehofer, O. Bunk, G. Falkenberg, L. Lottermoser, R. Feidenhans'l, E. Landemark, M. Nielsen and R.L. Johnson, submitted to Surf. Sci.

2.5.9 Nanoclusters of the CWD Compound $Rb_{0.3}MoO_3$, Blue Bronze, Grown on $SrTiO_3$, Studied by Synchrotron x-ray Diffraction

A.J. Steinfort, A.B. Smits, P.M.L. O. Scholte, A. Ettema, and F. Tuinstra, *Department of Applied Physics, Delft University of Technology, The Netherlands,* M. Nielsen and J. Baker *Department of Solid State Physics, Risø National Laboratory, Denmark*

Films of the compound $Rb_{0.3}MoO_3$ (blue bronze) are grown and characterized in anticipation of studies of their charge density related electronic behaviour. In these films interesting new mesoscopic phenomena are anticipated.

Blue bronze is grown by laser ablation on a substrate of $SrTiO_3$ (001). AFM and x-ray analysis of layers with an approximate thickness of 300 nm have shown that the film consists of elongated clusters with typical dimensions of 0.5 by 2 micron. The blue bronze is monoclinic with the b*-axis along the long direction of the clusters which in turn are oriented parallel to the principal axis of the substrate. The clusters have their $(\bar{2}01)$ direction parallel to the substrate normal.

X-ray diffraction measurements have been performed on the diffractometer at the BW2 wiggler beam line in HASYLAB, Hamburg, on both thin films of about 1.5 nm to establish the condition for initial growth and on thick films of about 300 nm to analyze epitaxy, facet structure and strain conditions of the clusters. The thin films show island growth with full orientational epitaxy and little or no strain.

For thicker films similar epitaxial behaviour is observed. Furthermore streak shaped satellite reflections are measured as illustrated in the figure below, and they signal a uniform morphology of the clusters. In this interpretation the satellite peaks are truncation rods from the cluster facets and their positions are determined by the slope of the facet surface to the substrate surface. However, analysis of the full data set reveals that final size effects, internal strains and possibly stacking faults are important. The data analysis is in progress.

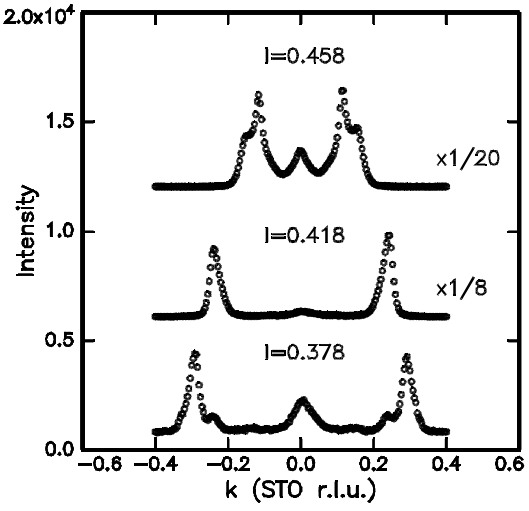

Fig. 1. Measured x-ray scattering profiles around the blue bronze $(\bar{2}\,0\,1)$ reflection perpendicular to the b*-axis at different heights in the reciprocal space above the substrate surface. The side peak positions are determined by the vertical momentum transfer l and they signal planar facets on the clusters. The upper curves are displaced by 600 and 1200 in intensity.

2.5.10 Cu Films on Ni(100), Internal Faceting and Embedded Clusters Studied by Synchrotron x-ray Diffraction

M. Nielsen, J. Baker, F. B. Rasmussen and R. Feidenhans'l, *Department of Solid State Physics, Risø National Laboratory, Denmark.* R. L. Johnson, G. Falkenberg and L. Seehofer, *II Institut für Experimentalphysik, Universität Hamburg, Germany*

The formation of internal facets and nanoscale Cu-clusters on Ni(100) single crystal surfaces after deposition of Cu thin films were studied by x-ray diffraction. Cu atoms are 2.6 per cent larger than Ni atoms and the first 20 monolayers (ML) of Cu were thought to grow pseudomorphically on Ni(100), with the Cu atoms simply extending the Ni lattice despite the misfit. It was recently discovered[1] using scanning tunneling microscopy that stripes are formed on the surface, where the Cu atoms protrude about 0.6 Å above the level of the surface. The authors concluded that the strain associated with the misfit is partly relaxed by the formation of wedges as illustrated in panel (a) beneath. The atoms inside the wedges are displaced half a lattice spacing in the long direction of the clusters and a little, 0.4-0.6 Å upwards. The buried surfaces of the clusters are (111) facets. This internal faceting model may be quite general in epitaxial crystal growth.

At the wiggler beamline BW2 in HASYLAB, Hamburg, we have studied the wedge-shaped clusters in 9 ML and in 20 ML Cu films by x-ray diffraction. The clusters are regular and monodispersed and give a very distinctive scattering response at the positions of the truncation rods from the facets as illustrated in panels (b) and (c). Due to the half lattice spacing shift of all atoms inside the wedge, these will scatter either in phase or out of phase with the Cu atoms outside, when the proper scans are chosen. The mechanism driving the cluster formation is strain relaxation, and from the diffraction results we can determine the inhomogeneous strain fields both inside and outside the wedges. Panel (c) illustrates the sensitivity of x-ray scattering to the strains. The asymmetry of the profiles arises from the inhomogeneous strain.

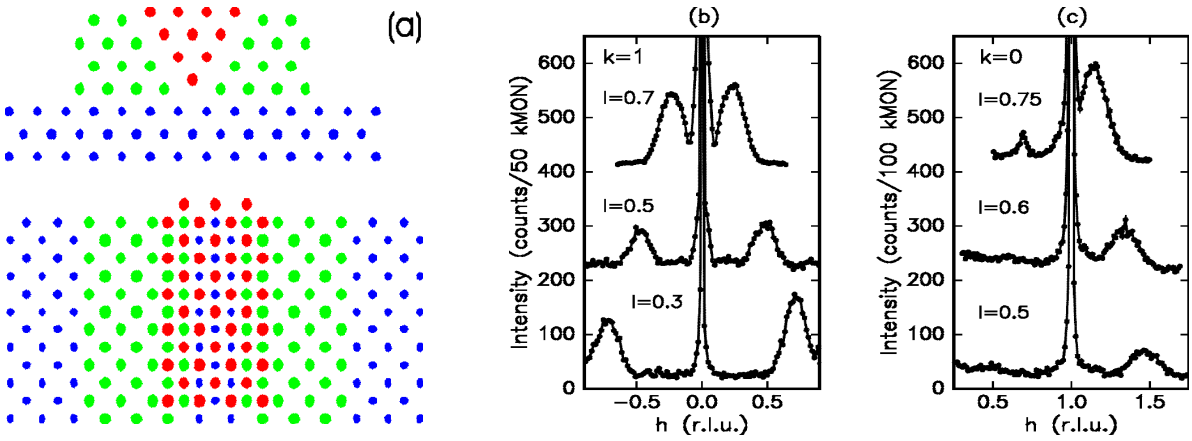

Fig. 1. (a) The wedge-shaped cluster, red atoms, are displaced half a nearest neighbour distance along the wedge axis and about 0.6 Å upwards. The Cu atoms outside the wedge, green atoms, are pseudomorphic with the Ni-substrate, black atoms. (b) "Transverse" x-ray scans. The side-peak scattering is from clusters with the long axis along the k-direction. (c) "Longitudinal" x-ray scans. The side-peak scattering is again from clusters lying along the k-direction. The asymmetry is due to inhomogenous strain.

[1] B. Müller, B. Fischer, L. Nedelmann, A. Fricke and K. Kern, Phys. Rev. Lett. **76**, 2358 (1996)

2.5.11 Surface X-Ray Diffraction Study of Si(001)-(3x4)-In

O. Bunk, L. Seehofer, G. Falkenberg, R. L. Johnson, *II. Institut für Experimental-physik, Universität Hamburg, Germany,* M. Nielsen, R. Feidenhans'l, E. Landemark, *Department of Solid State Physics, Risø National Laboratory, Denmark*

A new structural model for the indium-induced 3x4 reconstruction on Si(001) has been derived from surface X-Ray diffraction measurements. Despite some previous studies on this system[1,2,3] there is still no established model for this surface reconstruction. The sample was prepared in a STM sytem under UHV (base pressure < $4x10^{-11}$ mbar) by the deposition of 0.5 ML In on the clean Si(001) (2x1) surface and annealing at 350°C. It was then transferred under UHV to the diffractometer on the wiggler beamline BW2 at HASYLAB in Hamburg. The recorded dataset consists of 235 symmetry inequivalent in-plane reflections, 133 measurements along six fractional order rods and 42 measurements along one crystal truncation rod. The Patterson function is shown in Fig. 1a. Within the radius of one unit-cell dimension there is no strong peak in the Patterson function. Therefore, In-In dimers are probably not a significant structural element in this reconstruction in contrast to the (2x2) reconstruction[4] and to some of the previously suggested models for the (3x4) reconstruction [3] The main distances (1-3 in Fig. 1.) can be found e.g. in a model which includes parallel rows of In-Si dimers. The basic structural model is shown in Fig. 1b. It includes six In atoms per unit cell, of which four replace Si atoms leaving two additional In atoms. This is in agreement with the STM measurements which revealed of 6±1 In atoms and some displaced Si atoms.

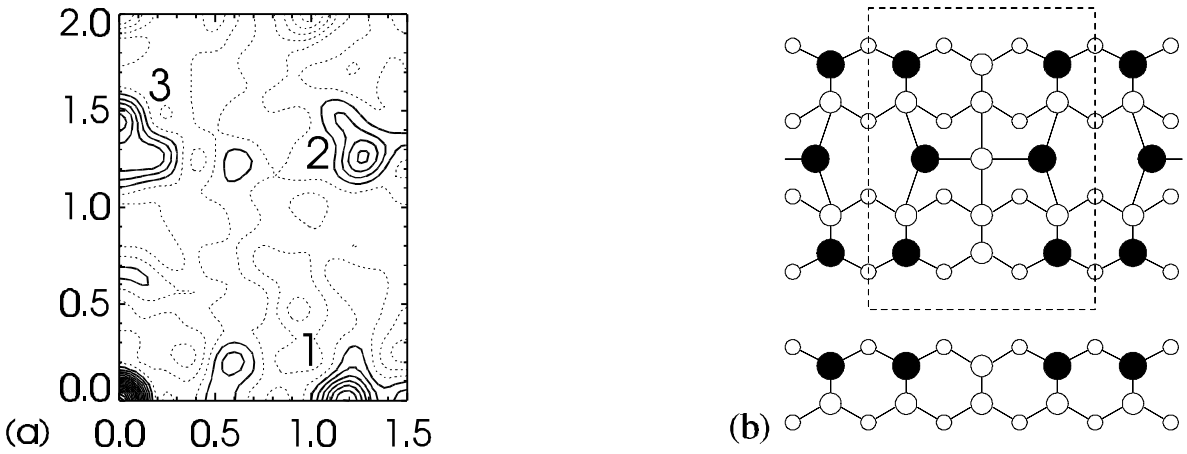

Fig. 1. a) Patterson function of the in-plane projected electron density calculated from the fractional order reflections. (The asymmetric unit is shown; the dotted lines are negative contour.) b) Structural model for the In on Si(001) (3x4) reconstruction with In-Si dimers and six In atoms. (Open circles represent Si atoms and filled circles In atoms.

1 J. Knall, J.-E. Sundgren. G. V. Hansson and J. E. Green, Surf. Sci. **166** (1986)
2 A. A. Baski, J. Nogami and C. F. Quate, Phys. Rev. B **43**, 9316 (1991)
3 B. E. Steele, D. M. Cornelison, Lian Li and I. S. T. Tsong, Nucl. Instr. Meth. B **85,** 414 (1994)
4 H. Sakama, K. Murakami, K. Nishikata and A. Kawazu, Phys. Rev. B **53**, 1080 (1996)

2.5.12 X-ray Surface Structure Studies on Organic Crystals of Benzamide

R. Edgar, *Department of Materials and Interfaces, Weissmann Institute, Israel*, R. Feidenhans'l, T. Schultz, *Department of Solid State Physics, Risø National Laboratory, Denmark*, L. Leiserowitz, *Department of Materials and Interfaces, Weissmann Institute, Israel*

Probing the surface structure of organic crystals arises many questions which were addressed to semiconductor and other inorganic surfaces only. The complexity and diversity of organic matter make this new field exciting for both pure and applied studies.

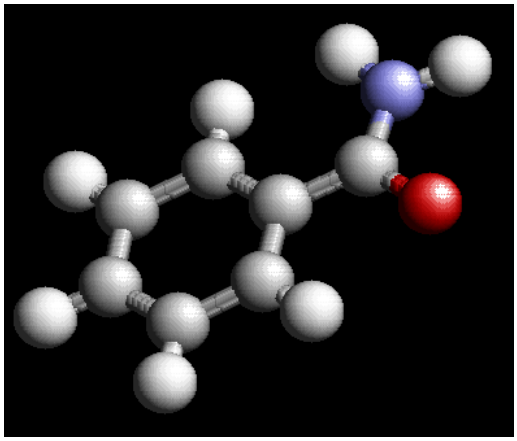

Fig. 2: One benzamide molecule, visualized using the Rasmol 2.6 programme.

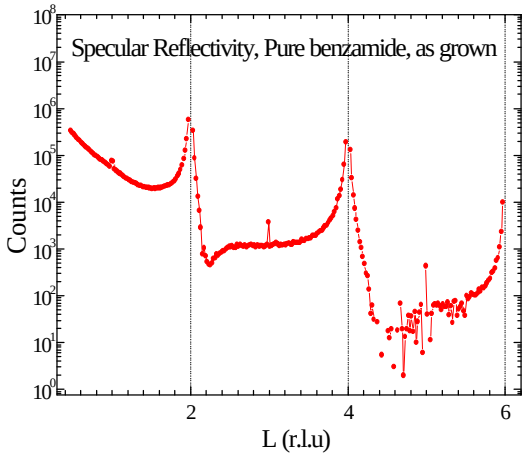

Fig. 3: Specular reflectivity curve for pure benzamide, as grown.

Benzamide (see fig. 1) is a simple organic molecule which packs in a triclinic space group $P2_1/c$ with four molecules in the unit cell. Dry single crystals of benzamide, grown from alcoholic solution to yield large (001) surface areas of ca. 12x12 mm and thicknesses of about 5mm, were mounted on the 6 circle surface diffractometer at BW2. The crystals were measured as grown (se specular rod fig.2) or freshly cleaved along the (001) face (see fig. 3). In addition crystals grown from solutions containing acetamide and trifluoroacetamide were measured.
The results presented here are so recent, that no data analysis has been perfomed yet. The data from the surface X-ray scattering experiment are of a very high quality, and therefore we aim to determine and refine the suface structure of benzamide, and thereby gaining knowlegde on the differences between the bulk and surface structure. If we succed in that, it will be the first time the surface structure of a organic crystal has been determined and refined.

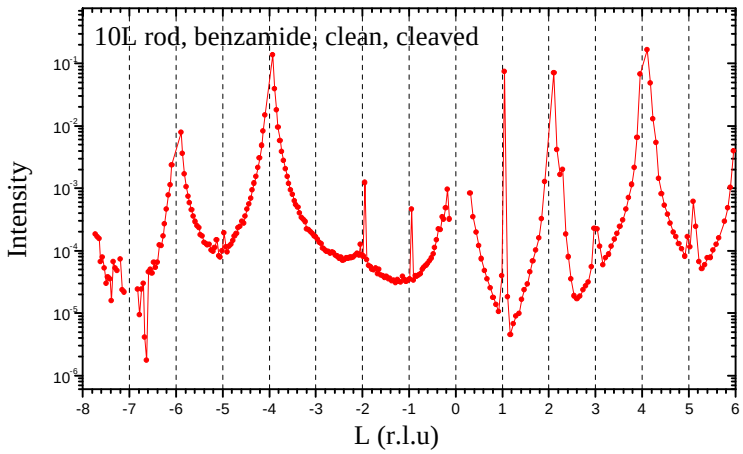

Fig. 4: 10*l* crystal truncation rod from pure, cleaved benzamide.

2.6 Langmuir Films

2.6.1 X-ray Diffraction from Curved Thin Films

P. B. Howes and K. Kjær, *Department of Solid State Physics, Risø National Laboratory, Denmark*

X-ray diffraction has proved to be a powerful technique in the study of Langmuir monolayers. It is well known that diffraction from a flat, two-dimensional, crystalline monolayer leads to rods of scattering in reciprocal space which are sharp in the directions parallel to the surface, $\boldsymbol{q}_{xy}$, but extended perpendicular to the surface: along $\boldsymbol{q}_{z}$. A number of experiments on amphiphilic mono- or multi-layers have given rise to diffraction which, instead of exhibiting the expected Bragg rod (see Fig. 1a), are additionally extended along a curved line[1] which follows the Scherrer ring of constant $(q_{xy}^2 + q_z^2)^{1/2}$ (see Fig. 1b). Such scattering can be explained by a mosaic spread in the normals of flat crystallites.[2] Another possible explanation is that the individual crystallites may be curved (Fig 1c); however it is not immediately obvious if this would give rise to the observed peak profile, or whether an X-ray diffraction experiment could distinguish the two cases. To investigate this phenomenon, we have performed numerical simulations of the X-ray scattering from both curved crystallites and mosaic distributions of flat crystallites. The simulations were performed on one-dimensional crystals (Fig 1c). The electron density of the long, linear molecules was taken to be a Gaussian ellipse for simplicity. For the curved domains, the scattered intensity was calculated as the coherent sum in reciprocal space of the Fourier transforms of N molecules on a circularly curved line with radius R. For the case of a mosaic spread of flat crystallites the Fourier transform of the density of a single crystallite was first calculated then added incoherently to that from other crystallites with different tilts.

It was found that the two different kinds of surface gave broadly similar scattering. In both cases the Bragg rod was extended along the Scherrer ring (Fig 1b). However, whereas the mosaic crystallites lead to a constant q_{xy}-width, the curved layer diffraction becomes broader with increasing diffraction order. Thus it is, in principle, possible to distinguish the two cases experimentally .

Fig. 1. Calculated diffraction peak profiles for a flat monolayer (N=30) (a) and a curved monolayer (N=30, R=120 intermolecular spacings) (b). Real space electron density of the curved monolayer is shown in (c).

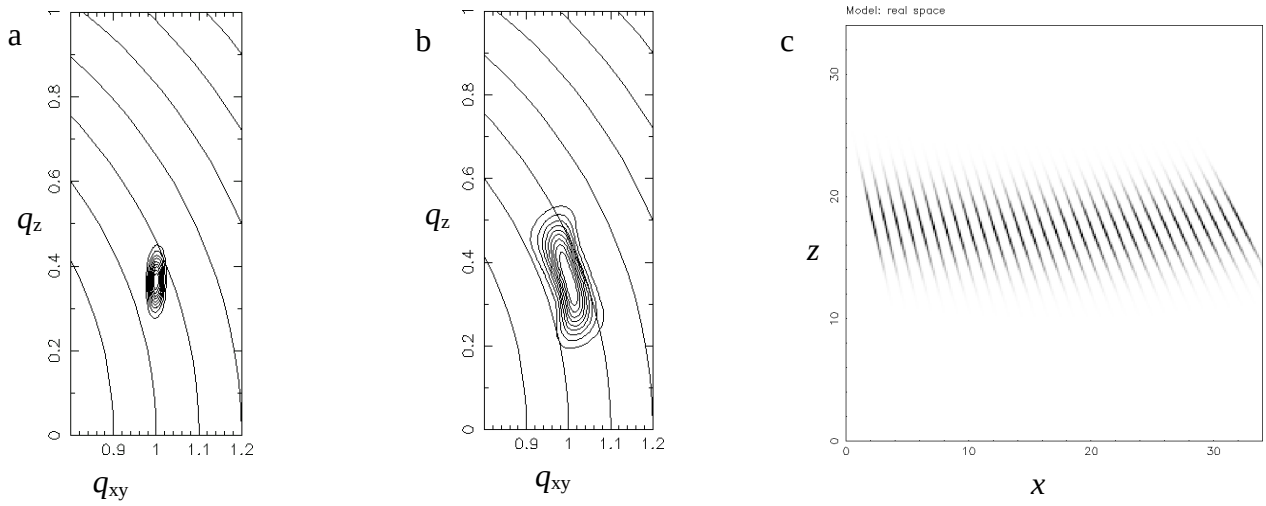

[1] S. P. Weinbach *et al.,* Ann. Rep. Solid State Physics Dept., Risø, 1994, 2.6.12 and Adv. Mater. **7,** 857 (1995)
[2] W. Bouwman and K. Kjær, Ann. Rep. Solid State Physics Dept., Risø, 1994, 2.6.1

2.6.2 Studies of Phase Transitions in Langmuir Monolayers of a Triple Chain PE

F. Bringezu, G. Brezesinski, H. Möhwald, *Max-Planck-Institute for Colloids and Interfaces, Germany*, P. Howes and K. Kjær, *Department of Solid State Physics, Risø National Laboratory, Denmark*

Branched-chain phospholipid monolayers provide interesting model systems for the study of the interplay between the polar head group region and the hydrophobic chains. We have investigated condensed phases of a triple chain 1($2C_{16}$-18:0)-2H-PE (**a,** *cf.* Fig. 1) by means of Grazing-Incidence X-ray Diffraction (GIXD), using the liquid surface diffractometer at the undulator beamline BW1 in HASYLAB at DESY, Hamburg. The lipid consists of three hydrocarbon chains and one glycerophosphoethanolamine head group. In this case the molecular area is influenced by two factors. First, three chains require more space in the monolayer than the small head group. Second, regardless of the large hydrophobic part of the molecules interactions between the hydrophilic head-groups must be taken into account.[1]

The pressure (π) *vs.* molecular area (A) ,isotherm at 20°C indicates a phase transition at $\pi \cong 9$ mN/m (Fig. 1). ΔA yields a transition enthalpy of 16.7 kJ/mol (Clausius-Clapeyron equation). GIXD experiments were performed between 0 and 37 mN/m at 20°C. At $\pi \cong 0$ a centred-rectangular lattice with chains tilted in a symmetry direction towards nearest neighbours (NN) was observed with in-plane area *per molecule* $A_{xy} \cong 42$ Å^2. With increasing π the tilt decreases from 13.5° ($\pi \cong 0$ mN/m) to 5.7° ($\pi \cong 11$ mN/m). At $\pi \cong 15$ mN/m only one sharp diffraction peak with a *d*-spacing of 4.86 Å appears, indicating a hexagonal lattice of upright oriented chains. Further increase of π leads to decreasing *d*- and A_{xy}-values (4.82 Å, 40.8 Å^2 at $\pi \cong 37$ mN/m). Fig. 1 compares the isotherm and the A_{xy} -values from the GIXD-measurements. The change in the molecular area in the isotherm is apparently not only due to a change in the lattice of the hydrocarbon chains. The phase transition from centred-rectangular to hexagonal occurs between 11 and 15mN/m and not at $\pi \cong 9$ mN/m as inferred from the isotherm. Brewster angle microscopy studies showed that, on expansion, monolayer inhomogeneities, resulting from an anisotropy contrast due to the tilting of the chains, appear between 13 and 11 mN/m. At around $\pi \cong 10$ mN/m inhomogeneities resulting from unoccupied areas in the monolayer are observed for parallel polarizers as well. In previous work[2] with DPPE a model of head group ordering was deduced from analysis of Bragg rod profiles. Possibly, the tilting of the triple-chain PE leads to an analogous orientational ordering of the head group dipoles. Thus, the surprising behaviour of **(a)**, showing large differences between the molecular areas derived from isotherm and X-ray measurements below 10 mN/m, could be due to electrostatic repulsion between condensed phase domains.

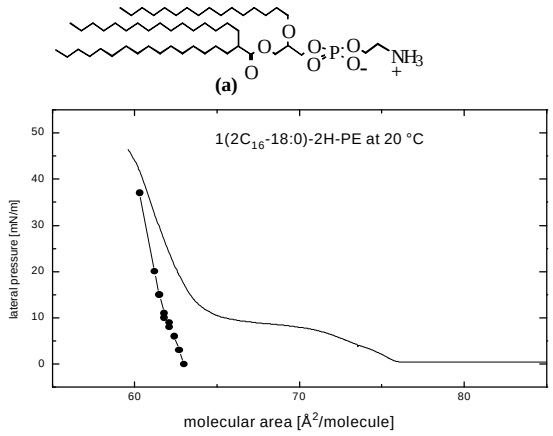

Fig. 1. Isotherm (_) and A_{xy} per molecule calculated from GIXD data (•).

[1] F. Bringezu, G. Brezesinski, H. Möhwald, B. Struth, W.G. Bouwman, K. Kjær, Annual Report for 1995

[2] C. Böhm, H. Möhwald, L. Leiserowitz, J. Als-Nielsen and K. Kjær, Biophys. J., **64**, 553 (1993)

2.6.3 Influence of Head Group Methylation on the Phase Behaviour of Lipid Monolayers

F. Bringezu, G. Brezesinski, H. Möhwald, *Max Planck Institute for Colloids and Interfaces, Germany* and K. Kjær, *Department of Solid State Physics, Risø National Laboratory, Denmark*

In phospholipid monolayers the interaction between adjacent head groups is one of the basic factors which influences the arrangement of the hydrophobic chains. The present investigations focus on the effect of systematic changes in head group methylation in triple- chain phospholipids on the structure of monolayers formed at the air-water interface. Therefore we have studied monolayers of the racemic 1-(2C_{14}-16:0)-2H-PE$(CH_3)_n$ [n=0 (**a**), 1 (**b**), 2 (**c**), 3 (**d**)] (*cf.* Fig. 1). From isotherm measurements we conclude that with increasing number of methylene groups the characteristic temperatures of the monolayers change systematically. *E. g.*, the temperature T_0 (at which the liquid-expanded phase appears) decreases from **a**: 16°C to **b**: 13°C, **c**: 11°C and **d**: 6°C. Grazing-incidence diffraction (GIXD) measurements (performed at the liquid surface diffractometer on the undulator X-ray beamline BW1 at HASYLAB, DESY, Hamburg) show that at 5°C and $\pi \cong 0$ mN/m monolayers of **a** exhibit 2 diffraction peaks indicating a rectangular unit cell. The molecules are tilted in symmetry direction towards nearest neighbours (NN). Increasing pressure leads to a phase transition from rectangular to hexagonal symmetry with vertical chains. On introduction of methyl groups at the nitrogen the area per head group increases continuously. The diffraction patterns of **b**, **c** and **d** at 5°C and low pressures are very similar to that of **a**, however the tilt angles are increased (see Fig.1). Methylation of the head group increases the transition pressures to the hexagonal phase. This corresponds to increasing differences of space requirement between head and tail region in the monolayer. At 15°C **a** shows only one sharp diffraction peak, indicating hexagonal packing of upright chains, even at ≅ zero pressure. Tilted phases were observed for **c** and **d** only (see Fig.1).

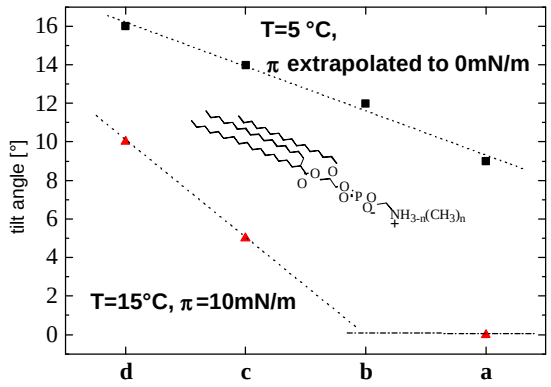

Fig.1. Tilt angle as function of methylation degree.

For further discussion it is interesting to note that for all these triple-chain lipids the phase transition from NN to hexagonal is characterised by a pressure region where the in-plane components Q_{xy} of the two peaks coincide while the out-of-plane components Q_z differ (see Fig.2). This indicates an undistorted hexagonal lattice even though the symmetry is broken by the tilted chains. Despite the large cross-sectional area of the chains one observes an influence on the phase behaviour of triple-chain phospholipids of head group size and their resulting ability to form hydrogen bonds.

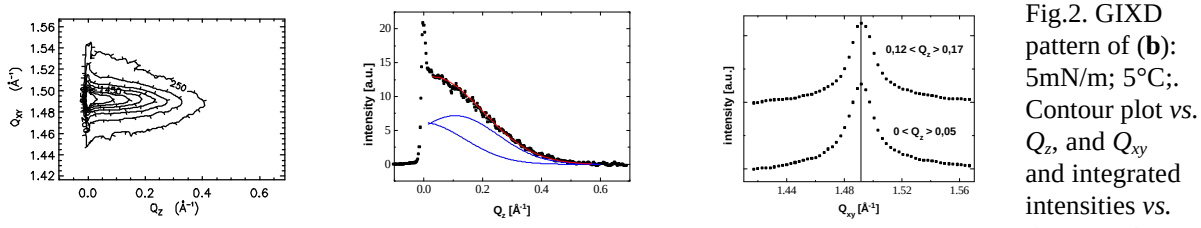

Fig.2. GIXD pattern of (**b**): 5mN/m; 5°C;. Contour plot *vs.* Q_z, and Q_{xy} and integrated intensities *vs.* Q_z, resp. Q_{xy}

2.6.4 Binary Phase Diagram of Monolayers of Simple 1,2-Diol Derivatives

G. Brezesinski, F. Bringezu, H. Möhwald, *Max-Planck-Institute for Colloids and Interfaces, Germany,* P. Howes and K. Kjær, *Department of Solid State Physics, Risø National Laboratory, Denmark*

In order to obtain information about the interplay in Langmuir films between polar head groups and hydrophobic tails it is helpful to resort to simple model systems. Therefore, the phase behaviour of monolayers of several amphiphilic 1,2-diol derivatives has been characterised in recent years. Here we report on the miscibility behaviour of 1-palmitoylglycerol (**1**) with 1-hexadecylglycerol (**2**) (*cf.* Fig. 1). The different chemical linkage of the chain to the glycerol (via an ester bond in (**1**) and an ether bond in (**2**)) leads to different molecular conformations and different interactions between the hydrophilic head groups. Because of the similarity of the transition pressures of (**1**) and (**2**) we investigated the miscibility behaviour by comparing the lattice structures measured by means of Grazing Incidence X-ray Diffraction (GIXD). At all pressures up to 44 mN/m monolayers of compound (**1**) exhibit a rectangular lattice with chains tilted in a symmetry direction towards nearest neighbours (NN). On increasing lateral pressure the parameters *a* and *b* of the rectangular unit cell decrease continuously. For (**2**) the tilt direction changes towards next nearest neighbours (NNN) at a lateral pressure of 18 mN/m. This transition is connected with an increase of *b* and a decrease of *a*. Further pressure increase leads to a drastic decrease of *b* (long axis of the unit cell along the tilt direction) but a small change of *a*. Comparing the tilt angles of (**1**) and (**2**) one observes that at low lateral pressures (**1**) has a lower tilt angle than (**2**), and *vice versa* at high pressures. For a 1:3 mixture of (**1**) and (**2**) the measurements indicate a NN tilted phase between 10 and 30 mN/m. At 35 mN/m the tilt direction changes towards NNN. For a 1:1 mixture this phase transition is shifted to a lateral pressure between 40 and 45 mN/m. Since the transition pressure is higher the increase of *b* during the NN-NNN transition is smaller (see Fig. 1). The dependence of this transition pressure on the mixing ratio points to complete miscibility of (**1**) and (**2**) in all phases, so that a theoretical pressure of 67 mN/m for the transition NN-NNN of (**1**) can be extrapolated. The smaller *a*-values of compound (**1**) than of (**2**) at low pressures may indicate an orientation of the polarised carbonyl group along the *a*-axis. The NN-NNN transition seems to be connected with a reorientation of these carbonyl groups and therefore a higher energy (higher pressure) is needed for this transition in case of (**1**). The carbonyl groups stabilise the NN-tilted rectangular phase obviously not only by dipole-dipole interactions: Different molecular conformations of (**1**) and (**2**) must be assumed.

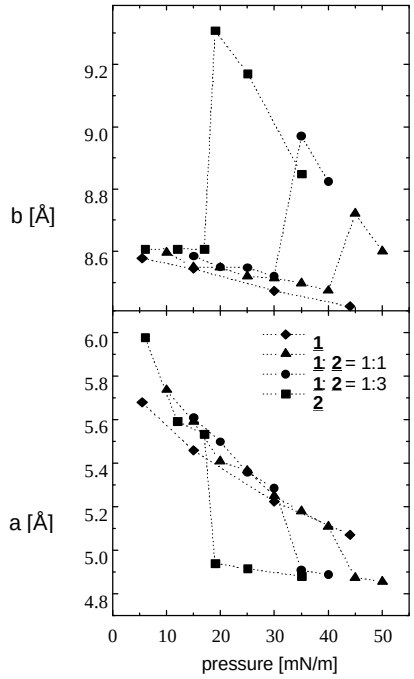

Fig.1. Lattice parameters *a* and *b* of the rectangular unit cell vs. pressure at 20 °C.

2.6.5 Influence of Polyelectrolyte Coupling on the Structure of Charged Monolayers

K. de Meijere, G. Brezesinski, H. Möhwald, *Max Planck Institute for Colloids and Interfaces, Germany* and K. Kjær, *Department of Solid State Physics, Risø National Laboratory, Denmark*

Langmuir monolayers of charged lipids coupled to polyelectrolytes of opposite charge are of interest for understanding the importance of different interactions on the structure of the monolayer. The present investigations focus on structural changes, shifts of phase transitions and the phase diagram of negatively charged 1,2-dipalmitoyl phosphatidic acid (DPPA) at the air/water interface at normal *pH*, bound to the positively charged polyelectrolyte PDADMAC (see Fig. 1, left) using pressure/area isotherms, fluorescence microscopy and Grazing-Incidence X-Ray Diffraction (GIXD) at the liquid surface diffractometer on the undulator beamline BW1 at HASYLAB, DESY, Hamburg, Germany.

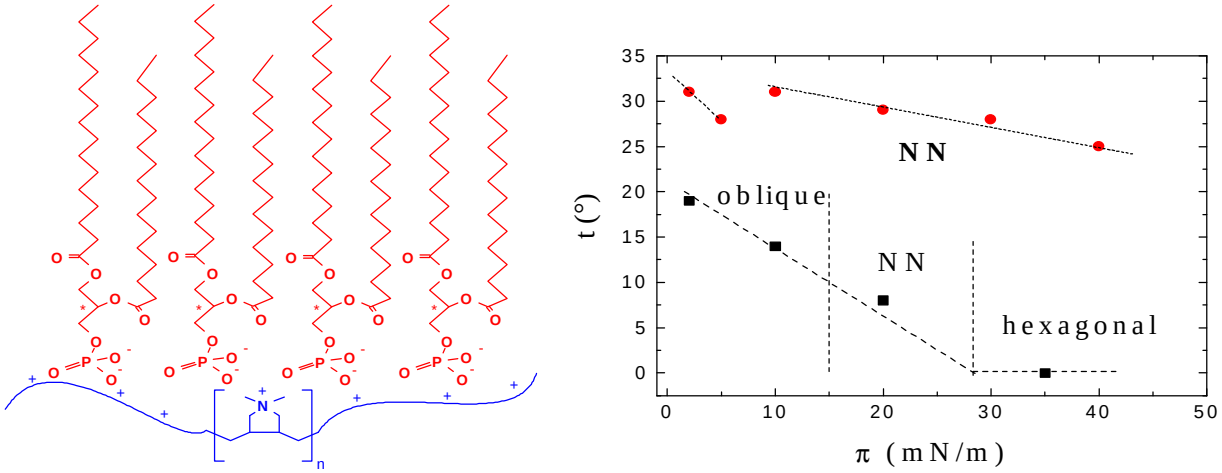

Fig. 1. Left: Chemical structures of the lipid DPPA and the polyelectrolyte PDADMAC (poly-[$CH_2CHCH_2N^+(CH_3)_2CH_2CHCH_2$]). Right: phase diagram of DPPA on water (■) and DPPA on PDADMAC (•).

The isotherms show that binding to the polymer causes an expansion of the DPPA monolayer. At low lateral pressure coexistence of ordered and disordered regions, with possible protrusion of polymer into the disordered monolayer regions, is observed by fluorescence microscopy. On increase of pressure, the inhomogeneities are gradually removed. At high lateral pressures (>20 mN/m) polymer insertion into the film can be excluded by comparing the molecular areas derived from isotherm and GIXD measurements. Fig. 1 (right) shows a schematic phase diagram (tilt angle t versus lateral pressure π) deduced from GIXD. At all pressures investigated the film of the coupled system exhibits two X-ray diffraction peaks, indicating a rectangular structure with uniform chain tilt. The tilt angle decreases only slightly with increasing lateral pressure while on pure water DPPA has a much lower tilt angle at all pressures, decreasing to zero for π > 28 mN/m. Binding to the polyelectrolyte leads to a decrease of the lateral lipid density, and to optimise van der Waals interaction the lipid responds by an increase of the tilt angle. The pure acid film has the phase sequence oblique-rectangular-hexagonal. The removal - for DPPA bound to PDADMAC - of the oblique phase at low pressure is apparently due to destruction of the head group lattice by the polyelectrolyte. The well-defined rectangular structure of the DPPA monolayer coupled to the polyelectrolyte may be due to the 1:1 stoichiometry of the complexes[1] where the packing constraints are determined by the polymer because of its strong entropic forces.

[1] H. Dautzenberg, J. Hartmann, S. Grunewald, F. Brand, Ber. Bunsenges. Phys. Chem. **100**, 1024 (1996)

2.6.6 Superlattices of Crystalline Copper Complexes of α-Amino Acid Amphiphiles at the Air-Aqueous Solution Interface

I. Weissbuch, M. Berfeld M. Lahav, L. Leiserowitz, *Department of Materials & Interfaces, The Weizmann Institute of Science, Israel*, J. Als-Nielsen, *Niels Bohr Institute, H.C. Ørsted Laboratory, Denmark*, P. Howes and K. Kjær, *Department of Solid State Physics, Risø National Laboratory, Denmark*

The reaction between insoluble amphiphiles and soluble ions from the subphase can lead to the formation of self-assembled crystalline monolayers of complex systems in 2D superstructures involving several molecules.[1] The present study describes the effect of the length and nature of the hydrocarbon chain of zwitterionic α-amino acid amphiphiles, R-CH(NH_3^+)CO_2^-, on the packing of their crystalline copper complexes, self-assembled at the air-aqueous solution interface. Fig. 1 (left) shows the grazing-incidence X-ray diffraction (GIXD) pattern for a monolayer of the amphiphile with R=$C_{15}H_{31}$-CONH-$(CH_2)_4$ (enantiomerically pure) spread on a 1mM copper acetate aqueous solution at normal *pH*. Assignment of all the Bragg peaks yielded a cell (a_S =14.40Å, b_S =12.77Å γ_S =103°) that can be interpreted as a superstructure (a_S =3*a-b;* b_S =2*b*) of a subcell (*a*=4.79Å, *b*=6.38Å, γ=77.4°, *A*=29.9Å^2) *i. e.* with one molecule per subcell. The reflections of this subcell, presumably with contribution mainly from the hydrocarbon chains, are marked with arrows in Fig. 1. By contrast, the copper complex with a longer amphiphile, R=$C_{21}H_{31}$-CONH-$(CH_2)_4$, yielded a GIXD pattern showing only the contribution from the chains (see Annual Report for 1994). Fig. 1 (right) shows the GIXD pattern obtained from a monolayer of the enantiomerically pure amphiphile with R=$C_{16}H_{33}$ spread on a 1mM copper acetate aqueous solution. Assignment of all the Bragg peaks yielded a cell (a_S =15.65Å, b_S =14.63Å γ_S =104.74°) that can be interpreted as a superstructure (a_S =3*a;* b_S =3*b-2a*) of a distorted-hexagonal subcell (*a*=5.22Å, *b*=5.22Å, γ=64.66°, *A*=24.6Å^2; one molecule per cell). The GIXD pattern of the racemic counterpart (not shown) gave a cell (*a*=8.06Å, *b*=6.10Å, γ=92°, *A*=49.14Å^2) corresponding to a complex unit in which the copper is linked to two ligand molecules, presumably of opposite handedness. Thus the racemic amphiphile forms a racemic copper complex monolayer.

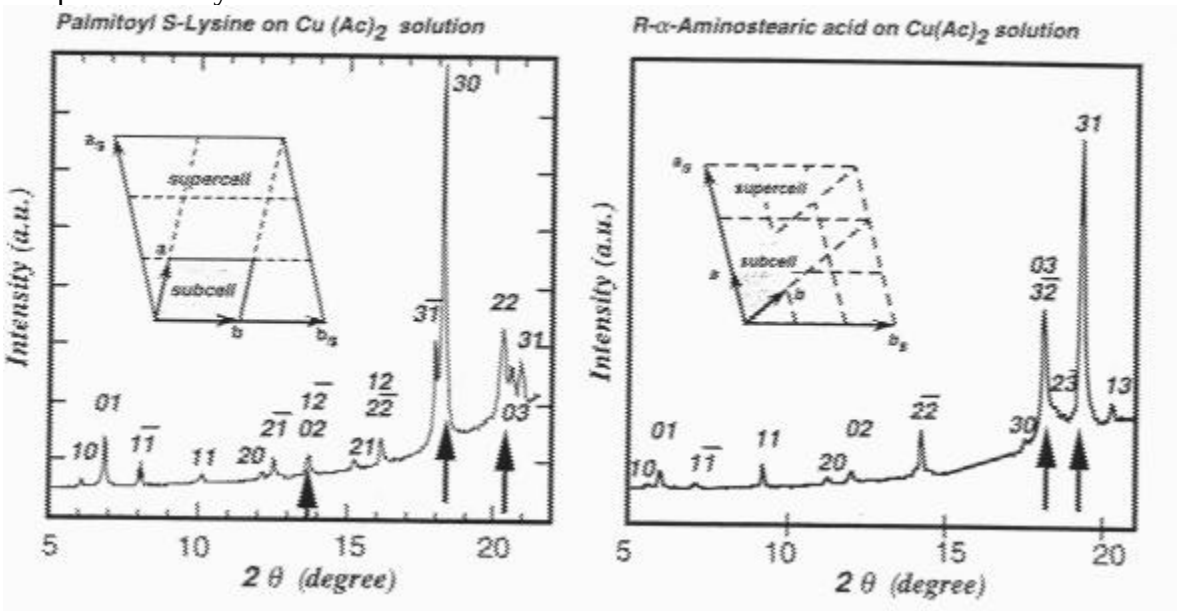

[1] F. Leveiller *et al.* Langmuir **10**, 819 (1994); C. Böhm *et al.*, Langmuir **10**, 830 (1994)

2.6.7 Supramolecular Architecture Prepared *in-situ* at the Air-Aqueous Solution Interface; Thin Films of a 3x3 Grid Silver Complex

I. Weissbuch, L. Leiserowitz, M. Lahav, *Department of Materials & Interfaces, Weizmann Institute of Science, Israel,* P. Howes**,** K. Kjær, *Department of Solid State Physics, Risø National Laboratory, Denmark,* J. Als-Nielsen, *Niels Bohr Institute, Denmark* and P. Baxter, J.-M. Lehn, *Laboratoire de Chimie Supramoléculaire, Université Louis Pasteur, France*

We report on self-assembled crystalline domains of a 3x3 silver grid complex with a specific orientation at the interface, as determined by grazing incidence synchrotron X-ray diffraction (GIXD). Evidence is provided for the self-assembly process of a complex between nine silver(I) metal ions and six ligands, $[Ag_9L_6]^{9+}$ $\bullet 9CF_3SO_3^-$, where *L* is 6,6'-bis[2-(6-methylpyridyl)]-3,3'-bipyridazine, (Fig. 1, left). The process of film preparation, involving spreading a ligand solution in chloroform onto the surface of a 1mM aqueous solution of silver triflate ($Ag^+CF_3SO_3^-$) in the dark, could be monitored by the surface pressure *vs.* area isotherm which showed a significant difference in shape from that of the ligand spread on water. The GIXD pattern measured for the ligand on water, (Fig. 1, mid) yields a rectangular 2-D unit cell of dimensions a=8.12Å, b=20.01Å and molecular area of 81.2Å^2. Bragg rod intensity profiles exhibit maxima that occur at q_z values of 0, 0.6 and 1.2Å^{-1} indicating an orthorhombic unit cell a vertical spacing of 10.5Å ($\cong 2\pi/\Delta q_z$). Indeed, analysis of powder synchrotron X-ray data from 3-D material confirmed the orthorhombic unit cell. In the packing arrangement obtained (space group *Pcab*) the long molecular axis is parallel to the *ab* plane. Since this crystalline plane of the multilayers is parallel to the water surface according to GIXD data, we conclude that the nucleation was initiated by molecules lying flat on the water surface. The GIXD pattern obtained from the ligand spread on a silver triflate aqueous solution, Fig. 1 right, is significantly different. Given the known 3-D crystal structure of the 3x3 silver grid complex (a=28.58Å, b=31.494Å, c=22.45Å, β=116.36°, space group $P112_1/n$, c unique axis) all the Bragg peaks can be easily assigned (*hk*) Miller indices. Such an assignment implies that the crystalline domains adopt a structure akin to that of the 3-D crystal and are oriented with their (001) plane parallel to the liquid surface. Other preferred orientations of the complex crystals would imply the appearance of a strong reflection at q_{xy} of ~0.372Å^{-1} not observed in our measured pattern. Hence the crystallites must be oriented with their *ab* plane parallel to the water surface. The crystalline domains are ~20Å thick, in agreement with the estimate from scanning force microscopy. This value corresponds to an (001) bilayer of the complex units which are related by centers of inversion within each layer, and make interlayer contact by twofold screw symmetry along the vertical *c* axis.

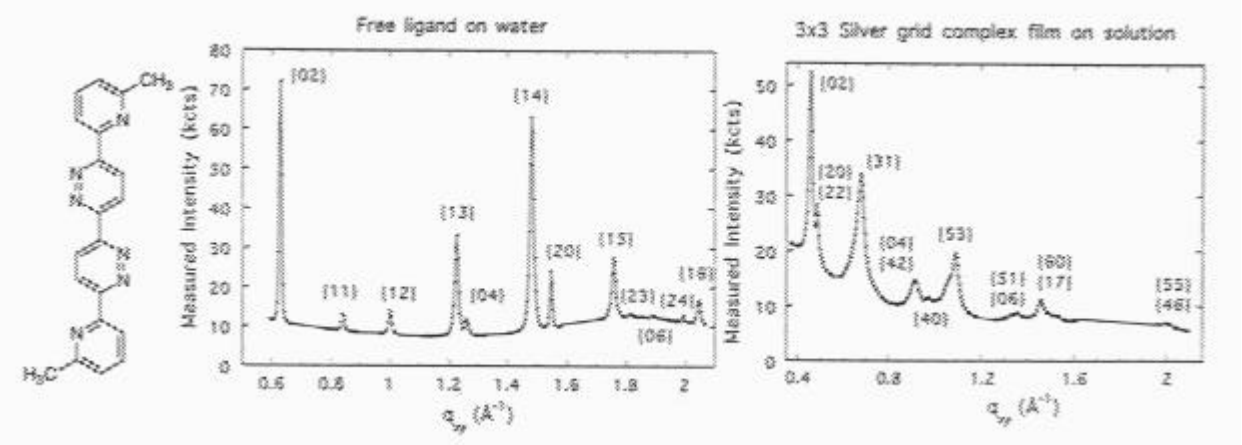

2.6.8 Oriented Crystalline Multilayers of Metal Dicarboxylic Acid Salts Self-Assembled at the Air-Aqueous Solution Interface

I. Weissbuch, M. Lahav, L. Leiserowitz, *Department of Materials & Interfaces, Weizmann Institute of Science, Israel*, J. Als-Nielsen, *Niels Bohr Institute, H.C. Ørsted Institute, Denmark*, P. Howes and K. Kjær, *Department of Solid State Physics, Risø National Laboratory, Denmark*

The present study describes the self-assembly of symmetric dicarboxylic acid molecules, $HOOCC_{22}H_{44}COOH$, on aqueous subphases containing divalent Cd, Pb, Ca, Cu or monovalent Ag ions. These positive ions have a dramatic influence on the packing of the diacid molecules: they bind to both ends of the molecules and force the long hydrocarbon chain to lie parallel to the water surface and to crystallise as multilayer domains about 50-60Å thick. In these crystalline multilayers the bound ions are aligned in columns perpendicular to the surface, with a lateral coherence length in the range of 700-1000Å.

Diacid films spread on a 1.0 mM $CdCl_2$ subphase yield a diffraction pattern exhibiting Bragg peaks up to 15th order, (Fig. 1, left) and, on a 1mM $PbNO_3$ subphase, up to 20th order (Fig. 1, right), much stronger than observed on any other Langmuir film. All normalised peak positions $Q_{xy}/a^* = a\,Q_{xy}/2\pi$ are precisely on integer values corresponding to a lattice spacing of a=33.11Å for Cd salt and a=33.36Å for the Pb salt, very close to the estimated length of an extended molecule. The Q_Z-width of the corresponding Bragg rods yield an estimate of the multilayer thickness of ~55Å.

Some information about the packing of the molecules in the plane normal to the molecular axis is obtained from two peaks at $Q_z > 0$ (not shown). For the Cd^{++} system the peaks occur at total scattering vectors Q_{tot} =1.55Å^{-1} and Q_{tot} =1.69Å^{-1} corresponding to lattice spacings of 4.05 and 3.72Å, respectively. These spacings are close to those found in crystal packing of long-chain molecules. The widths of the peaks correspond to coherently diffracting regions of about 50 Å, i.e. similar to the thickness deduced from the widths of all the harmonic Bragg rods. Independent information on the total thickness, of ~59Å, of the multilayer crystallites was obtained from specular reflectivity data measured for the Cd^{++} system.

For the Pb^{++} system the two peaks occur at Q_{tot}= 1.41Å^{-1} and 1.48Å^{-1} corresponding to lattice spacings of 4.56Å and 4.24Å, respectively.

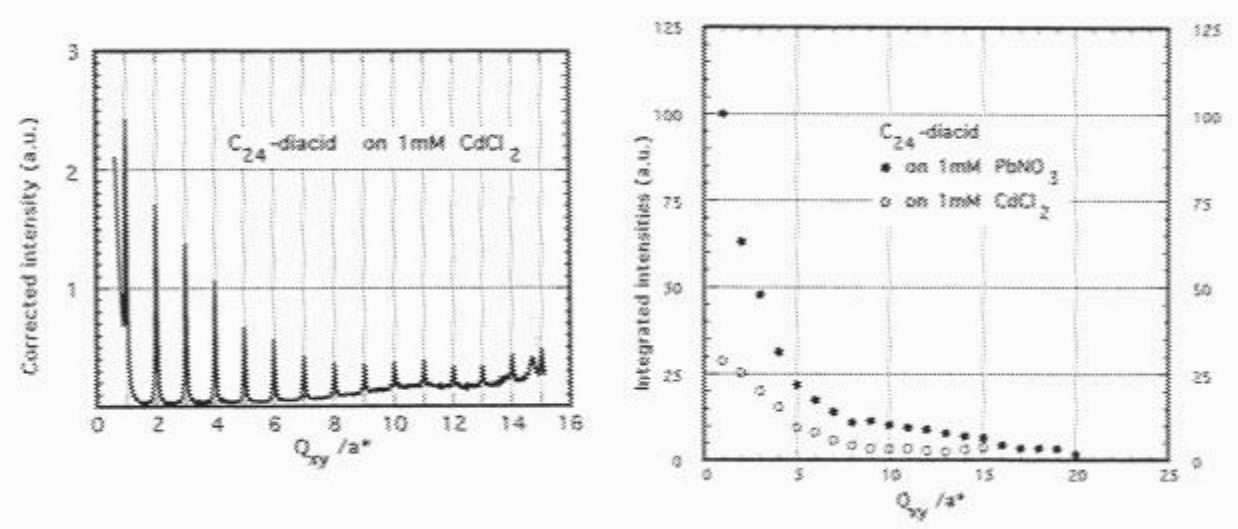

Fig. 1. Left: Scattered intensity *vs.* Q_{xy} for the Cd^{++} system. Right: Integrated intensities for Cd^{++} and Pb^{++} systems.

2.6.9 Chiral Separation of Diastereomeric Monolayers at the Air/water Interface

I. Kuzmenko, M. Lahav, L. Leiserowitz, *Department of Materials & Interfaces, Weizmann Institute of Science, Israel*, J. Als-Nielsen, *Niels Bohr Institute, H. C. Ørsted Institute, Denmark* and K. Kjær, *Department of Solid State Physics, Risø National Laboratory, Denmark*

In bulk, racemic mixtures (R,S) can sometimes be separated by co-crystallisation with suitable chiral agents R' (or S'), utilising differences in solubility and enthalpies of formation of the resulting diastereomeric compounds (R,R' and S,R'). In two dimensions, spontaneous chiral separation of long chiral aminoacids in Langmuir films has recently been observed by grazing-incidence X-ray diffraction (GIXD).[1,2] Here we demonstrate that strong diastereomeric interactions may be used to achieve chiral segregation in 2D crystallites at the air/water interface. A 1:1 mixture of (R)-para-pentadecylmandelic acid [$C_{15}H_{31}$-C_6H_4-CH(OH)-COOH, (R)] and (R)-para-tetradecylphenylethylamine [$C_{14}H_{29}$-C_6H_4-$CH(CH_3)$-NH_2, (R')] forms stable highly crystalline Langmuir monolayer films according to GIXD data (Fig.1, top curve). Indexing of the diffraction pattern brings out an oblique cell (a=5.59 Å, b=9.45 Å, γ=101.45°). The unit cell contains two independent molecules: acid and amine. The GIXD pattern of the second diastereomeric mixture (R,S') (Fig.1, bottom curve) is different from that of (R,R'). The constants of the oblique unit cell are (a=5.55 Å, b=9.55 Å, γ=104.72°). An equimolar mixture of the four components (R,R',S,S') gives rise to a diffraction pattern almost identical to that of the (R,R') mixture (Fig.1 middle curve). Since the oblique unit cell contains only two molecules and the monolayer is highly crystalline, we may conclude that the (R,R',S,S') mixture is separated into (R,R') and (S,S') domains.

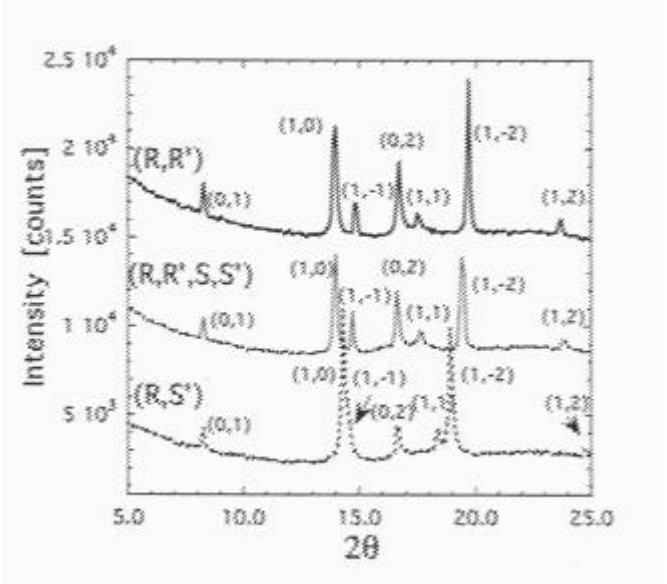

Fig.1

[1] Nassoy, P., Goldmann, M., Bouloussa, O. & Rondelez, F. *Phys. Rev. Letters* **75**, 457 (1995)
[2] Weissbuch, I., *et al. J. Am. Chem. Soc.* (submitted) and Annual Report for 1995

2.6.10 Interdigitated Chiral Architectures at the Air/liquid Interface: Role of Diastereomeric Interactions

I. Kuzmenko, S. Isz, M. Lahav, L. Leiserowitz, *Department of Materials & Interfaces The Weizmann Institute of Science, Israel*, J. Als-Nielsen, *Niels Bohr Institute, H. C. Ørsted Institute, Denmark*, P. Howes and K. Kjær, *Department of Solid State Physics, Risø National Laboratory, Denmark*

The long-chain chiral water-insoluble molecules [(R)-*para*-pentadecylmandelic acid, $C_{15}H_{31}$-C_6H_4-CH*(OH)-COOH, C_{15}-MA] may interact with their water-soluble chemical counterparts [phenylethylamine, C_6H_5-CH*(CH_3)-NH_2, PEA] at the air/solution interface and form mixed amorphous monolayers that, upon compression, transform into crystalline interdigitated trilayers.[1] Grazing incidence X-ray diffraction (GIXD) was used to monitor the process of two-dimensional crystallisation *in-situ* and provide data of near-atomic resolution. The crystallisation is dependent upon the chirality (R,S,R',S') of both components (in these experiments every molecule had one chiral centre) and is likely to be correlated with crystallisation properties of the analogous water-soluble diastereomeric salts (MA, PEA).[1]

We have now extended our surface studies to a more complex system that included the same surfactant C_{15}-MA molecules [of (R)-handedness], whereas ephedrine (C_6H_5-CH*(OH)CH*(CH_3)NH-CH_3, EPH) bearing two chiral centres [(R',R''), (R',S''), (S',R'') or (S',S'')] served as a water soluble component. All the four diastereomeric systems [(R,(R',R'')), (R,(R',S'')), (R,(S',R'')) or (R,(S',S''))] display similar pressure-molecular area (π *vs. A*) isotherms (not shown). They are very expanded and reach a plateau region at A~45Å^2 to ~15Å^2/molecule as for the mixtures of (C_{15}-MA, PEA),[1] suggesting intercalation of the solute molecules between long-chain amphiphilic molecules. Only one chiral combination, namely [R,(R',R'')] gave rise, upon compression, to a strong GIXD diffraction pattern (Fig.1) that appears to correspond to an interdigitated crystalline film with a rectangular lattice (a=11.6Å, b=11.91Å; two acid and two amine molecules per unit cell).

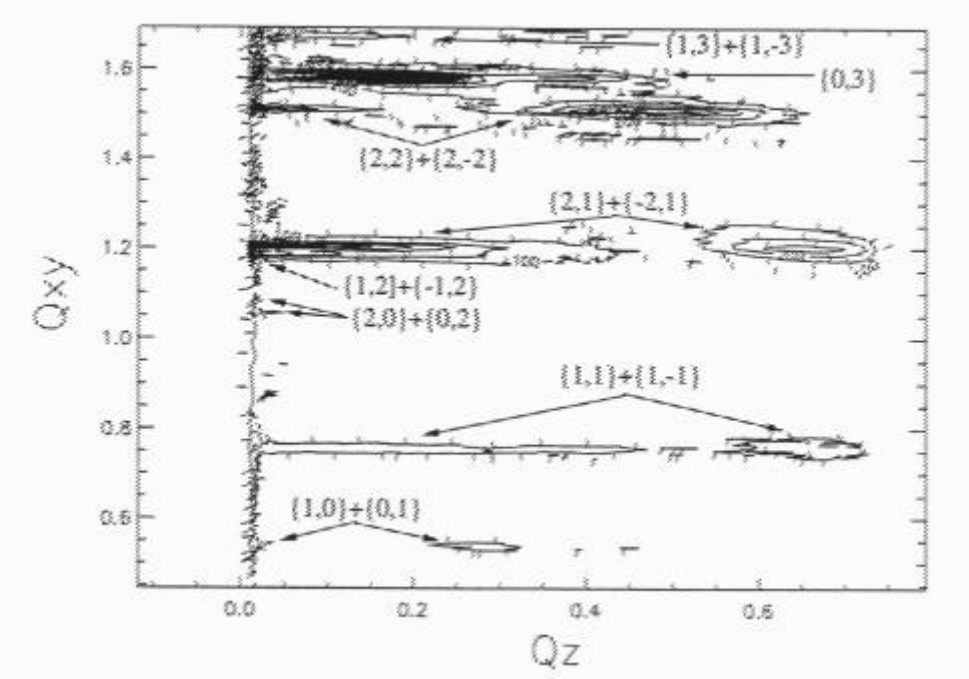

Fig.1

[1] Kuzmenko, I., *et al*. *Science* (in press) and Annual Report for 1995

2.6.11 X-Ray Synchrotron Studies of Polymer-Modified Lipid Monolayers on Water

J. Majewski, G.S. Smith, *MLNSC, Los Alamos National Laboratory, USA*, T. Kuhl, J. Israelachwili, *Department of Chemical and Nuclear Engineering, University of California at Santa Barbara, USA, Denmark,* J. Als-Nielsen, *Niels Bohr Institute, University of Copenhagen, Denmark* and K. Kjær, M. Gerstenberg, *Department of Solid State Physics, Risø National Laboratory, Denmark*

An exciting idea in the area of advanced drug delivery is the use of liposomes composed of macromolecular assemblies of lipids and cholesterol molecules to encapsulate drugs.[1] However, simple liposomes tend to be removed from the bloodstream by the macro phage system (MPS).[1] Recently, it was discovered that by including a small percentage of PEG-lipids (phosphatidyl choline with poly-ethylene oxide or poly-ethylene glycol (PEG) chemically bound to the head group) in the bilayer membrane, the removal of the liposomes by the MPS is greatly reduced and the *in-vivo* bloodstream half-life is increased from hours to days.[2] To gain insight into the physical properties of lipid-polymer/lipid system we performed a series of x-ray reflection and grazing incidence diffraction (GIXD) experiments at BW1 beamline at HASYLAB. We studied monolayers composed of mixtures of distearoyl phosphatidyl ethanolamine (DSPE) mixed with 1.3 and 9% of the same lipid but modified by polyethylene glycol chains (PEG, MW=2000) covalently linked to its head group (DSPE-PEG). Monolayers were spread on a water subphase in a thermostated Langmuir trough. The GIXD data for the pure DSPE and DSPE/DSPE-PEG monolayer yielded three in-plane reflections: {1,0}, {1,1} and {2,0} leading to a hexagonal unit cell of the hydrocarbon chains (a_H =4.7Å, area per lipid molecule for the *crystalline phase* = 38.26Å^2 independent of PEG concentration). The coherence lengths of the 2-D lipid crystallites decreased from 360Å for the pure lipid to 280Å and 230Å for 1.3% and 9.0% DSPE-PEG, respectively. The FWHM(q_z) of each of the Bragg rods increased with PEG-lipid concentration suggesting that the lengths of the coherently diffracting part of the hydrocarbon chains changed from 23Å for the pure lipid to 20Å and 18Å, for 1.3% and 9.0% of the PEG-lipid, respectively. X-ray reflectivity profiles show that both the density and the extension of the polymer segments increase with DSPE-PEG concentration and can be well modelled with a parabolic density profile despite a very weak electron density contrast between the PEG polymer and the water subphase. The roughness of the interface increases with the DSPE-PEG concentration, perhaps indicating that the bulky hydrophilic polymer disrupts the lipid monolayer (Fig.1). The disruption is attributed to two mechanisms: an increase in lipid protrusions due to the increased solubility of the PEG-lipids, and a relaxation of the lateral force between PEG portions by staggering of the lipid headgroups.

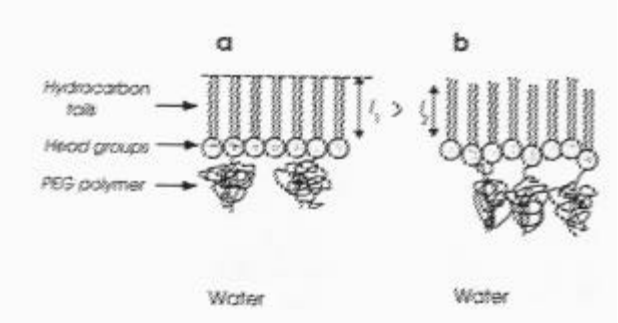

Fig.1. Schematic structure of mixed DSPE with (a) 1.3% and (b) 9.0% DSPE-PEG monolayers showing the decrease in length l of the coherently scattering lipid tails due to the greater out of plane protrusions of the DSPE–PEG molecules.

[1] D. R. Woodle, D. D. Lasic, Biochim. Biophys. Acta, **1113**, 171 (1992). and references therein
[2] T. M. Allen, *et al*, Biochim. Biophys. Acta, **1061**, 56 (1991)

2.6.12 Cyclic Peptides Forming Nanotubes at the Air-Water Interface

H. Rapaport, M. Lahav, L. Leiserowitz, *Department of Materials and Interfaces, The Weizmann Institute of Science, Israel,* J. Als-Nielsen, *Niels Bohr Institute, H. C. Ørsted Institute, Denmark,* P. Howes, K. Kjær, *Department of Solid State Physics, Risø National Laboratory, Denmark,* M.R. Ghadiri and H.S. Kim, *Department of Chemistry, Scripps Research Inst., California, USA*

Cyclic peptides made up of even number of alternating *D*- and *L*- amino acids are ring-shaped and form intermolecular hydrogen bonds, creating tubular structures with a hydrophilic core and a hydrophobic rim[1] (shown schematically for *cyclo*[-*L*-Ser-*D*-Leu-(*L*-Trp-*D*-Leu)$_3$-] in Fig.1). These architectures are expected to have applications as size selective channels in artificial membranes. Three types of cyclic-peptide films spread at the air-water interface, that provides a simple model of membrane environment, were studied by Grazing-Incidence X-ray Diffraction (GIXD).

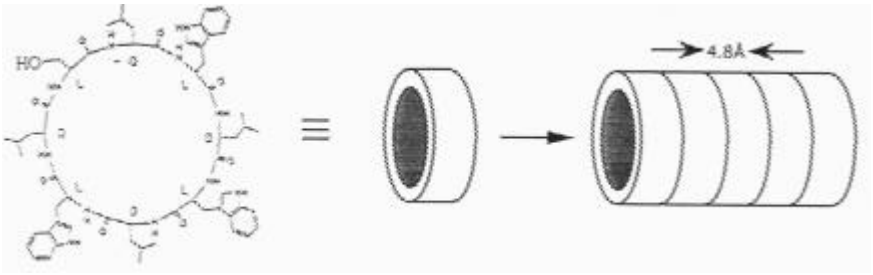

Fig. 1.

For films of *cyclo*[-*L*-Ser-*D*-Leu-(*L*-Trp-*D*-Leu)$_3$-] the GIXD pattern (Fig. 2) exhibits a Bragg rod at q_{XY}=1.3Å^{-1}, peaking at q_Z=0, thus corresponding to nanotubes aligned with the ring plane normal to the water surface and stacked with a 4.8Å lateral spacing. The skewed Bragg rod suggests that the tubes have a mosaic distribution on the water surface. The width of the Bragg rod indicates a film ~35Å thick corresponding to two layers of tubes. The extent of crystalline order along the nanotube is ~60 stacked rings according to the width of the Bragg peak. The film of the similar derivative *cyclo*[-(*L*-Trp-*D*-Leu)$_4$-] formed no ordered structures.
Cyclo[-(*L*-Phe-*D*-N-MeAla)$_4$-] (designed by addition of methylene groups to be devoid of hydrogen-bond donation from one face of the molecule, formed a 2D crystalline film of horizontal rings stacked in antiparallel dimers (Fig. 3). A tetragonal unit cell *a*=*b*=16.8Å was assigned to the GIXD pattern. The widths of the Bragg rods indicate film 25-35Å thick (≅3 layers). The positions of the Bragg rod maxima are in keeping with a body centred unit cell as found in the 3D crystal structure.[2]

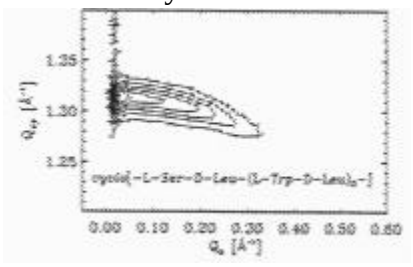

Fig. 2 Bragg rod of *cyclo*[-*L*-Ser-*D*-Leu-(*L*-Trp-*D*-Leu)$_3$ -]

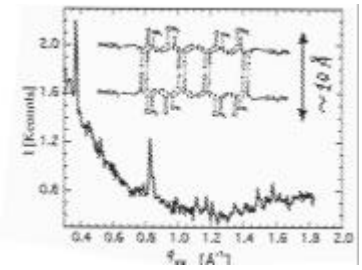

Fig. 3 GIXD pattern of *Cyclo*[-(*L*-Phe-*D*-N-MeAla)$_4$-] inset shows the horizontal ring-dimers.

[1] M. R. Ghadiri *et al.*, Nature, **369**, 301 (1994)
[2] M. R. Granaja *et al.*, Angew. Chem. Int. Ed. Engl.., **34**, 93 (1995)

2.6.13 Crystallography of Monomolecular Protein Surface Layers Using X-ray GIXD

P. Howes, K. Kjær, *Risø National Laboratory, Denmark,* B. Wetzer, D. Pum, U. B. Sleytr, *University for Agriculture, Austria,* S. A. W. Verclas, N. A. Dencher, *Hahn-Meitner-Institute, Germany,* M. Weygand and M. Lösche, *University of Leipzig, Germany*

Protein crystallography has revolutionised our understanding of biological processes, enabling a correlation, in molecular detail, of structure and function for a steadily growing number of biomolecules. The bottleneck is the formation of well-ordered three-dimensional (3D) crystals.[1] Many important biological processes are mediated by proteins which in their functional state are either associated with or incorporated into biomembranes.[2] Unfortunately, such proteins are the least amenable to 3D crystallisation, and only a handful of structures of membrane proteins have been solved by crystallography to date.[3] Because of this problem, electron crystallography has been developed,[4] for which 2D protein crystal sheets are prepared at an interface and analysed under UHV conditions in the electron microscope after heavy ion staining or cryo-fixation. A problem here is the inaccessibility of the surface normal ("hidden cone problem").[5] Using a different approach, we have attempted crystallography of monomolecular protein layers floating on the surface of an aqueous buffer, by means of grazing-incidence X-ray diffraction (GIXD). While GIXD has been widely employed for the structural characterisation of lipid surface layers,[6] its application to proteins[7] met with a number of technical problems which we have solved at HASYLAB's beam line BW1. Advantages of the method are its extreme sensitivity (diffraction from samples that contain as few as 10^{12} molecules!), the "natural" environment of the proteins during investigation that reduces preparation artefacts (sample on top of buffer interface; no need for stain or cryo-fixation) and an increased probability for the formation of 2D protein crystals, as opposed to 3D crystals, in particular of interface-bound membrane proteins. On the other hand, GIXD from 2D protein crystals currently has a quite limited signal-to-noise ratio, limiting the resolution to about 8Å. Also, the data evaluation has yet to be rigorously established. So far, we have investigated 4 proteins bound in different ways to the buffer/air interface. After completing test measurements with streptavidin we obtained useful GIXD also from:

(•) Purple membrane patches, the protein/lipid crystal films containing bacteriorhodopsin (bR) trimers.[8] The preparation procedure was optimised earlier in fluorescence microscopy experiments using labelled membrane patches. Diffraction was observed up to order (h,k)=(4,3) (hexagonal unit cell), corresponding to a resolution of ~ 8Å. Beam damage was not a problem.

(•) Two different bacterial S(urface)-layer proteins (from *B. sphaericus* CCM2177[9] and from *B. coagulans* E38-66[10]) were crystallised under phospholipid monolayers at buffer surfaces and were found to diffract with higher efficiency than bR. Beam damage was severe but careful dose management meant that samples could survive for 10 hours. Data was collected out to Q_{xy} ~ $2\pi/8$Å (*cf.* Fig. 1).

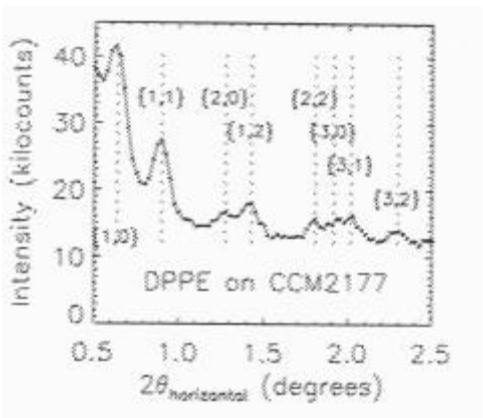

[1] Feher & Kam, in: Methods in Enzymol., **114**, 77 (1985)
[2] Travis, Science, **260**, 906 (1993)
[3] Deisenhofer *et al.*, Nature, **318**, 618 (1985)
[4] Uzgiris & Kornberg, Nature, **301**, 125 (1983)
[5] Darst *et al.*, Biophys. J., **59**, 387 (1991)
[6] Als-Nielsen *et al.*, Physics Reports, **246**, 251 (1994)
[7] Haas *et al.*, Biophys. J., **68**, 312 (1995)
[8] Grigorieff *et al.*, J. Mol. Biol., **259**, 393 (1996)
[9] Pum & Sleytr, Coll. Surf. A, **102**, 99 (1995)
[10] Pum *et al.*, J. Bacteriol., **175**, 2762 (1993)

2.6.14 Temperature and Time Dependent Investigations of Cd-and Uranyl- Stearate Multilayers by means of Neutron Reflectivity Measurements[1]

A. Bolm, U. Englisch, F. Penacorada, and U. Pietsch, *University of Potsdam,Institute of Solid State Physics, Germany*, M.C. Gerstenberg, *Department of Solid State Physics, Risø National Laboratory, Denmark*

Langmuir-Blodgett multilayers of Cd- and Uranyl- stearate salts, prepared by sequential transfer of deuterated and non-deuterated bilayers on a silicon support, have been investigated by neutron reflectivity measurements at the beam line TAS8 at Risø. Already freshly prepared L.B. multilayers show an intermixing of the bilayers which is interpreted by incomplete monolayer transfer from the water surface on solid support.[2] This becomes visible via the reduced intensity of that superlattice peak probing the scattering length density contrast between deuterated and non-deuterated monolayers. Further experiments reveal that the intermixing increases as a function of temperature.[3]
The kinetics of this process was investigated now by combined temperature and time dependent X-ray and neutron reflectivity measurements. For annealing temperatures below 55°C Cd-stearate films show a dramatically decrease of the superstructure peak intensity, indicating an increase of intermixing. Taking into account that the X-ray reflectivity pattern remain nearly unchanged the intermixing is interpreted by discrete hopping of fatty acid salt molecules between various bilayer sites. Its time constant decreases as a function of temperature and vanishes close to the melting point of the stearic acid phase at about 75°C. The Arrhenius like activation energy for the hopping process was estimated to be about 1.9 eV.
For Uranyl-stearate samples we observed complete intermixing already at about 40°C which is interpreted by the reduced lateral interaction among the hydrocarbon chains induced by the bigger counter ions.

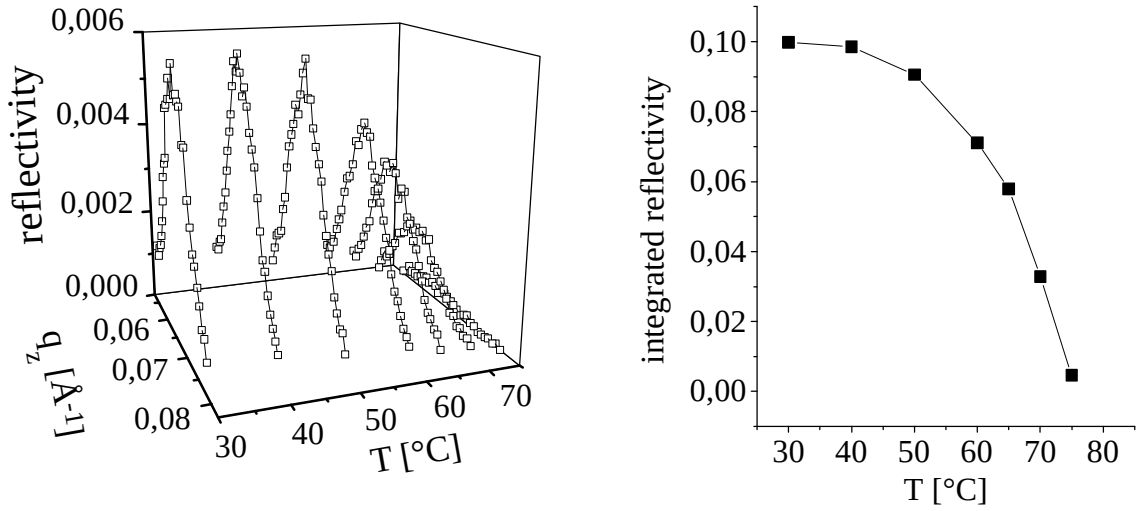

Fig. 1. Temperature dependent variation of the superstructure peak intensity. The integrated reflectivity varies like the order parameter near the order-disorder transition of an AB-alloy. "Domain melting" can be neglected because the FWHM of the ω -scans (not shown here) is nearly constant.

---

1 The results have been presented on ECOF6, Sheffield, September 1996, to be published in Supramolecular Science (this abstract) and on the 1st European Conference on Neutron Scattering, Oct 1996 in Interlaken, Switzerland

2 M.R. Buhenko, M.J. Grundy, R.M. Richardson, S.J. Roser, Thin Solid Films **159**, 253 (1988)

3 U. Englisch, T.A. Barberka, U. Pietsch, H. Hoehne, Thin Solid Films **266**, 234 (1995)

2.7 Microemulsions, Surfactants and Biological Systems

2.7.1 Isotropic Lifshitz Behavior in Block Copolymer-Homopolymer Blends

F.S. Bates, W. Maurer, T.P. Lodge, M.F. Schulz, M.W. Matsen, *Department of Chemical Engineering and Material Science, University of Minnesota, USA*, K. Almdal and K. Mortensen, *Department of Solid State Physics, Risø National Laboratory, Denmark*

Blends of homopolymers and diblock copolymers offer unique physical systems in which one may expect critical phenomena with competing length-scales. While block copolymer tend to phase separate on a microscopic length scale given by the polymer radius of gyration (characteristic momentum $q^* \sim R_g^{-1}$) resulting in an ordered phase, homopolymer blends phase separate macroscopically ($q^*=0$). Theory predicts that in such systems a line of order-disorder transitions with wavevector $q^*>0$ will meet a λ-line of second-order critical points with $q^*=0$ at an isotropic Lifshitz point,[1] as shown in Fig.1. Above the λ-line the system is disordered. Adding homopolymer to the lamellar phase continuously increases the repeat distance *D* until a transition, *UT*, where the system separates into two phases. Lifshitz critical behavior have been discussed widely in theory, however, up to the present no experiments have confirmed the existence of an isotropic Lifshitz point, *LP*.

We have studied the phase diagram of a three-component mixture of poly(ethylene), PE, (N_{PE}=392), poly(ethylenepropylene), PEP, (N_{PEP}=409) homopolymers and PE-PEP symmetric block copolymer ($N_{PE\text{-}PEP}$=1952).[2] The results included in Fig.1 show remarkable agreement with the theoretical picture, including the *LP*-point at ϕ=0.91. In the disordered phase above the ODT-line, the scattering function follows the Leibler-function with a peak in intensity at $q^* \neq 0$, whereas Ornstein-Zernike ($I^{-1} \propto q^2$) characteristics is found above the line of demixing. In the mean-field picture, i.e. ignoring renormalizations due to fluctuations, the second-order fluctuation term in the Landau-free energy vanish at the Lifshitz-point,[1] implying $I^{-1}(q) \propto q^4$ and $I^{-1}(q=0) \propto T^{-1}$ characteristic. This is exactly the form found experimentally,[2] which seems quite surprising knowing that fluctuations markedly renormalizes the behavior in both block copolymers and homopolymer blends. Fig.2 shows this meanfield character of *I(q=0)* and χ.

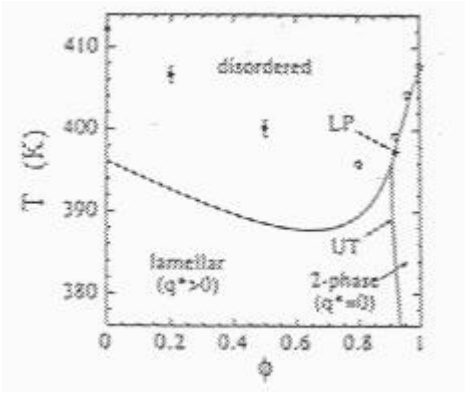

Fig.1. Phase diagram for the PE-PEP block copolymer-homopolymer phasediagram.

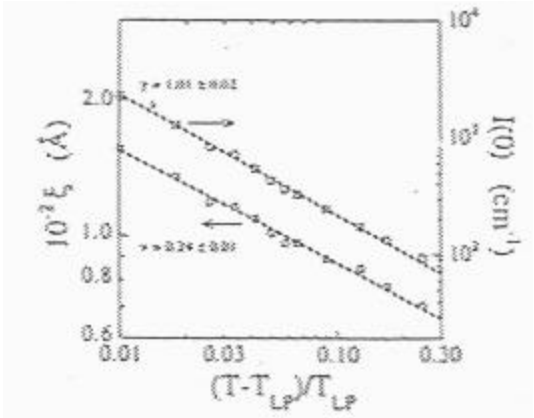

Fig.2. Correlation length and zero angle scattering versus reduced temperature, revealing mean-field behavior

[1] D. Broseta, G.H. Fredrickson, G.H. J. Chem. Phys. **93** 2927 (1990)

[2] F.S. Bates, W. Maurer, T.P. Lodge, M.F. Schulz, M.W. Matsen, K. Almdal, K. Mortensen, Phys. Rev. Letter **75**. 4429 (1995)

2.7.2 Pressure Dependence of the Phase Behavior of PEP-PDMS Diblock Copolymer[1]

K. Mortensen and K. Almdal, *Department of Solid State Physics, Risø National Laboratory, Denmark,* D. Schwahn and H. Frielinghaus, *Forschungszentrum Jülich GmbH, Germany*

Studies of the phase behavior of polymer systems has proven that the sensitivity to fluctuations is much more distinct than originally anticipated based on theoretical arguments. In blends of homo-polymers, studies have revealed that fluctuations give rise to significant re-normalised critical behaviour, showing cross-over from mean-field to 3d-Ising character at a well defined Ginzburg value.[2] In block copolymers the fluctuations have even more pronounced effects, as it changes the second order critical point at f=0.5 to first order and additional complex phases are stabilised. It has been argued that the free volume causes an entropic contribution, χ_σ, to the Flory-Huggins interaction parameter, $\chi=\chi_h/T+\chi_\sigma$, and is thereby responsible for the re-normalised critical behaviour. In binary homopolymer blends this was proven by application of hydrodynamic pressure which directly probe the dependence of free volume.[3] Pressure was found generally to shift the phase boundaries to higher temperatures in agreement with the relation between free volume and χ_σ.

The phase behaviour of diblock copolymer are studied by measuring the structure factor *S(q)* in scattering experiments. *S(q)* represents various parameter's which all change discontinuous at the first order T_{ODT}. In a study of the symmetric diblock copolymer, PEP-PDMS 6, three parameters could be obtained from *S(q)* which all changes discontinuously at the order-disorder temperature.[1] These are the peak intensity, *S(q*)*, the peak width, (1/x), and peak position q^*. The change in q^* was identified through a marked unexpected singularity in the conformational compressibility. The phase diagram of PEP-PDMS as determined from the three parameters is shown in Fig.1. The phase boundary between disordered and ordered phases has unique character with re-entrant ordered structure. While pressure has marked and unexpected effect on the general phase behavior, it apparently does not affect the Ginzburg number significantly, indicating that the order parameter is much less influenced by the compressibility as compared to binary homo-polymers blends.

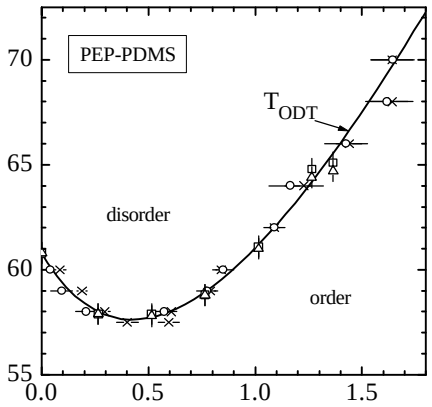

Fig. 1. Phase diagram of the PEP-PDMS diblock copolymer in the temperature-pressure representation, as determined from discontinuity in hight and width in *S(Q*)* and conformational compressibility at T_{ODT}.

1 D.Schwahn, H.Friedlinghaus, K. Mortensen, K. Almdal, Phys.Rev.Lett. **77,** 3153, (1996); K. Mortensen, K. Almdal, D.Schwahn, H.Friedlinghaus, Macromolecular Symposia, *in press*

2 D. Schwahn, G. Meier, K. Mortensen, S. Janssen, J. Phys.II (France) **4**, 837, (1994)

3 S.Janssen, D.Schwahn, T.Springer, K.Mortensen, Macromolecules **28**, 2555 (1995); D. Schwahn, T. Schmackers, K. Mortensen, Phys.Rev.E **52,** R1288, (1995)

2.7.3 Diblock Copolymer Blends with Small Amounts of Homopolymer

V.T. Bartels, M. Stamm, V. Abetz, *Max Planck Institut für Polymerforschung, Germany* and K. Mortensen, *Department of Solid State Physics, Risø National Laboratory, Denmark*

The phase behavior of diblock copolymer melts has been the subject of intense research over the past two decades, and the general phase behavior of pure systems are approaching a relative well understanding, including the role of fluctuations and polymer asymmetry.[1] Block copolymers synthesised via anionic polymerisation are, however, usually not pure but contain small amounts of un-reacted homopolymers. The changes in the phase behavior by the presence of such homopolymers may significantly change the phase-diagram, and may include the Lifshitz critical point where macroscopic phase separation meets the regime of microphase separation.[2] The appearance of small amounts of homopolymer in diblock copolymer melts is expected to change the structure-factor, *S(q)*, with the result that *S(q)* does not vanish at small scattering momentum *q*, and the peak-position *q** may expected to be shifted to lower values.[3]
Experimentally, we have studied the influence of small amounts of polystyrene, PS, homopolymers in a diblock copolymer of polystyrene-poly(paramethylstyrene), PS-PPMS, in which the polystyrene blocks were deuterated.[4] The structure factor was measured using small-angle neutron scattering. At small scattering vectors, $q \rightarrow 0$ the structure factor is finite, as theoretically predicted, with a clear temperature dependence. Furthermore, the *q*-value of maximum intensity, *q**, is shifted to smaller values, as seen in Fig.1a. On the other hand, the peak width *w* and the microphase separation (order-disorder) temperature T_{ODT} do not significantly change with the amount of homopolymer and the qualitative temperature dependencies of *q** and *w* are unchanged (Fig.1). The stretching of the copolymer chains at the order-disorder transition appear to be smaller with the presence of homopolymers, as seen in Fig.1a, probably as a result of the dilution.

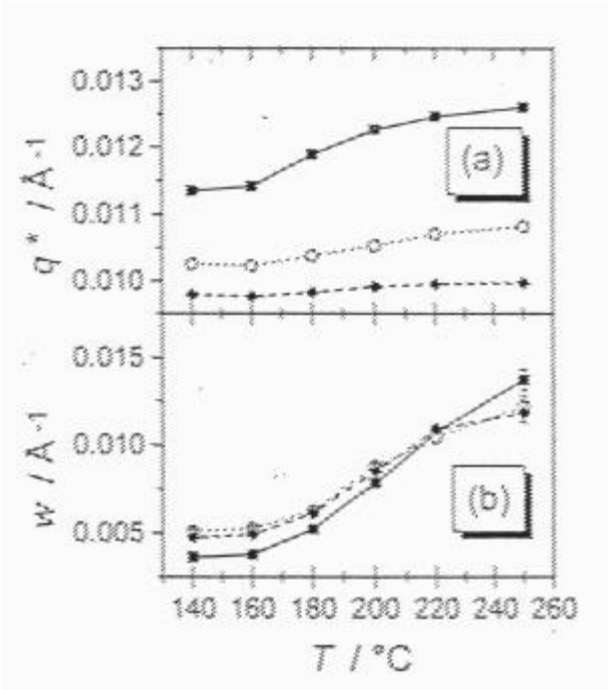

Fig.1 Characteristics of the structure factor of PS-PPMS with different amounts of PS-homopolymers (0, 5% and 10%). a) Maximum position *q**, and b) peak width *w* as a function of temperature near T_{ODT}.

1 F.S. Bates, M.F. Schultz, A.K. Khandpur, S. Förster, J.H. Rosedale, K. Almdal, K. Mortensen, Trans. Faraday Soc., **98**, 7, (1994)
2 F.S. Bates, W. Maurer, T.P. Lodge, M.F. Schulz, M.V. Matsen, K. Almdal, K. Mortensen, Phys. Rev. Lett. **75** 4429 (1995)
3 N. Nojima, R.J. Roe, Macromolecules **20** 1866 (1987)
4 V.T. Bartels, M. Stamm, V. Abetz, K. Mortensen, *submitted*

2.7.4 Micro-phase Separation in Polymer Electrolyte Models PPO-$LiClO_4$ and PPO-$Mg(ClO_4)_2$

P. Carlsson, L.M. Torell, *Department of Physics, Chalmers University of Technology, Sweden,* M. Käll, *Department of Applied Physics, Chalmers University of Technology, Sweden* and K. Mortensen, *Department of Solid State Physics, Risø National Laboratory, Denmark*

Polymer electrolytes have recently attracted great attention because of promising applications in new polymer based batteries. The mechanism of ion conduction is generally believed to be linked to the polymer segmental mobility, but detailed knowledge about the structural characteristics needed for achieving high conductivity is totally lacking. The aim of the present work is to provide experimental data to correlate the transport properties and with structure.

Previous structural investigations of polymer electrolytes have been focused on crystalline polymer electrolytes, even though it is the amorphous phase which is conducting. We have studied two model systems of amorphous poly(propylene oxide), PPO, electrolytes with very different electric characteristics: the conducting PPO-$LiClO_4$, and the non-conducting PPO-$Mg(ClO_4)_2$. With molecular weight $M_w \approx 4000$, the former material is a viscous liquid whereas the latter is rubbery in character. The solvated cations can act as a coordination centre of several ether oxygens, and it is suggested that they thereby also can act as transient cross links between neighbouring chains. Recent reports based on segmental mobility[1,2] studies, measurements of the glass transition temperature[3,4,5] and structural relaxation dynamics[6,7] and photon correlation measurements indicates microscopic two-phase structure in salt-polyether complexes, which has been attributed to salt-depleted and salt-rich regions.

In Fig.1, the scattered function *S(q)*, as measured by SANS, is plotted versus momentum transfer, *q*. The data are obtained for PPO-$LiClO_4$ with ether oxygens per cation concentration 10:1 and data for PPO-$Mg(ClO_4)_2$ with concentration 20:1 Large differences for the two materials can be observed in *S(q)*. In case of the conducting Li^+-systems the small angle scattering is weak and structure less indicating a homogeneous material. In contrast, the non-conducting Mg^{++} system shows a pronounced peak. The SANS results of the latter indicates thus fluctuations on a length scale of roughly $(2\pi/0.08Å^{-1}) \approx 80Å$, giving evidence for micro-phase separation into salt-rich and salt-depleted regions. The characteristic length scale can be interpreted as the distance between the salt-rich regions.

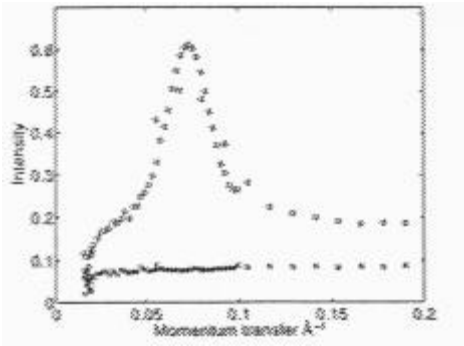

Fig.1 The intensity versus momentum transfer from small angle neutron scattering measurements on PPO-$Mg(ClO_4)_2$ of concentration 20:1 (o) and PPO-$LiClO_4$ of concentration 10:1 (x).

1 P. Carlsson, J. Swenson, R.L. McGreevy, B. Gabrys, W.S. Howells, L. Börjesson, L.M. Torell. Physica B *in press*
2 L.M. Torell and C.A. Angell. British Polymer Journal, **20**, 173, (1988)
3 Q.~Lu and C.A. Angell. *To be published*
4 C. Vachon, M. Vasco, M. Perrier, and J. Prud'homme. Macromolecules, **26**, 4023, (1993)
5 C. Vachon, C. Labréche, A. Vallée, S. Besner, M. Dumont, and J. Prud'homme. Macromolecules, **28** 5585 (1995)
6 R. Bergman, L. Börjesson, G. Fytas, and L.M. Torell. Journal of Non-crystalline Solids, **172,** 830, (1994)
7 R. Bergman, A. Brodin, D. Engberg, Q. Lu, C.A. Angell, and L.M. Torell. Electrochimica Acta, **40** 2049, (1995)

2.7.5 Structure of PS-PEO Diblock Copolymers in Solution and the Bulk State Probed using Mechanical, Dynamic Light Scattering and Small-angle Neutron Scattering

K. Mortensen, K. Almdal , *Department of Solid State Physics, Risø National Laboratory, Denmark,* W. Brown, E. Alami, *Department of Physical Chemistry, Uppsala University, Sweden* and A. Jada, *Centre de Researches sur la Physico-Chimie des Surfaces Solides, France*

While many block copolymers undergo order-disorder transitions as a consequence of enthalpy-driven phase-separation, ordering on the mesoscopic length scale may also occur when one of the blocks crystallises. Block copolymers of poly(ethylene oxide) typically shows such ordering.[1] In selective solvent, i.e. solvent which is which is good for one block but a bad for the other block, the polymers self-association into well defined structures. These may be micellar aggregates spherical, rod-like or discs form depending on the molecular details and the location in the phase diagram. In aqueous systems, block copolymers with poly(ethylene oxide) as the water-soluble part have recently attracted great interest both for their application and in basic research.[2] The present report[3] describes small-angle neutron and light scattering and rheological studies which are used to elucidate the structural features of the bulk as well as D_2O solutions of a low molecular weight diblock copolymer of polystyrene, PS (M_w=1000) and polyethylene oxide, PEO (M_{PEO}=3000). At low temperature the bulk block copolymer forms a lamellar mesophase driven by the crystallisation of PEO (Fig.1). The melting point of PEO, $T\approx64$ °C, is accompanied by an order-to-disorder transition. The melt is typified by single exponential correlation functions in the dynamic light scattering spectra, observed in the temperature range 60-100 °C. In aqueous solutions up to roughly 20% polymer concentration, PS-PEO self-associates into spherical micelles (Fig.2 and 3) with core size of $R_c\approx56$Å and interaction radius $R_{hs}\approx115$Å, corresponding to an aggregation number of 470. The hydrodynamic radius R_h=140Å obtained from dynamic light scattering is close to, but somewhat larger than the interaction radius, as expected.

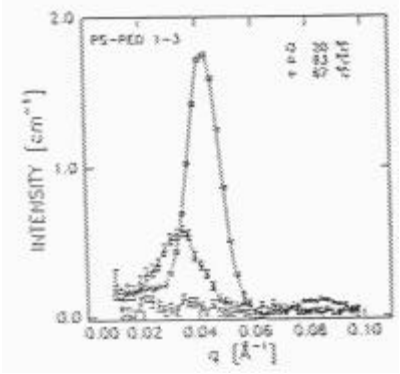

Fig.1 Small-angle neutron scattering data of bulk PS-PEO~1-3, as obtained at temperatures 20, 63 and 67 °C.

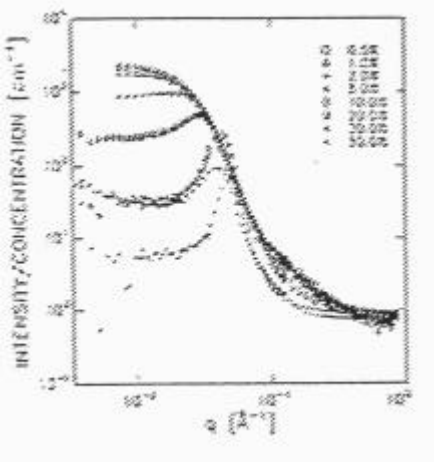

Fig.2 Small-angle neutron scattering data of aqueous solutions of PS-PEO1-3, as obtained at T=20 °C.

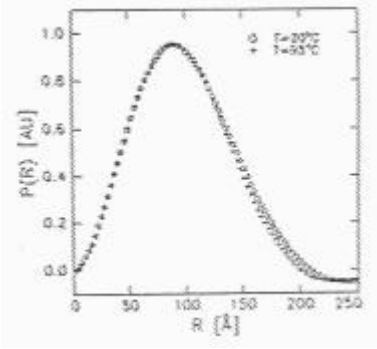

Fig.3 Fourier transform of 1% aqueous solutions of PS-PEO 1-3 as resulting from scattering data.

---

1 M. Hillmyer, F.S. Bates, K. Almdal, K. Mortensen, A. Ryan, Science **271** 976 (1996) 271, 976

2 K. Mortensen, J.Physics Condensed Matter **8** A103 (1996)

3 K M ortensen, K. Almdal, W. Brown, E. Alami, A. Jada, Langmuir *submitted*

2.7.6 Cubic Phase in a Connected Micellar Network of Poly(Propylene Oxide) Poly(Ethylene Oxide)-Poly(Propylene Oxide) Triblock Copolymers in Water

K. Mortensen, *Department of Solid State Physics, Risø National Laboratory, Denmark*

Block copolymer surfactants presently attract great interest both as a result of their commercial utility, and because of their novel physical behavior. Many studies have been performed on aqueous solutions of triblock copolymer of poly(ethylene oxide), PEO, and poly(propylene oxide), PPO as recently reviewed.[1] It is well established that aqueous solutions of PEO-PPO-PEO in wide temperature/concentration ranges associate into spherical micellar aggregates along with rod-like and possibly layered micelles. The spherical micelles constitute the basis for gel formation in the form of a body-centred cubic (BCC) mesophase, formed by simple hard-sphere crystallisation.

Aqueous suspensions of the reversed block copolymer architecture, PPO-PEO-PPO, show rather different phase behavior.[2] But also this system is dominated by spherical micelles in a wide region of the phase diagram. Due to the hydrophobic blocks situated at both ends, however, the block-copolymer associate into a network of micelles rather than the independent micelles given in PEO-PPO-PEO systems. Small-angle neutron scattering studies are presented in the solid aqueous gel phase of the Pluronic-R polymer, 25R8, which is a triblock copolymer with a central poly(ethylene oxide) block symmetrically surrounded by poly(propylene oxide) blocks: $PO_{15}EO_{156}PO_{15}$. At copolymer concentrations of the order of 50-65%, these copolymers associates into a homogeneous phase constituting an interconnected network of micelles, in which micellar cores of hydrophobic poly(propylene oxide) are interconnected by hydrophilic poly(ethylene oxide) strands.[2] At temperatures below 40^{o}C, the materials form three solid gel phases. Neutron scattering show that two of these phases have characteristics of cubic structures.[3] The third phase constitutes a mixture of ordered micelles and a lamellar phase of crystalline PEO. The cubic phase close to the order-disorder transition can by shear be aligned into a mono (or twinned) domain structure, resulting in a novel polymer network in which the micellar knots are positioned on a lattice.

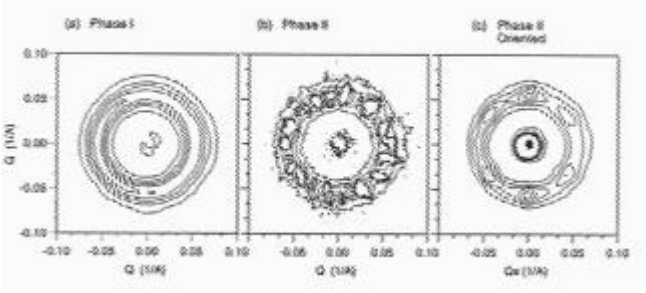

Fig.1 Two-dimensional scattering pattern of a 55% 25R8 suspension obtained in a) the liquid micellar phase (55% polymer at 43 ^{o}C); b) the solid cubic phase (55% polymer at 41 ^{o}C) when quenched from phase I and c) when shear-aligned.

[1] K. Mortensen, J. Physics Condensed Matter **8** A103 (1996)
[2] K. Mortensen, W. Brown, E. Jørgensen, Macromolecules **27** 5654 (1994)
[3] K. Mortensen, Macromolecules,in press

2.7.7 Scattering Studies of Aerogels During Gel-formation and Ageing

M.B. Kirkedelen, J. Samseth, *IFE, Norway*, M.-A. Einarsrud, A. Hansen, *NTNU, Norway and* K. Mortensen, *Department of Solid State Physics, Risø National Laboratory, Denmark*

Silica aerogels are porous materials that can contain up to 99% air. Thus, they are good insulators and have potentially a broad range of applications. There are several aspects of these gels that can be studied by small-angle neutron scattering, SANS. We have studied both the dynamic formation of the aerogels and the structural characteristics of aged gels that have been aged under different conditions both with respect to duration and with respect to post-processing temperatures.

The scattering patterns from the aged gels show typical a fractal behavior. Each curves usually contains several fractal regions with well defined crossovers between them. The fractal dimensions and the crossovers vary from sample to sample, but so far there is no clear correlation between structural characteristics and the different parameters that are important during ageing and post-processing.

The formation of wet gels was followed by SANS as their structure evolved. The system we studied was tetraethoxysilane, abbreviated TEOS, in a solvent of ethanol, HCl and ammonia. The samples were carefully prepared and put into the neutron beam almost immediately in order to look at the early stages of the gelation process. Spectra were then taken at fixed time intervals of a few minutes. Some results are shown in the Fig.1. At the beginning of the gelation process, the scattering is only weak and structure-less, indicating that no aggregates are present. As time goes by the scattering intensity increases, reflecting the formation of clusters. The size of these initial clusters are a few nanometers.

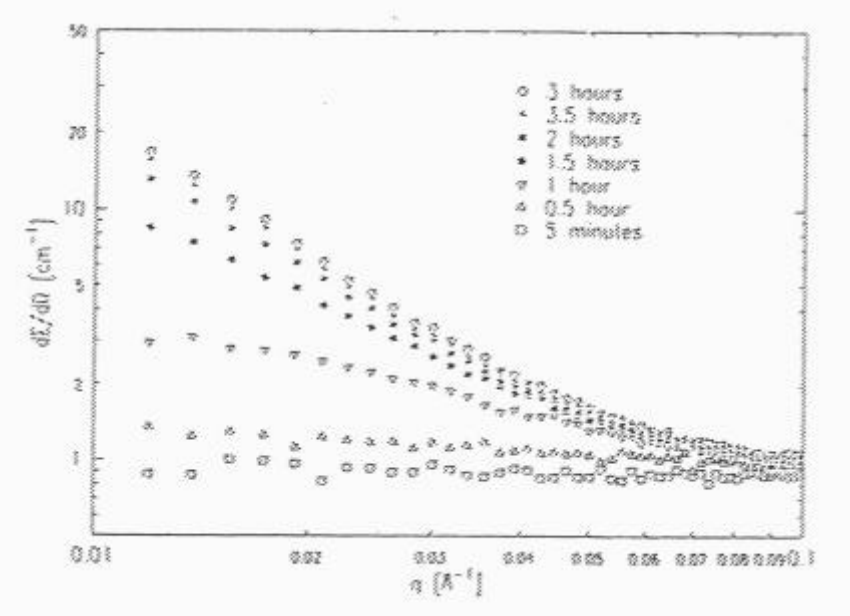

Fig. 1. Small-angle scattering data of TEOS in solvent of ethanol, HCl and ammonia, as obtained at various times, between five minutes and three hours, during the gel-formation.

2.7.8 The Effect of Short Chain Alcohols on SDS Micelles

G. Førland, *Department of Chemistry, University of Bergen, Norway,* J. Samseth, *IFE, Norway,* and K. Mortensen, *Department of Solid State Physics, Risø National Laboratory, Denmark*

Sodium Dodecyl Sulphate (SDS) form micelles in water. Their size and shape depend upon parameters such as temperature and salt concentration. Addition of short chained alcohols will in analogy to salts modify the interactions between the head groups of the SDS molecules. This is due to the polar character of the OH-group of the alcohol.

We have studied the effect of 3 alcohols; 1-propanol, 1-butanol and 1-pentanol, which all showed significant effects on the size and shape of the SDS-micelles. The SDS concentration was kept constant at 0.04 molal, and NaCl was added (0.4 molal) in order to avoid interactions between the micelles. The experimental scattering functions were all well fitted to ellipsoidal form. Common for all alcohols is that the micellar shape is prolate (or spherical) object. In Fig.1 is shown the length and width of the ellipsoidal micelles, as obtained from fits to the experimental data. The pristine SDS-micelles are prolate with aspect ratio of about 2. By adding propanol the prolate object gets shorter and approaches spherical form at ~1.5 molal propanol. With more alcohol the micelles become significant smaller as they approach the limit where the micelle might disintegrate. In the case of butanol a peculiar behavior is observed. When butanol is added in small amounts (<0.1molal), the micelles grow. As more is added the micelle becomes shorter and reaches a plateau close to a spherical shape. By adding even more alcohol the micelle again grow. Pentanol causes the micelle to grow to a long objects that is about 10 times longer than the pristine SDS-micelles, and the micelles get slightly thinner.

The diverging effects of the three alcohols may be related to the differences in molecular polarity. Pentanol is less polar because of its longer hydrocarbon tail and prefers to integrate with the micelle rather than in the aqueous phase, thus increasing the micellar length. Propanol is most polar and is readily dissolvable in water. This will reduce the polarity of the solvent and the micelle will tend to disintegrate. Butanol shows with an intermediate size hydrocarbon chain signature of both characteristcs.

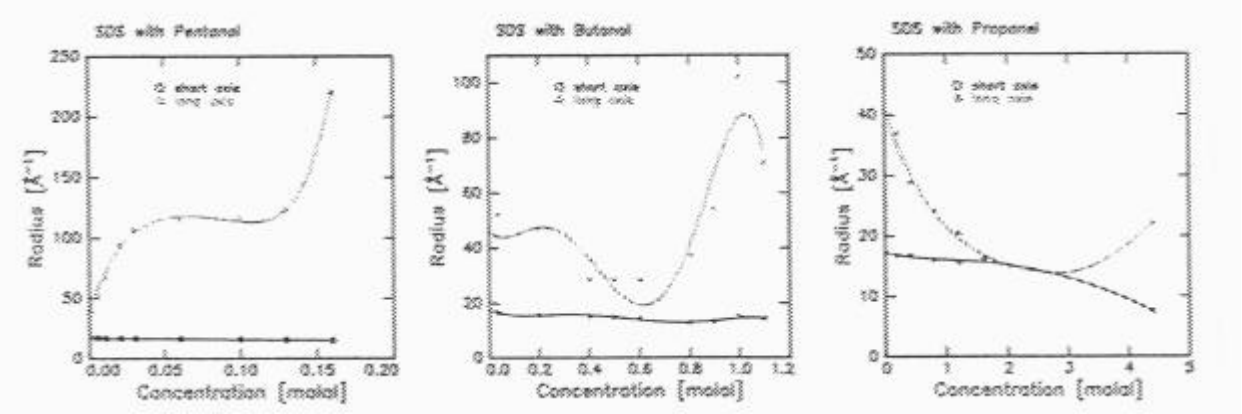

Fig. 1 Size of micellar ellipsoids as obtained from fits to the experimental SANS data of SDS with various concentration of a) 1-pentanol, b) 1-butanol, and c) 1-propanol.

2.7.9 Reverse (Water-in-oil) Micelles of Amphiphilic Block Copolymers: A Small-angle X-ray and Neutron Scattering Investigation

P. Alexandridis, B. Svensson, U. Olsson, B. Lindman, *Center for Surface and Colloid Science, University of Lund, Sweden* and K. Mortensen, *Department of Solid State Physics, Risø National Laboratory, Denmark*

Di- and tri-block copolymers are known to associate into micelles when dissolved in selective solvents.[1,2,3] One such example are polyoxyalkylene block copolymers composed of poly(ethylene oxide) (PEO) and poly(propylene oxide) (PPO) which form spherical micelles in water, a selective solvent for the PEO block.[2,3] Depending on the copolymer PEO/PPO composition, the micelles can pack into a body-centered cubic lattice when their effective concentration reaches that required for hard-sphere crystallization.[3] Hexagonal and lamellar lyotropic liquid crystalline structures can also be formed at higher copolymer concentrations.[3] Little is still known about the solution behavior of polyoxyalkylene block copolymers in organic solvents. $EO_{13}PO_{30}EO_{13}$ (Pluronic L64) does not form micelles in o-xylene; however, micelles with hydrated PEO core and a PPO corona can be formed by L64 in o-xylene in the presence of water at concentrations higher thatn 0.15 water molecules per EO segment.[4] In our investigation of the complete phase diagram of the $EO_{13}PO_{30}$ EO_{13}-water-p-xylene system at 25°C, it appear that the copolymer is miscible with p-xylene in all proportions and formed an isotropic solution (L2 region) along the copolymer-oil axis of the ternary phase diagram; 2 water molecules per EO segment could be solubilized in p-xylene.[5] L2 regions have now been identified in a number of PEO-PPO/water/p-xylene systems. The present SANS investigation aims in determining the dimensions and structure of PEO/PPO reverse (water-in-xylene) micelles as affected by the micelle volume fraction, the copolymer molecular weight, and the solution temperature. The reverse micelle radius was found on the order of 70 Å and increased with increasing copolymer mol. weight. The reverse micelles can crystallize (increased order) into a cubic lattice for sufficiently high copolymer mol. weight. Contrast matching of the water and the xylene revealed that the reverse micelles have a core (of radius 20 Å) consisting mainly of water and an extended PEO/PPO interfacial region (of thickness 30 Å). The reverse micelle radius did not vary with the copolymer+water (dispersed phase) concentration at a fixed water/copolymer ratio. The reverse micelle radius increased with temperature.

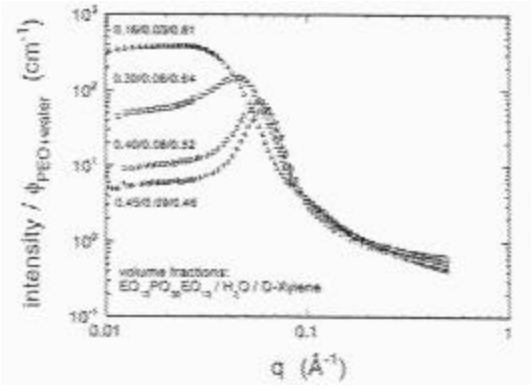

Fig.1 Scattering function of $EO_{13}PO_{30}$ EO_{13} reverse micelles at different copolymer + water composition and T=25°C. The water / EO ratio was constant, 1.2.

1 P. Alexandridis, T.A. Hatton, In *The Polymeric Materials Encyclopedia*, Salamone, J. (Ed); CRC Press (1996)
2 P. Alexandridis, T.A. Hatton, Colloids Surfaces **A 96** 1 (1995)
3 K. Mortensen, J. Phys.: Condens. Matter **8** A103 (1996)
4 G. Wu, Z. Zhou, B Chu, Macromolecules **26** 2117 (1993)
5 P. Alexandridis, U. Olsson, B. Lindman, Macromolecules **28** 7700 (1995)

2.7.10 Surface Induced Ordering of Triblock Copolymer Micelles at the Solid-Liquid Interface

M.C. Gerstenberg, J.S. Pedersen, *Department of Solid State Physics, Risø National Laboratory, Denmark,* G. Smith and Manual Lujan Jr. *Neutron Scattering Center, LANSCE, Los Alamos National Laboratory, USA*

The amphiphilic triblock copolymer P85[1] aggregates in aqueous solution *e.g.* as spherical micelles, hexagonal rods, or prolate ellipsoids. For polymer concentrations between 15 to 25 % wt and temperatures between 30 to 60 ^{o}C in the bulk micellar regime the scattering length density profiles obtained from neutron reflection measurements of the solution-single crystalline quartz interface showed micellar ordering close to the quartz surface. In an effort to model the ordering we have performed Monte Carlo simulations of hard spheres confined in space between two walls for hard-sphere volume fractions ranging from 0.05 to 0.46.

The density of hard spheres, which give the distribution of the centres of the micelles, obtained from the Monte Carlo simulations could be expressed as a numerical function of the hard-sphere volume fraction and the distance from the wall (See Fig. 1). The expression was found to be valid for volume fractions up to the crystallisation value of 0.53. In order to account for the shape of the micelles, the centre distribution of the micelles was convoluted with the projected radial density of either a solid sphere or a solid sphere with polymers attached to the surface. These models for the micelles have previously been shown to represent the bulk micelles.[2,3] The obtained density function can, when the solvent density is taken into account, model the experimentally determined scattering length density profiles (See Fig. 2). The quality of the fits improved when the micelles were treated as solid spheres with Gaussian polymer chains attached to the surface. From the fits a water layer of 20 Å ± 5 Å was found to form on the surface of the quartz crystal, hence no adsorption on the crystal took place. In the case of the polymer chains tethered to the sphere an excellent agreement between the hard-sphere interaction radius and the radius of the sphere plus two radius of gyration for the polymer chains was found For 25 % wt, close to the BCC crystallisation of the micelles, the model was not able to fit the scattering length density profiles suggesting a pre-crystallisation close to the quartz surface.

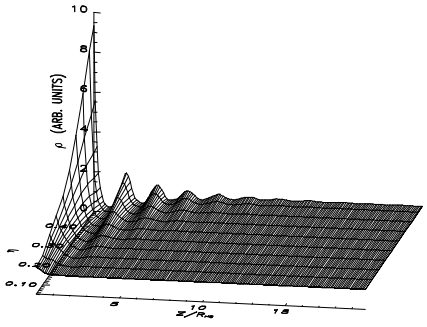

Fig. 1. The parameterization for the density, ρ, of the hard sphere at a hard wall obtained from Monte Carlo simulations as a function of the hard-sphere volume fraction, η, and the distance from the wall, *z*.

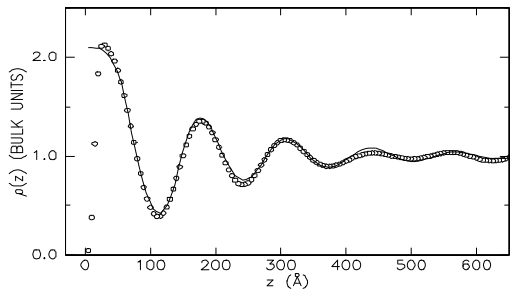

Fig. 2. The fit (solid line) to free-form profile of 20 % wt P85 at a temperature of 50 ^{o}C (open circles). The fit to the data is obtained by convoluting the density of the hard sphere centres (parameterized MC simulations) with the projected density of solid spheres with Gaussian polymer chains tethered to the surface.

---

1 Annual Progress Report of the Department of Solid State Physics, 1 January - 31 December 1995, contribution 2.7.1

2 J.S. Pedersen and M.C. Gerstenberg, Macromolecules **29**, 1363 (1996)

3 K. Mortensen and J.S. Pedersen, Macromolecules **26**, 805 (1993)

2.7.11 Neutron Reflection from Biosensors

S. Roser, *University of Bath, School of Chemistry, UK*, D. Caruana, *Department of Biomedical Sciences, University of Malta, Malta* and M.C. Gerstenberg, *Department of Solid State Physics, Risø National Laboratory, Denmark*

This work is aimed at determining the detailed structure of an electrochemically produced biosensor, consisting of the enzyme Glucose Oxidase embedded in an electrochemically produced poly(phenol) film. In previous reports we have shown the accurate detail of the polymer film density and thickness that can accrue from measurements at the solid/liquid interface, and how measurements at different subphase contrasts illuminate the extent of solvent penetration into films grown on gold plated electrodes.[1]
Here, we show how neutron reflection can be used to characterise the oxidative growth of a layer of poly(phenol) on silicon single crystals, including as a function of time. During the oxidation process an electrochemically active layer of silicon hydroxide is produced between the solid and the polymer film whose scattering length density depends on the subphase. The thickness and density of this inner film has been monitored as a function of applied potential and time (see Fig. 1), and the resultant trace modelled. Two different modes of deposition are noted depending on whether the potential step is ramped or stepped. It is found that the ramped potential leads to a more diffuse polymer. With the extra clarity that the silicon substrate yields over the gold electrodes it has been possible to start measuring the effect of adsorbed protein molecules on the reflectivity profile.

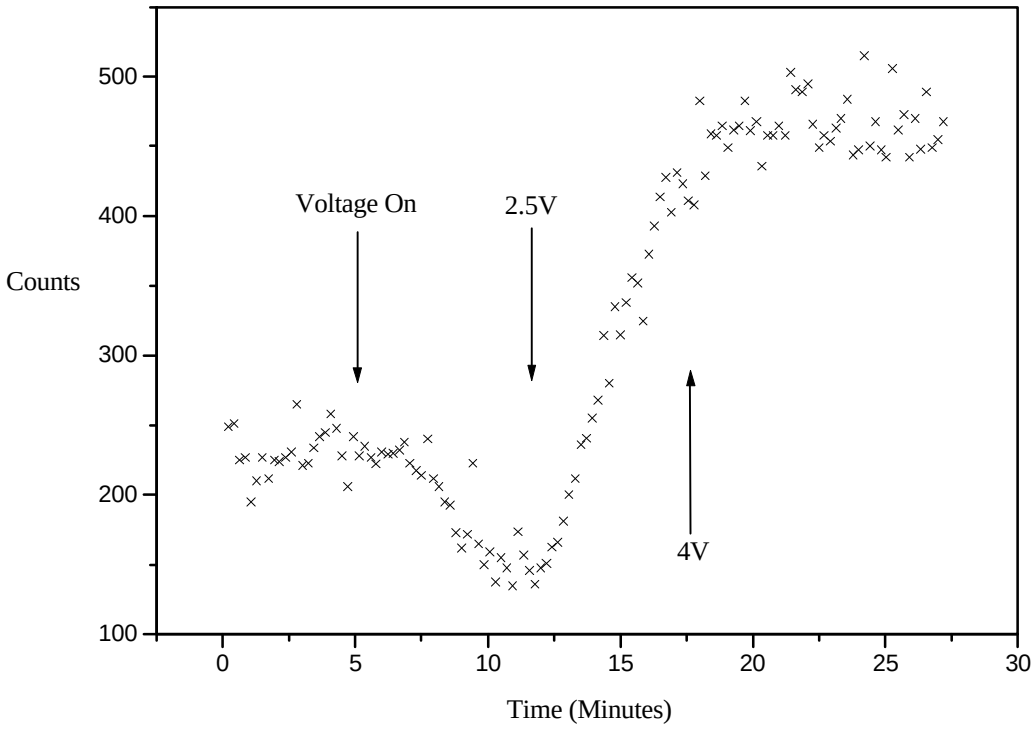

Fig. 1. Deposition of poly(phenol). The intensity monitored as a function of time and applied voltage at momentum transfer Q=0.01 Å^{-1}.

[1] S.J.Roser, D.Caruana, M.Gerstenberg, J.Electrochim. Acta , in final preparation

2.7.12 Order, Disorder and Composition Fluctuation Effects in Low Molar Mass Hydrocarbon-Poly(dimethylsiloxane) Diblock Copolymers

K. Almdal, K. Mortensen, *Department of Solid State Physics, Risø National Laboratory, Denmark*, A.J. Ryan, *Manchester Materials Science Centre, UMIST, UK, and CCLRC Daresbury Laboratory, UK* and F.S. Bates, *Department of Chemical Engineering and Materials Science, University of Minnesota, USA*

The phase behaviour of diblock copolymers are investigated in the short chain limit. The size of the window in composition and temperature where complex phases diblock copolymers are observed is dependent on the chain length of the block copolymer. However, in the limit of very short diblocks close to the order-to-disorder transition which are characterised by very large incompatibilities between the blocks we expect the trends observed for long chains to break down. In the short chain limit, the molecules would behave more like rigid rods rather than flexible chains. Rigid rods are well established to form nematic and smectic phases. Thus, we expect that as the block copolymer molar mass is progressively reduced, while maintaining χN~10, the stability window of the lamellar phase will increase and eventually the complex mono- and bicontinuous phases will be squeezed out.

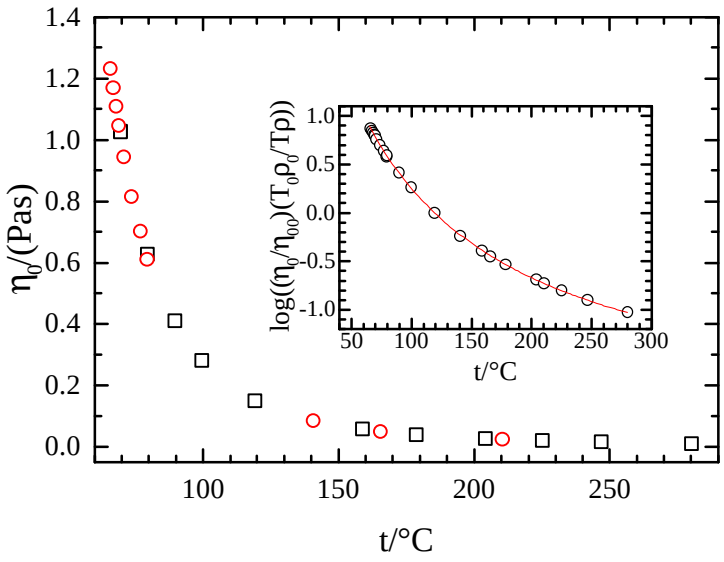

Figure 1. Viscosity of sample PEP-PDMS-6 as a function of temperature. Data was taken while heating (□) and cooling (○). In the inset the viscosity data is normalised to represent WLF shift-factors. The dotted line is a fit to the WLF equation $\log(a_T=-c_1^0(T-T_0)/(c_2^0+T-T_0)$, ($c_1^0$=2.17, c_2^0=187.4°C, and T_0=119.1°C. η_0, and ρ are the viscosity and density, respectively. The subscript zero refers to the reference temperature T_0.

Four block copolymer melts - two poly(isoprene-*block*-dimethylsiloxane) (PI-PDMS) and two poly(ethylene-*alt*-propylene *block*-dimethylsiloxane) (PEP-PDMS) - have been investigated through rheological measurements, SANS, and SAXS[1]. In both systems lamellar to disorder and Ia$\bar{3}$d bicontinuous to disorder transitions have been observed. Upon heating the sequence of phases, lamellae, modified layers, bicontinuous Ia$\bar{3}$d, disorder is observed in the f = 0.65 PEP-PDMS sample. Composition fluctuations dominate the disordered state properties over an unprecedented wide temperature window in the f = 0.49 PEP-PDMS sample. The fluctuations are evident both in SANS measurements and through the temperature dependence of the viscosity. The phase behaviour of these relatively low molar mass block copolymer melts, which range from 6 to 10kg/mol, are qualitatively anticipated by the trends reported earlier for high but progressively lower molar mass diblock copolymers. The viscosity (see Fig. 1) was measured over a wide temperature range. Fitting these data to the WLF-equation afford a determination of the Vogel-temperature, T_∞, of the sample. Due to composition fluctuation T_∞ is much higher than expected from the corresponding two homopolymers.

[1] K. Almdal, K. Mortensen, A. J. Ryan, F. S. Bates. Macromolecules, **29**, 5940-5947 (1996)

2.7.13 Composition Fluctuations at the Order-to-Disorder Transition in a Sheared Asymmetric Diblock Copolymer Melt

K. Almdal, K. Mortensen, *Department of Solid State Physics, Risø National Laboratory, Denmark*, K.A. Koppi, M. Tirrell and F.S. Bates, *Department of Chemical Engineering and Materials Science, University of Minnesota, USA*

A diblock copolymer was examined near the order-to-disorder transition temperature, T_{ODT}, by small-angle neutron scattering as a function of shear rate, $d\gamma/dt$[1]. The sample PEP-PEE-7 is an asymmetric partially deuterated poly(ethylene-propylene)-poly(ethylethylene) (PEP-PEE) diblock copolymer with M_w=1.07×10^{5}g/mol and M_w/M_n=1.07. Heating in the absence of shear disorders the material from a hexagonal structure at T_{ODT} =155°C±1°C. Application of a reciprocating simple shear field markedly influences the phase behaviour near the ODT. Application of shear while heating increases T_{ODT} consistent with the theoretical prediction, T_{ODT}~$(d\gamma/dt)^2$. During fast cooling studies we observe an additional characteristic temperature, T_S, at which the material spontaneously orders, which we interpret as a stability (*i.e.*, spinodal) limit. This result also agrees with the theoretical prediction, τ_S ~$(d\gamma/dt)^{-1/3}$. Upon cessation of shear at temperatures close to but above the quiescent T_{ODT} a transient phase is observed before the system macroscopically disorders. The transient structure has a symmetry compatible with spheres arranged on a body e cubic (BCC) space lattice, or undulating cylinders of the minority component (PEE). Anisotropic (*i.e.* lattice pinned) fluctuations can also be observed close to, but below, T_{ODT} upon heating the hexagonal structure under shear free conditions. In Fig. 1 the shear rate dependent T_{ODT} is given. Thus, it has been shown that a shear field in the form of reciprocating shear increases the order-to-disorder transition temperature, T_{ODT} in the case of an asymmetric diblock copolymer. The temperature, T_S, at which this polymer spontaneously orders on cooling in the shear field is an increasing function of shear rate. The functional form of the curves T_{ODT} and T_S is in accordance with theoretical predictions based on the concept of shear field mediated suppression of the composition fluctuations which dominate diblock copolymer thermodynamics close to the ODT under quiescent conditions. The disordered state composition fluctuations are spherical-like domains of the minority component in the majority component matrix rather than a worm-like topology suggested earlier.

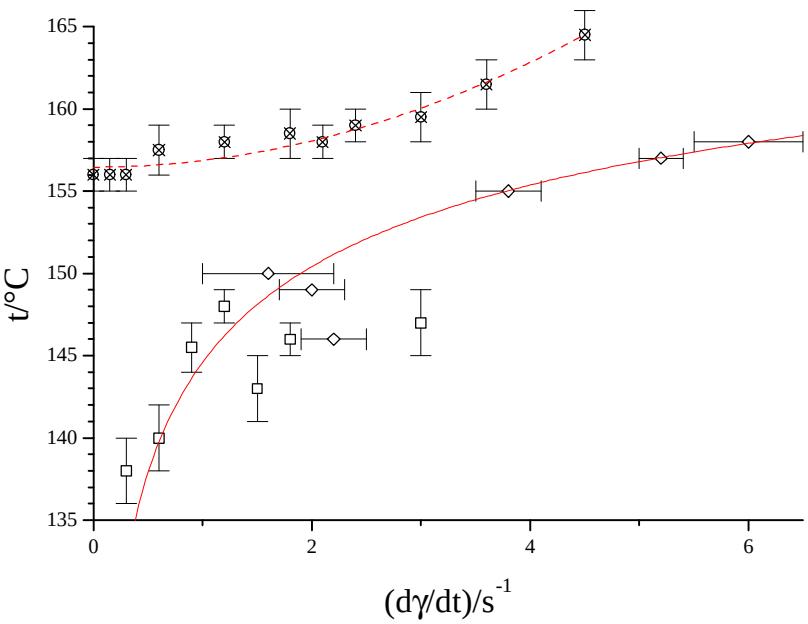

Fig. 1. The shear rate dependent order-to-disorder transition temperature of sample PEP-PEE-7. T_{ODT} was measured while heating under constant reciprocating shear (⊗), while cooling at constant shear rate (□), and while increasing the shear rate at constant temperature(◊). The dotted line is a fit to a parabola and the solid line has the functional form $A/(B(d\gamma/dt)^{-1/3}+1)$.

[1] K. Almdal, K. Mortensen, K.A. Koppi, M. Tirrell, F S. Bates. J. Phys. II, **6**, 617 (1996)

2.7.14 Phase Behaviour in Poly(ethyleneoxide)-*block*-poly(ethylethylene) Diblock Copolymers

M.A. Hillmyer, F.S Bates, *Department of Chemical Engineering and Materials Science, University of Minnesota, USA.* K. Almdal, K. Mortensen, *Department of Solid State Physics, Risø National Laboratory, Denmark,* A.J. Ryan and J.P.A. Fairclough. *Manchester Materials Science Centre, UMIST, UK, and CCLRC Daresbury Laboratory, UK*

Two asymmetric poly(ethyleneoxide)-*block*-poly(ethylethylene) (PEO-PEE) diblock copolymers with the volume fraction, *f*, of PEO equal to 0.7 and 0.72 and $M_n \approx 1.5$kg/mol were investigated under solvent free conditions with small angle neutron and x-ray scattering (SANS and SAXS) and dynamical mechanical measurements.[1] This particular set of block copolymer melts represent an experimental effort to branch the gap between unsolvated block copolymers and surfactant solutions. These two sets of 'soft materials' share a common set of ordered microstructures. The PEO-PEE block copolymers are similar to the well known alkane-oxyethylene (C_nEO_m) non-ionic surfactants. The general phase behaviour in these materials has similarities with both the higher molar mass block copolymer analogues and the lower molar mass surfactant solutions. In the two block copolymer melts described here thermally induced order-to-order transitions (OOT's) were found.

The cubic gyroid structure with Ia$\bar{3}$d space group symmetry were found in both materials. Upon heating from the semi crystalline lamellae found below 45°C both materials showed a range of phase transitions as evidenced by sharp changes increase in the dynamical mechanical shear modulus G′. In the *f*=0.70 sample a sequence of 5 phases was identified by rheology and scattering: semi-crystalline lamellae, lamellae, modified lamellae, Ia$\bar{3}$d and disorder. In the *f*=0.72 sample the sequence of 6 phases semi-crystalline lamellae, lamellae, modified lamellae, Ia$\bar{3}$d, hexagonal and disorder was observed. Upon cooling form the cubic state considerable hysteresis in the phase behaviour occurs. In the *f*=0.70 sample the cubic phase changes directly to lamellae and in the *f*=0.72 sample the cubic state is preserved until the PEO block crystallises. The PEO crystallisation appears to force the system back into a layered state. It is not clear which of the states lamellae or cubic Ia$\bar{3}$d is the equilibrium phase in the temperature window where the lamellae are observed on heating. The kinetic hindrance of the phase transition appears related to a mismatch in inter planar spacing associated with the ordered state which was measured by SANS. In the *f*=0.72 sample where the transition between lamellae and cubic Ia$\bar{3}$d most complicate this mismatch is as much as 16% where as the comparable number for the *f*=0.70 sample is only 5%.

[1] M.A. Hillmyer, F.S. Bates, K. Almdal, K. Mortensen, A.J. Ryan, J.P.A. Fairclough. Science, **271**, 976 (1996)

2.7.15 Heat-induced Aggregation of β-Lactoglobulin Studied by Small-Angle Neutron Scattering

M. Verheul, S.P.F. M. Roefs, C.G. de Kruif, *Technology Department, Netherlands Institute for Dairy Research, The Netherlands* and J.S. Pedersen, *Department of Solid State Physics, Risø National Laboratory, Denmark*

β-Lactoglobulin (β-lg) is the major whey protein in bovine milk. Heating induces denaturation and subsequent irreversible aggregation of β-lg. At neutral pH and low ionic strength transparant dispersions or gels are formed, while at high ionic strength turbid systems are formed. In this study the heat-induced aggregation of β-lg at 68.5 °C was investigated. Samples with pD=7.1 were heated for various times, NaCl concentration varied from 0 to 0.5 M and β-lg concentrations were in the range of 6 to 57 g/l. Figure 1 shows SANS spectra of 35 g/l β-lg in 0.2 M NaCl heated for various times at 68.5 °C together with the results of a Static Light Scattering (SLS) measurement on the sample that was heated for 8 hours. The inset in Fig. 1 shows the fractional decrease of the native protein as a function of heating time. The scattered intensity at low q values increases enormously with increasing conversion of native protein, indicating that large aggregates are formed. A limiting slope of 2.0 ± 0.1 is reached in the double-logarithmic plot at long heating times, which points to fractal structures. In the q range between 0.03 $Å^{-1}$ and 0.2 $Å^{-1}$ the scattered intensity decreases with increasing conversion of native β-lg. This indicates that the elementary subunit of the aggregates does not correspond to the native β-lg molecule. Figure 2 shows SANS spectra of heated β-lg solutions (35 g/l) with various NaCl concentrations (0 M, 0.1 M, 0.2 M and 0.5 M). In all samples approximately the same amount of protein (± 40%) has been converted into aggregates. At low ionic strength a correlation peak is seen at $q \approx 0.02$ $Å^{-1}$, indicating that a rather homogeneous system of interacting aggregates is formed. With increasing NaCl concentration the correlation peak disappears and larger aggregates without preferential distances are formed. Aggregate size increases with NaCl concentration and the limiting slope at 0.5 M NaCl is steeper (2.3 ± 0.1) than at 0.2 M NaCl (2.0 ± 0.1). At q values higher than 0.06 $Å^{-1}$ the SANS spectra of the heated β-lg samples at different ionic strengths are identical, so the subunits of the aggregates will have a similar structure on the corresponding length scale.

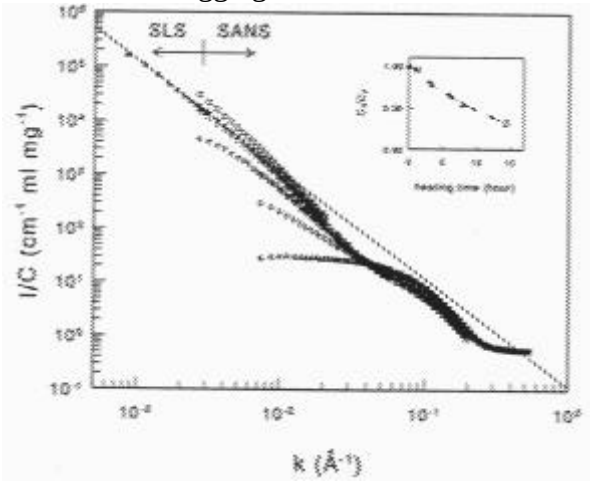

Fig 1. SANS spectra of 35 g/l β-lg solutions (0.2 M NaCl, pH 7.1) heated at 68.5 °C for various times; inset: fractional decrease of native protein concentration as a function of heating time.

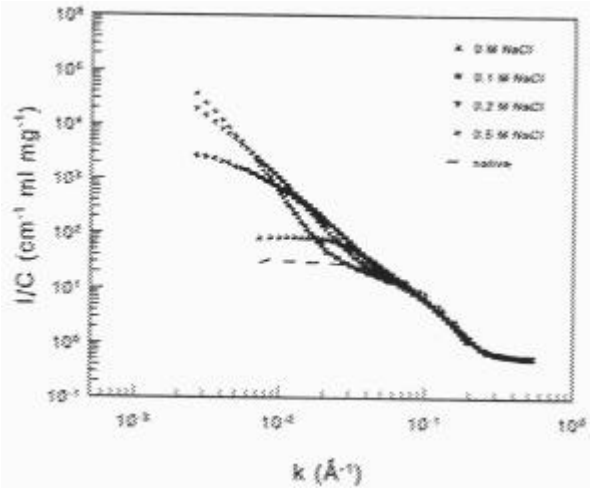

Fig 2. SANS spectra of heated 35 g/l β-lg solutions (68.5 °C) with various NaCl concentrations; all samples still contain approximately 60 % native β-lg; dotted line: unheated β-lg solution.

2.7.16 A Small-angle Scattering Study of the Polydispersity of Microemulsion Droplets

L. Arleth and J.S. Pedersen, *Department of Solid State Physics, Risø National Laboratory, Denmark* and T. Zemb, *Service de Chimie Moléculaire, France*

At certain compositions and temperatures ternary mixtures of water, alkane and the amphiphile molecule AOT form clear and termodynamically stable solutions of almost spherical AOT-covered water droplets in alkane. Small-angle neutron scattering measurements are performed on such microemulsions of AOT/water/isooctane and AOT/water/decane. At fixed temperature the radius of the droplets depends mainly on the AOT/water ratio, whereas the polydispersity and shape fluctuations of the droplets seem to be determined by the alkane type. Explicit information about the size distribution of the microemulsion droplets is obtained by measuring the scattering at zero angle for different protonated alkane/deuterated alkane ratios. Analysis of these contrast variation data show that the microemulsion droplets in AOT/water/iso-octane are more polydisperse than those in AOT/water/decane. This is in agreement with previous light-scattering results.[1]

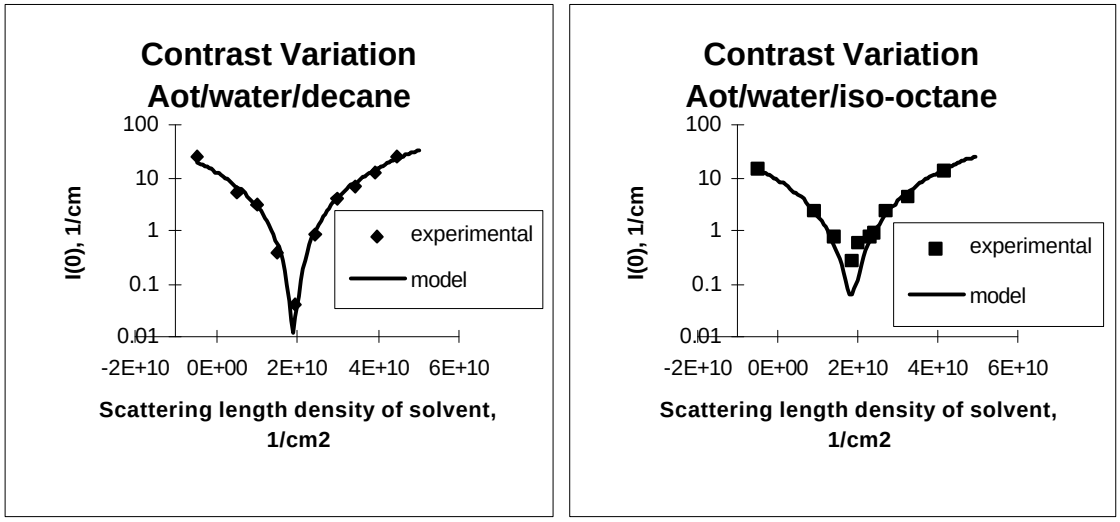

Figures**:** Scattering at zero angle as function of scattering length density of the solvent. In the model fits we assume that the micelles are spherical core-shell objects. We use a Schulz size distribution and calculate the effective structure factor from a polydisperse hard sphere model.[2] For the AOT/water/decane droplets we find a mean radius of 50 Å and a polydispersity $(s / \overline{R})$ of 10%. For the AOT/water/iso-octane droplets we find a mean radius of 35 Å and a polydispersity of 30%.

[1] S. Christ and P. Schurtenberger, J. Phys. Chem. **98**, 12780 (1994)
[2] A. Vrij, J. Chem. Phys. **71**, 3267 (1979)

2.7.17 Structural Model of the 70S E. Coli Ribosome and Its RNA from Solution Scattering

D.I. Svergun, M.H.J. Koch, *European Molecular Biology Laboratory, Hamburg, Germany*, J.S. Pedersen, *Risø National Laboratory, Denmark* , V.V. Volkov, M.B. Kozin, *Institute of Crystallography, Russia*, W. Meerwink, H.B. Stuhrmann, *GKSS Research Centre, Germany*, G. Diedrich, N. Burkhardt and K.H. Nierhaus, *Max Planck Institute for Molecular Genetics, Germany*

Contrast variation neutron solution scattering experiments were performed on hybrid 70S E.Coli ribosomes reassembled from specifically deuterated subunits, and on the free 30S and 50S subunits. The authenticity of the partially deuterated particles was controlled by parallel X-ray measurements. The contrast variation data set (42 curves in total) proved to be consistent with a description of the ribosome as a four component system composed of the RNA and protein moieties in its large and small subunits, and thus provided ten times more information than a single solution scattering curve. A model independent comparison of these data with the scattering curves calculated from recent electron microscopic reconstructions in vitreous ice[1,2] indicated that the ribosome is unlikely to have a “Swiss-cheese”-like structure with a pronounced net of channels. A solid body four phase low resolution model of the 70S ribosome was build from the envelope functions of the entire 30S and 50S subunits and of those of the corresponding RNA moities. The four envelopes were parameterized at a resolution of 3.5 nm using spherical harmonics taking into account interface layers between the phases. The initial approximation for two envelopes - those of the subunits - was taken from the model[1] and an optimized four phase model (Fig. 1) was obtained by non-linear minimization to fit the available experimental curves. The refined envelopes of the subunits differ only by about 10% from the starting approximation, whereas the rRNA moities are significantly different from those inferred from the electron microscopy. The RNA moiety in the 30S is more anisometric than the subunit itself, whereas in the 50S RNA forms a compact core. Both RNAs protrude to the surfaces of the subunits and occupy approximately 30% of the surface areas.

Fig. 1 Four phase model of the 70S ribosome. Envelopes of the subunits are drawn in wireframes, rRNA moities as solid bodies. Left: 30S is closer to the viewer, right - the entire model turned 45^{o} clockwise around Y.

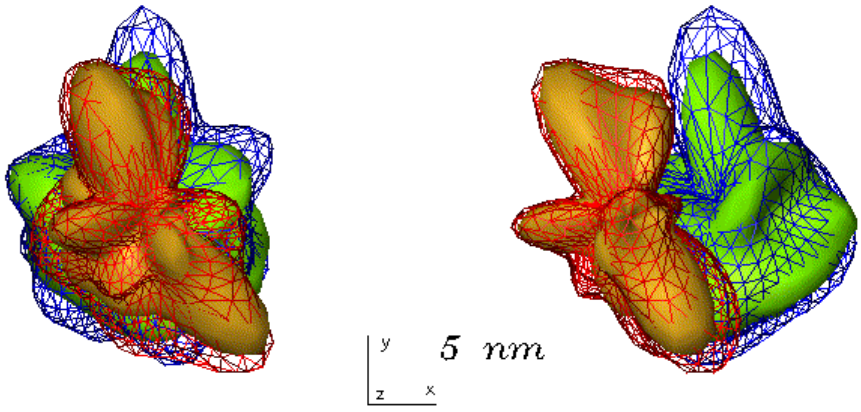

[1] J. Frank *et al.*, Nature (London) **376**, 441 (1995)
[2] H. Stark *et al.*, Structure **3**, 815 (1995)

2.7.18 Static Structure Factor of Worm-like Micelles

G. Jerke, P. Schurtenberger, *Institut für Polymere, ETH Zürich, Switzerland* and J.S. Pedersen, *Department of Solid State Physics, Risø National Laboratory, Denmark*

In our recent study we have performed small-angle neutron scattering (SANS) and static light scattering (SLS) measurements of the static structure factor, $S(q)$, of worm-like micelles formed by soybean lecithin and trace amounts of water in deuterated isooctane. The structure and flexibility of the aggregates have been investigated in detail as a function of the solution composition. In former investigations of various worm-like micelles it was shown that the concentration dependence of $S(0)$ can be recovered if one combines micellar growth and intermicellar interaction effects in the framework of conformation space renormalization group theory, whereas the influence of intermicellar interaction effects on $S(q)$ on different length scales is still an unresolved problem.[1,2] In particular a precise determination of the intrinsic flexibility of worm-like micelles requires knowledge of $S(q)$ as a function of micellar size, flexibility, cross-section structure and interactions. The starting point in our approach is a non-linear least-squares fitting procedure based on a parametrization of the results from a recent Monte Carlo simulation study of the single scattering functions of worm-like chains with excluded volume effects.[3,4] A typical fit to the combined data set from SLS and SANS measurements is shown in Fig.1. The only relevant fit parameter is the flexibility (in terms of Kuhn lengths); all the other input parameters of the fit procedure were determined mainly by applying indirect Fourier transformation techniques to the high-q part of the data.[5] The determined apparent Kuhn length (Fig. 2) shows a pronounced concentration dependence which reflects that the intermicellar interaction effects contribute significantly even on intermediate length scales.[6] This finding is consistent with recent results from Monte Carlo simulation studies of many chain systems.

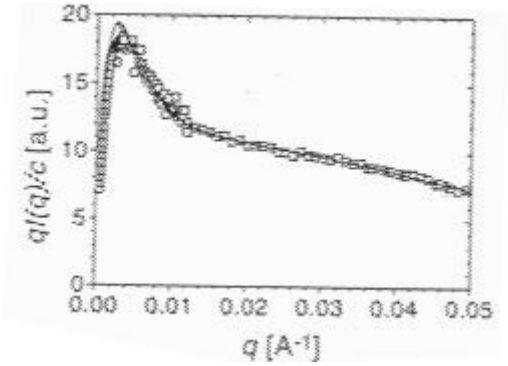

Fig.1. Scattered intensity, $qI(q)/c$, as a function of scattering vector q for lecithin reverse micelles in deuterated isooctane (molar water-to-lecithin ratio w_0 = 2.5, lecithin concentration c = 1.2 mg/ml). Data shown are obtained from SLS and SANS measurements. Also shown is the fit to the data from a non-linear least squares fitting procedure.

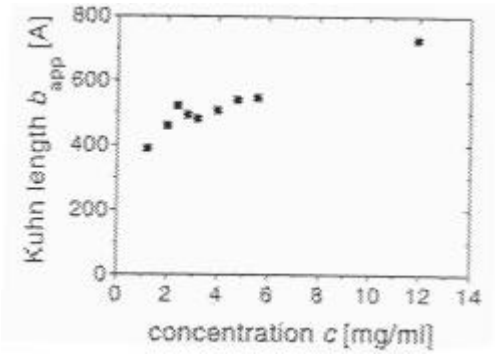

Fig.2. Concentration dependence of the apparent Kuhn length b (molar water-to-lecithin ratio w_0 = 1.5).

1 P. Schurtenberger, C. Cavaco, J. Phys. II (France) **3** 1279 (1993)
2 P.Schurtenberger, C. Cavaco, F. Tiberg, O. Regev, Langmuir **12** 2894 (1996)
3 J.S. Pedersen, M. Laso, P. SchurtenbergerPhys. Rev. E **54**, 5917 (1996).
4 J.S. Pedersen, P. Schurtenberger. Macromolecules **29**, 7602 (1996)
5 P. Schurtenberger, G. Jerke, C. Cavaco, J.S. Pedersen, Langmuir **12** 2433 (1996)
6 G. Jerke, S.U. Egelhaaf, J.S. Pedersen, P. Schurtenberger (1996). In Preparation

2.7.19 Aggregation Processes in AOT Water-in-Oil Microemulsions

W.F.C. Sager, J. Smeets, G.J.M. Koper, *Department of Physical and Macromolecular Chemistry, Leiden Institute of Chemistry, The Netherlands*, and J.S. Pedersen, *Department of Solid State Physics, Risø National Laboratory, Denmark*

Droplet phase microemulsions, especially AOT (sodium di-2-ethyl-hexylsulfosuccinate) stabilised water-in-oil (w/o) microemulsions, have been studied intensively over the last 2 decades, using static and dynamic light scattering as well as small-angle X-ray and neutron scattering. It is now established that the droplet size depends linearly on the water-to-surfactant ratio and that the minima in the form factor (spherical Bessel function) are not only smeared out by the size polydispersity but also by form fluctuations of the droplets. Both quantities depend on the elastic properties of the interfacial film, *e.g.* rigidity and spontaneous curvature. Interactions between the droplets have so far been treated by applying liquid state theories using hard sphere or sticky hard sphere models.[1]

The aim of this investigation is to study by SANS and SAXS the droplet aggregation phenomena which have been observed for AOT w/o microemulsions as the temperature is increased. The aggregation has been found by means of e.g. conductivity, viscosity, fluorescent quenching and temperature jump experiments, for a recent overview see.[2] We hope to obtain enough information about the structural changes taking place with temperature over the whole one-phase region that we will be able to address droplet aggregation in the same framework as the (temperature) evolution of phases occurring in surfactant-water-oil systems; namely by looking at the changes in the properties of the interfacial film separating water and oil domains. So far we have performed SAXS measurements (in collaboration with M.H.J. Koch, EMBL-outstation) at DESY for different droplet sizes and volume fractions and SANS measurements for one droplet size for temperatures between the lower and the upper phase boundary of the w/o microemulsion region. Both SAXS and SANS measurements reveal a single droplet population at low temperatures with a distribution width corresponding to a polydispersity of about 20%, which is in agreement with work published earlier.[3] With increasing temperature a second peak shows up in the pair distance distribution function *p(r),* obtained by indirect Fourier transformation, with a maximal radius corresponding to twice the radius of the single droplet. With increasing temperature the fraction of aggregated droplets increases. For small droplet sizes (w_o = [H2O] / [AOT] = 45) a second structural transition occurs. At temperatures close to the upper phase boundary the *p(r)* curves reveal a shape which is typical for cylinders. Analysing the scattering curves *I(q)* at intermediate temperatures using a simple model, that assumes a distribution of monomeric droplets and dimers calculated by the Debye formulae (retaining spherical symmetry), shows that the situation at hand is more complicated. The *p(r)* curves, as well as shift in the position of the first minimum in the curves obtained in the shell-contrast SAXS experiments, indicate that the mean radius of the single droplet decreases systematically as temperature is increased. More SAXS measurements at the exact contrast matching point are required to study the structure of the aggregates formed.

[1] S.H. Chen, C.Y. Ku, J. Rouch, P. Tartaglia, C. Cametti, and J. Samseth, Journal de Physique IV, **3**, 143 (1993)
[2] G.J.M. Koper , W.F.C. Sager, J. Smeets, and D. Bedeaux, J. Phys. Chem. **99,** 13291 (1995)
[3] M. Kotlarchyk, S.H. Chen, and J.S. Huang, J. Phys. Chem. **86,** 3273 (1982)

2.7.20 Microemulsions as Model Systems for Hard and Soft Spheres

P. Schurtenberger, *Institut für Polymere, ETH Zürich, Switzerland*, U. Olsson, V. Rajagopalan, *Physical Chemistry 1, Centre for Chemistry and Chemical Engineering, Lund University, Sweden*, K. Mortensen, and J.S. Pedersen, *Department of Solid State Physics, Risø National Laboratory, Denmark*

Microemulsions are thermodynamically stable liquid mixtures of water, oil and surfactant. Under certain conditions, it is possible to stabilize spherical droplets of, say, oil in water with a low polydispersity and a concentration independent size. This can be achieved with a finite but not too low spontaneous curvature of the surfactant film and a system which is saturated with the dispersed oil, *i.e.* conditions which are reached close to the so-called emulsification failure line. We have recently investigated in detail such a system with the nonionic surfactant pentaethylene glycol dodecyl ether ($C_{12}E_5$), water and decane.[1] Spherical oil droplets were prepared with a surfactant-to-oil ratio $\phi_s/\phi_o=0.815$, where ϕ_s and ϕ_o are the surfactant and oil volume fraction, respectively, over a large range of droplet volume fractions $\phi = \phi_s+\phi_o$. The microemulsion particles can be considered as spherical oil droplets of (hydrocarbon) radius r_{hc} covered by dense brush of end-grafted penta ethylene oxide chains, where the grafting density is approximately 45 $Å^2$ per chain, *i.e.* a situation quite analogous to sterically stabilized 'solid' colloid particles. A characterization of the static and dynamic properties of these microemulsions using static and dynamic ligth scattering, small angle neutron scattering, NMR self diffusion and viscosity measurements has demonstrated that the droplets behave to a very good approximation like hard spheres.[2] An interesting possibility in this system arises from the fact that the microemulsion droplets can be charged in a controlled way by adding small amounts of ionic surfactants. This allows a detailed investigation of the static structure factor of a suspension of colloidal particles where the interaction potential gradually changes from a hard sphere to a soft sphere (Yukawa-) type. We have investigated the structure factor over an extended range of q values for systems with volume fractions between $0.05 \leq \phi \leq 0.3$ and 0-100 charges per particle. We are currently analyzing the experimentally obtained structure factors using integral equation schemes.

1 U. Olsson and P. Schurtenberger, Langmuir **9**, 3389 (1993)
2 U. Olsson and P. Schurtenberger, to appear in Prog. Colloid Polym. Sci.

2.7.21 Phase Behaviour of Hydrocarbon-poly(dimethylsiloxane) Diblock Copolymer Melts Related to Temperature and Their Volume Fraction of Hydrocarbon

M.E. Vigild, S. Ndoni, and K. Almdal, *Department of Solid State Physics, Risø National Laboratory*. I.W. Hamley, *School of Chemistry, University of Leeds, UK*, J.P.A. Fairclough, and A.J. Ryan, *Manchester Materials Science Centre, UMIST, UK*

In this study we present the first promising results showing the features of the phase diagramme for an asymmetrically composed poly(ethylene-alt-propylene)-poly(dimethylsiloxane) (PEP-PDMS) copolymer system. Samples are very carefully synthesised by ”living” anionic polymerisation (please see K.Almdal et al. elsewhere in this report). Di-block copolymers are known to form different phases under conditions given by the molar mass and the strength of interaction between the chemically distinct units of the polymer. This dependence is summarised in the variable χN (the Flory-Huggins interaction parameter χ times the molar mass N) as is illustrated along the y-axis in Fig. 1. χN is inversely related to the temperature. Individually synthesised block copolymers are mapped along the x-axis in Fig. 1 as a function of the volume fraction of hydrocarbon. This constitutes a semi-phase diagramme of the PEP-PDMS system falling in the two ranges of the volume fraction: 0.3 to 0.5 and 0.6 to 0.7.

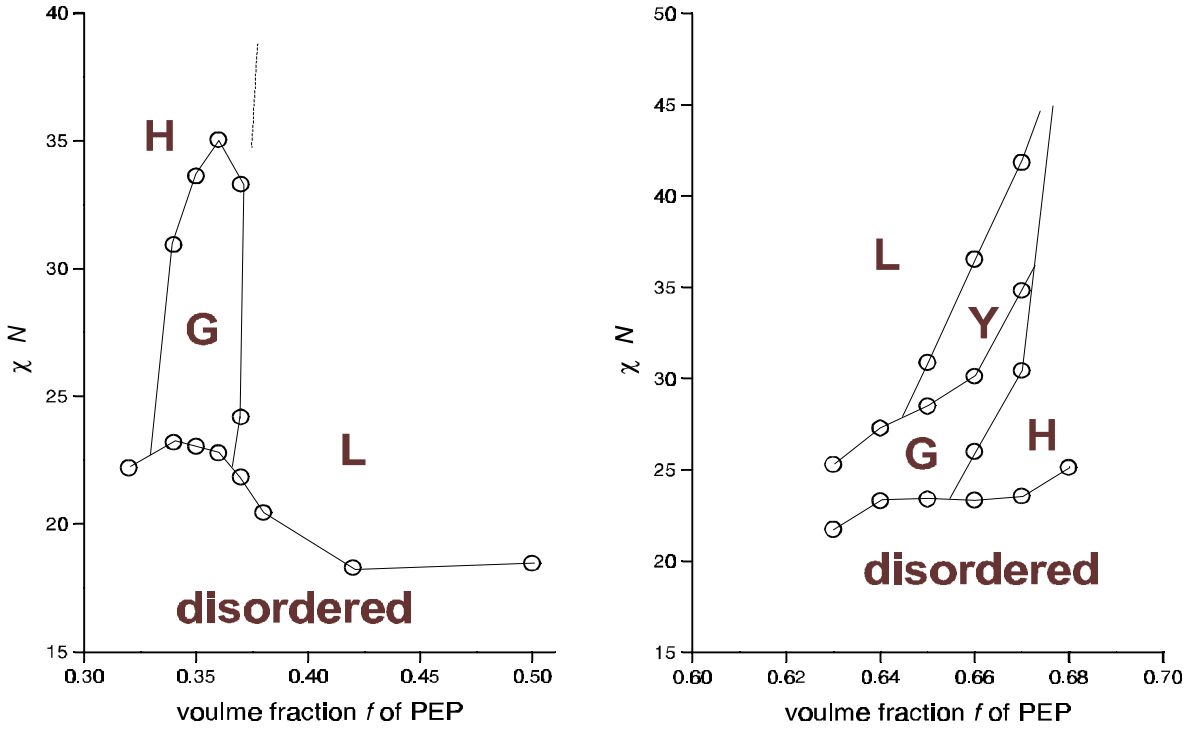

Fig. 1. Semi-phase diagrammes of PEP-PDMS falling in the volume fraction ranges of 0.3 to 0.5 and 0.6 to 0.7.

Phase transition temperatures between ordered states, T_{OOT}, and from ordered to disordered states, T_{ODT}, are determined by dynamical mechanical spectroscopy measuring the value of the elastic shear modulus G' as a function of temperature. The phase structures in the ordered states are analysed by using small angle x-ray scattering (SAXS). Our investigation shows that especially the asymmetrically composed PEP-PDMS system transforms through a series of morphologies as the temperature rises until, eventually, the polymer disorders. The phases identified are lamella (L), hexagonal (H), gyroid (G), and at the present an unidentified metastable phase (Y).

2.7.22 A Small-Angle Neutron Scattering (SANS) Study of Aggregates Formed From an Aqueous Mixture of Sodium Dodecyl Sulphate (SDS) and Dodecyl Trimethyl-ammonium Bromide (DTAB).

M. Bergström and J.S. Pedersen, *Department of Solid State Physics, Risø National Laboratory, Denmark*

We have studied several different samples of SDS (anionic surfactant) and DTAB (cationic surfactant) in D_2O with SANS, where the surfactant molar ratios ranges between 20:80 and 80:20 and the total amount of surfactants between 0.125 and 5 wt %. Small unilamellar vesicles (450 Å < $\langle R_I$ < 700 Å) is seen in the very dilute samples of compositions 20:80 and 80:20, *i.e.* when one of the surfactants is in excess. A typical example of the scattering intensity as a function of the scattering vector q for a sample where vesicles is found is given in Fig. 1. We have also included the scattering intensity function as predicted from a one-shell model of unilamellar vesicles and fitted by means of conventional least-squares methods with respect to parameters such as vesicle size, polydispersity, intervesicular interactions etc. The previously[1,2] theoretically predicted value of the (number weighted) polydispersity, $\sigma_R / \langle R_I = 0.36$, seems to be in good agreement with our experiments for the most diluted samples. However, when the total amount of surfactants decreases there is an evident decrease of the polydispersity. Since intervesicular interactions seem to be of considerable importance, even for the dilute samples in which we find vesicles, we have tried to include excluded volume interaction effects into our previous theory. In this way, we are actually able to account for the observed polydispersity decrease upon increasing the surfactant concentration. The entropically stabilised vesicles at the most diluted concentrations become energetically stabilised by intervesicular interactions at higher surfactant concentrations. It remains to analyse the samples in which there are other structures than unilamellar vesicles. Most notably, large multilamellar bilayer structures seems to form when equimolar composition is approached and in the more concentrated samples of the surfactant molar ratios where vesicles form, there seem to exist globular micelles.

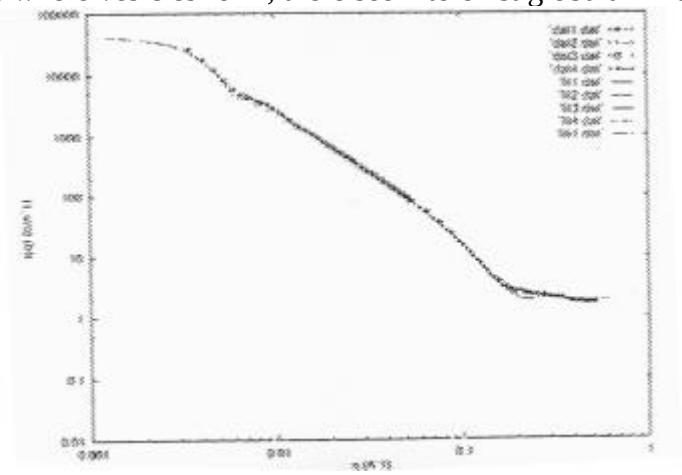

Fig. 1. Normalised scattering intensity as a function of scattering vector q for a sample with a surfactant molar ratio of SDS:DTAB 20:80 and a total amount of surfactants 0.5 wt %. Individual symbols represent data obtained with different combinations of neutron wavelength and sample-detector distance. The lines represent the results from a fit with a one-shell vesicle bilayer model.

[1] Bergström, M., Eriksson, J. C., Langmuir, submitted for publication
[2] Bergström, M, Langmuir, **12**, 2454 (1996)

2.7.23 The Influence of Shape Fluctuations on the Size Distributions of Spherical Bilayer Vesicles and Droplet Microemulsions

M. Bergström, *Department of Solid State Physics, Risø National Laboratory, Denmark*

The free energy per unit area of an arbitrarily shaped lipid/surfactant mono- or bilayer is usually described by the so-called Helfrich expression,[1] $g(H,K) = g_0 + 2k_c(H - H_0) + k_c K$, which, in essence, is a Taylor expansion to second order in mean and Gaussian curvatures $H \equiv (c_1 + c_2)/2$ and $K \equiv c_1 c_2$, respectively, where c_1 and c_2 denote the two principal curvatures. H_0 is the spontaneous curvature and the two (solution state-dependent) constants k_c and k_c, related to *H* and *K*, are generally referred to as the rigidity and the saddle splay constant, respectively. By means of combining the Helfrich expression with a conventional multiple equilibrium approach, we have investigated the influence of shape fluctuations on the size distributions of spherical bilayer vesicles and microemulsion droplets.[2] Shape fluctuations is shown to contribute with a factor proportional to R^2 to the size distribution functions for both aggregates. From the derived size and shape distribution functions we have related the thermodynamical parameters from the Helfrich expression k_c, k_c and H_0 with the, in principle, experimentally available quantities average size $\langle R \rangle$, average shape $\langle c \rangle$ and polydispersity $s_R/\langle R \rangle$. For a symmetrical bilayer vesicle, H_0 is shown to equal zero, resulting in a polydispersity of vesicles which is independent on k_c and k_c.

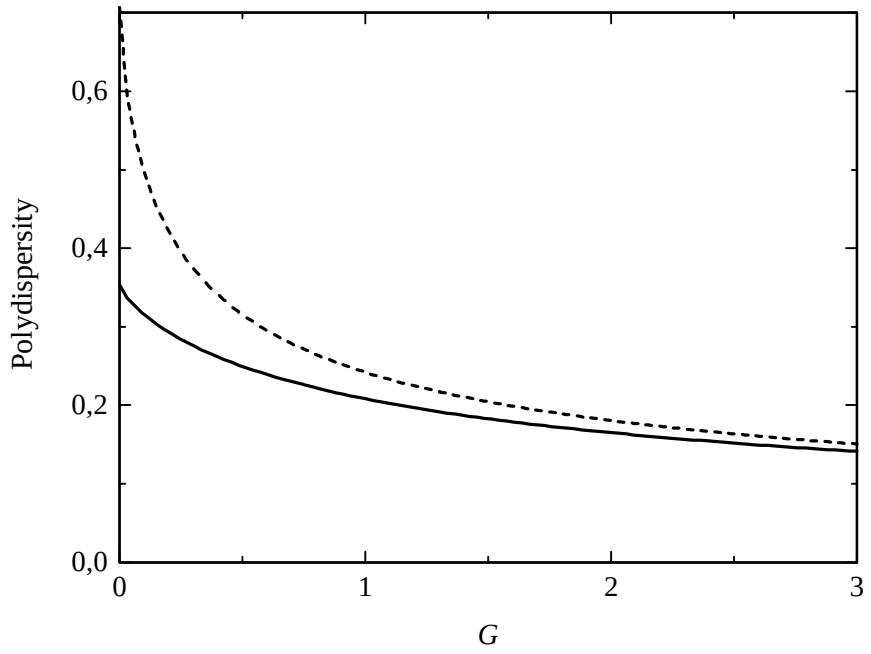

Fig. 1. The polydispersity s_R / R_{max} of microemulsion droplets plotted against the thermodynamic parameter $G = 4k_c^{-} H_0^{-}/(g_0 + 2k_c H_0^{-})kT$. The lower curve (solid line) is derived from the volume fraction density distribution whereas the polydispersity in the upper curve (dashed line) is defined from a number density size distribution.

[1] Helfrich, W., Naturforsch., **28c**, 693, (1973)
[2] Bergström, M., J. Chem. Phys., submitted for publication

2.7.24 An X-ray Photon Correlation Spectroscopy Experiment on a Diblock Copolymer System

C.M. Papadakis, K. Mortensen, *Department of Solid State Physics, Risø National Laboratory, Denmark.* D. Posselt, *Institute of Mathematics and Physics, Roskilde University, Denmark* D.-M. Smilgies, D.L. Abernathy and G. Grübel, *European Synchrotron Radiation Facility, France*

Whereas the static structural properties of diblock copolymer systems in the bulk are relatively well understood, the dynamic processes in these systems are still under intensive discussion.[1] Dynamic light scattering (DLS) has been the most important technique used for investigations of the dynamics. X-ray photon correlation spectroscopy (XPCS) constitutes a new method to study these processes on a time-scale between milliseconds and ca. 100 sec and covering larger *q*-values than is possible with DLS.[2] Such experiments are feasible using synchrotron radiation.

We have studied the dynamics of a symmetric polystyrene-polybutadiene diblock copolymer sample in the disordered state using XPCS. This low molar-mass sample (M_N = 9200 g/mol) has previously been studied using dynamic light scattering[3] and four processes have been identified, two of which are related to the diblock structure: one related to single chain diffusion and another attributed to internal chain relaxation and chain stretching. However, the time-dependent correlation function of the scattered intensity is dominated by a slow process (~100 s), attributed to long-range heterogeneities (~100 nm), which hampers the characterization of the other modes.[3] As the intensity due to the long-range heterogeneities decreases with increasing *q*, XPCS may allow more detailed studies of the other modes.

The experiment was conducted at the TROIKA beamline at the ESRF. In order to achieve a transversally coherent incoming beam, an 8 mm pinhole was inserted into the beam. The time-dependent autocorrelation function of the scattered intensity was measured in a *q*-range between 0.0036 and 0.015 $Å^{-1}$ and decays with a relaxation time of ca. 10 ms. This relaxation time is in accordance with the relaxation times of the diffusive mode observed in DLS-experiments.

1 P. Stepanek and T. P. Lodge, in "Light Scattering. Principles and Development", Oxford 1996
2 *e.g.* I.K. Robinson *et al*., Phys. Rev. B, **52**, 9917 (1995)
3 C.M. Papadakis, W. Brown, R.M. Johnsen, D. Posselt, and K. Almdal, J. Chem. Phys., **104**, 1611 (1996)

2.7.25 The Effect of Cholesterol, Short Chain Lipids, and Bola Lipids in Small Amounts on Lipid-bilayer Softness in the Region of the Main Phase Transition

J. Lemmich, K. Mortensen, *Department of Solid State Physics, Risø National Laboratory, Denmark.* T. Hønger, J.H. Ipsen, O.G. Mouritsen, *Department of Chemistry, The Technical University of Denmark, Denmark and* Rogert Bauer, *Department of Physics, Royal Veterinary and Agricultural University of Denmark, Denmark*

In recent work, we studied the temperature dependence of the small-angle neutron scattering (SANS) from fully hydrated multilamellar phospholipid bilayers, specifically DMPC and DPPC with deuterated acyl-chains, DMPC-d_{54} and DPPC-d_{62}, close to the main phase transition.[1,2]
The observation of an anomalous swelling behavior in the phase transition region, in the sense that the repeat distance displays a peak at the transition, was interpreted as an indication of bilayer softening and thermally reduced bending rigidity.

In the present work, we have studied the effect of the incorporation of small amounts (~ 1 mole%) of amphiphilic solutes, such as cholesterol, a short-chain lipid ($DC_{10}PC$), and bola lipid, into multilamellar DMPC-d_{54} bilayers by differential-scanning calorimetry and SANS. Small amounts of the solutes are found to maintain or even enhance the size of the swelling peak and therefore the bilayer softness in the transition region[3] (See Fig. 1). In the case of cholesterol, a systematic study with $x_{cholesterol}$ = 0.5, 1, 2, and 4 mole% was performed. The data set in Fig. 2 clearly shows that the anomalous swelling peak is enhanced for $x_{cholesterol}$ = 2 mole%, whereas the peak is completely removed for $x_{cholesterol}$ = 4 mole%. This indicates that the effect of small amounts of cholesterol (≤ 3 mole%) is a softening of the bilayers in the transition region, whereas larger cholesterol contents lead to the well-known effect of rigidication.[4]

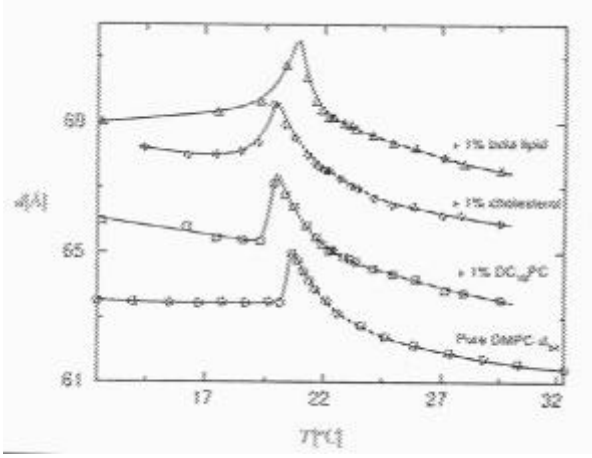

Fig. 1. Temp. dependence of the lamellar repeat distance , *d*, as obtained from SANS measurements in a region around the phase transition temperature of multilamellar bilayers of pure DMPC-d_{54}, and DMPC-d_{54} with 1 mole% of $DC_{10}PC$, cholesterol, or bola lipid. Each data set above that for pure DMPC-d_{54} has been displaced by 2 Å relative to that below.

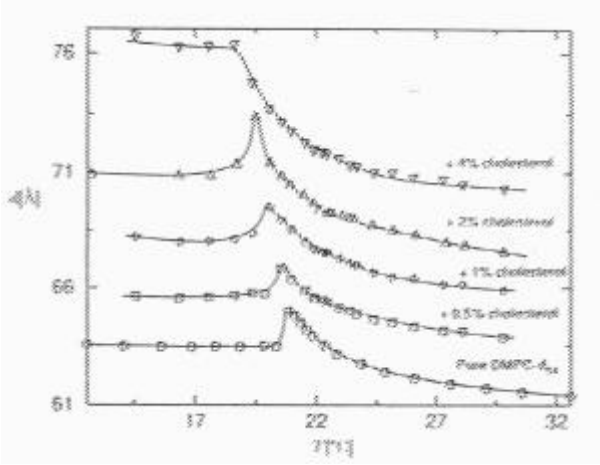

Fig. 2. Temp. dependence of the lamellar repeat distance , *d*, as obtained from SANS measurements in a region around the phase transition temperature of multilamellar bilayers of pure DMPC-d_{54}, incorporated with cholesterol in concentrations 0, 0.5, 1, 2, or 4 mole%. Each data set above that for pure DMPC-d_{54} has been displaced by 2 Å relative to that below.

1 T. Hønger *et al*., Phys. Rev. Lett. **72**, 3911 (1994)
2 J. Lemmich *et al*., Phys. Rev. Lett. **75**, 3958 (1995)
3 J. Lemmich *et al*., Biophys. Lett. *In press* (1996)
4 J. Lemmich *et al*., Eur. Biophys. J. *Submitted* (1996)

2.8 Polymers

2.8.1 Holographic Data Storage Using Peptide Oligomers (DNO)

R.H. Berg, S. Hvilsted, P.H. Rasmussen, *Department of Solid State Physics, Risø National Laboratory, Denmark* and P.S. Ramanujam, *Optics and Fluid Dynamics Department, Risø National Laboratory, Denmark*

Photoanisotropic liquid-crystalline polymers[1] and photorefractive polymers[2] are currently being investigated for the development of media for optical data storage. In recent work,[3] we have described a new family of organic materials - oligopeptides containing azobenzene chromophores, referred to as DNO oligomers - which appear particularly promising for erasable holographic data storage applications. The rationale for the DNO approach is to use the structural properties of peptide-like molecules to impose orientational order on the chromophores, and thereby optimize the optical properties of the resulting materials. The molecular architecture of DNO is inspired by that of DNA (see Fig. 1). The results show that holographic gratings with large first-order diffraction efficiencies (up to 80%) can be written and erased optically in DNO films only a few micrometres thick. The holograms also exhibit good thermal stability, and are not erased after exposure to 180 ^{o}C for one month. The peptide strategy used permits efficient solid-phase assembly of large numbers of diverse molecular structures by Merrifield synthesis and thus could expand considerably the framework for the design of organic molecular materials for optics.

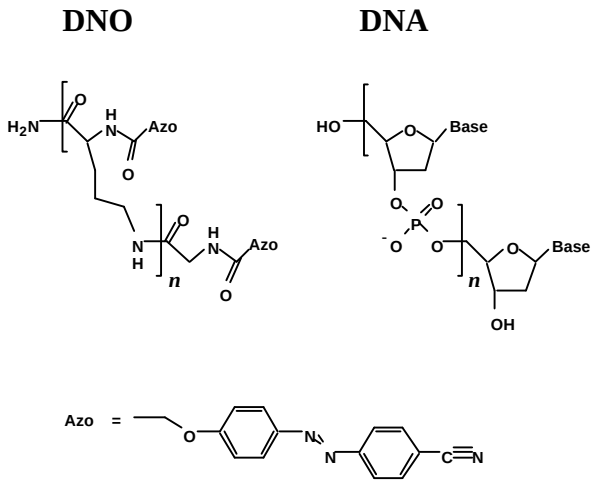

Fig. 1. Chemical structures of DNO and DNA.

[1] M. Eich, J. H. Wendorff, B. Reck, and Ringsdorf, H. *Makromol. Chem. Rapid Commun.* **8,** 59 (1987)
[2] S. Ducharme, J. C. Scott, R. J. Twieg, and W. E. Moerner, *Phys. Rev. Lett.* **66,** 1846 (1991)
[3] R. H. Berg, S. Hvilsted, and P. S. Ramanujam, *Nature* **383,** 505 (1996)

2.8.2 New Azobenzene Side-Chain Polyesters for Optical Information Storage

M. Pedersen, S. Hvilsted, *Department of Solid State Physics, Risø National Laboratory, Denmark,* P.S. Ramanujam, N.C.R Holme, *Optics and Fluid Dynamics Department, Risø National Laboratory, Denmark* and J. Kops, *Department of Chemical Engineering, The Technical University of Denmark, Denmark*

Photosensitive chromophores in thin films of azobenzene side-chain polyesters are investigated for use in holographic data storage. The polyesters are prepared in a transesterification of a mesogenic diol containing an azobenzene moiety and a diphenyl ester. Aiming at the comprehension of the role of the substituent a large number of polyesters with different substituents (**CN, NO_2, OCH_3, H, CF_3, CH_3, $(CH_2)_3CH_3$, C_6H_5** and the halogens: **F, Cl** and **Br**) in the 4-position of the azobenzene side-chain have been synthesized with 4 and 12 methylene groups in the main-chain, respectively. In addition, copolyesters employing a mixture (50:50) of two different diols (**CN-NO_2, CN-F,** and **NO_2-F**) have been prepared.
Polarization holographic measurements were performed on thin unoriented films cast from chloroform solutions of the polyesters on glass substrates in order to study the diffraction efficiency as well as the spatial resolution of the storage. Diffraction gratings were recorded in a two-beam set-up[1] with three intensity levels (50, 75 and 100 mW/cm^2) of the 488 nm line of an Argon ion laser and the read outs were performed at 633 nm with a HeNe laser (Table 1).

Table 1. First-order diffraction efficiency (%) in thin polyester films cast from chloroform solutions (The polyester is identified with **Pnxm** where **n** is the number of methylene groups in the side-chain, **m** is the number of methylene groups in the main-chain and **x** symbolizes the substituent: a = **CN**,b = **NO_2**).

Polymer (Subst.)	Film thickness (μm)	Intensity (mW/cm^2)	Irradiation time (s)			Irradiation time (s)	Intensity (mW/cm^2)		
			10	30	60		50	75	100
			Diffraction efficiency (%)				Diffraction efficiency (%)		
P6a12 (CN)	1.8	75	60	61	61	60	55	61	9
P6b12 (NO_2)	2.6	75	5	18	35	60	5	35	50
P6ab12 (CN-NO_2)	3.3	75	50	54	70	60	67	70	72

The highest diffraction efficiency obtained was on the order of 72 % which is close to the maximum achievable and among the highest found in organic materials. This was disclosed in the copolyester containing a mixture of **CN** and **NO_2** (**P6ab12**). However, also the **OCH_3, H, CF_3, CH_3,** and **F** substituted polyesters displayed diffraction efficiencies higher than 50 % in the series of the tetradecanedioate (**m** = 12) but not in the adipate series (**m** = 4). In some polyesters (**C_6H_5, $(CH_2)_3CH_3$** and **Br** substituted) the determined diffraction efficiencies were close to zero and the explanation for this is still under investigation. The induced gratings in the films are in general stable at room temperature but can be completely erased by heating the films upon the isotropization temperature of the polymers (appr. 80 °C).

[1] P. S. Ramanujam, C. Holme, S. Hvilsted, M. Pedersen, F. Andruzzi, M. Paci, E. L. Tassi, P. Magagnini, U. Hoffman, I. Zebger and H. W. Siesler, Polymers for Advanced Technologies, **7**, 768 (1996)

2.8.3 Side-Chain Liquid Crystalline Polyesters for Optical Information Storage

S. Hvilsted, *Department of Solid State Physics, Risø National Laboratory, Denmark*, P.S. Ramanujam, *Optics and Fluid Dynamics Department, Risø National Laboratory, Denmark*, H.W. Siesler, *Department of Physical Chemistry, University of Essen, Germany*, P. Magagnini, *Chemical Engineering Department, University of Pisa, Italy*, and F. Andruzzi, *CNR, Chemical Engineering Department, University of Pisa, Italy*

This project, LICRYPOIS, is a collaborative focused fundamental research performed by the above consortium with the objective to develop materials for optical information storage. The project is supported financially in part by the European Economic Community in the framework of the Brite/EuRam programme and the project management is in the department.

It is shown through intensive differential scanning calorimetry measurements and X-ray,[1] synchroton, and polarization optical microscopy investigations,[2] FTIR and optical anisotropy measurements[3] and through polarization holography[4] that side-chain liquid crystalline polyesters are admirably suited for erasable optical storage. A grating recorded in 1992 in a film of such a polyester with its undiminished diffraction efficiency testifies to the potential for optical storage in these polyesters. After a thorough investigation it is found that polyesters with 6 or 8 methylene groups in the flexible spacer, a cyano substituted azobenzene as the photoactive chromophore in the side chain, 12 methylene groups in the acidic part of the main chain, with a molar mass between 20,000 and 70,000 are eminently suited for optical storage.

As they stand, the polyester films can be used for the storage of medical documents, x-ray pictures, satellite images and the like.

There are still several unexplained observations which require more investigations: 1) the phenomenally strong influence of a red-laser irradiation subsequent to the blue-laser in some polyesters and copolyesters. Much more than a simple *cis-trans* isomerization is hidden behind these observations. 2) the role of aggregation: the evidence has been indirect through FTIR and optical investigations. Again preliminary work with the synchroton irradiation seems to point to a change in structure when the film is irradiated while undergoing a cooling process. 3) the role of dipole moment: it is clear that the substituent with the largest dipole moment (nitro) is poor from an optical point of view. At present it is unknown what parameter determines the efficiency and speed of storage.

---

1 P.S. Ramanujam, C. Holme, S. Hvilsted, M. Pedersen, F. Andruzzi, M. Paci, E.L. Tassi, P. Magagnini, I. Zebger, U. Hoffman, H.W. Siesler, Polymers for Advanced Technologies **7**, 768 (1996)

2 P.S. Ramanujam, N.C.R. Holme, S. Hvilsted, Appl. Phys. Lett. **68**, 1329 (1996)

3 N.C.R. Holme, P.S. Ramanujam, S. Hvilsted, Appl. Opt. **35**, 4622 (1996)

4 L. Nikolova, T. Todorov, M. Ivanov, F. Andruzzi, S. Hvilsted, P.S. Ramanujam, Appl. Opt. **35**, 3835 (1996)

2.8.4 New Polyester Materials with Exceptionally Short Optical Storage Recording Times

S. Hvilsted, C. Kulinna, E.T. Kristensen, *Department of Solid State Physics, Risø National Laboratory, Denmark*, and P.S. Ramanujam, *Optics and Fluid Dynamics Department, Risø National Laboratory, Denmark*

Many azobenzene side-chain liquid crystalline polyesters possess the necessary potential to become future analog optical storage media. Thus, in two-beam interoferometry by use of orthogonally circularly polarized Argon ion laser light they demonstrate high permanent diffraction efficiency (> 50%) with high resolution (> 3000 lines/mm). However, the time necessary to achieve these merits are normally on the order of tenth of seconds which for industrial applications are considered too long.

In the search for fast optically responding polyesters, one particular class, having a chiral S(-)-2-methyl-1-butoxy substituent on the azobenzene, has revealed promising properties including unusually short recording times. However, the optical responce is strongly depending on the polyester architecture and a delicate balance between both main-chain and side-chain spacing is apparently needed. After a systematic preparative work the most prosperous combination is found in a polysebacate (8 methylene chain) with a decamethylene side-chain spacing, **P10>c<8**. This polyester is able to achieve > 50% 1st order diffraction efficiency by 300 ms exposure to an Ar laser power of 100 mW/cm^2 (see Fig. 1), or after 1 s with 30 mW/cm^2. A sizable diffraction efficiency has been detected in as short as 50 ms which by far is the best performance recorded in any organic (polymeric) material.

Ongoing investigations have shown that isomeric polyesters employing the achiral analogue perform optically almost as well. This points to the decisive character of the substituent rather than the necessity for chirality. Additionally, the achiral building block is simpler to prepare which is an advantage from an exploitationable point of view.

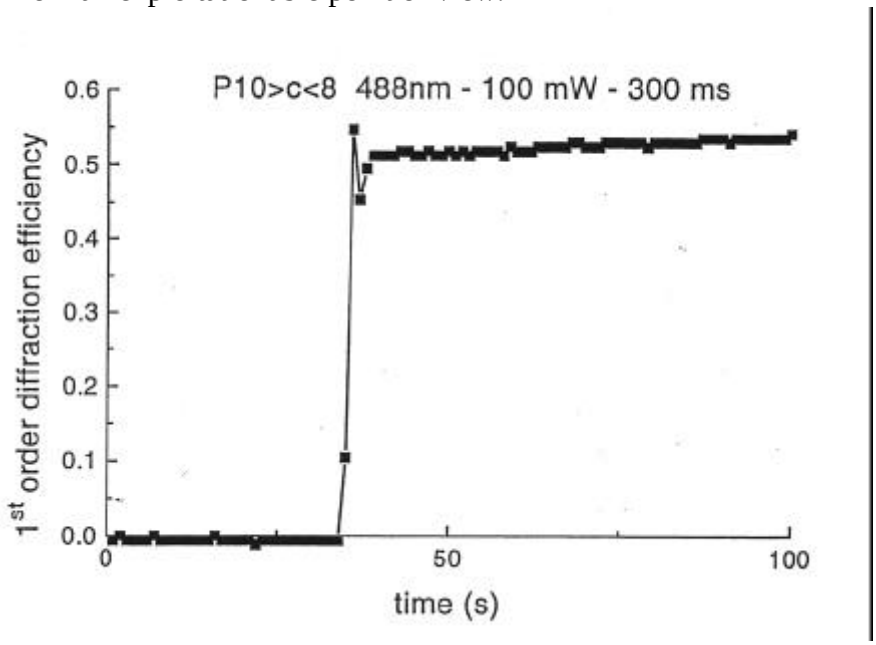

Fig. 1. Development of 1st order diffraction efficiency in the polyester, **P10>c<8**, after exposure to 300 ms of orthogonally circularly polarized argon laser light at 100 mW/cm^2

2.8.5 Laser Induced Segmental Orientation in Cyanoazobenzene Side-Chain Polyesters

C. Kulinna, S. Hvilsted, *Department of Solid State Physics, Risø National Laboratory, Denmark*, and P.S. Ramanujam, *Optics and Fluid Dynamics Department, Risø National Laboratory, Denmark*

Investigations by atomic force and scanning near-field optical microscopic investigations have revealed[1] that laser induced optical anisotropy in cyanoazobenzene side-chain polyesters is associated with the development of a topographic undulation. However, if a grating is produced by polarization holography the resulting polarization is preserved across the pronounced surface roughness. It has therefore long been speculated that not only the photo sensitive azobenzene chromophores are responsible for the induced anisotropy but additionally other polyester segments could contribute.

With properly deuterium labeled polyesters it is possible to study the anisotropic influence on the different polyester segments by polarization FTIR spectroscopy. In particular, it is possible to focus on the dichroic behaviour of (CD_2) vibrational modes and remaining (CH_2) absorptions originating from different segments of the same polyester. A large variation of selectively deuterated polyesters have been prepared and spectroscopically investigated after exposure to laser irradiation.

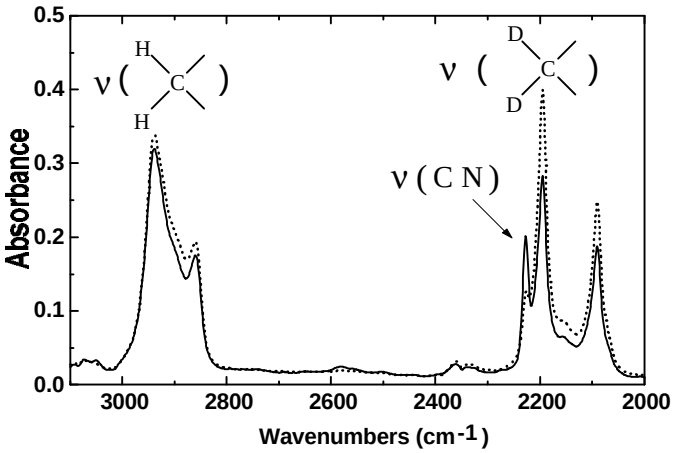

Fig. 1. FTIR polarization spectra of a main-chain deuterated cyanoazobenzene side-chain polyester (**P6a12$_d$**), recorded with infrared radiation polarized parallel (┈) and perpendicular (—) to the argon ion laser polarization.

Table 1. Dichroic ratio, R, and order parameter, S, of selected group vibrations of main-chain deuterated polytetradecandioates.

Polyester	azobenzene chromophore $\nu_s(C=C)_{ring}$		main-chain spacer $\nu_s(CD_2)$		side-chain spacer $\nu_s(CH_2)$	
	R	S	R	S	R	S
P6a12$_d$	4.04	0.50	0.68	0.24	0.81	0.14
P8a12$_d$	4.62	0.55	0.63	0.28	0.68	0.24
P10a12$_d$	7.63	0.69	0.59	0.32	0.62	0.29

A characteristic example is depicted in Fig. 1. Assuming a uniaxial orientation, quantitative evaluations can be carried out by calculating the order parameter, S, defined by the second term of the Legrendre polynom employing the dichroic ratio, R. Table 1 presents these merits for different polyester segments as a function of side-chain spacer length. The laser power has been adjusted to achieve maximum values for S.

From Table 1 it is evident that the aliphatic spacer length (6, 8, or 10 methylenes) exhibits a pronounced influence on the laser induced alignment of different structural segments. Moreover, although only the orientational behaviour of the azobenzene chromophore is directly influenced by the irradiation process, the infrared spectroscopic investigations have shown that all major polyester structural segments are integrated into the induced anisotropy and are therefore contributing to the storage process.

[1] P.S. Ramanujam, N.C.R. Holme, S. Hvilsted, Appl. Phys. Lett. **68**, 1329 (1996)

2.8.6 Studies on a Dilithium Initiator

J. Zhou, S. Ndoni and K. Almdal *Department of Solid State Physics, Risø National Laboratory, Denmark*

The dilithium initiator (DLi) based on *sec*-butyllithium/1,3-bis(1-phenylethenyl)benzene (BuLi/PEB) has been studied for many years. It is the basis for important methods to prepare ABA triblock copolymers and difunctional polymers.[1] The exact stoichiometric control of the addition of BuLi to PEB is imperative for the formation of the diadduct only (equation below), without the disturbance of monoadduct.

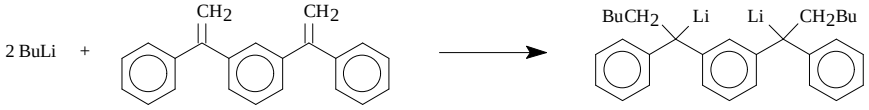

However, when it is empolyed to initiate isoprene to obtain low molar mass polyisoprene (PI) in apolar solvents, i.e. cyclohexane, unlike PI initiated by *sec*-butyllithium or the monolithium initiator based on *sec*-butyllithium/1,1-diphenylethylene in cyclohexane, the size exclusion chromatography (SEC) curve of the PI initiated by the DLi shows that the molar mass distribution is bimodal and very broad (Fig. 1). The measured molar masses of peak A and peak B are 3000 g/mol and 1000 g/mol, respectively.

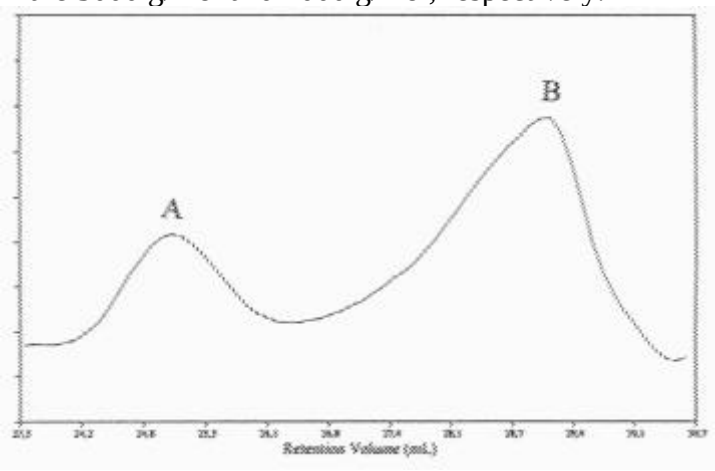

Fig.1 SEC curve of PI initiated by DLi in cyclohexane and terminated by trimethylchlorosilane, then methanol.

The phenomenon has been investigated using trimethylchlorosilane as terminator. The polymer is analysized by ^{1}H NMR spectra. The studies conclude that in cyclohexane, the polymer chains corresponding to peak A grow only in one direction. Peak A arises from the monofunctional growth species and grow faster than peak B to form the higher molar mass fraction. The monofunctional growth species is speculated to be due to the steric effect. Peak B arises from polyisoprenyldilithium or difunctional growth. The low molar mass is consistent with the suggestion [2] that association of the difunctional species leads to slower growth.

The fact that 3,4 content of peak B is higher than that of peak A shows that when isoprene molecules are added slowly, more 3,4 units enter the polymer chains in spite of the use of cyclohexane as solvent.

---

1 R. P. Quirk, J.-J. Ma, Polymer International, **24**, 197-206 (1991)

2 G. Y.-S. Lo, E. W. Otterbacher, A. L. Gatzke, L. H. Tung, Macromolecules, **27**, 2233-2240 (1994)

2.8.7 Dilute Solution Properties of Segmentwise Deuterated Star-Shaped Polystyrenes

S. Ndoni, J.S. Pedersen and K. Almdal, *Department of Solid State Physics, Risø National Laboratory, Denmark*

We investigated by small angle neutron scattering (SANS) the conformation of relatively long-arm regular star polystyrenes in dilute solution with a good solvent, as dependent on the functionality of the star and on the position relative to the branching point. The experimental results were compared with Monte Carlo (M.C.) computer simulations.

Monodisperse six-, three- and two- arm star polystyrenes were prepared by living anionic polymerization in cyclohexane under inert (argon) atmosphere followed by coupling with hexa-, tri- and di- chloro-alkylsilane compounds, respectively. The single arms of a given type (*i.e.* sequence of (d)euterated and (h)ydrogenated blocks) were prepared first, by sequential addition of deuterated and hydrogenated monomer (styrene) and the living chains (capped with few units of butadiene in order to permit for complete coupling) were used to prepare the respective 2-,3- and 6- arm stars. This procedure provided the same arm length for the stars of a given arm type. From 4 synthesis there were obtained 12 polymers: $(hhh\text{-})_i$, $(ddh\text{-})_i$, $(hdd\text{-})_i$, and $(dhd\text{-})_i$ (i=6,3,2), where hhh- stays for fully hydrogenated, ddh- stays for hydrogenated at the 1/3 inner part and deuterated at the 2/3 outer part of the arms and so on. The average molar masses per arm were in the range $(1{,}1\pm0{,}1)\cdot10^5$g/mol.

SANS measurements were conducted at the Risø National Laboratory. The covered *q*-range was $7\cdot10^{-3}$Å^{-1}-0.5Å^{-1}. The measurements were made on dilute solutions with a good solvent (dry deuterated tetrahydrofurane (d_8-THF)); three concentrations were prepared for each sample: 0.25%; 0.5% and 1%. The scattering length of THF matches within 1% that of the styrene repeating unit, therefore only the hydrogenated parts are 'visible'. ^{1}H-NMR measurements on the SANS samples were used to correct for eventual solvent remained in the polymer after drying.

A Kratky-Porod worm-like chain model with fixed valence angles and free rotation of bonds was used for the off-lattice M.C. computer simulations. The simulations were based on a Pivot algorithm with coordinate corrections and 'zippering' for overlap. A hard core potential was adopted to account for the excluded volume interaction in good solvents. After choosing 6 spheres per Kuhn length (600 spheres per arm), each simulation consisted of 10^6 M.C. steps, with 10^4 calculations of the structure factor *S(q)*. The resulting error is of the order of 0.5%. Fig.1 shows the simulated scattering plots as compared with the experimental data for the case of 6-arm stars. A good general fit is obtained. The small discrepancies at low *q* are under investigation.

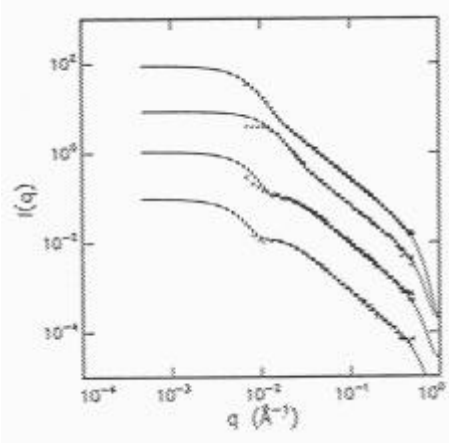

Fig. 1. Comparison of the M.C. simulations (solid lines) with the SANS data for the 6-arm polystyrene samples (0.25% by mass in d_8-THF). From the top: fully labeled (hydrogenated) arms, labeled in the central 1/3 section, labeled in the middle 1/3 section and labeled in the outer 1/3 section of the arms.

2.8.8 Synthesis of Hydrocarbon-Poly(dimethylsiloxane) Diblock Copolymers

K. Almdal, *Department of Solid State Physics, Risø National Laboratory, Denmark* and M.A. Hillmyer, *Department of Chemical Engineering and Materials Science, University of Minnesota, USA*

Anionic polymerisation of hexamethylcyclotrisiloxane (D_3), which can be initiated by sufficiently nucleophilic species, are usually performed in tetrahydrofuran (THF) solution. However, in the polymerisation of diene monomers the choice of solvent have a strong influence on the structure of the prepared polymer and THF is often not a desirable choice. A method has been developed that allows for the anionic polymerisation D_3 in hydrocarbon solvent. The enhanced flexibility in choice of polymerisation conditions for D_3 has been utilised for synthesis of a series of hydrocarbon-PDMS block copolymers.

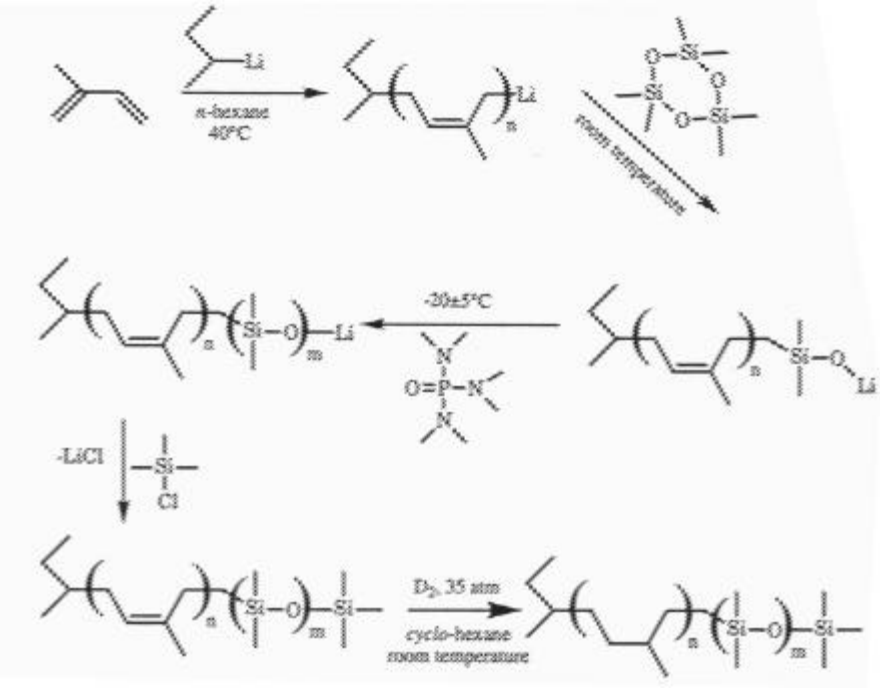

Sequential anionic polymerisation of butadiene or isoprene and of (D_3) were performed in either a hydrocarbon solvent or tetrahydrofuran (THF) with lithium as the counter ion. *n*-hexane or *cyclo*-hexane was used for the polymerisation of butadiene and isoprene to yield high 1,4 addition. Addition of hexamethylphosphoric triamide (HMPA) in these non-polar solvents facilitates the polymerisation of D_3. Termination was effected by addition of a 1.5 fold excess of trimethyl chlorosilane. The resulting hydrocarbon-PDMS block copolymers were saturated with deuterium at 35 atm using Palladium (5%) on calcium carbonate as catalyst. This procedure yields block copolymers of PDMS and the saturated hydrocarbon polymers poly(1,2-butylene- *ran*-1,4-butylene) with 90% 1,2-units (PEE90) and 7% 1,2-units (PE), and poly(ethylene-*alt*-propylene) (PEP). The synthetic procedure is outlined in Scheme 1.

2.8.9 Microstructure of Electropolymerized Polypyrrole Films

A.R. Hillman, *Department of Chemistry, University of Leicester, UK,* A. Glidle, *Department of Bioelectronics, Glasgow University, UK,* P.M. Saville, R.W. Wilson, *Department of Chemistry, University of Leicester, UK* and M.C. Gerstenberg, *Department of Solid State Physics, Risø National Laboratory, Denmark*

In the long term we wish to arrive at an understanding of the effects of polypyrrole thickness, solvent and ion content, and film redox state, on the spatial distributions of polymer (redox sites) and solvent. The correlation of this information is key to understanding electrochemical response. In this experiment reflectivity measurements were made on polypyrrole films, electropolymerized in the presence of different electrolyte species, against different solvent contrasts.

Pyrrole (20 mmol dm^{-3}) was electropolymerized by cycling the potential between 0 and 0.9 V vs SCE until the desired film thickness was reached. The dopants used in polymerization included p-toluenesulphonate, perchlorate and trifluoromethanesulfonate (as tetraethyl ammonium or lithium salts) at concentrations of 0.3 mol dm^{-3} in acetonitrile (acetonitrile results in a more uniform film than obtained from aqueous solvents). Reflectivity measurements were then made on the films in aqueous solutions using H_2O, D_2O or quartz contrast matched water as solvent.

Figure 1 shows the reflectivity profiles of the four films studied against D_2O. Counter ion has an obvious effect on film structure. Polypyrrole from tosylate appears to be the most uniform.

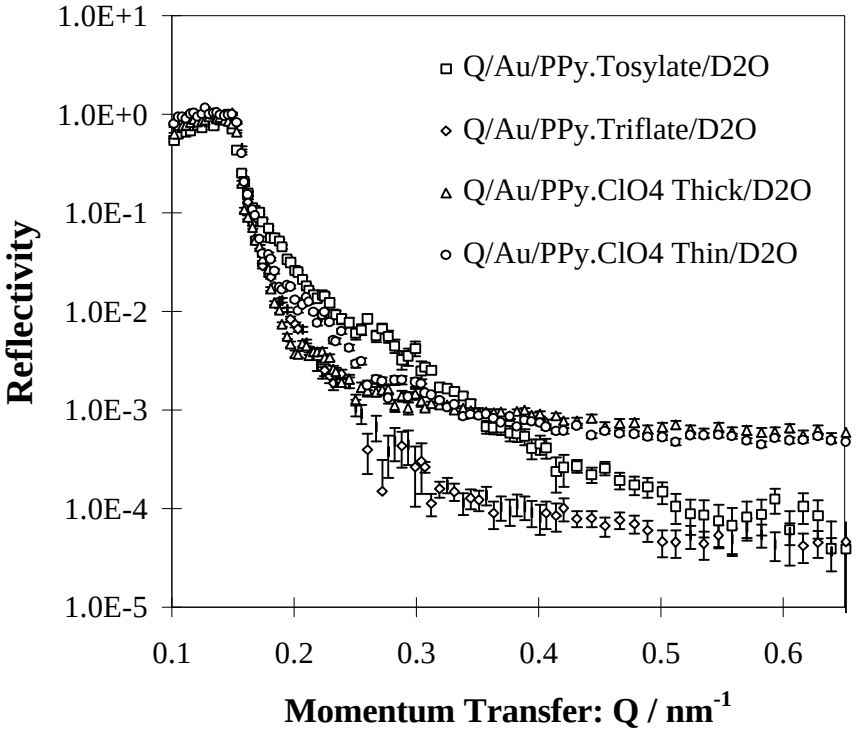

Fig. 1. Reflectivity profiles of four polypyrrole films polymerized with different electrolyte species, tetraethylammonium *p*-toluene sulphonate (tosylate), tetraethyl ammonium perchlorate (ClO_4), and lithium trifluoromethyl sulphonate (triflate).

2.9 Organic Chemistry

2.9.1 Synthesis, Structure and Properties of 4,8,12-Trioxa-12c-phospha-4,8,12,12c-tetrahydrodibenzo[cd,mn]pyrene a Molecular Pyroelectric

F.C. Krebs, P. Sommer-Larsen, J. Larsen, *Department of Solid State Physics, Risø National Laboratory, Denmark,* C.S. Jacobsen, *Department of Physics, Technical University of Denmark,* C. Boutton, *Laboratorium voor Chemische en Biologische Dynamica, Belgium* and N. Thorup, *Department of Chemistry, Technical University of Denmark*

The title compound was synthesised and its crystalline structure was determined. The structure was found to belong to a relatively rare space group, *R3m,* for organic molecules. The molecule has a C_{3v} point symmetri and a considerable dipole moment, 3.3 D, which when combined with the particular structure results in a permanent polarisation and consequent pyroelectric properties.[1]
The pyroelectric properties were determined in the temperature range from 28 ^{o}C to 110 ^{o}C. The room temperature pyroelectric coefficient had a value of -3 C m^{-2} K^{-1} which was found to be in good agreement with a calculated value of -3.2 C m^{-2} K^{-1}. The calculated value was based on a simple model,

$$\frac{dP(T)}{dT} = p_3(T) = -\frac{Z}{\left(aT^2 + 2bT + \frac{b^2}{a}\right)}\begin{pmatrix}0\\0\\\mu\end{pmatrix}$$

P(T) being the polarisation, *T* the temperature, *Z* the number of molecules in the unit cell, μ the molecular dipole moment, *a* and *b* being coefficients in the expression for linear expansion (the unit cell volume $V(T) = aT + b$). The linear expansion of the material was determined by measuring the unit cell volume in the temperature range from -93 ^{o}C to 200 ^{o}C. The material was further considered for use as a detector material in infrared detection. A determination of the relative permittivity tensor at optical frequencies, at 35 GHz and the isotropic permittivity at low frequencies (1 KHz, and 120 Hz) along with a calculation of the heat capacity allowed for a calculation of the detectivity merit factor for the title compound. The material has a detectivity merit factor well above many inorganic detector materials currently in use but still below the most performing detector materials known.

Fig. 1. The molecular structure of the molecule along with the unambigously assigned direction of the molecular dipole moment.

[1] F.C. Krebs, P. Sommer-Larsen, J. Larsen, C.S. Jacobsen, C. Boutton, N. Thorup, *JACS*, in press

2.9.2 Synthesis of Labile Molecules for Scanning Probe Microscopy-Induced Chemical Reactions

S.B. Wilkes and K. Bechgaard, *Department of Solid State Physics, Risø National Laboratory, Denmark*

The scanning tunnelling microscope (STM) can be considered as a potential tool for the *in-situ* manipulation and study of electrochemically, photochemically and thermally labile molecules since the energy of tunnelling is within the range of many chemical processes. In conjunction with our work on photochemically labile molecules,[1] a series of suitable molecules have now been prepared intended for electrochemical analogies. Two new variants of a 2,6-dialkoxy-9,10-bis(1,3-dithiol)-dihydroanthracene of type **1** (Fig. 1) and a series of 1,4-dithiafulvenes of type **2** (Fig. 2) have been synthesised for this purpose. The bis(1,3-dithiol) derivatives **1** are known to undergo a reversible 2-electron wave oxidation at low potentials (*ca*. +0.3 V) from the neutral to dication state[2] (see Fig. 1). Similarly, the 1,4-dithiafulvenes **2** dimerise to the neutral dimeric species under oxidative/reductive conditions[3] (see Fig. 2). In both sets of molecules, as the redox properties are altered, so are the structural and conformational properties. Therefore, depending on whether an initial physisorbed monolayer can be suitably imaged, these molecules seem ideal candidates for subsequent *in-situ* manipulation and imaging using an electrochemical STM set-up. STM work on these molecules along these lines is currently in progress.

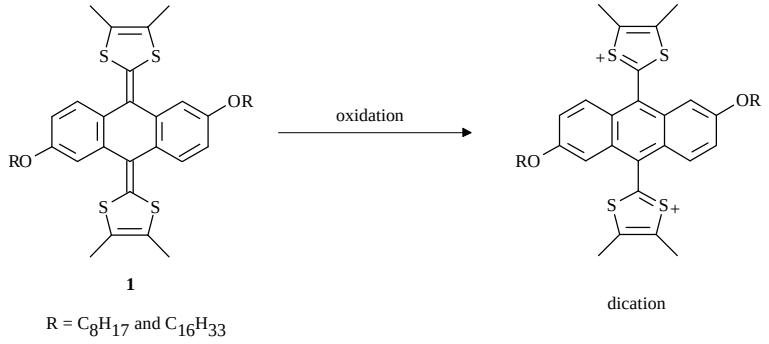

1

Fig. 1. Oxidation of 2,6-dialkoxy-9,10-bis(1,3-dithiol)-dihydroanthracene.

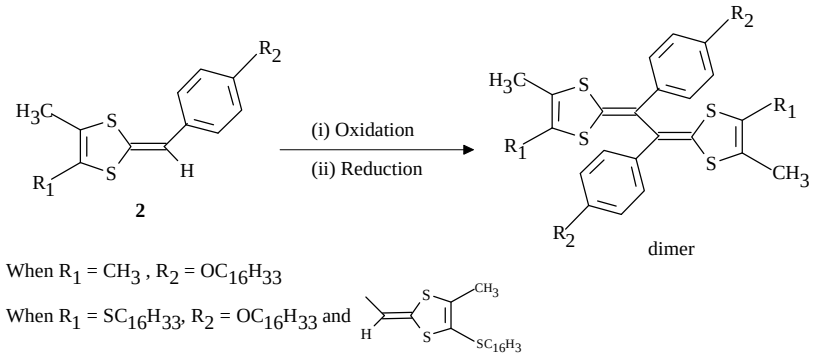

2

Fig. 2. Dimerisation of substituted 1,4-dithiafulvenes.

---

1 S.B. Wilkes, K. Bechgaard, T. Hansen, S. Itoua, T. Bjørnholm and K. Schaumburg, in the Risø Annual Progress Report of the Department of Solid State Physics, Risø-R-863(EN), 1 January-31 December 1995, 68

2 G. J. Marshallsay and M. Bryce, J. Org. Chem., **59**, 6847 (1994)

3 D. Lorcy, R. Carlier, A. Robert, A. Tallec, P. Le Magueres and L. Ouahab, J. Org. Chem., **60**, 2443 (1995)

2.9.3 Synthesis of Some Novel 12c-Derivatives of 1,5,9-Trioxa-3,7,11-tris(tert-butyl)-tricornane

A. Faldt, I. Johannsen, *Department of Solid State Physics, Risø National Laboratory, Denmark*
and K. Boubekeur, *IMM, University of Nantes, France*

Since Martin *et al*[1] first synthesised the 1,5,9-trioxatricornan and investigated the great stability of the cation by cyclic voltammetry derivatives of this system has attracted much attention. Both the cation and the free radical has been investigated by means of NMR and ESR.[2] One way of making the trioxatricornan molecule more steric demanding is the introduction of relatively large groups at the periphery, at the centre or at both places. The synthesis of the 1,5,9-trioxa-3,7,11-tris(tert-butyl)-tricornane has been described earlier[3] but our synthesis has introduced some significant improvements in yields and shortening the total synthesis. Synthesis of the PF_6 salt of **1** (see Fig. 1., R=PF_6^-) gives the starting material for the introduction of several 12c-derivatives by nucleophilic addition and the reduction of the ethylether by $NaBH_4$ results in the 1,5,9-trioxa-3,7,11-tris(tert-butyl)-12c-H-tricornane(R=H). This substituent is expected to introduce the least deviation from the total planar cationic derivative (R=PF_6^-).
Treatment of the ethylether derivative with $Mo_6Cl_{14}^{2-}$ (formed *in situ* from $MoCl_2$ and HCl) gave compound **2** as orange needles which precipitated from the solution. The crystal structure has been investigated by means of X-ray crystallography at 200 K where the unit cell belong to the $P2_{1/n}$ spacegroup and the unit cell dimensions where, a= 17.199 Å; b= 11.186 Å; c= 18.450 Å; R=0.0367 (2991 data).[4]

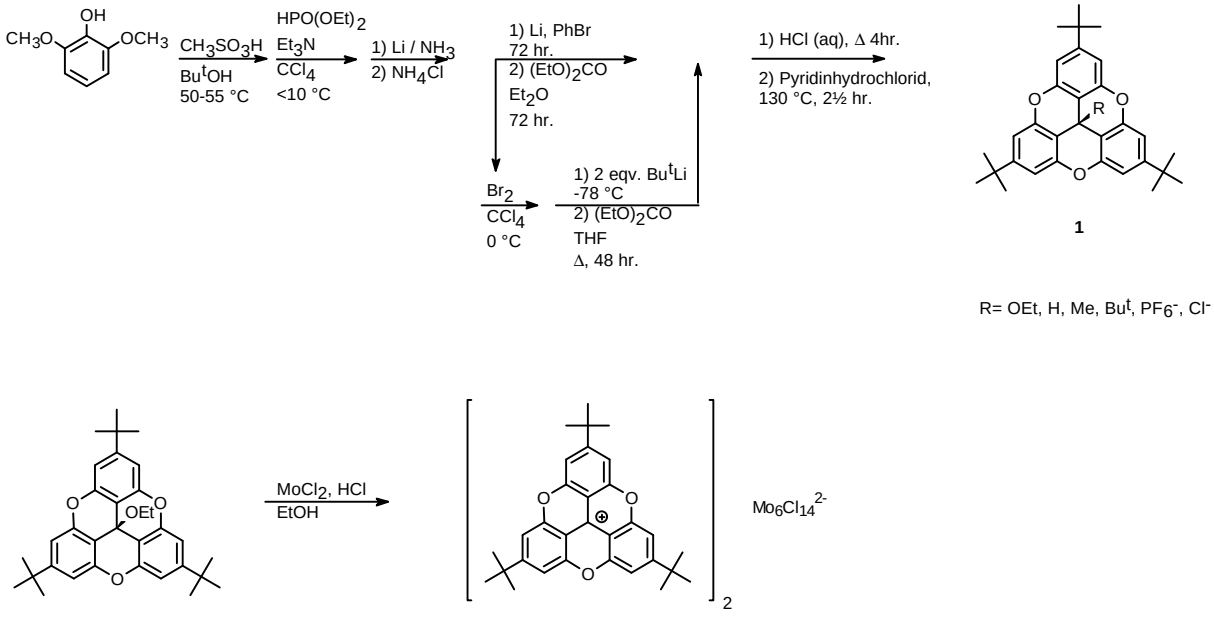

Fig. 1

---

1 J.C. Martin, R.G. Smith, *J. Am. Chem. Soc.*, **86**, 2252-2256 (1964)
2 W.T. Bowie, M.R. Feldman, *J. Am. Chem. Soc.*, **99**, 4721-4726 (1977)
3 M. Lofthagen, R. VernonClark, K.K. Baldridge, J.S. Siegel, *J. Org. Chem.*, **57**, 61-69 (1992)
4 The front page of this Annual Progress Report shows the structure

2.9.4 Synthesis of Two Container Molecules With Potential Liquid Crystalline Properties

A. Faldt and K. Bechgaard, *Department of Solid State Physics, Risø National Laboratory, Denmark*

The compounds CTV and CTTV (CycloTriVeratrylene **1** and CycloTeTraVeratrylene **2** respectively) have been known for a long time[1,2] but have recently received a growing attention because derivatives have shown liquid crystalline properties. This type of compounds is prone to act as host molecules since they have a rigid structure (this does not apply for **2** which exists as two interconverting isomers at room temperature) allowing inclusion of guest molecules in their cavities. We first tried to synthesise the triketone of CTV (**3**) using a broad range of oxidations known to result in specific benzylic oxidation but all attempts failed. This result can be explained using molecular modelling which indicates that the lack of space in the lower rim (the distance between two axial hydrogen atoms located at the lower rim (CH_2-groups) is approx. 2 Å) only allows oxidation of **1** to the monoketone. The triketone might be interesting since reduction by an alkali metal (sodium etc.) would result in the radical anion with special magnetical and electrical properties. Similar experiments attempted on CTTV also failed to produce the tetraketone. In order to enhance the solubility of **1** and **2** synthesis of the butyloxy-derivatives **4** and **5** has been performed and preliminary DSC-experiments on compound **4** showed no glass transition in the temperature region 10 °C<T<160 °C (T_m=134 °C).

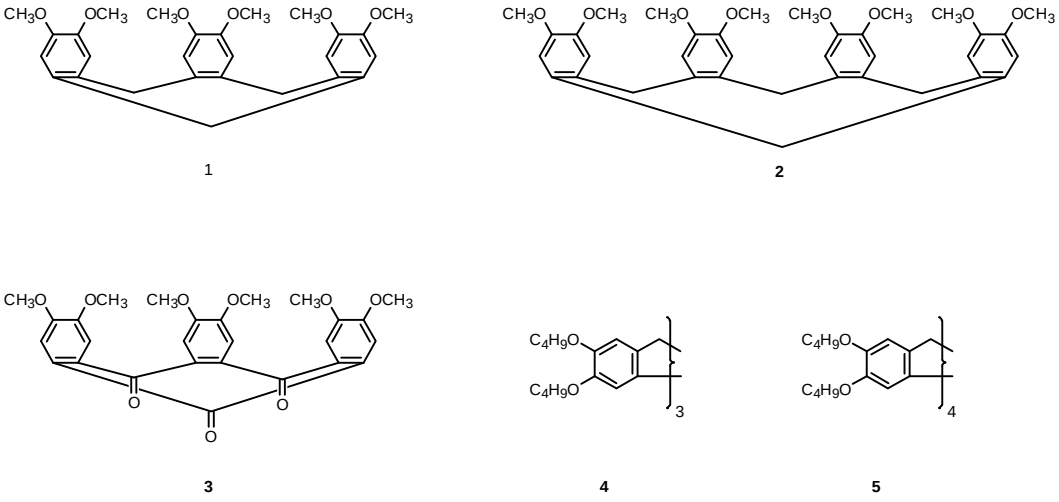

Fig. 1

[1] A.S. Lindsey, *J. Chem. Soc.*, 1685 (1965)
[2] A. Goldup, A.B. Morrison, G.W. Smith, *J. Chem. Soc.*, 3864 (1965)

2.9.5 Selective Halogen-Lithium Exchange Reaction of Bromine Substituted 25,26,27,28-Tetrapropoxycalix[4]arenes

M. Larsen and M. Jørgensen, *Department of Solid State Physics, Materials Chemistry, Risø National Laboratory, Denmark*

Calix[4]arenes are a class of macrocyclic organic molecules which are easily synthesized and have been widely used in the study of supramolecular host-guest systems in the solid state as well in solution. They are bowl-shaped and therefor very interesting building blocks in the synthesis of artificial receptor systems, which can recognize small organic molecules or ions. In order to obtain a selectivity towards certain analyt molecules, it is necessary to control the regio-chemsistry. We have developed a very useful method to introduce functionalities in the so called *upper rim*, which are the *para*-positions of the benzene moieties. The starting compound is a bromine substituted calix[4]arene where we can selective exchange bromine with lithium with either *n*-BuLi or *t*-BuLi in tetrahydrofuran. These lithiated intermediates can then be used to introduce a variety of substituents: carbon in different oxidation states, deuterium, hydrogen, boron, sulfur. The selective bromine to lithium exchange reaction thus offers a simple route to substituted calix[4]arenes with a variety of functionalities and regio-control. By this method it is possible to achieve mono-lithiated, dilithiated and tetralithiated calix[4]arenes (See Fig. 1). Several new calix[4]arenes have been synthesized by this method.[1]

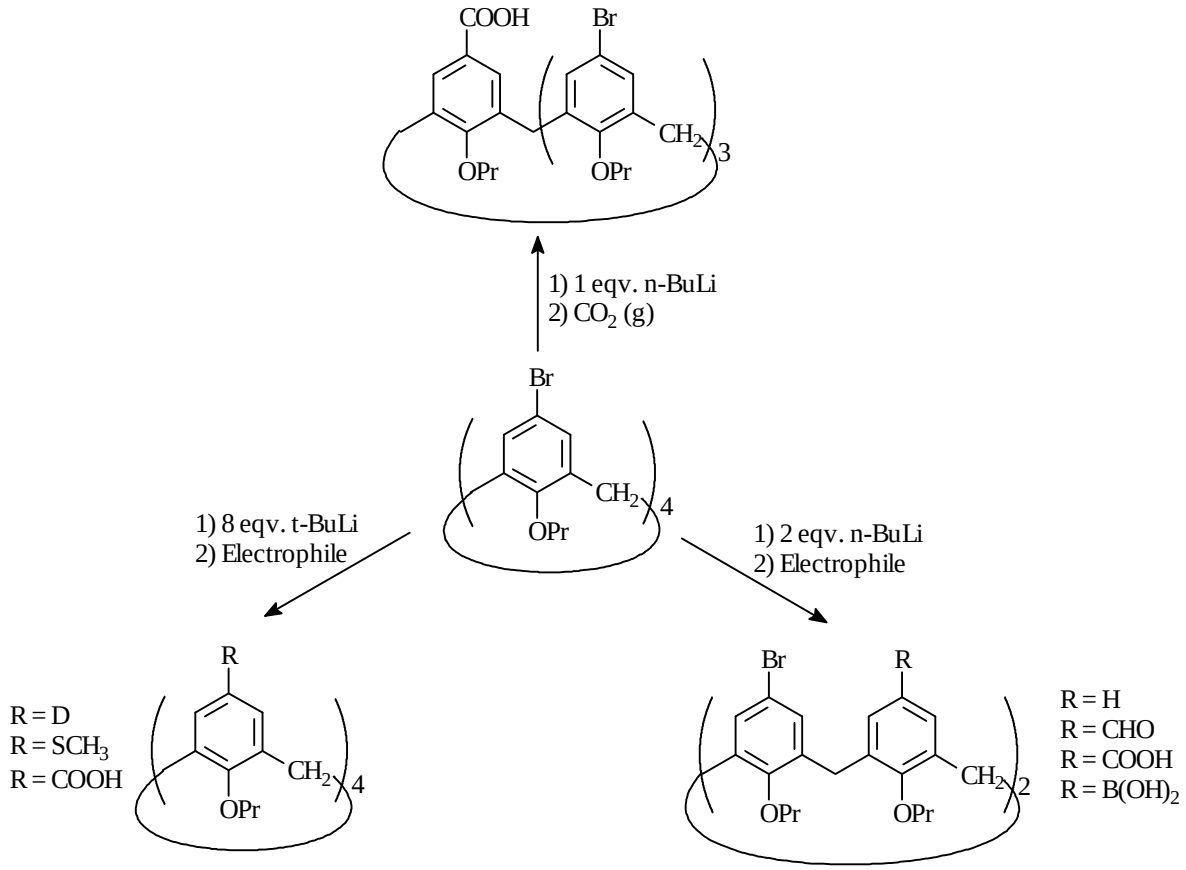

Fig. 1.

[1] M. Larsen and M. Jørgensen, J. Org. Chem. **61**, 6651 (1996)

2.9.6 Biaryl Cross-Coupling Reactions on 25,26,27,28-Tetrapropoxycalix[4]arenes

M. Larsen and M. Jørgensen, *Department of Solid State Physics, Materials Chemistry, Risø National Laboratory, Denmark*

Only few biaryl cross-coupling reactions on calixarenes has been reported in the litterature. Arduini *et al.*[1] synthesized a calix[4]arene which was substituted in the *upper rim* with four phenyl groups. This was carried out by either photolysis of 5,11,17,23-tetraiodo-25,26,27,28-tetrakis(2-ethoxyethoxy)calix[4]arene in benzene (15 % yield) or by a Negishi type reaction in which tetraiodocalix[4]arene was reacted with PhZnCl and $Ni(PPh_3)_4$ as a catalyst (95 % yield). Another reported cross-coupling is described by Haino *et al.*[2] They synthesized a *upper rim* substituted dibromocalix[5]arene which was substituted with two benzene units *via* a Suzuki type coupling reaction using $Pd(PPh_3)_4$ as catalyst in 69 % yield.
With these two reported cross-coupling reactions, we find that it was necessary to investigate the cross-coupling reaction in more detail, because new calix[4]arene derivatives could be synthesized and that these new compounds could have interesting properties in the field of supramolecular chemistry *i.e.* host-guest systems and artificial receptor systems.
We have synthesized several new phenylsubstituted calix[4]arenes *via* the methods developed by Suzuki (figure 1) and Negishi (figure 2) in good yields and in gram-scale. It is known that biphenyl systems are highly fluorescent. This property is very useful, because with the right substitution on the aromatic ring it will be possible to monitor a complexation between the sensor and analyt molecule.

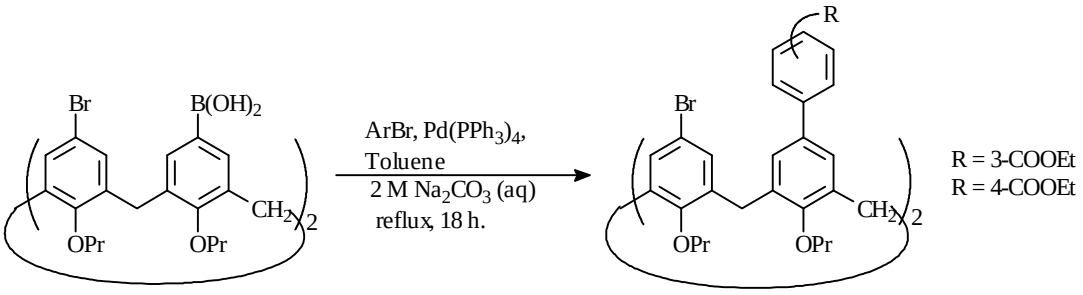

Fig. 1.

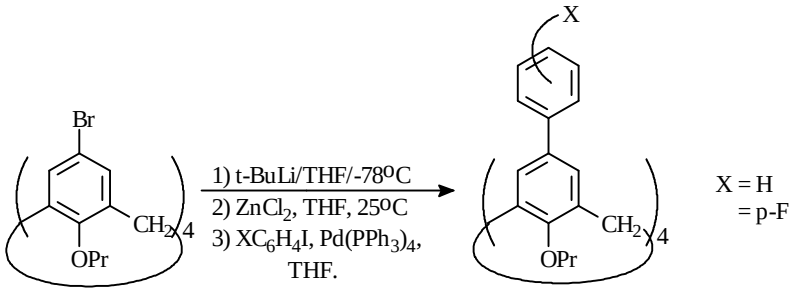

Fig. 2.

[1] A. Arduini, A. Pochini, A. Rizzi, A. Sicuri, R. Ungaro, *Tetrahedron Letters*, **31**, 4653, (1990)
[2] T. Haino, T. Harano, K. Matsumura, Y. Fukazawa, *Tetrahedron Letters*, **36**, 5793, (1995)

2.9.7 Van der Waals Interactions between Pyrene Substituted Calix[4]arene and Naphthalene

M. Larsen and M. Jørgensen, *Department of Solid State Physics, Materials Chemistry, Risø National Laboratory, Denmark*

Large molecules with an internal cavity capable of including guest molecules are of great interest to workers in supramolecular chemistry. The interest in calix[4]arene chemistry is rapidly increasing because its derivatives can form inclusion complexes with cations or small neutral organic molecules. Much work has been done in the development of cation sensors based on functionalized calix[4]arene. Sensors capable of binding small organic molecules especially saccharides has recently gained much attention. The interaction between the sensor molecule and the analyt in these saccharide sensors are covalent bonding. The calix[4]arene is functionalized with boronic acids and it is well known that cis-1,2 and cis-1,3-glycols reacts with boronic acids to give the corresponding cyclic esters.

Here we wish to report a system where the interactions are purely van der Waals interactions. We have functionalized the calix[4]arene with two pyrene units (figure 1). Pyrene is widely used as a chromophore in many systems. The special photophysical property of pyrene is that it shows excimer fluorescence at high concentrations and monomer fluorescence at low contrations. The reason why we have chosen pyrene is that it serves both as a ligand and as a chromophore.

We have shown that a possible ground state complex as shown in figure 1 exists in ethanol but not in 1,2-dichloroethane at room temperature. When naphthalene is added to the sensor in 1,2-dichloro-ethane, no fluorescence quenching is observed. In ethanol there is a remarkable quenching. The reason why there is no quenching in 1,2-dichloroethane is probably due to the polarity of the solvent. Ethanol which is a polar solvent favors the complexation, because the cavity between the two pyrenes is very lipophilic and naphthalene are less solvated in ethanol than between the pyrenes.

The quenching can not be dynamic because the singlet energy of naphthalene is higher than the singlet energy of pyrene. Therefor the quenching is static which means that a ground-state complex exists.

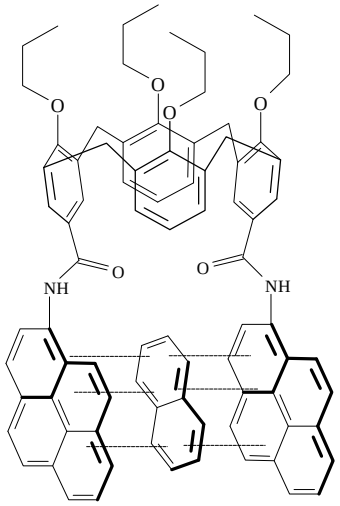

Fig. 1.

2.9.8 NMR Investigation of Solvent Dependant Conformational Change in Calix[4]arene Based Systems

M. Jørgensen, M. Larsen, P. Sommer-Larsen, *Department of Solid State Physics, Risø National Laboratory, Denmark* and H. Eggert, *University of Copenhagen, Denmark*

Calix[4]arenes are used as building blocks in an ongoing project to make supramolecular sensors for small molecules. They are easily constructed bowl shaped molecules with four phenolic residues arranged in a ring. During synthesis of a dimeric calix[4]arene sensor compound **1** was prepared.[1] Two flat 4-nitrophenylamine residues are connected on opposite sides of the calixarene via amide groups. Characterization of compound **1** by ^{1}H-NMR in two different solvents: deutero-chloroform ($CDCl_3$) and deutero-dimethyl sulfoxide (DMSO-d_6) showed remarkable differences in chemical shift values. Fig. 1 shows the low field part of the ^{1}H-NMR spectra of **1** in DMSO-d_6 and $CDCl_3$. Forcefield calculations (BIOSYM software) indicated that two conformers can exist with the two 4-nitrophenylamine groups either flattened outward or periplanar with each other. The solvent dependant ^{1}H-NMR data can then be explained if one conformer is predominant in DMSO-d_6 and the other in $CDCl_3$ as shown in Fig. 1. Two-dimensional Nuclear Overhauser NMR spectra of compound **1** in the two solvents where used to measure the relative distances between selected pairs of different protons confirming the structural assignment of the two conformers.
The presence of two conformers has dramatic influence when compound **1** is used as a sensor for flat aromatic type molecules. Only the periplanar structure found in $CDCl_3$ is able to bind molecules like anthracene or pyrene.

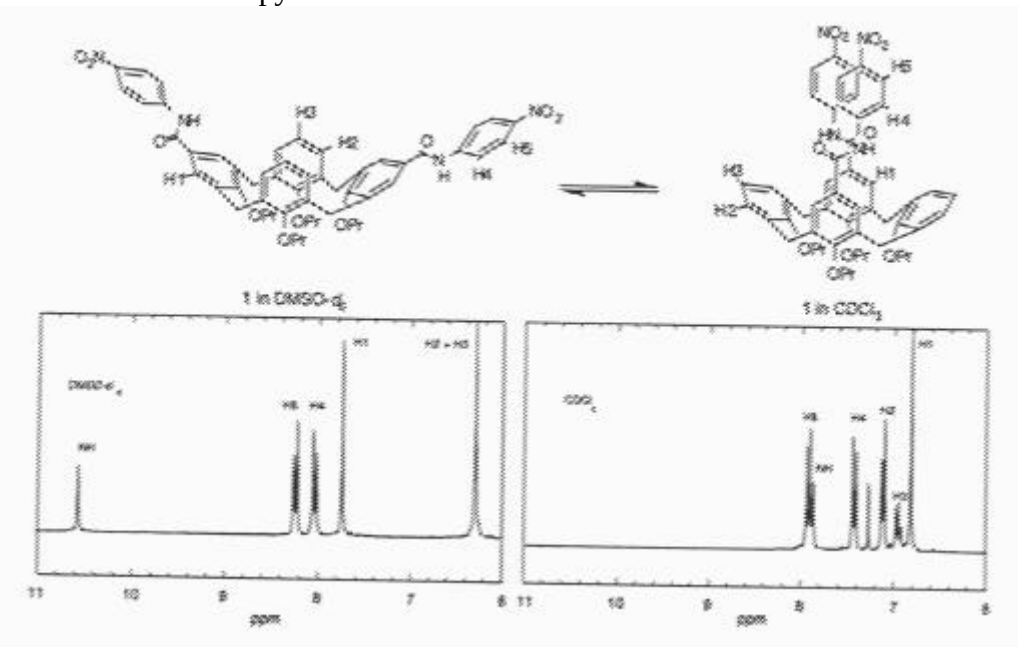

Fig.1. ^{1}H-NMR spectra and conformations of calixarene **1** in DMSO-d_6 and $CDCl_3$.

[1] Annual Progress Report of the Department of Solid State Physics 1995, 132

2.10 Instrumentation

2.10.1 Flux Measurements on RITA

K.N. Clausen, D.F. McMorrow and K. Lefmann, *Department of Solid State Physics, Risø National Laboratory, Denmark*, G. Aeppli, *NEC, USA*

The construction phase of the RITA spectrometer was completed in the early part of the summer, at which time the commissioning phase began. The main task during this period has been to characterise the key components of the system, including the performance of the new monochromator assembly. In order to increase the flux delivered to the PG(002) monochromator a short section (c. 1.5 m) of supermirror (m=3.3) guide has been placed between the cold source and the monochromator. (For more details of the construction of RITA see Mason *et al.*)[1] For the flux measurements, further sections of supermirror guide were used between the monochromator and the sample position. In this configuration the flux at the sample position was measured using a standard gold-foil technique.[2] After making the usual corrections (including one for the $\lambda/2$ component in the beam) the flux was found to be 2.8×10^7 n/s/cm^2 at 5 meV and 3.5×10^7 n/s/cm^2 at 14 meV. The horizontal divergence of the beam before the monochromator at these two energies is calculated to be approximately 100' and 55' respectively. The flux gain relative to the old TAS6 instrument is shown in Fig. 1, where is can be seen that the for most wavelengths of interest the gain factor is between 1.5 and 5. It can also be seen that the measured gain factor is in excellent agreement with the results of ray-tracing calculations[1].

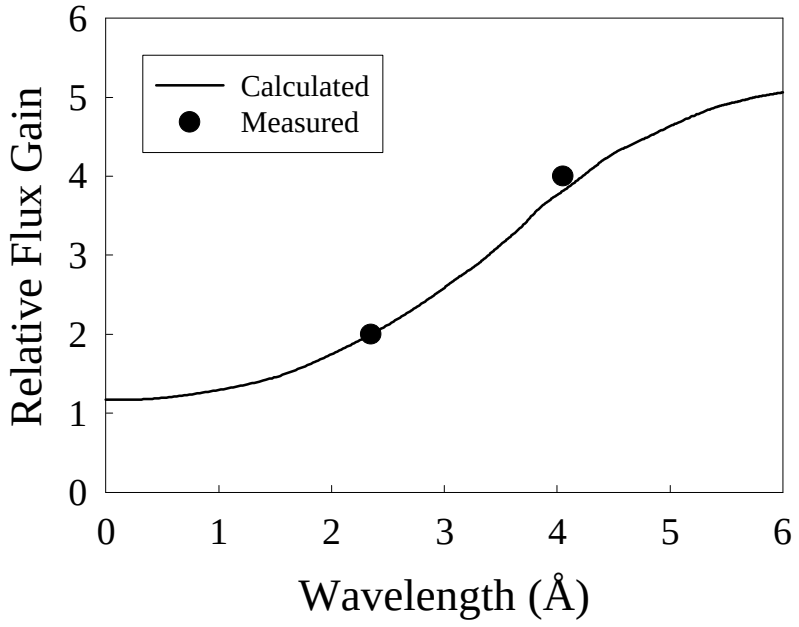

Fig.1. The gain in incident flux on RITA relative to the old TAS6 as a function of wavelength. Key: solid line, calculated gain; closed circles, measured.

[1] T.E. Mason *et al.*, Can. J. Phys. **73**, 697(1995)
[2] J. Als-Nielsen, Nuc. Inst. Meth. **50**, 191(1967)

2.10.2 The Facility for Deformation of Germanium Wafers to be used as Monochromators

B. Lebech, K. Theodor, B. Breiting, J. Lebech, S.Aa. Sørensen, K.N. Clausen, *Department of Solid State Physics, Risø National Laboratory, Denmark* and P.G. Kealey, *School of Physics and Space Research, University of Birmingham, UK*

Inspired by the deformed germanium composite wafer monochromator developed and produced by Axe et al.[1] at Brookhaven National Laboratory some years ago, we have developed and installed a facility for deformation of single crystal germanium wafers using the same principle. The facility consists of a commercial tube furnace with a maximum operating temperature of 1200°C. The furnace can radiate heat to the tools used for deformation or flattening of the wafers. These tools, for either deformation or flattening, are exchangeable and mounted inside a glass vacuum enclosure which fits into the furnace. The facility requires minimal attention. It is semi-automatic and all movements are done by a robot controlled by a PLC-control system which also controls the temperature. The production of deformed wafers started in the beginning of February 1996 and by the end of September 1996 about 150 wafer were deformed and quality controlled by measuring the rocking curves of the (511) reflection in a perfectly focused diffraction set-up using incident neutrons from the (333) reflection from a perfect Ge monochromator. Figure 1 shows a summary of the test data for the first twenty wafers deformed using the facility. The filled points in (a) show the full width at half maximum (FWHM) for the wafer stack and the unfilled points the FWHM for the individual wafers. The filled points in (b) show the peak area for a stack of wafers, while the solid curves show the corresponding data obtained by summation of the peak areas of the individual wafers. In (c) is shown the development of the peak as the wafer stack builds up.

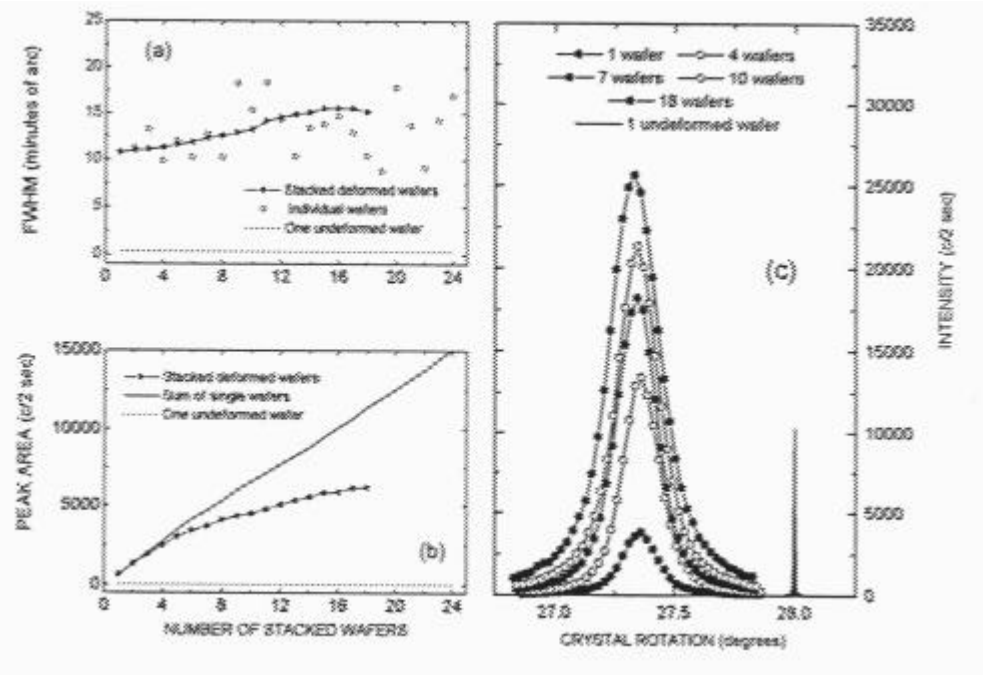

Fig. 1. Summary of the results of the tests of the first twenty wafers deformed at Risø.

[1] J. D. Axe, S. Cheung, D.E. Cox, L. Passell, T. Vogt and S. Bar-Ziv, J. Neutron Research **2,** 85 (1994)

2.10.3 Polarised Neutrons at the Neutron Reflectometer, TAS8

M.C. Gerstenberg, S.Aa. Sørensen, K.N. Clausen, *Department of Solid State Physics, Risø National Laboratory, Denmark,* P. Høghøj, *Institute Laue-Langevin, France*

Full polarisation analysis has been implemented at the neutron reflectometer, TAS8, for neutrons of wavelength 4.75 Å, in a collaboration between the Instrumentation Group at ILL and Risø. The two polarizers on the incident and scattered beam are each made up of two supermirrors,[1] which consist of 108 bilayers of Fe-Si on a glass substrate with a period ranging from 95 Å to 105 Å (m=3). The supermirrors are arranged in a double reflection geometry, i.e. the neutrons, which are reflected by the first mirror, reflect from the second mirror before exiting the device. A thin sheet of cadmium absorb the transmitted beam to avoid contamination. In effect the doubly reflected neutrons are displaced parallel to the incident beam by approximately 4.6 mm. The devices are placed in between two collimating slits up- and downstream of the sample, respectively. With different apertures of the slits the flipping ratio, i.e. the ratio of the intensity of the two neutron spins, was found to be consistently above 30 independent of whether the up- or downstream Mezei flipper was used. Consequently, each device has a flipping ratio above 60. The Mezei flippers were inserted in the guide field, which was placed along the whole neutron path. The maximum width of the beam measured was 2.4 mm. The polarising device had a reflectivity of one spin direction of approximately 83 %. As an advantage the device posed no difficulties in alignment and can be inserted with ease.

To test the device we measured several samples. Fig.1 shows reflectivity of the triblock copolymer P85[2] at 20 wt % in aqueous solution (D_2O) on single crystalline quartz in an applied guide field of 20 Gauss. The neutrons enter the side of the 100 x 10 x 50 mm^3 quartz crystal, traverse through the crystal, and reflect off the solid-liquid interface. The neutrons are only attenuated by 20 % in traversing 100 mm of quartz. The aim of the polarised measurements is to quantify and remove the incoherent signal from hydrogen. The analysis of the data is still in progress.

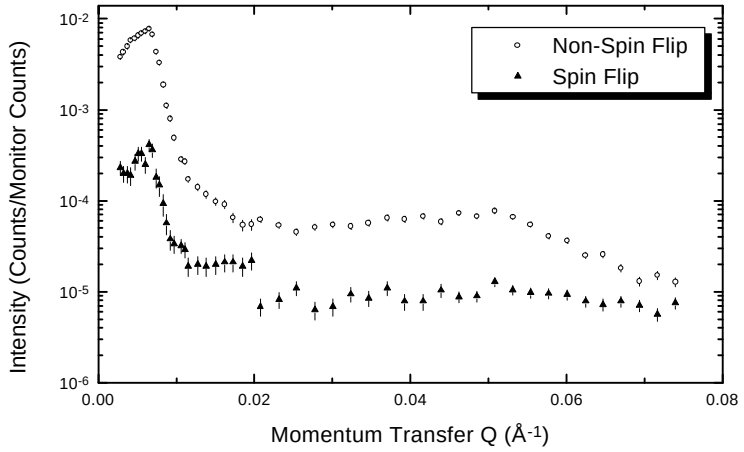

Fig. 1. The raw data from reflectivity measurements of the four different cross sections of the triblock copolymer P85 at 20 wt % at a temperature of 40 ^oC on single crystalline quartz. Only two curves are shown since the two scans of the non-spin flip and the spin flip, respectively, give similar results

[1] Manufactured and supplied by ILL, Grenoble, France
[2] See contribution 2.7.10 this report

2.11 Training and Mobility of Researchers - Access to Large Installations

K.N. Clausen, *Department of Solid State Physics, Risø National Laboratory, Denmark*

The CEC Large Installation Programme was initiated in order to make large national facilities available to users from the whole EU, to promote European collaboration and to make more facilities available to the less favoured regions in the EU. The cold neutron facilites at DR3 has been included in this programme since early 1992. The present TMR programme expires early 1999 and is a joint programme between Risø and NFL Studsvik in Sweden. This programme offers access to the neutron scattering facilities at DR3 Risø in Denmark and at NFL Studsvik in Sweden for scientists from all countries in the European Union and the associated States (Iceland, Israel, Liechtenstein and Norway). Deadlines for proposals are **April 1, August 1 and December 1** for beam-time during the periods June to September, October to January and February to May, respectively. News about the programme, information about the facilites and deadline for proposals can be found on WWW pages: http//www.risoe.dk/fys/lip.html and http://www.studsvik.uu.se.

Proposals for experiments at Risø and Studsvik are refereed by a group of six international experts, chaired by Prof. Jens Als-Nielsen, the University of Copenhagen. The TMR programme covers marginal expenses in connection with the neutron scattering experiments. These costs are (1) Travel and subsistence for the users, (2) salaries to staff employed to run the user programme, (3) consumables and other running costs in connection with the experiments.

During 1996 a new triple-axis spectrometer RITA (see contribution 2.10.1) and a new monochromator shielding and sample table for TAS3 were installed and commissioned, with major improvements for both spectrometers.

During 1996 a total of ~65 instrument weeks were used by 64 scientists from 7 different European countries. In total ~52 experiments were performed, and ~80 visits were supported by the programme.

The experiments carried out at Risø with support from the Commission of the European Communities during 1996 are listed below. The column marked applicant is the name of the principal applicant.

Applicant	Title
J.B. Booth	Incommensurate transition metal B_2O alloys
A.T. Boothroyd	Magnetic ordering of $PrBa_2Cu_3O_{6+x}$ under high pressure
A.T. Boothroyd	Magnetic ordering in $NdBa_2Cu_3O_{6+x}$
G. Caglioti	Reference System for Stress/Strain Evaluation
S. Coad	Magnetic behaviour of Quantum Spin-chain Paramagnets
R.A. Cowley	Magnetic Structure of Rare Earth Multilayers
R.A. Cowley	Magnetic Structure of Cs_2CuC_{l4} in zero applied fields
R.A. Cowley	Magnetic excitations pf MnW0
M.E. Fitzpatrick	Determination of the Components of Microstress Fields in Metal Matrix Composites by Stress Separation
J.P. Goff	Magnetic structure and interactions in light rare-earth superlattices
I.W. Hamley	Micellar structure in diblock copolymer solutions: A SANS study
I.W. Hamley	A SANS study of shear-induced order in complex phases formed by amphiphilic block copolymers
M.J. Harris	Soft-mode behaviour and lattice melting in Na_2CO_2
M.J. Harris	Diffuse magnetic scattering from geometrically-frustrated pyrochlores
A.R. Hillman	Microstructure of electropolymerized polypyrrole films
G.H. Jerke	Flexibility of polymers-like micelles
P. Klimanek	Investigation of isothermal grain growth in textured aluminium - correlation between texture and grain size
A. Lake	Magnetic excitations in K_2FeF_5
R.L. McGreevy	Structure/dynamics relations in polymer electrolytes
Don McK Paul	Neutron scattering study of $CuGeO_3$ in high magnetic fields
P. Müller	Spin structure determination of Na_6MnSe_4 and structure determination of new ternary hybrides
V.M. Nield	The structure of the plastic phase af ADAMANTANE by combined Bragg and diffuse scattering
J. A. Paixão	Investigation of the (H,T) magnetic phase diagram of $DyFe_4Al_8$
A. Pavese	Low Temperature single crystal neutron diffraction on partially disordered anorthite ($CaAl_2Si_2O_8$)
U. Pietsch	Neutron reflectivity of partially deuterated organic multilayers
H. Reynaers	Ordering phenomena in physical gels and stabilized polymer dispersions as observed by SANS
S. Roefs	Protein interactions: aggregation of beta-lactoglobulin and alpha-lactalbumin
S.J. Roser	Neutron Reflection from Biosensors
S.J. Roser	Neutron Reflection from Lithographic Films
J. Samseth	The effect of branched alcohols on micelle formation studied by SANS
J. Samseth	Phase and property studies of thermoplastic elastomer gels by SANS
O. Stockert	Magnetic phases of the heavy-fermion alloy $CeCu_5Ag$
D. Svergun	Contrast variation study of the 30S/70S ribosome E. Coli
R. Taylor	Measurement of internal stresses in thick plasma sprayed thermal barrier coatings
A.R. Wildes	Magnetic Bragg Rods in $MnPS_3$
E. Woldt	Correlation of texture changes and release of stored energy during the recrystallization of deformed copper
T. Zeiske	Phonon anomalies in copper due to a strong magnetic field

3 Publications, Educational and Organizational Activities, Colloqia

3.1 Publications in International Refereed Periodicals

Almdal, K., Mortensen, K, Ryan, A.J., Bates, F.S., Order, Disorder and Composition Fluctuation Effects in Low Molar Mass Hydrocarbon-Poly(dimethylsiloxane) Diblock Copolymers. Macromolecules, **29**, 5940-5947 (1996).

Almdal, K., Mortensen, K., Koppi, K.A., Tirrell, M., Bates, F.S., Isotropic and Anisotropic Composition Fluctuations Close to the Order-to-Disorder Transition in an Asymmetric Diblock Copolymer Melt Subjected to Reciprocating Shear Fields. J. Phys. II, **6**, 617-637 (1996).

Baker, J., Lindgård, P.-A., Monte Carlo determination of heteroepitaxial misfit structures. Phys. Rev. B54, R11137 (1996).

Barquin, L.F., Sal, J.C.G., Kaul, S.N., Barandiaran, J.M., Gorria, P., Pedersen, J.S., Heenan, R., Small-angle neutron scattering behavior of $Fe_{91}Zr_9$ glass under magnetic field. J. Appl. Phys., **79**, 5146-5148 (1996).

Bartels, V.T., Stamm, M., Mortensen, K., Change of phase behaviour of diblock copolymers upon application of pressure. Polym. Bull., **36**, 103-110 (1996).

Berg, R.H., Hvilsted, S., Ramanujam, P.S., Peptide oligomers for holographic data storage. Nature, **383**, 505-508 (1996).

Bergström, M., Thermodynamics of vesicle formation from a mixture of anionic and cationic surfactants. Langmuir, **12**, 2454-2463 (1996).

Bergström, M., Derivation of size distributions of surfactant micelles taking into account shape, composition, and chain packing density fluctuations. J. Colloid Interface Sci., **181**, 208-219 (1996).

Bouwman, W.G., Pedersen, J.S., Resolution function for two-axis specular neutron reflectivity. Journal of Applied Crystallography, **28**, 152-158 (1996).

Brecht, E., Schmahl, W.W., Miehe, G., Rodewald, M., Fuess, H., Andersen, N.H., Hanssmann, J., Wolf, T., Thermal treatment of $YBa_2Cu_{3-x}AL_xO_{6+d}$ single crystals in different atmospheres and neutron-diffraction study of excess oxygen pinned by the Al substituents. Physica C, **265**, 53-66 (1996).

Brezesinski, G., Meijere, K. de, Scalas, E., Bouwman, W.G., Kjær, K., Möhwald, H., Head-group variations and monolayer structures of diol derivatives. Progr. Colloid Polym. Sci., **100**, 351-355 (1996).

Casalta, H., Schleger, P., Harris, P., B. Lebech, B., Andersen, N.H., Ruixing Liang, Dosanjh, P. and Hardy, W. N., Neutron-scattering determination of the structural parameters versus oxygen content of $YBa_2Cu_3O_{6+x}$ single crystals. Physica C, **258**, 321-330 (1996).

Chang, L.J., Tomy, C.V., Paul, D.M.K., Andersen, N.H., Yethiraj, M., Magnetic order in HoNiBC and ErNiBC. J. Phys. Condens. Matter, **8**, 2119-2125 (1996).

Chang, L.J., Tomy, C.V., Paul, D.M.K., Andersen, N.H., Yethiraj, M., Neutron diffraction studies of $Ho_{1-x}Y_xNi_2B_2C$ compounds. Physica B, **223&224**, 119-122 (1996).

Christensen, A.N.; Andersen, N.H.; Emelchenko, G.A.; Maljuk, A.N., Superconducting cuprates and related oxides. 8. Composition and structure of the single crystals $La_{1.89}Sr_{0.11}CuO_4$ and $Nd_{1.81}Ce_{0.19}CuO_4$. Acta Chem. Scand. **50**, 1062-1063 (1996)

Christensen, J.B.; Schiodt, N.C.; Bechgaard, K.; Buch-Rasmussen,T., Preparation and properties of N,N,N',N'-tetrasubstituted 1,4-benzenediamines. Acta Chem. Scand. **50**, 1013-1019(1996)

Clausen, K. N., Lebech, B., McMorrow, D. F., Sørensen, S. Aa., Aeppli, G. and Mason, T. E., The Rita spectrometer at Risø. Neutron News, **7 (4),** 21-24 (1996).

Coad, S., Lussier, J.G., McMorrow, D.F., Paul, D.M., Neutron scattering and susceptibility measurements on single crystal of $Cu_{1-x}(Zn/Ni)_xGeO_3$. J. Phys. Condens. Matter, **8**, 6251-6266 (1996).

Coldea, R.; Tennant, D.A.; Cowley, R.A.; McMorrow, D.F.; Dorner, B.; Tylczynski, Z., Neutron scattering study of the magnetic structure of Cs_2CuCl_4. J. Phys. Condens. Matter. **8,** 7473-7491 (1996)

Dender, D.C., Davidovic, D., Reich, D.H., Broholm, C., Lefmann, K., Aeppli, G., Magnetic properties of a quasi-one-dimensional S=1/2 antiferromagnet: Copper benzoate. Phys. Rev. B, **53**, 2583-2589 (1996).

Deussen, H.J., Frederiksen, P., Bjørnholm, T., Bechgaard, K., A facile large scale preparation of racemic 2,2'-dihydroxy-1,1'-binaphthyl. Org. Prep. Proced. Int., **28** (no.4), 484-486 (1996).

Deussen, H.J., Hendrickx, E., Boutton, C., Krog, D., Clays, K., Bechgaard, K., Persoons, A., Bjørnholm, T., Novel chiral bis-dipolar 6,6'-disubstituted binaphthol derivatives for second-order nonlinear optics. Synthesis and linear and nonlinear optical properties. J. Am. Chem. Soc., **118**, 6841-6852 (1996).

Deussen, H.J., Shibaev, P.V., Vinokur, R., Bjørnholm, T., Schaumburg, K., Bechgaard, K., Shibaev, V.P., New 6,6'-disubstituted-binaphthol derivatives as chiral dopants: Synthesis and temperature dependence of molecular conformations. Liq. Cryst., **21**, 327-340 (1996).

Dobrzynski, L., Satula, D., Fjellvåg, H., Hauback, B. C., Baran, A., Suski, W., Wochowski, K., and Lebech, B., On the magnetic properties of $UFe_{4-x}Cu_xAl_8$ alloys. J. Alloys and Compounds, **236**, 121-131 (1996).

Egelhaaf, S.U., Pedersen, J.S., Schurtenberger, P., Shape transformations in biological mixed surfactant systems: From spheres to cylinders to vesicles. Progress in Colloid and Polymer Science, **98**, 224-227 (1995).

Eskildsen, M. R., and Smith, H., Surface acoustic waves and the magnetoconductivity of a two-dimensional electron gas. J. Phys.: Condens. Matter, **8**, 6597-6605 (1996).

Falcao, A.N., Pedersen, J.S., Mortensen, K., Boue, F., Polydimethylsiloxane networks at equilibrium swelling: Extracted and nonextracted networks. Macromolecules, **29**, 809-818 (1996).

Fernandez-Barquin, L., Gomez-Sal, J., Kaul, S.N., Barandiaran, J.M., Gorria, P., Pedersen, J.S., Heenan, R., SANS behaviour of $Fe_{91}Zr_9$ glass under magnetic field. Journal of Applied Physics **79**, 5146-5148 (1996).

Fiig, T., Andersen, N.H., Lindgård, P.-A., Berlin, J., Mouritsen, O.G., Mean-field and Monte Carlo calculations of the three-dimensional structure factor for $YBa_2Cu_3O_{6+x}$. Phys. Rev. B, **54**, 556-571 (1996).

Frielinghaus, H., Schwahn, D., Mortensen, K., Almdal, K., Springer, T., Composition fluctuations and coil conformation in a poly(ethylene-propylene)-poly(ethylethylene) diblock copolymer as a function of temperature and pressure. Macromolecules, **29**, 3263-3271 (1996).

Gabriel, J.-C., Pedersen, J.S., Bechgaard, K., Larsen, N.B., Larsen, M., Schaumburg, K., Ordering of Disk-like 2,3,6,7,10,11-hexakis-(hexylthio)-triphenylene (HHTT), in solution and at a liquid-solid interface. Langmuir, **12**, 1690-1692 (1996).

Gehring, P.M., Vigliante, A., McMorrow, D.F., Gibbs, D., Majkrzak, C.F., Helgesen, G., Cowley, R.A., Ward, R.C.C., Wells, M.R., Observation of two length scales above T_N in a holmium thin film. Physica B, **221**, 398-404 (1996).

Gerstenberg. M.C., Pedersen, J.S., Clausen, K.N., Neutron reflectometry from solid-solid and solid-liquid interfaces at the TAS8 spectrometer at Risø. Neutron News, **7 (4),** 25-30 (1996).

Gidalevitz, D., Weissbuch, I., Bouwman, W.G., Kjær, K., Als-Nielsen, J., Leiserowitz, L., Self-aggregated two-dimensional crystal structure of the mixed monolayer of triacontanoic acid and nanocosylamine. Evidence in favor of an ordered arrangement of ionized head groups. Langmuir, **12**, 1011-1017 (1996).

Goff, J.P., Bryn Jacobsen, C., Cowley, R.A., McMorrow, D.F., Ward, R.C.C., Wells, M.R., The magnetic structure and interactions in Nd/Pr superlattices. J. Magn. Magn. Mater., **156**, 263-264 (1996).

Greedan, J.E., Raju, N.P., Maignan, A., Simon, C., Pedersen, J.S., Niraimathi, A.M., Gmelin, E., Subramanin, M.A., Frustrated Pyrochlores, Y_2Mn2O_7, $Ho_2Mn_2O_7$ and $Yb_2Mn_2O_7$: Bulk magnetism and magnetic microstructure. Phys. Rev. B **54**, 7189-7200 (1996).

Gregorkiewitz, M., Lebech, B., Mellini, M. and Viti, C., Hydrogen positions and thermal expansion in Lizardite-1T from Elba: a low-temperature study using Rietveld refinement of netron diffraction data. American Mineralogist, **81**, 1111-1116 (1996).

Hack, T., Abetz, V., Stamm, M., Schubert, D.W., Mortensen, K., Siol, W., Spinodal decomposition of a polystyrene/poly(cyclohexylacrylate-stat-bytyl methacrylate) blend. Colloid Polym. Sci., **274**, 350-355 (1996).

Hamley, I.W., Garnett, S., Luckhurst, G.R., Roskilly, S.J., Pedersen, J.S., Richardson, R.M., Seddon, J.M., Orientational ordering in the nematic phase of a thermotropic liquid crystal: A Small angle neutron scattering study. Journal of Chemical Physics, **104**, 10046-10054 (1996).

Hansen, S., Bauer, R., Pedersen, J.S., Mortensen, K., Lomholt, S., Quist, K., Structure of casein micelles studied by small-angle neutron scattering. European Biophysics Journal, **24**, 143-147 (1996).

Hill, J.P., McMorrow, D.F., X-ray resonant exchange scattering: Polarization dependence and correlation functions. Acta Cryst. A, **52**, 236-244 (1996).

Hillmyer, M.A., Bates, F.S., Almdal, K., Mortensen, K., Ryan, A.J., Fairclough, J.P.A., Complex Lyotropic-Like Phase Behavior in Solvent-Free Nonionic Surfactants. *Science.,* **271**, 976-978 (1996).

Holme, N.C.R., Ramanujam, P.S., Hvilsted, S., 10,000 optical write, read, and erase cycles in an azobenzene sidechain liquid-crystalline polyester. Opt. Lett., **21**, 902-904 (1996).

Holme, N.C.R., Ramanujam, P.S., Hvilsted, S., Photoinduced anisotropic measurements in liquid-crystalline azobenzene side-chain polyesters. Appl. Opt., **35**, 4622-4627 (1996).

Jiang, Q.D., Smilgies, D.M., Feidenhans'l, R., Cardona, M., Zegenhagen, J., Surface morphology and in-plane-epitaxy of $SmBa_2Cu_3O_{7-d}$ films on $SrTiO_3$ (001) substrates studied by STM and grazing incidence x-ray diffraction. Solid State Commun., **98**, 157-161 (1996).

Jørgensen, O., Egsgaard, H., Larsen, E., Synthesis of deuterated clenbuterol. J. Labelled Comp. Radiopharm., **38**, 1007-1014 (1996).

Kakihana, M., Osada, M., Käll, M., Börjesson, L., Mazaki, H., Yasuoka, H., Yashima, M., Yoshimura, M., Raman-active phonons in $Bi_2Sr_2Ca_{1-x}Y_xCu_2O_{8+\delta}$ (x=0-1): Effects of hole filling and internal pressure induced by Y doping for Ca, and implications for phonon assignments. Phys. Rev. B, **53**, 11796-11806 (1996).

Kazimirov, A., Zegenhagen, J., Denk, I., Maier, J., Smilgies, D.-M., Feidenhans'l, R., X-ray characterization of a $SrTiO_3$ bicrystal interface. Surf. Sci., **352/354**, 875-878 (1996).

Kenn, R.M., Kjær, K., Möhwald, H., Non-rotator phases in phospholipid monolayers?. Colloids Surf. A, **117**, 171-181 (1996).

Khandpur, A.K., Förster, S., Bates, F.S., Hamley, I.W., Ryan, A.J., Bras, W., Almdal, K., Mortensen, K., The polyisoprene-polystyrene copolymer phase diagram near the order-disorder transition. Macromolecules, **28,** 8796-8806 (1995).

Larsen, J., Bechgaard, K., Direct oxidative cyclization of 1,2-bis(benzothiophene-2-yl)ethylenes as replacement of photocyclization in the syntheses of thiaheterohelicenes. J. Org. Chem., **61**, 1151-1152 (1996).

Larsen, J., Bechgaard, K., Thiaheterohelicenes 1. Synthesis of unsubstituted thia[5]-, [9]- and [13]heterohelicenes. Acta Chem. Scand., **50**, 71-76 (1996).

Larsen, J., Bechgaard, K., Thiaheterohelicenes 2. Synthesis of alkylated thiaheterohelicenes. Acta Chem. Scand., **50**, 77-82 (1996).

Larsen, J., Dolbecq, A., Bechgaard, K., Thiaheterohelicenes 3. Donor properties of a series of benzene-capped thiaheterohelicenes. Structure of a tetrathianonahelicene and its TCNQ salt. Acta Chem. Scand., **50**, 83-89 (1996).

Larsen, M., Jørgensen, M., Selective halogen-lithium exchange reaction of bromine-substituted 25,26,27,28-tetrapropoxycalix[4]arene. J. Org. Chem., **61**, 6651-6655 (1996).

Lefmann K., Rischel, C., Dynamical Correlation functions of the Nearest-Neighbor and Haldane-Shastry Heisenberg Antiferromagnetic S=1/2 chains in zero and applied fields. Phys. Rev. B, **54**, 6340-50 (1996).

Lefmann, K.,Tuoriniemi, J. T., Nummila, K. K., Vuorinen, R.T., and Metz, A., Neutron thermometry of highly polarized silver nuclei. Czech. J. Phys., **46 S5**, 2861-62 (1996).

Lemmich, J., Mortensen, K., Ipsen, J.H., Honger, T., Bauer, R., Mouritsen, O.G., Small-angle neutron scattering from multilamellar lipid bilayers: Theory, model, and experiment. Phys. Rev. E, **53**, 5169-5180 (1996).

*Lemmich, J., Mortensen, K., Ipsen, J.H., Honger, T., Bauer, R., Mouritsen, O.G.,*Solutes in small amounts provide for lipid-bilayer softness: cholesterol, short-chain lipids, and bola lipids. Eur. Biophys. J. (Biophys. Lett.) **25**, 61-65 (1996).

Lemmich, J., Mortensen, K., Ipsen, J.H., Hønger, T., Bauer, R., Mouritsen, O.G., Small-angle neutron scattering studies of lipid bilayer structure, softness, and the effect of cholesterol. Biophys J., **70**, A112 (1996).

Lindgård, P.-A., Bohr, H., Magic numbers in protein structures. Phys. Rev. Lett., **77**, 779-782 (1996).

Lodge, T.P., Xu., X., Ryu, C.Y., Hamley, I.W., Fairclough, J.P.A., Ryan, A.J., Pedersen, J.S., Structure and dynamics of concentrated solutions of asymmetric copolymers in slightly selective solvents. Macromolecules, **29**, 5955-5964 (1996).

Loewenhaupt, M Reif, T., Svoboda, P., Sieck, M., Wagner, S., Löheysen, G.E., Rotter, M., Lebech, B., Hauss, T. The magnetic phases of $NdCu_2$. Z. Phyzik B 101, 499-510 (1996).

Longmore, A., Boothroyd, A.T., Chen, C.K., Hu, Y.L., Nutley, M.P., Andersen, N.H., Casalta, H., Schleger, P., Christensen, A.N., Magnetic ordering in $PrBa_2Cu_{3-y}Al_yO_{6+x}$. Phys. Rev. B, **53**, 9382-9395 (1996).

Lussier, J.G., Coad, S.M., McMorrow, D.F., Paul, D.M., The temperature dependence of the spin-Peierls energy gab in $CuGeO_3$. J. Phys. Condens. Matter, **8**, L59-L64 (1996).

Malik, A., Schönfeld, B., Kostorz, G., Pedersen, J.S., Microstructure of Guinier-Preston zones in Al-Ag. Acta mater., **44 (12),** 4845-4852 (1996).

Mason, T.E., Clausen, K.N., Aeppli, G., McMorrow, D.F., Kjems, J.K., RITA: The reinvented triple axis spectrometer. Can. J. Phys., **73**, 697-702 (1995).

Mason, T.E., Schroder, A., Aeppli, G., Mook, H.A., Hayden, S.M., New magnetic coherence effect in superconducting $La_{2-x}Sr_xCuO_4$. Phys. Rev. Lett., **77**, 1604-1607 (1996).

McMorrow, D.F., Artificial magnetic superlattices, Neutron News, **7 (4)**, 16-20 (1996).

McMorrow, D.F., Swaddling, P.P., Cowley, R.A., Ward, R.C.C., Wells, M.R., The chemical structure of rare earth superlattices: A high-resolution x-ray scattering study. J. Phys. Condens. Matter, **8**, 6553-6567 (1996).

Montfrooij, W., McGreevy, R.L., Hadfield, R., Andersen, N.H., Reverse Monte Carlo analysis of powder patterns. J. Appl. Crystallogr., **29**, 285-290 (1996).

Mortensen, K., Structural studies of aqueous solutions of PEO-PPO-PEO triblock copolymers, their micellar aggregates and mesophases, A small-angle neutron scattering study. J. Phys. Condens. Matter, **8**, A103-A124 (1996).

Mortensen, K., Talmon, Y., Cryo-TEM and SANS microstructure study of Pluronic polymer solution. Macromolecules, **28,** 8829-8834 (1995).

Mortensen, K., Small-angle neutron scattering studies of mesophases and networks of block copolymer micelles. Neutron News, **7,** 31-35 (1996).

Nielsen, M., Smilgies, D.-M., Feidenhans'l, R., Landemark, E., Falkenberg, G., Lottermoser, L., Seehofer, L., Johnson, R.L., Hut clusters on Ge(001) surfaces studied by STM and synchrotron X-ray diffraction. Surf. Sci., **352/354**, 430-434 (1996).

Nikolova, L., Todorov, T., Ivanov, M., Andruzzi, F., Hvilsted, S., Ramanujam, P.S., Polarization holographic gratings in side-chain azobenzene polyesters with linear and circular photoanisotropy. Appl. Opt., **35**, 3835-3840 (1996).

Nummila, K. K., Tuoriniemi, J. T., Vuorinen, R. T., Lounasmaa, O. V., Lefmann, K., Clausen, K. N., Metz, A., Siemensmeyer, K., Lipinsky, L., Steiner, M., and Rasmussen, F. B., Neutron Experiments on Nuclear order in Silver at pK Temperatures. Czech. J. Phys., **46 S4**, 2201-02 (1996).

Paolasini, L., Lander, G. H., Shapiro, S. M., Caciuffo, R., Lebech, B. , Regnault, L.-P., Roessli, B., and Fournier, J.-M., Enhanced exchange in the itinerant ferromagnet UFe_2. Europhys. Lett., **34**, 459-464 (1996).

Paolasini, L., Lander, G. H., Shapiro, S. M., Caciuffo, R., Lebech, B. , Regnault, L.-P., Roessli, B., and Fournier, J.-M., Magnetic excitations in the itinerant ferromagnet UFe_2. Phys. Rev. B, **54**, 7222-7232 (1996).

Papadakis, C.M., Brown, W., Johnsen, R.M., Posselt, D., Almdal, K., The dynamics of symmetric polystyrene-polybutadiene diblock copolymer melts studied above and below the order-disorder transition using dynamic light scattering. J. Chem. Phys., **104**, 1611-1625 (1996).

Papadakis, C.M., Almdal, K., Mortensen, K., Posselt, D., Identification of an intermediate segregation regime in a diblock copolymer system. Europhysics Letters, **36(4)**, 289-294 (1996).

Pedersen, J.S., Hansen, S., Bauer, R., Aggregation behavior of zinc-free insulin studied by small-angle neutron scattering: Analysis by use of a thermodynamic equilibrium model. Progress in Colloid and Polymer Science, **98**, 215-218 (1995).

Pedersen, J.S., Gerstenberg, M.C., Form factor of block copolymer micelles. Macromolecules, **29**, 1363-1365 (1996).

Pedersen, J.S., Schurtenberger, P., Cross-section structure of cylindrical and polymer-like micelles from small-angle scattering data: I. Test of analysis methods. Journal of Applied Crystallography, **29,** 646-661 (1996).

Pedersen, J.S., Laso. M., Schurtenberger P., A Monte Carlo study of excluded volume effects in worm-like micelles and semi-flexible polymers. Physical Review E. (Rapid Communication). **54**, 5917-5920 (1996).

Pedersen, J.S., Schurtenberger, P., Scattering functions of semi-flexible polymers with and without excluded volume effects. Macromolecules, **29**, 7602-7612 (1996).

Pedersen, J.S., Horsewell, A., Eldrup, M., A small-angle neutron scattering and transmission electron microscopy study of Krypton bubbles in copper. Journal of Physics: Condensed Matter, **8**, 8431-8455 (1996).

Peterson, I.R., Kenn, R.M., Goudot, A., Fontaine, P., Rondelez, F., Bouwman, W.G., Kjær, K., Chiral and herringbone symmetry breaking in water-surface monolayers. Phys. Rev. E, **53**, 667-673 (1996).

Popovitz-Biro, R., Edgar, R., Majewski, J., Cohen, S., Margulis, L., Kjær, K., Als-Nielsen, J., Leiserowitz, L., Lahav, M., Self-aggregation of alpha,omega-alkanediols into two and three dimensional crystallites at the air-water interface. Relevance to ice nucleation. Croatica Chem. Acta, **69** (no.2), 689-708 (1996).

Poulsen, H.F., Zimmermann, M. von, Schneider, J.R., Andersen, N.H., Schleger, P., Madsen, J., Hadfield, R., Casalta, H., Liang, R., Dosanjh, P., Hardy, W., Structural phase transitions in bulk $YBa_2Cu_3O_{6+x}$ with x=0.35 and x=0.36. Phys. Rev. B, **53**, 15335-15344 (1996).

Raju, N.P., Greedan, J.E., Pedersen, J.S., Simon, C., Maignan, A., Niraimathi, A.M., Gmelin, E., Subramanian, M.A., Magnetic ordering in pyrochlore $Ho_2Mn_2O_7$. Journal of Applied Physics, **79**, 6173-6175 (1996).

Ramanujam, P.S., Holme, N.C.R., Hvilsted, S., Atomic force and optical near-field microscopic investigations of polarization holographic gratings in a liquid crystalline azobenzene side-chain polyester. Appl. Phys. Lett., **68**, 1329-1331 (1996).

Ramanujam, P.S., Holme, C., Hvilsted, S., Pedersen, M., Andruzzi, F., Paci, M., Tassi, E.L., Magagnini, P., Hoffman, U., Zebger, I., Siesler, H.W., Side-chain liquid crystalline polyesters for optical information storage. Polym. Adv. Technol., **7**, 768-776 (1996).

Ramanujam, P.S., Hvilsted, S., Berg, R.H., New polymer materials for erasable holographic storage. Holography. SPIE Int. Techn. Working Group Newslett., **6** (no.2), 2-3 (1996).

Reynders, K., Mischenko, N., Mortensen, K., Overborgh, N., Reynaers, H., Stretching induced correlations in triblock copolymer gels as observed by small-angle neutron scattering. Macromolecules, **28,** 8699-8701 (1995).

Rial, C.; Moran, E.; Alario-Franco, M.A.; Amador, U.; Andersen, N.H., On the structural properties and superconductivity of room-temperature chemically oxidized $La_{2-x}Ba_xCuO_{4+y}$ (0<=x<=0.15). Physica C **270**, 51-67(1996)

Roser, S.J., Caruana, D.J., Gerstenberg, M., Neutron reflection studies of poly(phenol) films, J. Electroanal. Chem., **411**, 153-160 (1996).

Rump, P.J., Arts, A.F.M., Wijn, H.W. de, Nielsen, M., Dynamics of couples electron-phonon modes in $LiY_{1-x}Ho_xF_4$. Physica B, **219/220**, 760-762 (1996).

Scherrenberg, R., Moonen, J., Mortensen, K., Small-angle neutron scattering study on the transamidition of polyamide-4.6. J. Polym. Sci. B, **34**, 335-340 (1996).

Schiødt, N.C., Bjørnholm, T., Bechgaard, K., Neumeier, J.J., Allgeier, C., Jacobsen, C.S., Thorup, N., Structural, electrical, magnetic, and optical properties of bis-benzene-1,2-dithiolato-Au(IV) crystals. Phys. Rev. B, **53**, 1773-1778 (1996).

Schulz, M.F., Khandpur, A.K., Bates, F.S., Almdal, K., Mortensen, K., Hajduk, D.A., S.M. Gruner, Phase behavior of polystyrene-poly(2-vinylpyridine) diblock copolymers. *Macromolecules*, **29**, 2857-2867 (1996)

Schurtenberger, P., Jerke, G., Cavacao. C., Pedersen, J.S., Cross-section structure of cylindrical and polymer-like micelles from small-angle scattering data: II. Experimental results. Langmuir, **12**, 2433-2440 (1996).

Schwahn, D., Frielinghaus, H., Mortensen, K., Almdal, K., Temperature and Pressure Dependence of the Order Parameter Fluctuations, Conformational Compressibility, and the Phase Diagram of the PEP-PDMS Diblock Copolymer. Phys. Rev. Lett., **77**, 3153-3156 (1996).

Seto, H., Schwahn, D., Nagao, M., Yokoi, E., Komura, S., Imai, M., Mortensen, K., Crossover from mean field to three-dimensional ising critical behavior in a three-component microemulsion system. Phys. Rev. E, **54**, 629-633 (1996).

Shibaev, P.V., Deussen, H.J., Vinokur, R.A., Schaumburg, K., Bechgaard, K., Bjørnholm, T., Alexandrov, A.F., Cholesteric mesophases induced by novel binaphtol derivatives. Izv. Akad. Nauk Ser. Fiz., **60 (4),** 50-57 (1996).

Simpson, J.A., Cowley, R.A., McMorrow, D.F., Ward, R.C.C., Wells, M.R., Carlile, C.J., Adams, M.A., Persistence of helical magnetic order in dysprosium holmium superlattices. J. Phys. Condens. Matter, **8**, L187-L194 (1996).

Simpson, J.A., Cowley, R.A., Jehan, D.A., Ward, R.C.C., Wells, M.R., McMorrow, D.F., Clausen, K.N., Thurston, T.R., Gibbs, D., Co-existence of long- and short-range magnetic correlations in holmium-erbium superlattices. Z. Phys. B, **101**, 35-46 (1996).

Smilgies, D.-M., Feidenhans'l, R., Scherb, G., Kolb, D.M., Kazimirov, A., Zegenhagen, J., Formation of tilted clusters in the electrochemical deposition of copper on *n*-GaAs(001). Surface Science, 367, 40-44 (1996).

Steiner, M., Metz, A., Siemensmeyer, K., Lounasmaa, O.V., Tuoriniemi, J.T., Nummila, K.K., Vuorinen, R.T., Clausen, K.N., Lefmann, K., Rasmussen, F.B., Neutron diffraction determination of the nuclear spin ordering in Cu and Ag at nano- and subnano-K temperatures. J. Appl. Phys., **79**, 5078-5080 (1996).

Steinfort, A.J., Scholte, P.M.L.O., Ettema, A., Tuinstra, F., Nielsen, M., Landemark, E., Smilgies, D.-M., Feidenhans'l, R., Falkenberg, G., Seehofer, L., Johnson, R.L., Strain in nanoscale Germanium hut clusters on Si(001) studied by x-ray diffraction. Phys. Rev. Lett., **77**, 2009-2012 (1996).

Swaddling, P.P., Cowley, R.A., Ward, R.C.C., Wells, M.R., McMorrow, D.F., Magnetic structures of holmium-lutetium alloys and superlattices. Phys. Rev. B, **53**, 6488-6498 (1996).

Vigild, M.E., Findeisen, E., Feidenhans'l, R., Barholm-Hansen, C., Bentzon, M.D., Hansen, J.B., Mass density and hydrogen content diamondlike carbon as related to the preparation by plasma-enhanced chemical vapor deposition. J. Appl. Phys., **79**, 4050-4056 (1996).

Vives, E., Castan, T., Lindgård, P.-A., Degenerate Blume-Emery-Griffiths model for the martensitic transformation. Phys. Rev. B, **53**, 8915-8921 (1996).

Ward, R.C.C., Wells, M.R., Bryn Jacobsen, C., Cowley, R.A., Goff, J.P., McMorrow, D.F., Simpson, J.A., MBE growth and characterisation of light rare-earth superlattices. Thin Solid Films, **275**, 137-139 (1996).

Weinbach, S.P., Kjær, K., Bouwman, W., Als-Nielsen, J., Leiserowitz, L., Elucidation of multilayer growth of amphiphiles on liquid surfaces. J. Phys. Chem., **100**, 8356-8362 (1996).

Yao, W., Knuuttila, T., Martikainen, J. E., Nummila, K. K., Oja, A. S., Lounasmaa, O. V., and Lefmann, K., A new Ultralow Temperature Cryostat in Helsinki. Czech. J. Phys, **46 S5**, 2793-94 (1996).

Yaron, U., Gammel, P.L., Huse, D.A., Kleiman, R.N., Oglesby, C.S., Bucher, E., Batlogg, B., Bishop, D.J., Mortensen, K., Clausen, K.N., Structural evidence for a two-step process in the depinning of the superconducting flux-line lattice (addendum to vol. 376, p. 753-755). Nature, **381**, 253 (1996).

Yaron, U., Gammel, P. L., Ramirez, A. P., Huse, D. A., Bishop, D. J., Goldman, A. I., Stassis, C., Canfield, P. C., Mortensen, K., and Eskildsen, M. R., Microscopic coexistence of magnetism and superconductivity in $ErNi_2B_2C$. Nature, **382**, 236-238 (1996).

Zegenhagen, J., Kazimirov, A., Scherb, G., Kolb, D.M., Smilgies, D.-M., Feidenhans'l, R., X-ray diffraction study of a semiconductor/electrolyte interface: n-GaAs(001)/H_2SO_4(:Cu). Surf. Sci., **352/354**, 346-351 (1996).

Zhao, J., Majumdar, B., Schulz, M.F., Bates, F.S., Almdal, K., Mortensen, K., Hajduk, D.A., Gruner, S.M., Phase Behavior of PE-PEE: Pure Diblocks and Binary Diblock Mixtures. Macromolucules, **29**, 1204-1215 (1996).

Zinkin, M.P., McMorrow, D.F., Hill, J.P., Cowley, R.A., Lussier, J.G., Gibaud, A., Grubel, G., Sutter, C., Synchrotron x-ray-scattering study of the normal-incommensurate phase transition in Rb_2ZnCl_4. Phys. Rev. B, **54**, 3115-3124 (1996).

3.2 Other Publications

Articles for a Broader Readership, Thesis and Reports

Andersen, N.H., Doping effects in high-Tc Superconductors, Risø Report: Risø-R-931(EN), 52 pp.

Berg, R.H., Hvilsted, S., Ramanujam, P.S., Novel Physically Functional Materials. Patent WO 96/38410 (1996).

Bates, F.S., Rosedale, J.H., Schulz, M.F., Almdal, K., Miscible Polyolefin Blends with Modifying Polyolefin having Matching Segment Lengths. US Patent 5, 571, 864 (1996).

Charvolin, J., Colmenero, L., Cummins, P., Mortensen, K., Richter, D., Thomas, B., Weil, G., Polymers and soft matter. *in* 'Scientific prospects for neutron scattering with present and future sources, ESF framework studies into large research facilities'. Ed. Lander, G., Curien, H., 52-63, (1996).

Clausen, K. N., Lebech, B., Mcmorrow, D. F., Sørensen, S. Aa., Aeppli, G. and Mason, T. E., Instrument development at Risø - The Rita neutron spectrometer and the germanium monochromator facility. www:http://www.risoe.dk/fys/lip.html 16 pp. (1996).

Hvilsted, S., Ramanujam, P.S., Andruzzi, F., Optical storage medium. US Patent, **5**, 496,670 A (1996).

Jørgensen, O., Egsgaard, H., Larsen, E., Syntese af deuterium-mærkede forbindelser til FØTEK projektet. Dansk Kemi, **77**, (no.6/7), 12-14 (1996).

Jørgensen, M., Bechgaard, K., Clausen, K.N., Feidenhans'l, R., Johannsen, I., (eds.), Annual progress report of the Department of Solid State Physics 1 January - 31 December 1995. Risø-R-863(EN),173 p. (1996).

Kirkegaard, P., Eldrup, M., Horsewell, A., Pedersen, J.S., Correction of bubble size distributions from transmission electron microscopy observations, Risø Report: Risø-R-789(EN). 43 pp.

Krebs, F.C., Specialerapport 1994-1996. Part 1: Syntese, struktur og egenskaber af 4,8,12-trioxa-12c-phospha-4,8,12,12c-tetrahydrodibenzo[cd,mn]pyrene et molekylært pyroelektrisk materiale, Part 2: Konstruktion af kloge materialer baseret på funktionaliserede organiske molekyler: Imod en kontrol af struktur og egenskab. 272, (1996).

Lefmann, K., Nuclear magnetic ordering in silver. Risø-R-850(EN), 226, (ph.d. thesis) (1995).

Lindgård, P.A. and Bohr, H. How many protein fold classes are to be found ? in*:* Protein Folds A Distance-Based Approach, CRC Press p. 98 (1996).Ed. Bohr, H. and Brunak, S.

Rønnow, H.M., Magnetic Properties of Holmium-Erbium Alloys, Ms.C. Thesis, Univ. of Copenhagen (1996).

Sommer-Larsen, P., Ed., ARTMUS - Artificial Muscles. A feasibility study of polymer based materials for actuator purposes. Report for project period I. Risø (1996).

Sommer-Larsen, P., Ed., ARTMUS - Artificial Muscles. A feasibility study of polymer based materials for actuator purposes. Report for project period II. Risø (1996).

Sommer-Larsen, P., Elgård Pedersen, P., Ed., ARTMUS - Artificial Muscles. A feasibility study of polymer based materials for actuator purposes. Final Report. Risø (1996).

Sommer-Larsen, P., Molecular Electronics. Notes for Course in Molecular Materials Science. Risø (1996).

3.3 Conferences

Alexandridis, P., Svensson, B., Olsson, U., Lindman, B., Mortensen, K., Reverse (Water-in-Oil) Micelles of Amphiphilic Block Copolymers: A Small-Angle Neutron Scattering Investigation. *Center for Surface and Colloid Science, University of Lund, Lund, Sweden,*

Almdal, K., Block copolymer phase behaviour and interactions in polymer melts. Meeting on polymer science. The Danish Academy for the Technical Sciences, Copenhagen (DK), (May).

Almdal, K., Rheological characterization of highly filled dental restorative composit in the uncured state. In: Polymer surfaces and interfaces. Conference on polymer surfaces and interfaces, Copenhagen (DK) (Oct).

Almdal, K., Mortensen, K., Bates, F.S., Order, disorder and conformational asymmetry in low molar mass hydrocarbon-poly(dimethylsiloxana) diblock copolymers. 1996 APS March meeting. Session E29: Block copolymer, St. Louis, MO (US) (Mar).

Almdal, K., Mortensen, K., Hillmyer, M.A., Bates, F.S., Conformational asymmetry effects in hydrocarbon-polydimethylsiloxane diblock copolymers. In: EPF'96. Book of abstracts. 6. European Polymer Federation symposium on polymeric materials, Crete (GR) (Oct).

Andersen, N.H., Superconductors in magnetic fields. Lecture series on mesoscopic physics. University of Copenhagen, Copenhagen (DK).

Andersen, N.H., Uimin, G., Model for the low-temperature magnetic phases of $YBa_2Cu_3O_{6+x}$. Magnetism in metals. A conference dedicated to the memory of Allan Mackintosh, Copenhagen (DK) (Aug).

Achiwa, N., Harris, P., Lebech, B. and Kawano, S., Weak-ferromagnetism and magnetic symmetry in $C_nH_{2n+1}NH_3)_2MnCl_4$ (n = 1, 2 and 3), $Co(HCOO)_2 \cdot 2(NH_2)_2CO$ and $Co(HCOO)_2 \cdot 2H_2O$. Workshop on Applications of Symmety Analysis to Diffraction Investigations, Krakow, (PL) (Jul).

Arleth, L., Posselt, D. Gazeau, D., Zemb, T., Larpent, C., Mortensen, K., Pedersen, J.S., "Charaterization of Tetraaza-AC8 -Asurfactant with cation complexing potential", Bombannes '96: "Third European Summer School on "Scattering Methods Applied to Soft Condensed Matter", Carcans-Maubuisson (FR) (Jun).

Arleth, L., Pedersen, J.S., and Zemb, T., A Small-angle Scattering study of the Shape and Polydispersity of Microemulsion droplets. Annual meeting of the Danish Physical Society, Nyborg, (DK) (May).

Arleth, L., Mortensen; K., Pedersen, J.S., Posselt, D., Gazeau, D., Larpent, C., and Zemb, T., A Small-Angle Scattering study of TAC8 - A Surfactant with cation complexing potential. Annual meeting in the European Colloid and Interface Society, Turku, (FI) (Aug).

Arleth, L., Pedersen, J.S., Zemb, T., A small-angle scattering study of the shape and structural interactions of microemulsion droplets. Annual meeting of the Danish Physical Society, Nyborg (DK) (May).

Baker, J., Lindgård, P.-A., Structure of surface layers of KBr on NaCl studied by Monte Carlo simulation. Annual meeting of the Danish Physical Society, Nyborg (DK) (May).

Bentzon, M.D., Poulsen, H.F., Garbe, S., Frello, T., Andersen, N.H., Abrahamsen, A., Zimmermann, M. von, In-situ synchrotron X-ray diffraction on BiSCCO-tapes during annealing. 1996 Applied superconductivity conference, Pittsburg, PA (US) (Aug).

Berg, R. H., Peptides for optical storage. Symposium on the applications of microtechnology in biotechnology, The Technical University of Denmark, Lyngby (DK) (Apr).

Berg, R. H., Peptides for optical storage. Minisymposium on molecules for advanced materials and nanostructures, The Danish Chemical Society, The H. C. Ørsted Institute, Copenhagen (DK) (May).

Berg, R. H., Hvilsted, S., Ramanujam, P. S., Peptide oligomers for optical holographic storage of information. 24th European Peptide Symposium, Edinburgh (GB) (Sep).

Berg Madsen, N., Chemical modification of inorganic fillers. In: Polymer surfaces and interfaces. Conference on polymer surfaces and interfaces, Copenhagen (DK) (Oct).

Bergström, M., Derivation of size distributions of surfactant aggregates from a multiple equilibrium approach. IIIrd European summer school on scattering methods applied to soft condensed matter, Bombannes (FR) (Jun).

Bergström, M., Reversibly formed bilayer vesicles: energetics and polydispersity. X. conference of the European colloid and interface society, Turku (FI) (Sep).

Bohr, H., Lindgård, P.-A., A physical classification of protein folds. Conference on bioinformatics structure, Jerusalem (IL) (Nov).

Bolm. A., English, U., Penacorada, F., Gerstenberg, M.C., Pietsch, U., Temperature and Time Dependent Investigations of Cd- and Uranyl-Stearate Multilayers by means of Neutron Reflectivity Measurements, ECOF6 - European Conference on Organized Films, Sheffield, (GB) (Sep).

Calderon, H.A., Caba-As-Moreno, J.G., Cruz, J.J., Pedersen, J.S., Analysis of anisotropic SANS patterns obtained from Ni-Al-Mo alloys with bimodal particle size distributions. XVII Congress and General Assembly of the International Union of Crystallography, Seattle, Washington (US) (Aug).

Charvolin, J., Colmenero, J., Cummins, P., Mortensen, K., Richter, D., Thomas, B., Weill, G., Polymers and soft matter. In: Scientific prospects for neutron scattering with present and future sources. ESF Exploratory workshop, Autrans (FR) (Jan)

Coad, S., Lussier, J.-G., Paul, D.M., McMorrow, D.F., Characterisation of the neel state in Zn and Ni doped $CuGeO_3$. IUCr 17. Congress and general assembly, Seattle, WA (US) (Aug).

Eskildsen, M.R., Andersen, N.H., Mortensen, K., Yaron, U., Gammel, P.L., Bishop, D.J., Flux-line lattice anisotropy in high-temperature superconductors. Annual meeting of the Danish Physical Society, Nyborg (DK) (May).

Falcao, A.N., Petersen, J.S., Mortensen, K., Butterfly pattern in scattering from swollen polymer networks: Experiments and new scaling model. 10. International conference on small-angle scattering (SAS-96), Sao Paulo (BR) (Jul).

Feidenhans'l, R., X-ray scattering from surfaces. IUCr 17. Congress and general assembly, Seattle, WA (US) (Aug).

Feidenhans'l, R., X-ray scattering from surfaces of organic crystals. Danish national meeting on crystallography. Danish Pharmaceutical Highschool, Copenhagen (DK) (Jun).

Feidenhans'l, R., X-ray scattering from surfaces outside UHV. Conference on surface science: Critical review and outlook, Hong Kong (HK) (Jun).

Feidenhans'l, R., Surface scattering. Summerschool on advanced methods in thin film analysis, Stockholm (SE) (Sep).

Feidenhans'l, R., Diffraction with a x-ray free electron laser. DESY, Hamburg (DE) (Sep).

Feidenhans'l, R., Interface studies by x-ray diffraction. Max-Lab, Lund (SE) (Jan).

Feidenhans'l, R., 'X-ray Scattering from Surfaces', XVII Congress and General Assembly of the International Union of Crystallography., Seattle, (US) (Aug).

Frello, T., Andersen, N.H., Madsen, J., Käll, M., Zimmermann, M. von, Schmidt, O., Poulsen, H.F., Schneider, J.R., Wolf, T., Dynamics of oxygen ordering in $YBa_2Cu_3O_{6+x}$ studied by neutron and high-energy synchrotron x-ray diffraction. NATO-ASI workshop on materials aspects of high-T_c superconductivity, Delphi (GR) (Aug).

Frello, T., Poulsen, H.F., Andersen, N.H., Bentzon, M.D., Süssenbach, J., Nowikow, D., Alignment of high-T_c superconducting crystallites in silver cladding studied by high-energy synchrotron x-ray diffraction. Annual meeting of the Danish Physical Society, Nyborg (DK) (May).

Frielinghaus, H., Schwahn, D., Mortensen, K., Almdal, K., Springer, T., Composition fluctuations and coil conformation in diblock copolymers as a function of temperature and pressure. 1996 APS March meeting. Session E29: Block copolymer, St. Louis, MO (US) (Mar).

Frielinghaus, H., Schwahn, D., Mortensen, K., Willner, L., Almdal, K., Pressure and temperature effects in homopolymer blends and diblock copolymers. 1st European Conference on Neutron Scattering, Interlagen (CH) (Oct).

Frielinghaus, H., Schwahn, D., Mortensen, K., Almdal, K., Springer, T., Pressure and temperature effects in homopolymer blends and diblock copolymers. 10. International conference on small-angle scattering (SAS-96), Sao Paulo (BR) (Jul).

Gammel, P.L., Yaron, U., Aeppli, G., Batlogg, B., Bishop, D.B., Boebinger, G.S., Bucher, E. Kleiman, R.N., Ramirez, A.P., Schiffer, P.E., Broholm, C., Mortensen, K., Neutron scattering from the vortex lattice in UpT_3. 1996-APS March-Meeting, St. Louis (US) (Mar).

Gammel, P.L., Yaron, U., Aeppli, G., Batlogg, B., Bishop, D.J., Boebinger, G.S., Bucher, E., Kleiman, R.N., Ramirez, A.P., Schiffer, P.E., Broholm, C., Mortensen, K., Neutron scattering from the vortex lattice in UPt_3. 1996 APS March meeting. Session N11: Vortex structure - imaging, St. Louis, MO (US) (Mar).

Garamus, V.M., Pedersen, J.S., Structure of graphitized carbon black aggregates in Triton X-100/water solutions by SANS. Xth International Conference on Small-angle Scattering, Campinas, São Paulo (BR) (Jul).

Gardner, J. S., Paul, D. McK. and Lebech, B., Neutron diffraction study of a La2Co4.15 single crystal. 1st European Conference on Neutron Scattering, Interlaken, (CH) (Oct).

Gerstenberg, M.C., Pedersen, J.S., Smith, G., Surface-induced ordering of micelles at the solid-liquid interface. Annual meeting of the Danish Physical Society, Nyborg (DK) (May).

Gerstenberg, M.C., Pedersen, J.S., Smith, G., Surface induced ordering of micelles at the solid-liquid interface. In: EPF'96. Book of abstracts. 6. European Polymer Federation symposium on polymeric materials, Crete (GR) (Oct).

Gerstenberg, M.C., The Surface Induced Ordering of Micelles at the Solid-Liquid Interface, Bombannes 96: Third European Summer School on “Scattering Methods Applied to Soft Condensed Matter”, Carcans-Maubuissson, (FR) (Jun).

Goff, J.P., Bryn-Jacobsen, C., McMorrow, D.F., Ward, R.C.C., Wells, M.R., Magnetic interactions in Nd/Pr superlattices. Neutron scattering conference. A satellite meeting to the 17. IUCR congress, Gaithersburg, MD (US) (Aug).

Hamley, I.W., Fairclough, J.P.A., Ryan, A.J., Lodge, T.P., Pedersen, J.S., The structure of block copolymer solutions: Small-angle scattering experiments. Xth International Conference on Small-angle Scattering, Campinas, São Paulo (BR) (Jul).

Hamley, I.W., Vigild, M.E., Almdal, K., Fairclough, J.P.A., Ryan, A.J., The dynamics of ordering in block copolymer melts: A synchrotron SAXS study. 10. International conference on small-angle scattering (SAS-96), Sao Paulo (BR) (Jul).

Hassager, O., Johannsen, I., Forskning og uddannelse ved Dansk Polymer Center. DSM's projektdag, Risø (DK) (May).

Hillmyer, M.A., Bates, F.S., Almdal, K., Mortensen, K., Ryan, A.J., Fairclough, J.P., Complex phase behavior in low-molecular-weight amphiphilic block copolymers. 1996 APS March meeting. Session E29: Block copolymer, St. Louis, MO (US) (Mar).

Holme, N.C.R., Ramanujam, P.S., Hvilsted, S., Pedersen, M., Near-field microscopy on liquid crystalline side-chain polyesters. Annual meeting of the Danish Physical Society, Nyborg (DK) (May).

Howes, P.B., The atomic structure of the Pb/Si(111) buried interfaces. 5. International conference on the structure of surfaces, Aix-en-Provence (FR) (Jul).

Hvilsted, S., Laser induced segmental orientation in cyanoazobenzene side-chain polyesters as origin of optical storage. Universita di Pisa. Dipartimento di Chimica e Chimica Industriale, Pisa (IT) (Mar).

Hvilsted, S., Berg, R.H., Ramanujam, P.S., Hendann, C., Rømer Holme, N.C., Pedersen, M., Rasmussen, R., Kulinna, C., The researh group on new materials for optical information storage at Risø National Laboratory. NorFA Nordic-Baltic workshop on molecular electrooptic materials, Göteborg (SE) (Jun).

Hvilsted, S., Kulinna, C., Ramanujam, P.S., Laser induced segmental orientation of side-chain liquid crystalline polyesters investigated by FTIR. In: 12th European symposium on polymer spectroscopy. Program. Book of abstracts. ESOPS 12, Lyon (FR) (Jul).

Hvilsted, S., Ramanujam, P.S., Optisk informationslagring. Ungdommens Naturvidenskabelige Forening. (UNF). H.C. Ørsted Institutet, København (DK) (Sep).

Jiang, Q.D., Smilgies, D.-M., Feidenhans'l, R., Cardona, M., Zegenhagen, J., In situ preparation of atomically flat $SrTiO_3$ (001) surface for high T_c thin film epitaxy. In: Applied superconductivity, 1995. 2. European conference on applied superconductivity, Edinburgh (GB), 3-6 Jul 1995. Dew-Hughes, D. (ed.), (Institute of Physics, Bristol, 1995) (Institute of Physics Conference Series, 148) p. 939-942 (1995).

Jerke, G., Cavaco, C., Pedersen, J.S., Schurtenberger, P., Cross-section structure of lecithin worm-like micelles.Workshop on worm-like micelles, Leiden (NL) (Feb).

Jerke, G., Pedersen, J.S., Schurtenberger, P., Micelles as equilibrium polymers: Light and neutron scattering experiments. Swiss Polymer Group: Spring meeting, Zuerich, (CH) (Mar).

Jerke, G., Pedersen, J.S., Schurtenberger, P., The static structur factor of polymer-like micelles: Light and small-angle neutron scattering studies. 3rd Liquid Matter Conference, Norwich (GB) (Jul).

Jerke, G., Pedersen, J.S. Egelhaaf, S.U., Schurtenberger, P., Structure and flexibility of worm-like micelles. Swiss Group of Colloid and Interface Science, General Assembly Meeting, Berne, (CH) (Sep).

Jerke, G., Pedesen, J.S., Schurtenberger, P., The static structure factor of polymer-like micelles: Light and small-angle neutron scattering studies. 20-th Gwatt Workshop. Gwatt (CH) (Oct).

Jerke, G., Pedersen, J.S., Egelhaaf, S.U., Schurtenberger, P., Static structure factor of worm-like micelles:A small-angle neutron scattering study. 1st European Conference on Neutron Scattering (ECNS), Interlaken (CH), (Oct).

Jørgensen, J.-E., Iversen, M.H., Andersen, N.H., On the structure of oxidized $Pb_2Sr_2Y_{0.5}Ca_{0.5}Cu_3O_8$. IUCr 17. Congress and general assembly, Seattle, WA (US) (Aug).

Jørgensen, M., Larsen, M., Facile Synthesis of a Doubly Bridged Bis-Calix[4]arene, ISMRI 9, Lyon (FR) (Sep).

Kolesik, M., Richards, H.L., Novotny, M.A., Rikvold, P.A., Lindgård, P.-A., Magnetization switching in nanoscale ferromagnetic grains: simulations of heterogeneous nucleation. Conf. on Magnetism and Magnetic Materials, St. Louis, (US) (Nov).

Kulinna, C., Hvilsted, S., Ramanujam, P.S., Selective deuterium labeling as a tool for the investigation of laser induced segmental orientation in cyanoazobenzene side-chain polyesters. In: EPF'96. Book of abstracts. 6. European Polymer Federation symposium on polymeric materials, Crete (GR) Oct).

Landemark, E., Nielsen, M., Smilgies, D.-M., Feidenhans'l, R., Lottermoser, L., Seehofer, L., Falkenberg, G., Johnson, R.L., Metal Induced Si(111) 3 x 1 Surface Structures Investigated by Surface X-ray Diffraction. V. International Conference on the Structure of Surface, Aix-en-Provence, (FR)(Jul).

Larsen, M., Jørgensen, M., Selective Substitution of Tetrapropoxy-Calix[4]arene Through Halogen to Lithium Exchange, ISMRI 9, Lyon (FR) (Sep).

Lebech, B., Sørensen, S.Å., Magnetic structure of MnSi - the effects of applied magnetic fields and hydrastatic pressure. Magnetism in Metals. A conference dedicated to the memory of Allan Mackintosh, Copenhagen (DK) (Aug).

Lebech, B., Theodor, K., Breiting, B., Lebech, J., and Sørensen, S. Aa., A facility for Production of deformed germanium wafers. Neutron Scattering - A Satellite Meeting to the XVII IUCr Congress, Gaithersburg (US) (Aug).

Lebech, B., Theodor, K., Breiting, B., Lebech, J., Sørensen, S.Å., A facility for production of deformed germanium wafers. Neutron scattering conference. A Satellite Meeting to the XVII IUCR Congress and General Assembly of the International Union of Crystallography, Gaithersburg, (US) (Aug).

Lefmann, K., Knuuttila, T., Martikainen, J. E., Nummila, K. K., Pohjola, T., and Yao, W., Improving the Transport Properties in Rh metal by Heat Treatment. Annual Conference of the Finnish Physical Society; Espoo (FI) (Mar).

Lefmann, K., Tuoriniemi, J. T., Nummila, K. K., Vuorinen, R. T., and Metz, A., Neutron thermometry of highly polarized silver nuclei. Low Temperature Conference LT-21, Prague, (CS) (Aug).

Lefmann, K., Nuclear magnetic order in silver. Neutron scattering conference. A satellite meeting to the 17. IUCR congress, Gaithersburg, MD (US) (Aug).

Lefmann, K., Tuoriniemi, J.T., Nummila, K.K., Metz, A., Extinction effects studied by varying the nuclear polarization. Neutron scattering conference. A satellite meeting to the 17. IUCR congress, Gaithersburg, MD (US) (Aug).

Lefmann, K., Knuuttila, T., Martikainen, J.E., Nummila, K.K., Pohjola, T., Yao, W., Heat treatment preparation of Rh metal samples for a nuclear ordering experiment. Ultralow temperature sattelite conference. ULT-21, Stara Lesna (CH) (Aug).

Lefmann, K., Nummila, K.K., Tuoriniemi, J.T., Vuorinen, R.T., Metz, A., Clausen, K.N., Lounasmaa, O.V., Rasmussen, F.B., Lipinski, L., Siemensmeyer, K., Steiner, M., Neutron and susceptibility measurements on nuclear ordering in silver. Ultralow temperature sattelite conference. ULT-21, Stara Lesna (CH) (Aug).

Lefmann, K., Nummila, K.K., Tuoriniemi, J.T., Vuorinen, R.T., Metz, A., Clausen, K.N., Lounasmaa, O.V., Rasmussen, F.B., Lipinski, L., Siemensmeyer, K., Steiner, M., Nuclear magnetic ordering in silver, studied by neutron diffraction. Magnetism in metals. A conference dedicated to the memory of Allan Mackintosh, Copenhagen (DK) (Aug). Unpublished.

Lefmann, K., Yao, W., Knuuttila, T., Martikainen, J.E., Nummila, K.K., Oja, A.S., Lounasmaa, O.V., A new ultra-low temperature cryostat for studying magnetic order in Rh. Magnetism in metals. A conference dedicated to the memory of Allan Mackintosh, Copenhagen (DK) (Aug).

Lemmich, J., Mortensen, K., Ipsen, J.H., Hønger, T., Bauer, R., Mouritsen, O.G., Small-angle neutron scattering studies of lipid bilayer structure, softness, and the effect of cholesterol. 40. Annual meeting of the Biophysical Society, Baltimore, MD (US) (Feb).

Lindgård, P.-A., Properties of magnetic nano-particles. 8. International symposium on small particles and inorganic clusters. ISSPIC 8, Copenhagen (DK) (Jul).

Lindgård, P.-A., Properties of magnetic nano-particles. European conference on physics of magnetism 96, Poznan (PL) (Jun).

Lindgård, P.-A., Bohr, H., Magic numbers in protein structures. Annual meeting of the Danish Physical Society, Nyborg (DK) (May).

Lindgård, P.-A., Bohr, H., Packing of protein structures in clusters with magic numbers. 8. International symposium on small particles and inorganic clusters. ISSPIC 8, Copenhagen (DK) (Jul).

*Lindgård, P.-A.,*Symmetry of Protein Folds. Protein Folding III, Copenhagen (DK) (Nov).

McMorrow, D.F.,Clausen, K.N., Lefmann, K., Aeppli, G., Mason, T.F.,Kjems, J.K. First Results from RITA. European Conference on Neutron Scattering, Interlaken (CZ) (Oct).

McMorrow, D.F., The magnetism of rare earth superlattices. Magnetism in metals. A conference dedicated to the memory of Allan Mackintosh, Copenhagen (DK) (Aug).

McMorrow, D.F., New possibilities for neutron scattering at Risø. Rutherford Appleton Laboratory, Chilton (GB) (Sep).

*Mortensen, K.,*1996-Annual Meeting of the American Institute of Chemical Engineers, Chicago (US) (Nov).

Mortensen, K., Studies of block copolymers melts and solutions. Danish Polymer Center meeting, Risø (DK) (Jun).

Mortensen, K., Selfassembling block copolymer: Melts and selective solutions. Nuclear and Technology Institute. Physics Department, Sacavem (PT) (Jun).

Mortensen, K., Polymer physics. Winterschool 1996, Sønderborg (DK) (Jan).

Mortensen, K., Almdal, K., Schwahn, D., Frielinghaus, H., Unusual temperature and pressure dependence of the phase behavior of a PEP-PDMS diblock copolymer. Annual meeting of the Danish Physical Society, Nyborg (DK) (May).

Mortensen, K., Almdal, K., Schwahn, D., Frielinghaus, H., Pressure dependence of the phase behavior of diblock copolymers. Rheology group meeting, Risø (DK) (May).

Mortensen, K., Almdal, K., Bates, F.S., Schwahn, D., Block copolymer micelles, mesophases and networks, studied by small angle neutron scattering. 10. International conference on small-angle scattering (SAS-96), Sao Paulo (BR) (Jul).

Mortensen, K., Almdal, K., Schwahn, D., Frielinghaus, H., Temparature and pressure dependence of the phase behavior of PEP-PDMS diblock copolymer. In: EPF'96. Book of abstracts. 6. European Polymer Federation symposium on polymeric materials, Crete (GR) (Oct).

Mortensen, K., Eskildsen, M.R., Andersen, N.H., Yaron, U., Gammel, P.L., Bishop, D., Flux-line lattices in type-II superconductors studied by small-angle neutron scattering. 10. International conference on small-angle scattering (SAS-96), Sao Paulo (BR) (Jul).

Mortensen, K., Reynaers, H., Block copolymers and polymer gels. 10. International conference on small-angle scattering (SAS-96), Sao Paulo (BR) (Jul).

Ndoni, S., Pedersen, J.S., Almdal, K. Dilute Solution properties of segmentwise labeled star-shaped polymers. Experiment & M.C.Computer Simulation. Poster presented at the 6th European Polymer Federation Symposium on Polymeric Materials, Crete, (GR) (Oct).

Paixao, J.A., Langridge, S., Sørensen, S.Å., Lebech, B., Goncalves, A.P., Lander, G.H., Brown, P.J., Burlet, P., Talik, E., Unusual sublattice interaction in compounds with the $ThMn_{12}$. 1. European conference on neutron scattering, Interlaken (CH) (Oct).

Paolasini, L., Lander, G.H., Shapiro, S.M., Caciuffo, R., Lebech, B., Regnault, L.P., Roessli, B., Fournier, J.-M., Enhanced exchange in the itinerant ferromagnet Ufe_2. 1. European conference on neutron scattering, Interlaken (CH) (Oct).

Papadakis, C.M., Almdal, K., Mortensen, K., Posselt, D., Identification of an intermediate segregation regime in a diblock copolymer system. In: EPF'96. Book of abstracts. 6. European Polymer Federation symposium on polymeric materials, Crete (GR) (Oct).

Papadakis, C.M., Posselt, D., Almdal, K., Mortensen, K., Phase behavior of symmetric diblock copolymers and of block copolymer blends. Annual meeting of the Danish Physical Society, Nyborg (DK) (May).

Pedersen, J.S., Jerke, G., Laso, M., Schurtenberger, P., Structure of polymer-like micelles: SANS and Monte Carlo simulation studies. XVII Congress and General Assembly of the International Union of Crystallography, Seattle, Washington (US) (Aug).

Pedersen, J.S., Jerke, G., Laso, M., Schurtenberger, P., Structure of polymer-like micelles: SANS and Monte Carlo simulation studies. 6th European Polymer Federation Symposium on Polymeric Materials. Aghia Pelaghia, Crete (GR) (Oct).

Reynders, K., Kleppinger, R., Mischenko, N., Mortensen, K., Koch, M.; Reynaers, H., Ordering phenomena in ABA triblock copolymer gels. 10. International conference on small-angle scattering (SAS-96), Sao Paulo (BR) (Jul).

Richards, H., Lindgård, P.-A., The effects of boundary conditions on magnetization switching in Ising clusters. Annual meeting of the Danish Physical Society, Nyborg (DK) (May).

Rønnow, H.M., Magnetic properties of holmium-erbium alloys. Annual meeting of the Danish Physical Society, Nyborg (DK) (May).

Rønnow, H.M., Magnetic properties of holmium-erbium alloys. Magnetism in metals. A conference dedicated to the memory of Allan Mackintosh, Copenhagen (DK) (Aug).

Scalas, E., Brezesinski, G., Bouwman, W.G., Kjær, K., Möhwald, H., Tilted monolayer phases of chiral diols. In: Short and long chains at interfaces. Proceedings of the 30th recontres de Moriond. Series: Moriond condensed matter physics. 30. Rencontres de Moriond, Villars sur Ollon (CH), 21-28 Jan 1995. Daillant, J., Guenoun, P., Marques, C., Muller, P., Tran Thanh Van, J. (eds.), (Editions Frontieres, Gif-sur-Yvette Cedex, 1995), 165-170 (1995).

Scherrenberg, R., Mortensen, K., Small-angle neutron scattering of polypropyleneimine dendrimers. 10. International conference on small-angle scattering (SAS-96), Sao Paulo (BR) (Jul).

Schultz, T., Hazell, R., Feidenhans'l, R., Larsen, M., Jørgensen, M., 2- and 3-dimensional crystallographic studies of a calix-4-arene. Danish national meeting on crystallography. Danish Pharmaceutical Highschool, Copenhagen (DK) (Jun).

Schultz, T., Larsen, F.K., Molecular rearrangements in tetramethylammonium tetrafluoroborate. IUCr 17. Congress and general assembly, Seattle, WA (US) (Aug).

Schwahn, D., Janssen, S., Frielinghaus, H., Mortensen, K., Pressure effects in polymer blends and diblock copolymers studied by small-angle neutron scattering. 5. European symposium on polymer blends, Maastricht (NL) (May).

Schönfeld, B., Malik, A., Kostorz, G., Bührer, W., Pedersen, J.S., Guinier-Preston zones in Al-rich Al-Cu and Al-Ag single crystals. 1st European Conference on Neutron Scattering (ECNS), Interlaken (CH) (Oct).

Sequeira, A.D., Kostorz, G., Pedersen, J.S., The Study of anisotropic single crystalline materials using small-angle neutron scattering. Xth International Conference on Small-angle Scattering, Campinas, São Paulo (BR) (Jul).

Slavomir, M., Mihalik, M., Kavecansky, V., Kovac, J., Menovsky, A.A., Structure, magnetic and electronic properties of (U,Ce)Ru_2Si_2. Annual meeting of the Danish Physical Society, Nyborg (DK) (May).

Sommer-Larsen,P., Modelling of Interphase Properties and Other Modelling Interests. Msi Polymer Users Group Meeting - 3^{rd}-5^{th} November 1996, Weetwood Hall, Leeds (GB) (Nov).

Sufi, M.A., Radiman, S., Wiedenmann, A., Mortensen, K., Performance of a new small angle neutron scattering instrument at the Malaysian Puspati Triga reactor. 10. International conference on small-angle scattering (SAS-96), Sao Paulo (BR) (Jul).

Svensson, B., Alexandridis, P., Olsson, U., Mortensen, K., Amphiphilic Block Copolymer - Water - Oil Systems: Effect of Polymer Molecular Weight on Self-Assembly and Order. 7th Annual Surface and Colloid Science Symposium, (FI) (Oct).

Sørensen, S.Aa., Lebech, B., Sans studies of magnetic structures with long periods. Neutron scattering conference. A satellite meeting to the 17. IUCR congress, Gaithersburg, MD (US) (Aug).

Tepe, T., Bates, F.S., Tirrell, M., Almdal, K., Mortensen, K., The effect of shear on a triblock copolymer melt. 1996 APS March meeting. Session G28: Dillon medal symposium, St. Louis, MO (US) (Mar).

Vigild, M.E., Almdal, K., Ndoni, S., Microphase behaviour of Di-block copolymers and mechanical properties. 3. European summer school on scattering methods applied to soft condensed matter, Bombannes (FR) (Jun).

Vigild, M.E., Ndoni, S., Almdal, K., Hamley, I.W., Fairclough, J.P.A., Ryan, A.J., Phase behaviour of hydrocarbon-poly(dimethylsiloxane) Diblock copolymer melts related to temperature and their volume fraction of hydrocarbon. In: EPF'96. Book of abstracts. 6. European Polymer Federation symposium on polymeric materials, Crete (GR) (Oct).

3.4 Lectures

Almdal, K., Janssen, P., Danish Society for Polymer Technology, Meeting on Polymer Surfaces and Interfaces: Rheological characterization of highly filled dental restorative composites in the uncured state, (Oct).

Almdal, K., The Danish Academy for the Technical Sciences, Meeting on Polymer Science: Block Copolymer Phase Behaviour and Interactions in Polymer Melts, (May).

Andersen, N.H., Uimin, G., Model for the low-temperature magnetic phases of $YBa_2Cu_3O_{6+x}$. Annual meeting of the Danish Physical Society, Nyborg (DK).

Berg, R. H., Peptider til holografisk lagring af information (Peptides for holographic storage of information). Risø National Laboratory, Roskilde (DK) (Apr).

Berg, R. H., Peptides for optical storage of information. Stockholm University, Stockholm (SE) (May).

Berg, R. H., Peptides for optical storage. The Technical University of Denmark, Lyngby (DK) (Nov).

Clausen, K.N., Optimisation of triple axis spectrometers. Two double-lectures at an IAEA Consultants meeting on 'Trends in Neutron Beam Instrumentation, Neutron Scattering', Bhabha Atomic Research Centre, Bombay, (IN) (Mar).

Eskildsen, M. R., The Magnetic Flux-Line Lattice in Type-II Superconductors, DTU International Summerschool on ''Physics and Electronics at Cryogenic Temperatures'' (BEST course): One lecture given at Risø National Laboratory, Roskilde (DK) (Jul).

Feidenhans'l, R., 'Surface Scattering', Summerschool on advanced Methods in Thin Film Analysis, Stockholm, (SE) (Sep).

Feidenhans'l, R., 'Diffraction with a X-ray Free Electron Laser', DESY, Hamburg (DE) (Sep).

Feidenhans'l, R., 'X-ray Scattering from Internal and External Facets', Lausanne (CH) (Nov).

Feidenhans'l, R. , 'Interface studies by X-ray diffraction', Lund, (SE) (Jan).

Frello, T., High-Tc Research at Risø National Laboratory, Structural Investigations of Single-crystal $YBa_2Cu_3O_{6+x}$ and Superconducting BiSCCO wires, DTU International Summer School on "Physics and Electronics at Cryogenic Temperatures" (BEST-course): Lecture given at Risø National Laboratory, Roskilde (DK) (Jul).

Gerstenberg, M.C., The Surface Induced Ordering of Micelles at the Solid-Liquid Interface, Annual Meeting of the Danish Physical Society, Nyborg Strand (May).

Hvilsted, S. and Ramanujam, P.S., Optisk Informationslagring (Optical Information Storage). Folkeuniversitetet i Roskilde (University Extension Services, Roskilde), Risø National Laboratory (Nov).

Hvilsted, S., Polarisations FTIR til studier af laserinducerede segmentbevægelser i selektivt deuterede polyestere (Polarization FTIR for studies of laser induced segmental mobility in selectively deuterated polyesters). User Meeting, Perkin Elmer, Allerød (DK) (Nov).

Lefmann, K., The second generation of nuclear cooling experiments on rhodium metal: Low Temperature Laboratory, Helsinki University of Technology; Espoo (FI) (Nov 1995).

Lindgård, P.-A., Properties of magnetic nano-particles. Odense Universitet. Fysisk Institut, Odense (DK) (Apr).

Lindgård, P.-A., Properties of magnetic nano-particles. Hahn-Meitner-Institut, Berlin (DE) (May).

McMorrow, D.F., Interplay between structure and magnetism in Ho-Pr alloys. ESRF, Grenoble (FR) (Mar).

McMorrow, D.F., Neutron and X-ray Scattering Studies from Thin Films and Superlattices. Ph.D. course on nanoscale physics, DTU, (DK) (Oct).

Mortensen, K., Polymer Physics. 1996-Sandbjerg Slot-Winterschool, Sønderborg, (DK) (Jan).

Mortensen, K., Neutron Scattering studies of polymer blends and block copolymers. Department of Solid State Physics, 1996-Annual Meeting, Risø (DK) (Apr).

Mortensen, K., Almdal, K., Schwahn, D., Frielinghaus, H., Pressure dependence of the phase behavior of diblock copolymers. Rheology Group Meeting, Risø, (DK) (May).

Mortensen, K., Studies of block copolymers melts and solutions. Danish Polymer Centre, Centre Meeting, Risø, (DK) (Jun).

Mortensen, K., Self-assembling block copolymer: Melts and in selective solutions. Physics Department, Nuclear and Technological Institute, Sacavem (PT) (Jun).

Papadakis, C.M., The dynamics of symmetric diblock copolymers studied using dynamic light scattering, Department of Mathematics and Physics, The Royal Veterinary and Agricultural University (DK) (Nov).

Pedersen, J.S., Monte Carlo simulations on the static properties of star polymers in dilute solutions with a good solvent. Rheology Group Meeting, Risø (DK) (Sep).

Pedersen, J.S., Instrumentation for small-angle scattering. The Third European Summer School on Scattering Methods applied to Soft Condensed Matter, Bombannes (FR) (Jun).

Pedersen, J.S., Analysis of small-angle scattering data: Modeling and least-squares fitting. The Third European Summer School on Scattering Methods applied to Soft Condensed Matter, Bombannes (FR) (Jun).

Sommer-Larsen, P., Molecular Electronics: Lecture given at Ph.D.-Course in Molecular Materials Science. Course given May 2. 1996 at CISMI, Univ. Of Copenhagen. (DK) (May).

Vigild, M.E., The phase diagramme of polyisoprene-polydimethylsiloxane. Rheology group meeting, Risø (DK) (May).

Vigild, M.E., Almdal, K., Fairclough, J.P.A., Ryan, A.J., Hamley, I.W., Synchrotron radiation used for small angle scattering examination of model Di-block copolymers melts. Part 1. Rheology group meeting, Risø (DK) (Sep).

3.5 Meetings and Courses Organised by the Department

3.5.1 Symposium on Magnetism in Metals

26-29 August 1996, The Royal Danish Academy of Sciences and Letters (Det Kongelige Danske Videnskabernes Selskab).

The symposium was attended by 69 scientists and was sponsored by

Royal Danish Academy of Sciences and Letters
Carlsberg Foundation
Novo Foundation
Danish Natural Science Research Council
Risø National Laboratory

The symposium was dedicated to the memory of Allan Mackintosh.

Organization

McEwen, K.A.,	Birkbeck College, London, England
Andersen, O. K.,	Max-Planck-Institut, Stuttgart, Germany
Falicov, L. M.,	University of California, USA
Als-Nielsen, J.,	Copenhagen University, Denmark
Clausen, K. N.,	Risø National Laboratory, Denmark
McMorrow, D. F.	Risø National Laboratory, Denmark
Jensen, J.,	Copenhagen University, Denmark

Programme

Memorial session in honour of Allan Mackintosh:

Mackintosh, I.,	England
Bjerrum Møller, H.,	Risø National Laboratory, Denmark,
McEwen, K. A.,	Birkbeck College, England
Andersen, O. K.,	Max-Planck-Institut, Stuttgart, Germany
Mackintosh, P.,	Denmark
Clausen, K.N.,	Risø National Laboratory, Denmark
Jensen, J.,	University of Copenhagen, Denmark

Elliott, R. J.,	University of Oxford, England. Magnetism since the war, 1946-1996.
Cowley, R. A.,	University of Oxford, England. Magnetic interactions and structures of the rare earths.
McEwen, K. A.,	Birkbeck College, London, England. Crystal-field effects in metallic magnetism.
Lander, G. H.,	EITU, Karlsruhe, Germany. Magnetism in the actinides.
Coles, B. R.,	Imperial College, London, England. Dilute magnetic alloys.
Brooks, M. S. S.,	EITU, Karlsruhe, Germany. Conduction electrons in magnetic metals.
Gibbs, D.,	Brookhaven National Laboratory, USA. X-ray magnetic scattering.
Lounasmaa, O.,	Helsinki Technical University, Finland. Nuclear magnetic ordering in metals.
Ikeda, I.,	KEK, Tsukuba, Japan. Neutron studies of disordered and fractal systems.
Jérome, D.,	Université Paris-Sud, France. Organic magnets.

McMorrow, D.F.,	Risø National Laboratory, Denmark. Rare earth superlattices.
Parkin, S. S. P.,	IBM Almaden Research Center, USA. Spin-dependent transport in magnetic nano-structures.
Fulde, P.,	Max-Planck-Institut, Stuttgart, Germany. Routes to heavy fermion behaviour.
Fawcett, E.,	University of Toronto, Canada. Antiferromagnetism in chromium.
Andersen, O. K.,	Max-Planck-Institut, Stuttgart, Germany. On the electronic structure of the cuprates.
Lynch, D. W.,	Iowa State University, USA. Photoemission from cuprate superconductors.
Shirane, G.,	Brookhaven National Laboratory, USA. Magnetism of copper-oxide compounds.
Johansson, B.,	University of Uppsala, Sweden. Localised and itinerant f-electrons.
Lonzarich, G. G.,	University of Cambridge, England. Itinerant electron magnetism.
Ott, H. R.,	ETH, Zürich, Switzerland. Magnetism in heavy electron metals.
Endoh, Y.,	Tohoku University, Sendai, Japan. Spin dynamics in strongly correlated electron compounds.
Mason, T. E.,	University of Toronto, Canada. Neutron scattering studies of heavy-fermion systems.

3.5.2 Danish Polymer Centre Lecture Series

A Danish Polymer Centre Lecture Series has been initiated in order to profile the Centre internally and externally towards the industrial partners and other interested parties. The lectures are delivered by estimated visiting, normally collaborating foreign scientists at either Risø National Laboratory (Risø) or Department of Chemical Engineering, Technical University of Denmark (TechUni).

Organization

The Lecture Series is coordinated by S. Hvilsted, Risø National Laboratory.

Programme

Brostow, W.,	Department of Materials Science, University of North Texas, Denton, USA. Reliability of Polymeric Materials (June, Risø).
McCullough, R.D.,	Department of Chemistry, Carnegie Mellon University, Pittsburgh, PE, USA. Self-Assembled and Chemically Responsive Regioregular Polythiophenes (June, Risø).
Feldthusen, J.,	University of Mainz, Germany. Synthesis of Amphiphilic Block Copolymers and Amphiphilic Networks by Combination of Living Cationic and Anionic Polymerizations (August, Risø).
Iván, B.,	Central Research Institute for Chemistry of the Hungarian Academy of Sciences, Budapest, Hungary. Molecular Engineering of Macromolecular Systems by Carbocationic Techniques. (September, Risø)
Maurer, F.H.J.,	Chalmers University of Technology, Göteborg, Sweden. Positron Annihilation in Polymers (October, TechUni).
Webster, O.W.,	DuPont Central Research and Development, Wilmington, DE, USA. Macromolecular Architecture (October, TechUni).

Valenza, A.,	Dipartimento di Ingegneria Chimica dei Processi e dei Materiali, University of Palermo, Italy. Dielectric Properties of Polymer Blends (October, TechUni).
Ulbricht, M.,	Humboldt-Universität zu Berlin, Germany. Photo-Grafting Surface Functionalizations of Polymeric Membranes (November, TechUni).

3.5.3 Polymer Research

20 May, Technical University of Denmark.

This meeting hosted by The Danish Academy of Technical Sciences in collaboration with the Danish Polymer Centre focused on how the Centre has accepted the challenge in strengthening the polymer research in Denmark. Current activities in the Centre were examplified in 5 presentations. In addition an English sister Centre was described and finally the future institutional Danish polymer research and its relationship to Danish Industry was debated. The meeting was well attended by 75 participants.

Organization

Hvilsted, S. Risø National Laboratory, Denmark
Johannsen, I. Risø National Laboratory, Denmark,
Hassager, O. Department of Chemical Engineering, Technical University of Denmark, *and*
Urban, C., Hempel's Marine Paints A/S, Denmark,
in collaboration with the Danish Academy of Technical Sciences.

Programme

Johannsen, I.,	Risø National Laboratory, Denmark and
Hassager, O.,	Technical University of Denmark. Brief Presentation of Danish Polymer Centre and Educational Initiatives at The Technical University of Denmark.
Hassager, O.,	Technical University of Denmark. Polymer Rheology and Processing.
Almdal, K.,	Risø National Laboratory, Denmark. Block Copolymer Phase Behaviour and Interactions in Polymer Melts.
Gregorius, K.,	M & E A/S, Denmark. New Surfaces for Covalent Immobilization of Small Molecules.
Christensen, S.F.,	Coloplast A/S, Denmark. Rheology of Adhesion.
Davies, G.R.,	University of Leeds, England. Interdisciplinary Research Centre in Polymer Science and Technology Hosted at the Universities of Bradford, Durham & Leeds.

Panel Discussion: The Future of Polymer Research in Denmark.

Abbås, K,	Borealis Denmark
Bechgaard, K.,	Risø National Laboratory, Denmark
Davies, G.R.,	University of Leeds, England
Hassager, O.,	Technical University of Denmark.
Hvilsted, S.	Risø National Laboratory, Denmark
Johannsen, I.	Risø National Laboratory, Denmark
Marcher, B.,	NKT Research A/S, Denmark

Schmidt, R., Wolff & Kaaber A/S, Denmark

3.5.4 Danish Polymer Centre Meeting

3 June, Risø National Laboratory.

Presentation of the ongoing research within Danish Polymer Centre attended by 40 scientists. The programme consisted of 9 lectures in addition to the exchange of formal and general information.

Organization

Hvilsted, S. Risø National Laboratory, Denmark
Johannsen, I., Risø National Laboratory, Denmark
Hassager, O. Department of Chemical Engineering, Technical University of Denmark
Urban, C., Hempel's Marine Paints A/S, Denmark

Programme

Jannasch, P., Novo-Nordisk A/S, Denmark. Development of Polymer Packing for Administration of Drugs.
Thulstrup, D., Nunc A/S, Denmark. Binding of Biomolecules to Polymer Surfaces.
Nielsen, L.V., ABB I.C. Møller A/S, Denmark. Heat Transport in Polymer Foam Materials.
Urban, C., Hempel's Marine Paints A/S, Denmark. Study of Epoxy Networks for Use in Coating Applications.
Jensen, B.H., Danfoss A/S, Denmark
Larsen, T.S., Grundfos A/S, Denmark
Chemical Thermal Aging of PPS and PA66 Polymer Composites.
Gao, B., Department of Chemical Engineering, Technical University of Denmark.
Preparation of Amphiphilic Block Copolymers
Mortensen, K., Risø National Laboratory, Denmark. Studies of Block Copolymer Melts and Solutions.
Jonsson, G., Department of Chemical Engineering, Technical University of Denmark.
Selectivity and Surface Properties of Polymer Membranes for Ultra and Micro Filtration.
Berg, R.H., Risø National Laboratory, Denmark. Peptide Based Materials for Optical Information Storage.

3.5.5 Polymer Surfaces and Interfaces

2 October, Domus Technica, Copenhagen, Denmark.

This Symposium under the auspices of Danish Society for Polymer Technology dealt with structure of surfaces and interfaces in polymer composites and polymer blends in addition to problems encountered with polymer surface wetting and adhesion. Nine lecturers covered both more fundamental aspects and a number of case stories. The Symposium had 51 participants with the majority from industry and 5 from the Department of Solid State Physics.

Organization

Lyngaae-Jørgensen, J., *Department of Chemical Engineering, Technical University of Denmark,*
Hvilsted, S., *Risø National Laboratory, Denmark.*

Programme

Lindquist, M.,	Technical University of Denmark. Polymer Surfaces an Introduction.
Maurer, F.H.J.,	Chalmers University of Technology, Sweden. Interfacial Properties of Polymer Blends and Alloys.
Badyal, J.P.,	University of Durham, England. Methods of Surface Characterization.
Eriksen, E.,	Aalborg University, Denmark. Characterization of Composite Surfaces by Stylus Instruments and Optical Profilers.
Hansen, C.M.,	FORCE Institute, Denmark. New Simple Method to Measure Polymer Surface Tension.
Madsen, N.B.,	Risø National Laboratory, Denmark. Chemical Modification of Inorganic Fillers.
Hennissen, L.,	Lapinus Fibres BV, The Netherlands. Systematic Modification of Filler/Fibre Surfaces to Achieve Maximum Compatibility with Matrix Polymers.
Almdal, K.,	Risø National Laboratory & Jansen, P., Wolff & Kaaber A/S, Denmark. Rheological Characterization of Highly Filled Dental Restorative Composite in the Uncured State.

3.5.6 Third European Summer School on "Scattering Methods Applied to Soft Condensed Matter"

2-8 June, Les Bruyères, Carcans-Maubuisson, Bombannes, France.

The aim of the school was to give advanced training for young researchers at post-graduate and post-doctoral level. 23 hours of general lectures were given by the 15 lectures. The school had 46 participants who also provided 16 hours of scientific contributions.

Organization

P. Lindner (chairman), Institut Laue-Langevin, Grenoble, France.
O. Glatter, University of Graz, Austria.
J.S. Pedersen, Risø National Laboratory, Denmark.
P. Schurtenberger, ETH Zürich, Switzerland.
T. Zemb, CEA Saclay, France.

Sponsors

Institute Laue-Langevin, Grenoble, France.
CEA Sacaly, France.
Risø National Laboratory, Denmark.
IFF Jülich, Germany.
PSI Villigen, Switzerland.
Austrian Foreign Ministery.

Programme

P. Pusey,	University of Edinburgh, UK, General Introduction to Scattering Experiments
J. Teixeira,	LLB Saclay, France, Initial Data Treatment, Absolute Intensity
O. Glatter,	University of Graz, Austria, Small Angle Scattering, Static Light Scattering
J.S. Pedersen,	Risø, Denmark, Instrumentation, Resolution Effects and Models
Th. Zemb,	CEA Saclay, France, General Theorems
C. Williams,	Collège de France, Synchrotron Radiation and Contrast Variation
R. Klein,	University of Konstanz, Germany, Interacting Systems
P. Pusey,	University of Edinburgh, UK, Dynamic Light Scattering
F. Boué,	LLB Saclay, France, Gels and Networks
A. Brûlet,	LLB Saclay, France, Quasi-elastic Neutron Scattering
B. Ewen,	MPIP Maniz, Germany, Polymers in Solution and Bulk
J. Als-Nielsen,	University of Copenhagen, Denmark, Specular Reflection of X-rays and Neutrons
R. May,	ILL, Grenoble France, Biological Applications
P. Schurtenberger,	ETH Zürich, Switzerland, Micelles and Microemulsions
P. Lindner,	ILL, Grenoble, France, Scattering Exp. under External Constraints
G. Porte,	Univ. of Montpellier, France, Scattering by Flexible Surfaces and Bilayers

3.6 Membership of Committees and Boards

Andersen, N.H.,
Consultant for the Swedish Superconductivity Consortium.

Bechgaard, K.,
Chairman of the Danish National Commitee for Chemistry.
Member of the Advisory Board of Journal of Materials Chemistry.
Member of the EEC COST D-4 Committee.
Member of the Academy Council of the Danish Academy of Technical Sciences.
Member of the NATO Special Programme Panel on Supramolecular Chemistry.

Berg, R. H.,
Member of the Editorial Advisory Board, Journal of Peptide Science.
Councillor of the European Peptide Society.

Clausen, K. N.,
Member of the Risø board of governors
Member of the EC-Round Table for Neutron Sources
Member of the IUPAP C.9 - Commission on Magnetism
ESS Science Working Group

Feidenhans'l, R.,
Secretary for the Danish National Commitee for Crystallography
Member of the Forschungsbeirat Synchrotronstrahlung HASYLAB, DESY, Hamburg (DE)
IUCr Commision on Synchrotron Radiation
Danish Representative in Nordsync.
Advisor for the Council of ESRF
Council Member of the European Synchrotron Radiation Society
Chaiman of the Working Group "Surfaces, Interfaces and Diffraction" for the X-ray Free Electron Project at HASYLAB, Hamburg (DE)

Hvilsted, S.,
Treasurer of The Danish Society for Polymer Technology.
Contributor to "The Great Danish Encyclopedia" (in Danish: "Den Store Danske Encyclopædi"), Copenhagen.
Local Organizing Committee for 12th International Congress on the Thermal Analysis and Calorimetry (ICTAC 2000), Copenhagen, August 2000.

Johannsen, I.,
Member of The Danish Technical Research Council.
Member of The Danish Biotechnology Research Board.
Chairman of the MODECS Research Forum.

Lebech, B.,

Member of the Commision on Neutron Scattering of the International Union of Crystallography
Member of the Danish National Commitee for Crystallography
Member of the Programme Commitee for the I. European Neutron Scattering Conference, Interlaken, CH.
Contributor to “The Great Danish Encyclopedia” (in Danish: “Den Store Danske Encyclopædi”), Copenhagen.
Danish Representative in ENSA, the European Neutron Scattering Assiciation

Lindgård, P.-A.,

Vicechaiman of the Magnetism Section of International Union of Pure and Applied Physics (IUPAP).
Chairman of the Condensed Matter Commitee at NORDITA.

Mortensen, K.,

Member of the Board of Solid State Decision of the Danish Physical Society.
Member of the European Spallation Source Scientific Working group on Large Scale Structures.

Pedersen, J. S.,

Coeditor of Journal of Applied Crystallography.
Member of the Commision for Neutron Scattering of the International Union of Crystallography.

3.7 Colloquia held at the Department

Bezryadin, A., Delft University of Technology, The Netherlands. Surface superconductivity and a quantum phase transition in superconducting film with a lattice of holes ("antidots") (January).

Lösche M., University of Leipzig, Germany. Composite Macromolecular Structures at Interfaces: From Membrane Models to Biosensors (January).

Robinson, I. R., University of Illinois, USA. Applications of Coherant X-ray Diffraction to Surfaces (January).

Pfleiderer, C., Centre d'Etudes Nucléaires de Grenoble DRFMC/SPSMS/LCP, France. Experimental Investigation of the Magnetic Quantum Phase Transition in MnSi (February).

Deuben, H-J., Department of Chemistry, University of Copenhagen, Denmark. Synthesis of Novel Chiral 6,6'- Disubstituted-Binaphthol Derivatives: Nonlinear Optical Properties and Twisting Power of Liquid Crystals (February).

Uimin, G., Landau Institute, Russia. Quadrupolar ordering in CeB_6 (March).

Rasmussen, F. B., Waals-Zeeman Institute, University of Amsterdam, The Netherlands. Nitrogen impurities in silicon studied by infrared absorption spectroscopy (March).

Bogdanov, A., University of Erlangen-Nuernberg, Germany. Magnetic vortex states in easy-axes and cubic helimagnets (April).

Lulek, T., A. Mickiewicz University, Poland. Symmetry description of Magnetic Structures in Crystals (June).

Achiwa, N., Faculty of Science, Kyushu University, Japan. Neutron Spin Echo Optics At Kurri (July).

Takayama-Muromachi, E., National Institute for Research in Inorganic Materials, Japan. Structural and Superconductors Prepared under High Pressure (August).

Andersen, K., Institut Laue-Langevin, France. High Resolution Measurements on Rotations in 4He (August).

Iván, B., Technical University of Denmark, Denmark. Molecular Engineering of Macromolecular Systems by Carbocationic Techniques (September).

Johansen, T. H., University of Oslo, Norway. Magneto-optic imaging - a powerful tool for studies of HTSCs (September).

Hedegård, P., NBI, University of Copenhagen, Denmark. The theory of high-T_c superconductivity (October).

Löhneysen, H. von, Physikalisches Institut, Universität Karlsruhe, Germany. Unusual Magnetic Phase Transitions (November).

Jung, T.A., IBM Research Division, Rüschlikon, Switzerland. Tuning Molecular Properties: Molecular and Conformational Identification by Scanning Tunneling Microscopy (November).

Rosengaard, N., Uppsala University, Sweden. Finite Temperature Studies of Itinerant Ferromagnetism in Fe, Co and Ni (December).

Smela, E., Univeristy of Linköping, Sweden. Polymer Micro-Actuators (December).

4 Staff and Guest Scientists

4.1 Scientific Staff

Aeppli, Gabriel (Consultant)
Almdal, Kristoffer
Als-Nielsen, Jens (Consultant)
Andersen, Niels Hessel
Bechgaard, Klaus (Head of the Department)
Berg, Rolf H.
Clausen, Kurt N. (Head of Research Programme)
Feidenhans'l, Robert (Head of Research Programme)
Hvilsted, Søren
Jensen, Jens (Consultant)
Johannsen, Ib (Head of Research Programme)
Jørgensen, Mikkel
Kjær, Kristian
Lebech, Bente
Lebech, Jens
Lindgård, Per-Anker
McMorrow, Des
Mortensen, Kell (Research Professor)
Nielsen, Mourits
Pedersen, Jan Skov
Pedersen, Walther Batsberg
Sommer-Larsen, Peter

Post-docs
Baker, Jeff (From August 1)
Bergström, Magnus (From January 12)
Howes, Paul (From February 12)
Jannasch, Patric (From March 1)
Jørgensen, Erling Bonne (From March 1)
Kulinna, Christian (Until October 31)
Käll, Mikael (Until August 31)
Larsen, Niels B. (From December 1)
Lefmann, Kim (From September 1)
Lemmich, Jesper (From September 1)
Lussier, Jean-Guy
Ndoni, Sokol
Papadakis, Christine Maria (From August 15)
Rasmussen, Frank Berg (From August 1)
Schiødt, Niels Chr. (From November 1)
Schröder, Almut
Wilkes, Stephen (Until November 31)

Ph.D. Students and other students
Arleth, Lise (On leave from July 31)
Christensen, Morten Jagd (On leave from April 30)
Eskildsen, Morten Ring
Flarup, Christina (From February 1)
Frello, Thomas
Gerstenberg, Michael C.
Krebs, Frederik
Larsen, Mogens
Larsen, Thomas Bjerggaard (From June 1)
Madsen, Anders (Until August 31)
Madsen, Jesper
Madsen, Nils Berg
Pedersen, Marianne
Rasmussen, Palle H.
Rønnow, Henrik M.
Schmidt, Ole
Schultz, Thomas (From February 1)
Sørensen, Steen Aagaard
Vigild, Martin E.
Zhou, Ji

Technical Staff
Bang, Steen
Berntsen, Allan Nørtoft
Breiting, Bjarne
Engelhardt, Stina (From September 1)
Hansen, Dorthe (Until January 31)
Hansen, Lone (From June 29 to July 19)
Hedeboe, Vivi (On leave from May 31)
Hubert, Lene
Jensen, Birgit
Johansen, Arne
Jørgensen, Ole
Kristensen, Eva Tulin (Until April 30)
Kjær, Torben
Lund, Morits
Nielsen, Anne Bønke
Nielsen, Carina (Until March 31)
Nielsen, Lotte
Nielsen, Steen
Rasmussen, Helle D.
Rasmussen, Ove
Saxild, Finn
Schmidt, Ewa Wanda (From August 15)
Sonberg, Tina Sonne (Until June 15)
Stahl, Kim
Theodor, Keld
Thomsen, Heidi (From October 1)

Thomsen, Ole Lystrup (Until June 30)
Thygesen, Maria (Until Januar 1)
Topp, John Erik (From September 16)

Secretaries
Frederiksen, Lajla
Liljenström, Anette (From May 15)
Schlichting, Bente O.
Studinski, Ca

Temporary Student Assistants
Abrahamsen, Asger (From July 8 to August 29)
Arentoft, Jesper (From April 1 to May 31)
Blicher, Thomas (From July 8 to August 30)
Kealey, P.G. (From August 1 to September 15)
Kofod, Guggi (From July 15 to August 23)

Guest Scientists, Temporary Scientific Staff and Long Time visitors
Faldt, André (Temporary from August 12)
Hendann, Claudia
Høghøj, Peter (From July 8 to Autust 12)
Ivan, Béla
Lay, Alexander (From April 1 to September 1)
Matas, Slavomir (From February 1)
Misaki, Yohji (Until 30-06-96)
Svejstrup, Jens (Temporary until March 31)

Degrees and Awards
Clausen, Kurt N., Adjunct professorship, University of Copenhagen

4.2 Short Time Visitors 1996

Barber, B.	Bell Laboratories, Lucent Technologies, Murray Hill, NJ, USA
Bates, F.S.	University of Minnesota, USA
Bishop, D.	Bell Laboratories, Lucent Technologies, Murray Hill, NJ, USA
Bradshaw, J.	Dept. of Preclinical Veterinary Sc., The Univ. of Edinburg, England
Bucher, R.	Institut für Angewandte Physik, Zürich, Switzerland
Calderon, H.	Inst. Politecnico Nacional, Dept. de Ingeniera Metalurgica, Mexico
Cruz, J.	Inst. Politecnico Nacional, Dept. de Ingeniera Metalurgica, Mexico
Gammel, P.	Bell Laboratories, Lucent Technologies, Murray Hill, NJ, USA
Goldman, A.	Iowa State University, USA
Hajduk, D.A.	University of Minnesota, USA
Hillmeyer, M.A.	University of Minnesota, USA
Høghøj, P.	Neutron Optics Lab., Institute Laue-Langevin, Grenoble, France
Iván, B.	Central Research Inst. For Chemistry of the Hungarian Academy of
Jerke, G.	Institut für Polymere, ETH Zentrum, Zürich, Switzerland
Kapral, S.	Fac. of Physics & Nuclear Techniques Academy, Poland
Kostorz, G.	Institut für Angewandte Physik, Zürich, Switzerland
Kuzma, M.	Migner Pedagogical School, Institute of Physics, Rzeszów, Poland
Lulek, T.	Adam Mickiewicz University of Poznan, Poland
Mannstaedt, S.	The Technical University of , Denmark, Denmark
Mason, T.	Theoretical and Nuclear Physics, Univ. of Toronto, Ontario, Canada
Maurer, W.	University of Minnesota, USA
Mentink, S.	Theoretical and Nuclear Physics, Univ. of Toronto, Ontario, Canada
Ramzan, A.	Dept. of Preclinical Veterinary Sc., The Univ. of Edinburg, England
Ramzi, A.	Structure & Morphology of Materials Section PAC-MC, Geleen, NL
Sager, W.	Dept. of Physical and Macromolecules Chemistry,Leiden, NL
Scherrenberg, R.	Structure & Morphology of Materials Section PAC-MC, Geleen, NL
Schneider, J. M.	Institut für Angewandte Physik, Zürich, Switzerland
Schönfeld, B.	Institut für Angewandte Physik, Zürich, Switzerland Sciences, Budapest, Hungary
Smeets, R.	Dept. of Physical and Macromolecules Chemistry, Leiden, NL
Szaszvari, P.	Institut für Angewandte Physik, Zürich, Switzerland
Takinouchi, H.	University of Minnesota, USA
Tepe, T.	University of Minnesota, USA
Uri, Y.	Bell Laboratories, Lucent Technologies, Murray Hill, NJ, USA
Wilkins, D. J.	Institut für Angewandte Physik, Zürich, Switzerland
Xu, G.	Johns Hopkins Univ., Dept.of Physics & Astronomy, Baltimore, USA

4.3 Short Time Visitors under the CEC-TMR programme 1996

Achu, E.W.	Department of Physics, University of Salford, England
Alexandridis, P.	Phys. Chem. 1, Chemical Center, Lund University, Sweden
Al-Kanani, H.J.	Department of Physics, University of Salford, England
Bolm, A.	Univ. of Postdam, Institute of Solid State Physics, Postdam, Germany
Boothroyd, A.	Clarendon Laboratory, University of Oxford, England
Booth, J.R.	Department of Physics, University of Salford, England
Brecht, E.	Institut für Nuklear Festkörperphysik, Karlsruhe, Germany
Brough, I.	UMIST; Materials Science Center, Manchester, England
Brugnami, D.	Universitá degli studi di Ancona, Italy
Bryn-Jacobsen, C.	Clarendon Laboratory, Oxford University, England
Caruana, D.	School of Chemistry, University of Bath, England
Caruana, D.	School of Chemistry, University of Bath, England
Coad, S.	Physics Department, University of Warwick, England
Coldea, R.	Clarendon Laboratory, University of Oxford, England
Cowley, R.	Clarendon Laboratory, University of Oxford, England
da Costa, M.M.R.	Department of Physics, University of Coimbra, Portugal
de la Fuenta, C.	Clarendon Laboratory, University of Oxford, England
de la Fuente, C.	Clarendon Laboratory, University of Oxford, England
Denef, B.	Department of Chemistry, K.U. Leuven, Belgium
Diedrich, G.	Max Planck Institut f. Mol. Gen., Germany
Englisch,U.	Univ. of Postdam, Institute of Solid State Physics, Postdam, Germany
Fairclough, J.P.A.	Department of Chemistry, University of Leeds, England
Fiori, F.	Universitá degli studi di Ancona, Italy
Fitzpatrick, M.	Faculty of Technology, Milton Keynes, England
Frenzen, A.	Universität Leipzig, Physik der Biomembrane, Germany
Frielinghaus, H.	Forschungszentrum Jülich GmbH, Germany
Förland, G.M.	Institutt for energiteknikk, Kjeller, Norway
Glidle, A.	Department of Electronics, Glasgow University, England
Goff, J.	Clarendon Laboratory, University of Oxford, England
Hamley, I.W.	Department of Chemistry, University of Leeds, England
Harris, M.,	ISIS Facility, RAL, England
Kierkedelen, M.	Institutt for energiteknikk, Kjeller, Norway
Kleppinger, R.	Department of Chemistry, K.U. Leuven, Belgium
Klimanek, P.	Freiberg University of Mining and Technology, Germany
Lake, B.	Clarendon Laboratory, University of Oxford, England
Lovell, M.	School of Chemistry, University of Bath, England
Lovell, M.	School of Chemistry, University of Bath, England
Mehnert, K.	Freiberg University of Mining and Technology, Germany
Mischenko, N.	Department of Chemistry, K.U. Leuven, Belgium
Moore, C.	School of Chemistry, University of Bath, England
Moore, C.	School of Chemistry, University of Bath, England
Müller, P.	Der Technischen Hochschule Aachen, Germany
Nield, V.	Physics Laboratory, University of Kent, United Kingdom
Olsson, U.	Phys. Chem. 1, Chemical Center, Lund University, Sweden
Paixao, J.A.C.	Department of Physics, University of Coimbra, Portugal
Pavese, A.	Dipartimento Scienze della Terra, Universitá di Milano, Italy
Pietsch, U.	Univ. of Postdam, Institute of Solid State Physics, Postdam, Germany
Prencipe, M.	Dipartimento di Scienze Mineralogiche e Petrologiche, Torino, Italy

Rainford, B.	Physics Department, University of Southampton, United Kingdom.
Reynolds, J.	Clarendon Laboratory, University of Oxford, England
Roefs, B.	Netherlands Institute for Dairy Research, Ede, The Netherlands
Roser, S.	School of Chemistry, University of Bath, England
Rouch, J.	CPMOH, University of Bordeaux I, France
Ryan, A.J.	Manchester Materials Science Centre, UMIST, England
Samseth, J.	Institutt for energiteknikk, Kjeller, Norway
Saville, P.M.	Department of Chemistry, University of Leicester, England
Schwahn, D.	Forschungszentrum Jülich GmbH, Germany
Schwingel, D.	UMIST; Materials Science Center, Manchester, England
Silva, M.R.	Department of Physics, University of Coimbra, Portugal
Stephan, V.	Hahn-Meitner-Institute Berlin, Germany
Stockert, O.	Physikalisches Institut, Universität Karlsruhe, Germany
Svensson, B.	Phys. Chem. 1, Chemical Center, Lund University, Sweden
Svergun, D.	EMBL, c/o DESY, Hamburg Outstation, Germany
Tennant, A.	Clarendon Laboratory, University of Oxford, England
Tribaudino, M.	Dipartimento di Scienze Mineralogiche e Petrologiche, Torino, Italy
Verheul, M.	Netherlands Institute for Dairy Research, Ede, The Netherlands
von Zimmerman, M.	Hamburger Synchrotronstrahlungslabor, HASYLAB, Desy, Germany
Watts, M.	Dept. of Materials Sc. & Metallurgy, Univ. of Cambridge, England
Weiss, L.	Hahn-Meitner-Institut, Berlin, Germany
Weygand, M.	Universität Leipzig, Physik der Biomembrane, Germany
Wildes, A.	Clarendon Laboratory, University of Oxford, England
Wilson, C.C.	ISIS Facility, RAL, England
Wilson, R.	Department of Chemistry, University of Leicester, England
Woldt, E.	Institut für Werkstoffe, Universität Braunschweig, Germany
Zeiske, T.	Hahn-Meitner-Institut, Berlin, Germany

Bibliographic Data Sheet **Risø-R-933(EN)**

Title and author(s)

Annual Progress Report of the Department of Solid State Physics
1 January - 31 December 1996

Edited by M. Jørgensen, K. Bechgaard, K.N. Clausen, R. Feidenhans'l, and I. Johannsen

ISBN
87-550-2233-2

ISSN
0106-2840
0907-0249

Dept. or group
Department of Solid State Physics

Date
January 1997

Groups own reg. number(s)

Project/contract no.

Pages	Tables	Illustrations	References
173	6	144	197

Abstract (Max. 2000 char.)
Research in the department is concerned with "Materials with Distinct Physical and Chemical Properties". The principal activities of the department in the period from 1 January to 31 December, 1996, are presented in this Progress Report.

Neutron and x-ray diffraction techniques are used to study a wide variety of problems in condensed matter physics and include: two- and three-dimensional structures, magnetic ordering, heavy fermions, high T_c superconductivity, phase transitions in model systems, precipitation phenomena, and nano-scale structures in various materials. The research in chemistry includes chemical synthesis and physico-chemical investigation of small molecules and polymers, with emphasis on polymers with new optical properties, block copolymers, surface modified polymers, and supramolecular structures. Related to these problems there is work going on in theory, Monte Carlo simulations, computer simulation of molecules and polymers and methods of data analysis.

Descriptors INIS/EDB
MAGNETISM, POLYMERS, PROGRESS REPORT, RESEARCH PROGRAMS, RISOE NATIONAL LABORATORY, SOLID STATE PHYSICS, SUPERCONDUCTIVITY

Available on request from:
Information Service Department,
Risø National Laboratory (Afdelingen for Informationsservice, Forskningscenter Risø)
P.O. Box 49, DK-4000 Roskilde, Denmark
Phone (+45) 46 77 46 77, ext. 4004/4005 - Telex 43 116 - Telefax (+45) 46 75 56 27